# Microwave Spectroscopic and Theoretical Investigations on Inter/Intra Molecular Bonding

A Thesis

Submitted for the Degree of

***Doctor of Philosophy***

in the Faculty of Science

by

**Abhishek Shahi**

**Department of Inorganic and Physical Chemistry**

**INDIAN INSTITUTE OF SCIENCE**

**BANGALORE- 560012, INDIA**

**July, 2014**

*Dedicated to My Dear Mother*

# Declaration

I hereby declare that the work presented in this thesis entitled ***Microwave Spectroscopic and Theoretical Investigations on Inter/Intra Molecular bonding*** has been carried out by me at the Department of Inorganic and Physical Chemistry, Indian Institute of Science, Bangalore, India, under the supervision of Professor E. Arunan.

Date Abhishek Shahi

# Certificate

I hereby certify that the work presented in this thesis entitled ***Microwave Spectroscopic and Theoretical Investigations on Inter/Intra Molecular bonding*** has been carried out by Mr. Abhishek Shahi at the Department of Inorganic and Physical Chemistry, Indian Institute of Science, Bangalore, India, under my supervision.

Date

Prof. E. Arunan

(Research Supervisor)

# ACKNOWLEDGMENTS

I would like to thank my research supervisor Prof. E. Arunan for giving me an opportunity to join his group and work with him. I remember those initial days when he started teaching me about science step by step and gave me full freedom to learn and grow. I greatly appreciate that despite a busy schedule, he always found time for discussion. Many times, through his discussion, I found a way to came out from my research related problems. Not only science, but I learned many inherent facts about the life just by observing his daily activity, like being regular, punctual and responsible. I sincerely thank him for all his help during my research and giving me a chance to explore the world.

I would like to thank Prof. P.C. Mathias for his kind helps towards maintaining the spectrometer and take us out from very difficult situations many times.

I take this opportunity to thank all the professors of the Chemical Dynamics Group. I find myself lucky to be a part of this group. The deep discussions during the talks introduced me to new areas of research. I thank Prof. E. Arunan, Prof. P.K. Das, Prof. K.L. Sebastian, Dr. A. Bhattacharya, Dr. U. Harbola and Dr. Sai G. Ramesh for their enthusiastic involvements during the talks.

I specifically want to thank Prof. K.L. Sebastian for his way of explaining the difficult topics in a very simple way. I also thank him for selecting as a teaching assistant under him. I learned many teaching techniques during the assistantship.

I would like to thank Prof. P. K. Das for his encouraging. I also thank him for providing all the good facilities in the department. I thank Prof. Sai G. Ramesh for fruitful discussions on various research topics and maintaining the wonderful computational facility at the department.

I express my sincere thanks to Prof. S. Umapathy for giving me a chance to participate in the ICORS-2012 conference. I enjoyed hearing from him on various topics during the ACS-2013 meeting.

I thank all IPC faculties for their friendly behavior and developing good environment in department.

I would also like to thank all IPC staff specially Mrs. Roopa, Mrs. Prabha, Mrs. Padma, Mr. Lokanathan and Mr. Arulnambi for their help.

I thank past Chairman, Prof. A. G. Samuelson, for good providing facilities in the department.

I gratefully acknowledge financial supports from CSIR and IISc during my Ph.D. tenure. I also acknowledge the financial grants from DST and IISc for attending the conferences abroad.

I sincerely acknowledge the SERC department, IISc for providing excellent computational facilities.

I feel at home inside the IISc while being at Sir's home. I thank Mrs. Arunan for inviting us on different festivals and making us feel at home with all those delicious meals.

I thank Dr. Santosh Mishra, Bhawana Bhabhi, Dr. Subinoy Da and Banani Di for their loving company and advices. I would like to thank IISc art of living group for conducting wonderful yoga and meditation courses in the campus.

I express my sincere thanks to my seniors Dr. Mausumi, Dr. Aiswaryalakshmi and Dr. Harish for their valuable advices. Special thanks to Dr. Devendra for thoroughly teaching me instruments and calculations. It has been a wonderful experience to work with my dear colleagues Devendra, Sharath, Kiran, Kunal, Sharon and Emmanuel. I enjoyed the time spending with them. I wish to thank all the summer students and visiting faculties of our lab.

I would like to thank Devendra for always being with me in tough situation, encouraging me and most of the time giving me solution of that problem. In his presence, I feel secure and worriless. I thank him for all his cooperation.

I feel privileged for being surrounded with some wonderful people. It gives me immense pleasure to mention the constant support of my friends during my research work. My special thanks to Devendra, Debarati, Chandrabhushan and Sharon for giving me some of the most wonderful moments of my life. I would like to specially thank Deepika for all her helps and care when she was in IISc, which still continues. I thank Debarati and Shron for their caring nature

towards me. I thank all of them for adding extra spice to all the special occasions of my Ph.D. life. Things would have not been so easy and smooth without these people in IISc. I am sure that I will miss them very much after leaving IISc.

I am thankful to all my friends, Shubhadip, Koushambi, Pallavi, Rati, Rekha, Himagshu, Deepika J., Deepika C., Rekha, Rohit, Himangshu, Saheli, Puja, Koushik, Bijayalaxmi, Aninadita, Balaji, Ravi, Joydeb, Ruchi, Yashpal, Rishi bhaiya and Bhawana di for making my tenure in IISc a wonderful experience. I would like to thank my friends Siva, Prabhat, Srikant, for all the wonderful times we spent together.

I would like to thank all the members of '2012' Al(l)chemists' club. It was fun working with them for arranging different programs of the department.

I thank my childhood friends Manish, Rajan, Ashwani, Mukesh, from depth of my heart for their evergreen friendship. I would also like to thank my close friends Maynak, Pawanesh, Anand, Vinay, Manoj, Indresh and Raju Mishra.

I owe my thanks to all my teachers who have helped me reach here. I would like to extend my sincere thanks to my favorite teacher Dr. B. M. Tripathi for his wonderful lessons on chemistry. I thank him for all his valuable advices at every crucial junctures of my academic life.

I would like to thank my uncle Dr. Ravi Prakash Shahi for taking care of me at and guiding me to solve each and every problem of my life. He is a father figure in my life. I would also like to thank another important person in my life Mr. Radheshyam Tiwari for his constant support.

I thank my each and every family members for all their love and affection. My special thanks to Kiran Bua, Kancha Bua, Anita Mausi, K. P. Mama, Hemant bhai, Sudha Bhabhi, S. R. Shahi, Jay Shahi, Rajan, Vivek and my late Grandparents for their support. I would like to thank all my well wishers who helped me directly or indirectly.

Finally, I would like to thank the divine figure of my life, my mother, Mrs. Rama Shahi, for all her efforts and sacrifices for making me what I am today. I would like to thank my younger brother for all his supports and love. We enjoyed a lot in our childhood time.

Abhishek Shahi

# Contents

# Summary

The importance of weak interactions between molecules to life and all parts of science and engineering is unquestionable and there have been an enormous interest in such interactions. Among all the weak interactions, hydrogen bonding is the most popular and it has enjoyed the most attention of the scientific community. Halogen bonding is gaining more popularity in the recent time, as its importance to biological molecules and crystal engineering has been recognized. In this work, a Pulsed Nozzle Fourier Transform Microwave spectrometer has been used to study the rotational spectra of molecules and hydrogen bonded complexes. Structural information is obtained from the rotational spectra. Ab initio electronic structure, Natural Bond Orbital (NBO) and Atoms in Molecules (AIM) theoretical methods have been used to characterize the weak intermolecular interactions, including hydrogen bonding, halogen bonding and lithium bonding.

In Chapter I, introduction to weak interaction is discussed. A brief introduction of different experimental and theoretical methods is presented.

Chapter II discusses in detail about the different methods used to investigate weak interaction, both experimentally and theoretically, in this work. In our lab, we use Pulsed Nozzle Fourier Transform Microwave spectrometer to determine the complexes spectra and structures. We generate MW radiation with the help of electronic devices and use Balle-Flygare cavity where molecular interaction takes place. We inject the sample inside the cavity in form of supersonic molecular beam through a pulsed nozzle, parallel to MW radiation. The detailed instrumental discussion about MW spectrometer has been done in this Chapter. We extensively use theoretical methods to probe weak bonding and characterize them. Ab initio and DFT calculations are used to optimize the structure of the complexes and predict their rotational spectra. Atoms in Molecules theory and Natural Bond Orbital theory are then used with the ab initio wave functions to understand the weak interactions in depth. Discussion about these methods and software used for the analysis will also be discussed.

In Chapter III, rotational spectrum of Hexafluoroisopropanol (HFIP) monomer is presented. HFIP is an interesting molecule as it offers many possibilities as hydrogen bond donor and

acceptor. It has the OH group which can both accept/donate a hydrogen bond and in addition it has a very acidic CH group. It is the only solvent that can dissolve polyethylene terephthalate, a normally difficult-to-dissolve polymer, and clearly it has unique interactions with this difficult to solve polymer. We have recorded and fitted rotational spectra of five different isotopologues of HFIP which helped us in determining its accurate structure. Though, it can exist in synclinical and antiperiplanar conformers, only the later has been detected in our molecular beam spectrometer. This happens to be the global minimum structure of HFIP. Combination of experimental observations and ab initio calculations provided many evidences which confirmed the presence of antiperiplanar conformer, experimentally. Since, the rotational constants for both conformers were very close, it was always challenging to pick up one conformer as experimentally observed structure. A prototype molecule, hexafluoroisobutene (HFIB) shows doubling of rotational transitions due to tunnelling/counter rotation of the two $CF_3$ groups through a small barrier. Interestingly, such motion has no barrier in HFIP and hence no splitting in transitions was observed. Potential energy surface calculated for counter-rotation of the two $CF_3$ groups is consistent with this observation. This barrier is different from eclipsed-staggered exchange barrier, observed by 60° counter rotation of both terminal $CF_3$ groups, for which the barrier height is very large and tunnelling cannot occur. The origin/lack of the small barrier in HFIB/HFIP has been explored using Natural Bond Orbital (NBO) method which helped in understanding intramolecular bonding in these molecules. Along with HFIB, other prototype molecules were also considered for the analysis e.g. hexafluoroacetone, hexafluoroacetone imine, hexafluoroisobutane, hexafluoroisopropylamine. In the last section of this Chapter, we have discussed the generalized behaviour of molecules which have $CF_3$-C-$CF_3$ groups.

In Chapter IV, rotational spectrum of HFIP•••$H_2O$ complex is presented. Aqueous solution of HFIP stabilizes α-helical structure of protein, a unique property of this solvent. The main objective of this Chapter is understanding the interaction between HFIP and $H_2O$. Microwave spectrum of HFIP•••$H_2O$ was predicted and recorded. Three isotopologues were investigated. Though, this complex could in principle have several structural conformers, detailed ab initio calculations predicted two conformers and only one was observed. Though,

the rotational constants for both structures were somewhat similar, lack of *a* dipole transitions, larger intensity of b-dipole transitions over c-dipole transitions and isotopic substitution analysis positively confirm the structure in which HFIP acts as the hydrogen bond donor. The linear O-H•••O hydrogen bond in HFIP-$H_2O$ complex is significantly stronger than that in water dimer with the H•••O distance of 1.8 Å. The other structure for this complex, not found in experiment is cyclic with both C-H•••O and O-H•••O hydrogen bonds, both of which are bent with H•••O distances in the range 2.2-2.3 Å. Both AIM and NBO calculations have been used to characterize the hydrogen bond in this complex.

In Chapter V, a comprehensive study on hydrogen bonding, chlorine bonding and lithium bonding have been done. A typical hydrogen bonded complex can be represented as A•••H-D, where A is the acceptor unit and H-D is the hydrogen bond donor unit. Many examples are known in literature, both experimentally and theoretically, in which the A-H-D bond angles are not linear. Deviation from linearity also results in the increase in A•••H bond lengths, as noted above for the two structures of HFIP•••$H_2O$ complex. Though this has been known for long, the distance between A and D being less than the sum of their van der Waals 'radii' is still used as a criterion for hydrogen bonding by many. Our group has recently shown the inappropriateness of van der Waals 'radii' and defined hydrogen bond 'radii' for various donors, DH and A. A strong correlation of DH hydrogen bond 'radii' with the dipole moment was noted. In this Chapter, we explored in detail the angular dependence of hydrogen bond 'radii'. Electron density topology around DH (D = F, Cl and OH) has been analyzed in detail and shown to be elliptical. For these molecules, the two constants for H atom treated as an ellipse have been determined. It is hoped that these two constants will be used widely in analyzing and interpreting H•••A distances, as a function of D-H•••A angles, rather than one 'radius' for H and acceptor atoms.

In Chapter VI, Detailed analysis and comparisons among hydrogen bond, chlorine bond and lithium bond, have been done. Hydrogen can be placed in group 1 as well as group 17 of the periodic table. Naturally, lithium bonding and halogen bonding have been proposed and investigated. There have been numerous investigations on the nature of hydrogen bonding and the physical forces contributing to it. In this Chapter, a total of one hundred complexes having H/Cl/Li bonding have been investigated using ab initio, AIM and NBO theoretical methods. Various criteria proposed in the literature have been examined. A new criterion has

been proposed for the characterization of closed shell (ionic/electrostatic) and open shell (covalent) interactions. It has been well known that the D-H bond weakens on the D-H•••A hydrogen bond formation and H•••A bond acquires a fractional covalency. This Chapter shows that for D-Li•••A complexes, the ionicity in D-Li is reduced as the Li•••A bond is formed This comprehensive investigation of H/Cl/Li bonding has led us to propose a conservation of bond order, considering both ionic and covalent contributions to both D-X and X•••A bonds, where DX is the X-bond donor and A is the acceptor with X = H/Cl/Li.

Hydrogen bond is well understood and its definition has been recently revised [Arunan et al. Pure Appl. Chem., Vol. 83, pp. 1619–1636, 2011]. It states "The X–H•••Y hydrogen bond angle tends toward 180° and should preferably be above 110°". Using AIM theory and other methods, this fact is examined and presented in Appendix A. In second part of appendix A, a discussion about calling $H_3^-$ complex as trihydrogen bond and its comparison with $FHF^-$ complex, is presented. In Appendix B, there is tentative prediction and discussion about the HFIP dimer. Condense phase studies show that HFIP have strong aggregation power to form dimer, trimer etc. During, HFIP monomer study, we have unassigned lines which are suspected to be from HFIP dimer. These are tabulated in the Appendix B as well.

# List of Abbreviations

| | |
|---|---|
| AIM | Atoms in Molecules |
| BCP | Bond Critical Point |
| BSSE | Basis Set Superposition Error |
| FID | Free Induction Decay |
| HFA | Hexafluoroacetone |
| HFIB | Hexafluoroisobutanol |
| HFIP | Hexafluoroisopropanol |
| MW | Microwave |
| NBO | Natural Bond Orbital |
| PNFTMW | Pulsed Nozzle Fourier Transform Microwave Spectrometer |
| RCP | Ring Critical Point |
| RF | Radio Frequency |
| SPDT | Single Pole Double Throw |
| SSBM | Single Side Band Mixer |
| ZPE | Zero point (vibrational) Energy |

# *List of Tables*

# *List of Figures*

# Chapter I. Introduction

## I.1. Intermolecular Interactions

Intermolecular interactions became popular when we realized their usefulness in our daily life. Nature has imbedded these interactions in biological and chemical systems very cleverly. Hydrogen bonding is the most important intermolecular interaction. It is responsible for the liquid state of water and also holds the two strands of DNA in the double helical structure.

Intermolecular interactions are also responsible for many physiological phenomena. These interactions are often utilized to design different macromolecules. Different names have been given to intermolecular interaction like non-covalent interaction, closed shell interaction, weak interaction, van der Waals interaction etc. These interactions are important to life and are complicated in nature, and no surprise that there have been numerous studies on these in the last two decades. Covalent bonding is almost a closed chapter because it is now well established and understood. However, intermolecular interactions are far from being completely understood and both theoreticians and experimentalists are continuously introducing new concepts and methods for it.

According to the ideal gas law, non-interacting gas particles or molecules follow the equation PV=nRT. This law was first given by Clapeyron as a combination of Boyle's and Charles's laws.[1] This assumption of 'non-interacting gas particle' indicates that they had some idea that some interaction might be present between two gas molecules which they did not understand at that time. Later, in 1873, van der Waals introduced his famous gas equation in which he included the terms corresponding to the attractive interactions between the gas molecules.[2] The understanding of intermolecular interactions, particularly hydrogen bond, began at the start of 19$^{th}$ century. Huggins (1919) was the first person who suggested the idea of hydrogen bonding and shortly after him this idea was advanced by Latimer and Rodebush (1920). There was a 10 years gap (1920-1931) for the further development of the understanding of hydrogen bond because community was enjoying quantum theory during this period. In 1931, Pauling interpreted the structure of $[FHF]^-$ ion the term 'Hydrogen Bridge' was used by Huggins. The first book on hydrogen bonding was written by Pimental and McClellen (1960).[3] Hydrogen bond is a chapter in Pauling's famous book[4] '*The Nature of the Chemical Bond*' (1939, 1940, 1960) which introduces the concept of hydrogen bond to the scientific

community. Another good book which discusses about the hydrogen bond is *Coulson's Valence*[5] revised by McWeeny and. Coulson.

Huggins termed 'hydrogen bond' as 'hydrogen bridge' because it was initially assumed to be 'simple electrostatic interaction' between two dipoles[6]. Pauling estimated about 5% covalency in O-H•••O hydrogen bond[4]. In Coulson's book[5], it is considered that electrostatic interaction is mainly responsible for intermolecular interactions, it says that *"these (induced dipole, van der Waals dispersion forces) are small points, and do not seriously disturb our conclusion that the bonds are essentially electrostatic in origin"* but after comparing the weightage of different resonance structures of strong hydrogen bonded complexes, they concluded that *"these short hydrogen bonds (β-form of oxalic acid) are not so completely electrostatic as the long ones."* However, some sources still consider hydrogen bonding as purely electrostatic[7].

Non-covalent interactions are simply used for those interactions which are not covalent.[8,9] Therefore, ionic and metallic bonds could also be considered as non-covalent interactions which are mostly much stronger than even the covalent bonds. Closed-shell interaction is another term used for the same. After observing covalency in intermolecular interactions,[4,5,10–14] it is important to rethink about calling it non-covalent. Both physical forces (polarization, exchange) and chemical bonding (VB approach) support the presence of covalency in the intermolecular interactions.

There are different types of intermolecular interactions. Hydrogen bond is the most popular one and enjoys much of the attention of the scientific community. Halogen bonding can be placed at the second position in terms of popularity. However, there are many more different types of intermolecular interactions which have been identified more recently and are discussed in the next few paragraphs. We can denote these complexes as A•••X-D where A is the acceptor which accepts the X-bonding and D is a part of donor which is covalently (or ionically) bonded with the X atom. For hydrogen bond X would be H, for halogen bond X would be a halogen atom and so on.

## I.1.1. Hydrogen Bond

Hydrogen bonding is the first detected intermolecular interaction and is comparatively well understood now. In the complex A•••H-D, D can be an atom or a part of molecule whose

electronegativity should be more than that of hydrogen. Electronegative nature of D part creates a partial positive charge on hydrogen which interacts with the electron rich part of the A. The acceptor A, can be atoms with lone pair of electrons ($NH_3$, $H_2O$), a source of π-electrons (benzene), a source of single electron ($CH_3$ radical), a source of σ-electrons ($H_2$), an electron rich region of a molecule (tetrahedral face of $CH_4$) and even an atom (like Argon). An example of hydrogen bond, Water dimer ($H_2O$•••H-OH) is presented in Figure I. 1 with the average charge on each atoms calculated by Atoms in molecule (AIM) theory (see Chapter VI for more information about calculation).

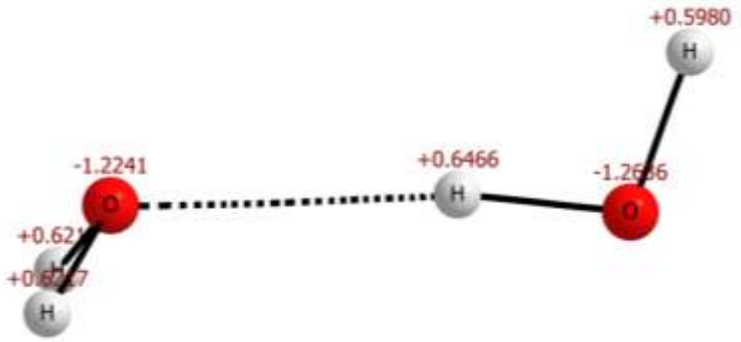


*Figure I. 1. Structure of water dimer at MP2(full)/aug-cc-PVTZ.*

As evident from this structure, hydrogen bonding is beyond dipole-dipole interaction. Contribution of covalency depends on the nature of A and D. Coulson named such contacts as short hydrogen bond[5] and mentioned that the weak hydrogen bonds are more appropriate to follow pure electrostatic model. Recently, Arunan et al.[13] have given a much broader and inclusive definition of hydrogen bond. Experiments for the detection of hydrogen bonds are touching new heights day by day. Last year, it has been shown that *Atomic Force Microscopy (AFM)* could be used to visualize the hydrogen bonds[15]. More recently, using 2D-IR spectroscopy, the effect of hydrogen bonding on intermolecular vibrational coupling in N-methylacetamide dimer has been observed[16]. Detailed discussion about the hydrogen bond and its properties are discussed in *Chapters IV to VI* of this thesis.

## I.1.2. Dihydrogen and Trihydrogen Bond

Now dihydrogen and trihydrogen bonds have also been proposed. The dihydrogen bond can be represented as M-$H^2$•••$^1$H-D ($^1$ and $^2$ are the labels to distinguish the two hydrogens). Here

[1]H-D is the donor part and it is the same as in the hydrogen bond case. M denotes a metal, which donates its electron to H[2]-atom and makes it a hydride (Figure I. 2) which facilitates the bonding with electron deficient hydrogen of H-D. Dihydrogen bonds are gaining popularity and a book has already been published on this interaction[17]. In 2011, a new interaction, trihydrogen bond ($H^-$•••H-H) was introduced[18]. Authors claimed it to be a new bond, and according to them such a structure (Figure I. 2) was unexpected. If we closely observe the structure of the $H^-$•••H-H complex, it is similar to $X^-$•••H-H, where $X^-$ may be negative charge atom (like $Cl^-$, $F^-$ or $Br^-$). The $F^-$•••H-H complex has been observed experimentally[19] and is not different from ($H^-$•••H-F) in many aspects. The detailed discussion comparing the so called trihydrogen bonds with the interaction in the $F^-$•••H-F complex has been presented in appendix A.

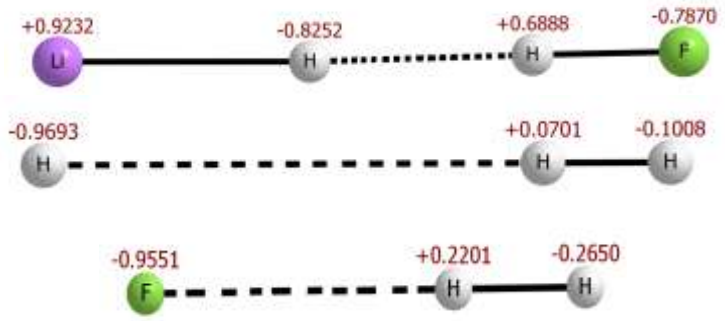


*Figure I. 2. Structure of dihydrogen bonding, trihydrogen bonding and $F^-$•••H-H complexes (from top to bottom) at MP2/6-311++G**.*

## I.1.3. Halogen Bonding

Halogen bonding is the second most popular intermolecular interaction and was first mentioned by Hassel in his Nobel lecture[20]. Benesi and Hildebrand (1949)[21] observed the halogen bond using UV-Vis spectroscopy. This interaction is often utilized in the crystal engineering and supramolecular chemistry. Halogen bonding can be represented as A•••X-D where X is a halogen atom and A is the halogen bond acceptor. In the case of hydrogen bond, hydrogen should have a partial positive charge. However, in the case of halogen bond, the charge on the halogen appeared not so important as both ClF and $Cl_2$ could form halogen bonded A•••ClF/$Cl_2$ complexes. Concept of electron deficient 'σ-hole' on halogen atoms can explain their interaction with another electron rich centre and thus the formation of halogen bonding.[22] The σ-hole is a region of positive electrostatic potential on the electron density

surface of halogen in the opposite direction of its directly bonded atom (D). This positive electrostatic potential interacts with the negative electrostatic site of the acceptor A. Initially, on the basis of available experimental data and chemical intuition, it was assumed that F atom cannot act as a halogen bond donor.[23] Later, Guru Row et al. published an experimental result which confirmed the presence of positive electrostatic site on fluorine and showed that fluorine can act as the halogen bond donor.[24] Recently, IUPAC has redefined halogen bonding.[25] An example of halogen bonding ($H_2O$•••Cl-OH) is presented in Figure I. 3.

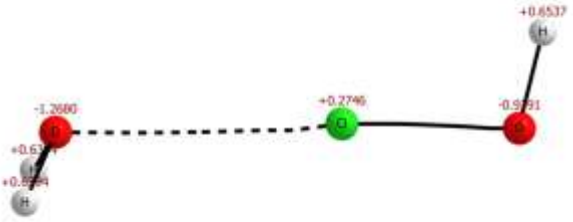


*Figure I. 3. Structure of halogen bonding at MP2/6-311++G**.*

## I.1.4. Lithium Bonding

Lithium bonding can be represented as A•••Li-D. It is the strongest interaction among all the A-X•••D interactions considering the same A and D. It is because the Li-D molecules have much larger dipole moment than H-D or Cl-D (where D=F/Cl/Br etc.) molecules. A•••Li bond is very close to being a pure electrostatic interaction. An example of lithium bonding ($H_2O$•••Li-OH) is presented in Figure I. 4.

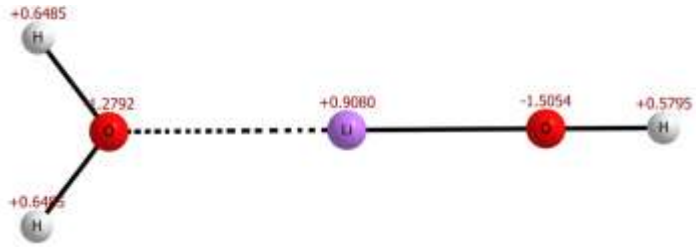


*Figure I. 4. Structure of lithium bonding at MP2(full)/aug-cc-PVTZ.*

## I.1.5. Chalcogen Bonding

Chalcogen bonds are the intermolecular interactions in which atoms of group VI act as electrophilic site i.e. S•••O, S•••Se or S•••Cl types of interactions. Chalcogen bonds can be

represented as A•••Chal-D. These interactions are similar to halogen bonds and are also termed as sister halogen bond[26]. In Figure I. 5, the chalcogen bonded complex $F_2C{=}S{\bullet\bullet\bullet}Cl^-$ is shown.[26] Like halogen bonding, chalcogen bonding can also be explained using the σ-hole concept.

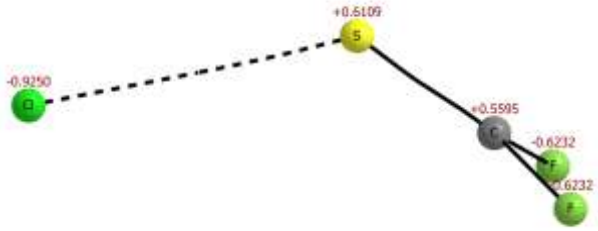


*Figure I. 5. Structure of Chalcogen bond at MP2/6-311++G**.*

## I.1.6. Agostic Bonding

Agostic bond is an interaction between metal (M) and C-H bond. It can be represented as M•••H-C. Initially it was defined as a covalent bond between H and the metal atom. It was considered that C-H donates a pair of electron to metal and forms a bond through hydrogen (see Figure I. 6(a)). It was considered as a 3c-2e bond like diborane. Later, in a review,[27] agostic bond was redefined stating "*agostic interactions are characterized by the distortion of an organometallic moiety which brings an appended C-H bond into close proximity with the metal center*"(Figure I. 6(b)) Many important reactions in organometallic chemistry proceed via agostic bonded intermediates where different stages of agostic bonds are involved. Examples of such reactions are hydroformylation,[28] Ziegler–Natta polymerization[29] and the activation of C-H bonds.[30]

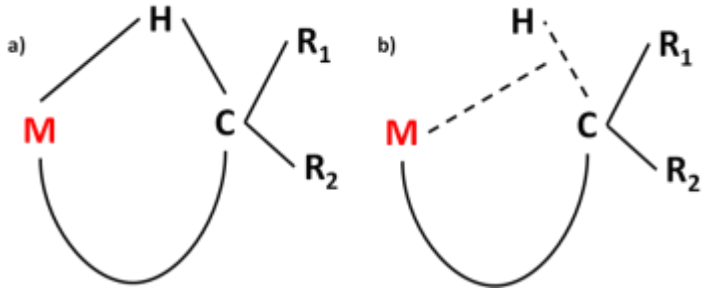


*Figure I. 6. Two models for agostic bonding.*

## I.1.7. Pnicogen Bonding

P•••N interaction is another new interaction which was proposed recently (2011) and is termed as a pnicogen bond.[31–35] There is direct interaction between P and N (Figure I. 7). This interaction is different in nature from other intermolecular interactions. In case of pnicogen bonded $H_3N•••PH_3$ complex, the lone pair orbital of phosphorus interacts with the σ*(N-H) orbital and the lone pair orbital of nitrogen interacts with the σ*(P-H) orbital. Both the antibonding orbitals σ*(N-H) and σ*(P-H) are in the direction of intermolecular bond path. Stabilization because of the l.p.(N)- σ*(P-H) interaction is more. Therefore, substitution on phosphorus affects the strength of the pnicogen bonding more than the substitution on nitrogen. Substitution of the hydrogen atom, which is aligned opposite to the bond path, with fluorine leads to a strong stabilization of the complex and its binding energy increases nearly fourfold (from 35.11 to 137.94 kJ/mol). Multiple substitution or substitution with Cl- or Br-atoms does not affect the binding energy much.[33] The structure of $H_3N•••PH_3$,[33] the first example of this interaction, is presented in Figure I. 7. In the figure, charges given are results from this work.

## I.1.8. Carbon Bonding

Carbon bonding has been proposed by Mani and Arunan in 2013.[36] It may be written as A•••C-D where C is a tetravalent C-atom. Tetrahedral face of methane has an electronegative centre and acts as hydrogen bond acceptor.[37] However, substitution of hydrogen with F (or some other electronegative atoms) makes the opposite tetrahedral face electropositive which can interact with electron rich centres. These complexes are like entrance and exit channel complexes of $S_N2$ reaction. We can say that agostic interaction and carbon bonding are good examples of prereactive complexes,[38] like hydrogen bond, which is a prereactive complex in proton transfer reaction. An example, $H_2O•••CH_3F$ is presented in Figure I. 8.

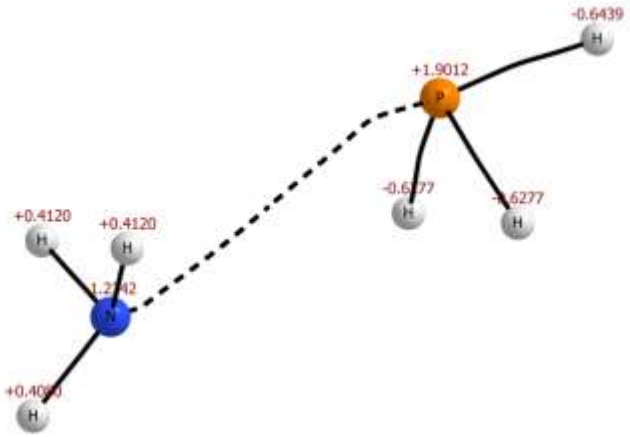


*Figure I. 7. Structure of $H_3P$•••$NH_3$ bonding at MP2/6-311++G**.*

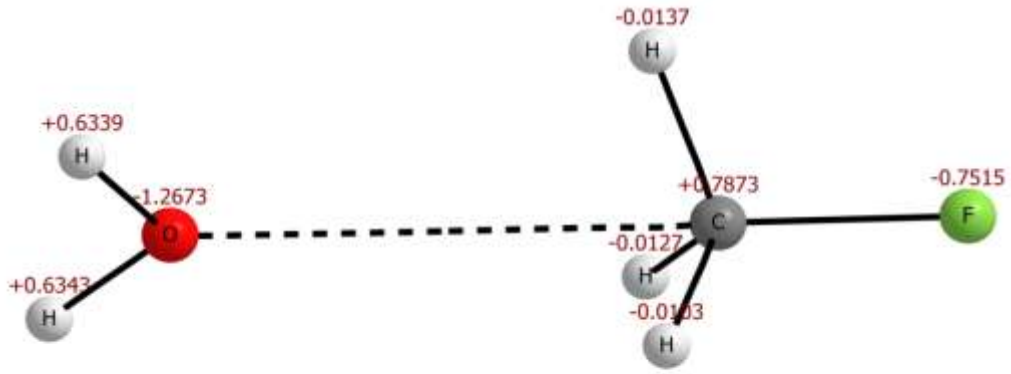


*Figure I. 8. Structure of Carbon bonding.*

## I.2. Theoretical and Experimental Methods

### I.2.1. Theoretical Methods

There are different purposes for performing ab initio calculations for intermolecular complexes. These can be to know about its binding energy, vibrational frequencies, geometrical parameters, rotational constants, nature of bond etc. Rotational constants and vibrational frequency calculations guide rotational and vibrational spectroscopic experiments, respectively. Different methods are used to get the optimum geometry for the complexes. These are molecular mechanics, semiempirical, Hartree-Fock (HF, ROHF, UHF),

post-Hartree-Fock (Moller-Plesset perturbation theory (MPn, where n=2-5)[39–42], DFT methods etc. Ab initio and DFT methods are used along with some basis sets. Ab initio calculations like MPn methods have very high computational cost which increases with the size of basis sets used. DFT methods are comparatively faster.

Natural Bond Orbital (NBO)[43] theory gives useful information about the nature of bonding. One of the most important information is second order perturbation energy, E(2). It is defined as the stabilization energy due to overlap between filled donor and vacant acceptor orbitals. Energy decomposition analysis is also possible by NBO theory and it is called as natural energy decomposition analysis (NEDA)[44]. Ionic and covalent character of a bond (inter or intramolecular) can also be estimated using the natural resonance theory (NRT)[45] which is inbuilt in the recent version, NBO 6.0,[46] of the program.

Atoms in Molecules (AIM)[47] theory is often helpful in identification and characterization of the intermolecular interaction. Electron density is the key information we get from this analysis. Topological analysis of this electron density results in the identification of different critical points, one such point being the bond critical point (BCP). The presence of BCP between two atoms and bond paths connecting the BCP to the atoms indicate interaction between the two atoms. This analysis also gives atomic properties of each atom inside a molecule. This method has been very successful so far and we have used it extensively in our study.

## I.2.2. Experimental Methods

Isolated weakly bound complexes can be produced in supersonic expansions using molecular beam technique. In such conditions, the spectra are highly simplified and the resolution is much better than condense phase or highly pressurized gas phase. For such gas phase studies, quantum chemical calculations are usually in quite good agreement with the experimental results. Different spectroscopy techniques such as IR, NMR, microwave etc. can be used to probe weak intermolecular interactions. Red-shift in the stretching frequency of the X-D bond is usually a direct probe of the strength of the A•••X-D weak interaction. However, some complexes with blue shift in the X-D stretching frequency upon complex formation are also known.[48–51] Due to the very high resolution of the available lasers, rotational features of the vibrational bands can easily be identified. Recently, in one such study tunable far IR

laser vibrational-rotational tunneling spectrometer[52] was used for the detection of water hexamer structure.[53] The spectral range of this spectrometer is 20-150 $cm^{-1}$ and it allows studying the transitions between vibrational and rotational energy levels. Besides structural information, dynamics of the hydrogen bonding can also be observed by using 2-D IR spectroscopy. Recently, effect of hydrogen bond on the intermolecular vibrational coupling has been observed.[16] N-methylacetamide molecule was used as an example and its dimer was observed as a hydrogen bonded complex. There was strong correlation between N-H and C=O oscillator, which changed significantly after complex formation.

In NMR technique, hydrogen peak shifts down-field if it is involved in hydrogen bonding. With the help of 2D-NMR, direct detection of hydrogen bond has been done.[54] In this experiment, J-coupling across the hydrogen bond was observed for a solid sample (N-{[[5-(phenylamino)methylene]-1,3-cyclopentadien-1-yl]methylene}-1,2,4-triazole-4-amine). This gives direct evidence for covalency in hydrogen bond. Hydrogen bond strength was observed qualitatively by using chemical shift and quadrupole coupling constants[55] and hydrogen bond length can also be measured quantitatively from dipolar coupling.[56]

There are some other techniques which are used for detecting hydrogen bonding and other weak interactions e.g. resonance-enhanced multiphoton ionisation (REMPI), hole burning spectroscopy, zero electron kinetic energy (ZEKE) spectroscopy etc. Review article by Muller-Dethlefs and Hobza discusses these methods in more detail.[8]

Hydrogen bonding in solid phase can also be observed by using different techniques. Recently, with the help of non-contact atomic force microscopy (NC-AFM), it has been possible to visualize the hydrogen bond formed between 8-hydroxyquinoline molecules (dimer) on the surface of Cu(111) face[15]. Direct structural and conformational information has been observed because this technique gives the resolution at atomic level. Carbon bonding has been proposed by Mani and Arunan[36] recently, and has also been observed experimentally by Guru Row *et. al*.[57]

Microwave spectroscopy has been used as the experimental technique for the work given in this Thesis. Brief introduction of this technique is given in the next section. Chapter II gives details of our home-built microwave spectrometer.

## I.3. Microwave Spectroscopy

### I.3.1. Introduction

Rotational levels in a molecule are quantized. Molecules can be divided into following four categories based on their principal moment of inertia, $I_a$, $I_b$ and $I_c$ along three principal axes *a*, *b* and *c* respectively.

a) Linear Top: ($I_a = 0$ $I_b = I_c$) ($CO$, $CO_2$)

b) Spherical Top: ($I_a = I_b = I_c$) ($CH_4$)

c) Symmetric Top: Two types.

   a) Prolate: ($I_a \leq I_b = I_c$)($CH_3Cl$)

   b) Oblate: ($I_a = I_b \leq I_c$) ($BF_3$)

d) Asymmetric Top: ($I_a < I_b < I_c$) ($H_2O$)

To observe the pure rotational spectrum of a molecule, it should possess a permanent dipole moment. Though, pure rotational transitions have been recorded for spherical top molecules (e.g $CH_4$) which possesses a small electrical dipole moment induced by distortion.[Oldani el al. *J. Mol. Spectrosc. 110*, 93-105, 1985] Moreover, homonuclear diatomic molecules give pure rotational Raman spectra because of the polarizability change during the rotation.

Rotational energy levels of a molecule can be calculated by solving the Schrödinger equation for rotational Hamiltonian. Detailed process of solving this Hamiltonian is given text books.[58,59] Under rigid rotor approximation, energy of a diatomic molecule is given by

$$E = B\,J(J+1)$$

Where, $B = (h^2/8\pi^2 I)$ and $I = \mu r^2$

B is the rotational constant of diatomic molecule, I is the moment of inertia, $\mu$ is its reduced mass and J is rotational quantum number. The above equation is for rigid rotor, but none of the molecules are perfect rigid rotors since molecular bonds stretch and bend (in case of polyatomic molecules) during rotation due to the centrifugal effects. Due to centrifugal stretching, the average bond distance, r, increases which results in decrease in the rotational

constant (B). Therefore, an extra term corresponding to the centrifugal distortion should be introduced in the above equation:

$$E = B\,J(J+1) - D_J\,[J\,(J+1)]^2$$

This term $D_J$ is called centrifugal distortion constant which is directly related to the vibration and rotation of the molecule. For the linear and symmetric top molecules analytical equations can be obtained by solving the Schrödinger equation. However, for the asymmetric molecules analytical solutions cannot be obtained. The details can be found in the book by Gordy and Cook.[58]

## I.3.2. Spectral Pattern

For symmetric top molecules spectral pattern is comparatively simple and for each of the J→J+1 transition a total of J+1 signals are observed which correspond to different values of K. The K is the projection of J on the molecular fixed symmetry axis, *a*-axis for the prolate top and *c*-axis for the oblate top molecules. Typical transition patterns for a prolate symmetric top molecule are shown in the Figure I. 9. In the absence of an external field, selection rules for the symmetric top molecules are $\Delta J = 0, \pm 1$, $\Delta K = 0$ and $\Delta M = 0$.

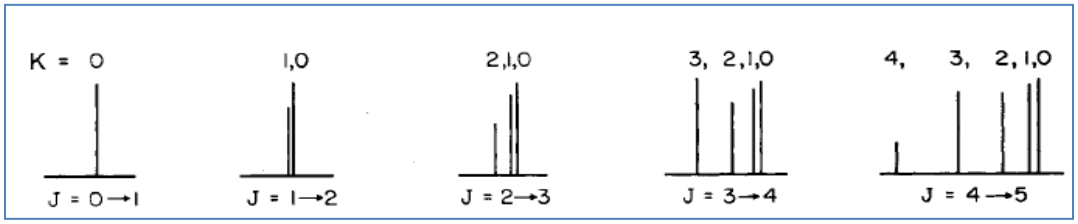


*Figure I. 9. Spectral pattern for a prolate symmetric top molecule.*[58]

For the asymmetric molecules, no two rotational constants are equal. Asymmetry in the molecules can be defined using Ray's parameter,κ, which is equal to (2B-A-C)/(A-C). For prolate and oblate symmetric top molecule κ is -1 and +1, respectively. Prolate and oblate tops are limiting cases for the asymmetric top molecules. For the asymmetric top molecules, κ value is in between -1 and +1. If the value of κ is close to -1 (say -0.98), spectral pattern of the molecule will be close to the spectral pattern of a prolate symmetric top molecule.

Energy levels for an asymmetric top molecule can be represented as $J_{K-1,\ K+1}$ where $K_{-1}$ and $K_{+1}$ are the 'K' quantum numbers for the limiting prolate and oblate top respectively. Selection rules for the asymmetric top molecules are as follows

| Transition | Selection rule |
|---|---|
| *a*-type | $\Delta J = 0, \pm1, \Delta K_a = 0; \Delta K_c = \pm1$ |
| *b*-type | $\Delta J = 0, \pm1, \Delta K_a = \pm1; \Delta K_c = \pm1$ |
| *c*-type | $\Delta J = 0, \pm1, \Delta K_a = \pm1; \Delta K_c = 0$ |

Qualitative estimation of the asymmetric top energy levels can be made by correlating the two energy levels of the limiting cases, prolate top and oblate top, as shown in the Figure I. 10. On X-axis, κ-values are taken and it varies from -1 to +1 as the values of rotational constants change. Any molecule falling in between this region is an asymmetric top. On the left side Y-axis, rotational energy levels of the prolate molecule is plotted for A=3 and B=C=1. Similarly, on the right side Y-axis, rotational energy level of oblate molecule is plotted for A=B=3 and C=1. At the center, where κ=0, rotational energy levels is plotted for the A=3, B=2 and C=1. This figure is adapted and redrawn from the book by Gordy and Cook.[58]

## I.3.3. Internal Rotation

Concept of internal rotation can be understood easily by the example of ethane molecule. In this molecule, the two $CH_3$ groups rotate with respect to each other. This rotation is not free and two extreme conditions arise, eclipse and staggered. In the eclipse form, H-C-C-H dihedral angle is zero and in the staggered form, it is 60°. Internal angular momentum arising due to such internal motions couples with the overall angular momentum of the molecule and leads to the splitting in the rotational transitions. Magnitude of the splitting depends upon the barrier height for the internal rotation. And the splitting pattern depends on the local symmetry of the internal rotor. Measuring the splitting in the transitions due to internal motion, barrier height corresponding to the motion can be calculated. For the free rotation there would be no splitting and for very high barrier height, splitting will be too small to be observed. Accuracy of barrier height estimations done in this way, are up to 5% or better.

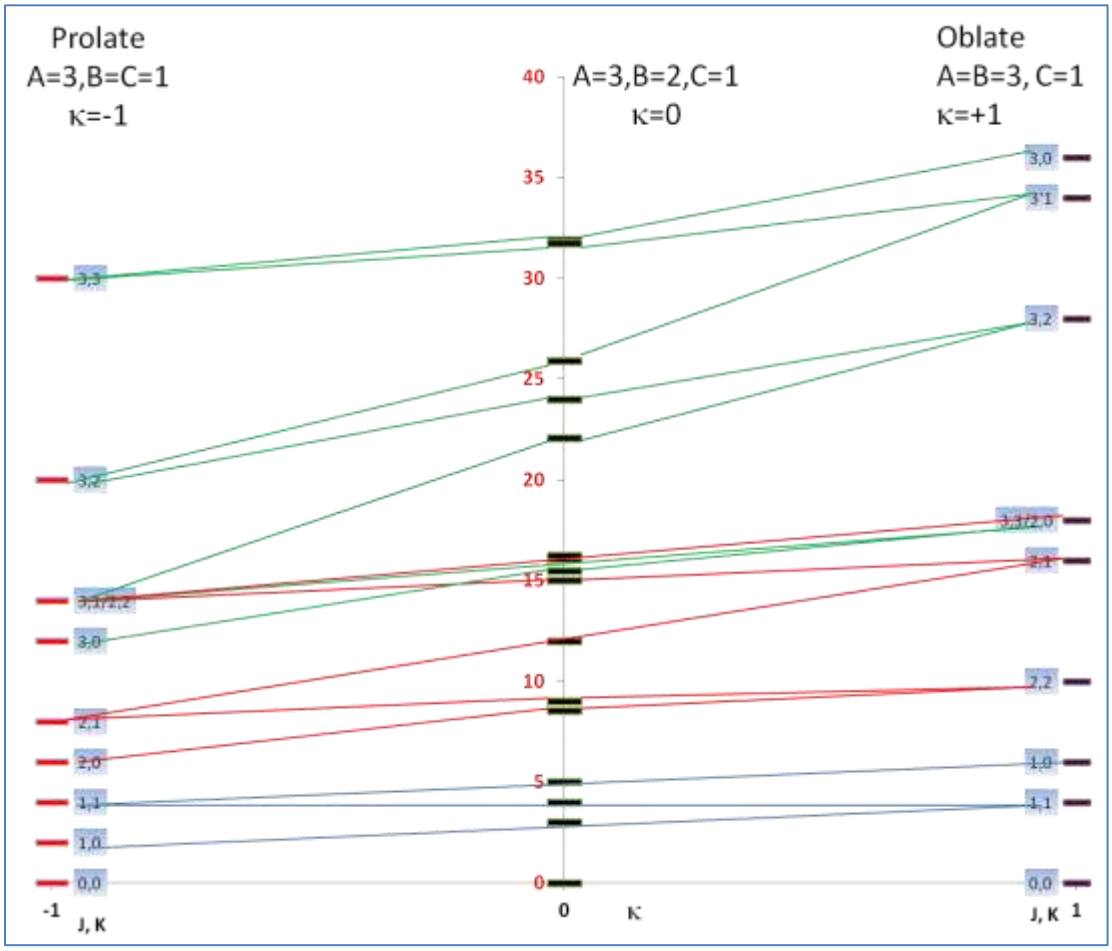


*Figure I. 10. Spectral pattern of asymmetric top.*

## I.3.4. Quadrupole Coupling Constant

Nuclear quadrupole moment describes effective shape of a nucleus. If the value of nuclear spin (I) is 0 or ½ , its shape is spherical and I ≥ 1 implies an ellipsoidal nucleus. Nuclear quadrupole moment of the nuclei with I ≥ 1 interacts with the electric field gradient of the molecule and gives rise to the hyperfine splitting in rotational transitions. Nuclei with spin 0 or ½ do not show hyperfine splitting. Fitting the hyperfine split rotational transitions to a suitable Hamiltonian one can obtain the nuclear quadrupole coupling constants. These constants give information about the electronic structure of the molecule. For example, the $^{35}$Cl nuclear quadrupole coupling constant for HCl and KCl are -67.819 and < -0.04 MHz, respectively. High value of the quadrupole coupling constant (-67.819 MHz) for HCl indicates a non-spherical electronic distribution around chlorine and its very low value (-0.04 MHz) in case of KCl indicates an almost spherical electronic distribution around chlorine.

This confirms that HCl bond has a very high covalent character and KCl bond has a very high ionic character.

### I.3.5. Microwave Spectrometers

Cavity based Fourier transform microwave spectrometer combined with molecular beam technique have very high resolution and sensitivity. Its sensitivity is so high that even the C-13 isotopologues can be probed in natural abundance. Signal resolution is very high for such spectrometer (about 4-6 kHz for our spectrometer). With such a high resolution spectral features like splitting due to internal rotation and nuclear quadrupole coupling can easily be resolved. Using different variants of the nozzle design various transient species like ions and radicals[60] as well as their complexes can be generated and studied using such spectrometers. Recently microwave spectroscopy using molecular beam cavity spectrometers has been used to observe chirality of a molecule.[61]

In our lab, we use a home-built Pulsed Nozzle Fourier Transform Microwave Spectrometer (PN-FTMW). The details of our spectrometer are presented in the Chapter II.

High resolution of these cavity based spectrometers comes with a cost and the high Q-factor of these cavities seriously limits its band width. In most of the frequency regions, only 1 MHz spectral width can be observed at a time which makes the experiments very time consuming. This limitation of the cavity based spectrometers has recently been overcome by the development of chirped pulse spectrometers, first developed by Pate's group.[62] These spectrometers have very high band width (11 GHz in case of Pate's spectrometer). Now almost every microwave group is updating their lab with one such spectrometer.[63] We are also planning to build a new chirp pulse based microwave spectrometer which will have the pulse width of 1 GHz and will cover the range of 1-12 GHz.[64,65] Now economic chirped pulse spectrometers are also available and are being introduced in the undergraduate labs.[66]

## I.4. Present Investigations

In this Thesis, study of monomer and weakly bound complexes has been done using microwave spectrometer and various theoretical methods. In Chapter II, instrumental details about our spectrometer are presented. In Chapter III, microwave spectroscopic study of

hexafluoroisopropanol (HFIP) and its comparison with its prototype hexafluoroisobutene (HFIB) have been reported. Five isotopologues (two deuterium and three C-13) of HFIP have been observed which helped in determining the structure of HFIP. In Chapter IV, microwave spectroscopic study of HFIP•••water complex and its two isotopologues has been presented. AIM and NBO theoretical methods have been used to characterize the intermolecular bonding. In Chapter V, a detailed discussion on the hydrogen bond radii and its angular dependence have been presented. Finally in Chapter VI, a comprehensive study on three intermolecular interactions has been done. These intermolecular interactions are hydrogen bonding, halogen bonding and lithium bonding. Using AIM and NBO methods, we have shown that there is bond conservation on complex formation and nature of bonding greatly depends on the nature of bond donor.

## I.5. References:


1. R. B. Thompson, *Illustrated Guide to Home Chemistry Experiments: All Lab, No Lecture*, O'Reilly Media, 2012.

2. J. D. van der Waals, *Doctoral Dissertation*, Leiden, 1873.

3. G. C. Pimentel and A. L. McClellan, *The Hydrogen Bond*, W. H. Freeman and Co., San Fransisco, 1960.

4. L. Pauling, *The Nature of the Chemical Bond and the Structure of Molecules and Crystals; An Introduction to Modern Structural Chemistry*, Cornell University Press, Ithaca, New York, 1960.

5. R. McWeeny and C. A. Coulson, *Coulson's Valence*, Oxford University Press, 3 Eddition., 1961.

6. M. L. Huggins, *J. Phys. Chem.*, 1936, **40**, 723–731.

7. J. N. Israelachvili, *Intermolecular and Surface Forces*, Academic Press, Third Edit., 2011.

8. K. Müller-Dethlefs and P. Hobza, *Chem. Rev.*, 2000, **100**, 143–68.

9. P. Hobza and K. Müller-Dethlefs, *Non-Covalent Interactions Theory and Experiment*, The Royal Society of Chemistry, Cambrdge, 2010.

10. S. J. Grabowski, *Chem. Rev.*, 2011, **111**, 2597–625.

11. E. D. Isaacs, A. Shukla, P. M. Platzman, D. R. Hamann, B. Barbiellini, and C. A. Tulk, *Phys. Rev. Lett.*, 1999, **82**, 600–603.

12. E. D. Isaacs, A. Shukla, P. M. Platzman, D. R. Hamann, B. Barbiellini, C. A. Tulk, B. Laboratories, L. Technologies, and M. Hill, *J. Phys. Chem. Solids*, 2000, **61**, 403–406.

13. E. Arunan, G. R. Desiraju, R. A. Klein, J. Sadlej, S. Scheiner, I. Alkorta, D. C. Clary, R. H. Crabtree, J. J. Dannenberg, P. Hobza, H. G. Kjaergaard, A. C. Legon, B. Mennucci, and D. J. Nesbitt, *Pure Appl. Chem.*, 2011, **83**, 1619–1636.

14. A. Shahi and E. Arunan, *Phys. Chem. Chem. Phys.*, 2014, **16**, 22935-52.

15. J. Zhang, P. Chen, B. Yuan, W. Ji, Z. Cheng, and X. Qiu, *Science*, 2013, **342**, 611–4.

16. L. De Marco, M. Thämer, M. Reppert, and A. Tokmakoff, *J. Chem. Phys.*, 2014, **141**, 034502.

17. V. I. Bakhmutov, *Dihydrogen bonds*, Wiley Interscience, John Wiley & Sons, Inc., Hoboken, New Jersey, 2008.

18. C. F. Matta, L. Huang, and L. Massa, *J. Phys. Chem. A*, 2011, **115**, 12451–8.

19. D. A. Wild, R. L. Wilson, Z. M. Loh, and E. J. Bieske, *Chem. Phys. Lett.*, 2004, **393**, 517–520.

20. "Odd Hassel - Facts". Nobelprize.org. Nobel Media AB 2013. Web. 18 Jan 2014. <http://www.nobelprize.org/nobel_prizes/chemistry/laureates/1969/hassel-facts.html>, .

21. H. A. Benesi and J. H. Hildebrand, *J. Am. Chem. Soc.*, 1949, **71**, 2703.

22. P. Politzer, P. Lane, M. C. Concha, Y. Ma, and J. S. Murray, *J. Mol. Model.*, 2007, **13**, 305–11.

23. T. Clark, M. Hennemann, J. S. Murray, and P. Politzer, *J. Mol. Model.*, 2007, 291–296.

24. V. R. Hathwar and T. N. Guru Row, *Cryst. Growth Des.*, 2011, **11**, 1338–1346.

25. *XB Halogen bonding*, http://www.halogenbonding.eu/, Web. 16 July 2014.

26. W. Wang, B. Ji, Y. Zhang, and C. Bond, 2009, 8132–8135.

27. W. Scherer and G. S. McGrady, *Angew. Chem. Int. Ed. Engl.*, 2004, **43**, 1782–806.

28. C.-F. Huo, Y.-W. Li, M. Beller, and H. Jiao, *Organometallics*, 2003, **22**, 4665–4677.

29. W. E. Piers and J. E. Bercaw, *J. Am. Chem. Soc.*, 1990, **112**, 9406–9407.

30. J. A. Labinger and J. E. Bercaw, *Nature*, 2002, **417**, 507–14.

31. U. Adhikari and S. Scheiner, *Chem. Phys. Lett.*, 2011, **514**, 36–39.

32. M. Solimannejad, M. Gharabaghi, and S. Scheiner, 2011, **024312**, 1–6.

33. S. Scheiner, *J. Chem. Phys.*, 2011, **134**, 094315.

34. S. Scheiner, *Chem. Phys.*, 2011, **387**, 79–84.

35. S. Scheiner, *J. Chem. Phys.*, 2011, **134**, 164313.

36. D. Mani and E. Arunan, *Phys. Chem. Chem. Phys.*, 2013, **15**, 14377–83.

37. B. Raghavendra and E. Arunan, *Chem. Phys. Lett.*, 2008, **467**, 37–40.

38. A. Legon, *Angew. Chem. Int. Ed. Engl.*, 1999, **38**, 2686–2714.

39. M. Head-Gordon, J. A. Pople, and M. J. Frisch, *Chem. Phys. Lett.*, 1988, **153**, 503–506.

40. J. A. Pople, J. S. Binkley, and R. Seeger, *Int. J. Quantum Chem.*, 2009, **10**, 1–19.

41. K. Raghavachari, J. A. Pople, E. S. Replogle, and M. Head-Gordon, *J. Phys. Chem.*, 1990, **94**, 5579–5586.

42. R. Krishnan and J. A. Pople, *Int. J. Quantum Chem.*, 1978, **14**, 91–100.

43. A. E. Reed, L. A. Curtiss, and F. Weinhold, *Chem. Rev.*, 1988, **88**, 899–926.

44. E. D. Glendening and A. Streitwieser, *J. Chem. Phys.*, 1994, **100**, 2900.

45. E. D. Glendening and F. Weinhold, *J. Comput. Chem.*, 1998, **19**, 593–609.

46. E. D. Glendening, J. K. Badenhoop, A. E. Reed, J. E. Carpenter, J. A. Bohmann, C. M. Morales, C. R. Landis, and F. Weinhold, *NBO6.0*, 2006.

47. R. F. W. Bader, *Atoms in Molecules: A Quantum Theory*, Oxford University Press, Oxford, 1990.

48. J. Joseph and E. D. Jemmis, *J. Am. Chem. Soc.*, 2007, **129**, 4620–32.

49. P. Hobza and Z. Havlas, *Chem. Rev.*, 2000, **100**, 4253–4264.

50. B. J. van der Veken, W. A. Herrebout, R. Szostak, D. N. Shchepkin, Z. Havlas, and P. Hobza, *J. Am. Chem. Soc.*, 2001, **123**, 12290–12293.

51. P. R. Shirhatti and S. Wategaonkar, *Phys. Chem. Chem. Phys.*, 2010, **12**, 6650–9.

52. G. A. Blake, K. B. Laughlin, R. C. Cohen, K. L. Busarow, D.-H. Gwo, C. A. Schmuttenmaer, D. W. Steyert, and R. J. Saykally, *Rev. Sci. Instrum.*, 1991, **62**, 1701.

53. K. Liu, M. G. Brown, C. Carter, R. J. Saykally, J. K. Gregory, and D. C. Clary, *Nature*, 1996, **381**, 501–503.

54. S. P. Brown, M. Pérez-Torralba, D. Sanz, R. M. Claramunt, and L. Emsley, *J. Am. Chem. Soc.*, 2002, **124**, 1152–1153.

55. R. K. Harris, P. Jackson, L. H. Merwin, B. J. Say, and G. Hägele, *J. Chem. Soc. Faraday Trans. 1 Phys. Chem. Condens. Phases*, 1988, **84**, 3649.

56. M. Hohwy, C. P. Jaroniec, B. Reif, C. M. Rienstra, and R. G. Griffin, *J. Am. Chem. Soc.*, 2000, **122**, 3218–3219.

57. S. P. Thomas, M. S. Pavan, and T. N. Guru Row, *Chem. Commun.*, 2014, **50**, 49–51.

58. W. Gordy and R. L. Cook, *Microwave Molecular Spectra. 2nd ed.*, New York: Wiley Interscience, 1984.

59. C. H. Townes and A. L. Schawlaw, *Microwave Spectroscopy*, Dover Publications, Inc., 1975.

60. T. Yoshikawa, Y. Sumiyoshi, and Y. Endo, *J. Chem. Phys.*, 2009, **130**, 094302.

61. D. Patterson, M. Schnell, and J. M. Doyle, *Nature*, 2013, **497**, 475–7.

62. G. G. Brown, B. C. Dian, K. O. Douglass, S. M. Geyer, S. T. Shipman, and B. H. Pate, *Rev. Sci. Instrum.*, 2008, **79**, 053103.

63. B. H. Pate and F. C. De Lucia, *J. Mol. Spectrosc.*, 2012, **280**, 1–2.

64. D. Mani, V. T. Bhat, K. J. Vinoy, and E. Arunan, *Indian J. Phys.*, 2012, **86**, 225–235.

65. D. Mani, *Ph. D. Dissertation, Indian Institute of Science*, 2013.

66. *International Symposium on Molecular Spectroscopy-2014.*, Talk no. RE01.

# Chapter II. Experimental and Theoretical Methods

## II.1. Introduction

Fourier transform microwave spectrometer is used to collect the rotational spectra of molecules and complexes in the gas phase. Initially, absorption cell based microwave spectrometers were used to record the rotational spectrum. However, the sensitivity of these spectrometers was not very good and therefore, it could mostly be used only for the detection of stable molecules. In 1979, Balle and Flygare developed a cavity based Fourier transform microwave spectrometer coupled with molecular beam technique.[1] The sensitivity of such spectrometers is very high and even C-13 isotopomers/isotopologues can easily be observed in their natural abundance. Moreover, very weak complexes such as those between two inert gas atoms like Ar•••Ne,[2] Kr•••Ar, Ne•••Kr,[3] Xe•••Ne, Xe•••Ar and Xe•••Kr[4] could be observed using these spectrometers. With time, there have been many modifications and advancements in the design of these cavity based spectrometers. These modifications include the use of heated nozzles to produce transient species such as radicals. Incorporation of laser ablation technique in the microwave spectrometers has helped in studying the solid samples as well. In 2008, development of chirp pulse Fourier transform microwave spectrometers has given a new direction to microwave spectroscopy.[5] Chirp pulse microwave spectrometers take much less time in data acquisition as compared to the cavity based microwave spectrometer. Band width of 11 GHz can be scanned in a single experiment using these spectrometers whereas using cavity based microwave spectrometers only 1 MHz band width can be covered at a time. This is the major advantage of chirp pulse microwave spectrometer over cavity based microwave spectrometer. However, the sensitivity of these spectrometers is much less as compared to the cavity based spectrometers.

In our lab, we use a conventional Pulsed Nozzle Fourier Transform Microwave (PNFTMW) spectrometer to record the pure rotational spectra. This spectrometer is based on the Balle-Flygare design and details about the spectrometer are discussed elsewhere.[6–9] A brief discussion about the spectrometer has been given in next few sections.

## II.2. PNFTMW spectrometer

The spectrometer can be divided into two parts: mechanical part and electrical part. The two parts are discussed below.

### II.2.1. Mechanical Part

The mechanical design of the PNFTMW spectrometer is shown in the Figure II. 1. The spectrometer has a cylindrical chamber which is vacuum sealed and is made of stainless steel (SS 304). It is 1000 mm long and has a diameter of 850 mm. Chamber houses two identical spherical aluminium mirrors. These mirrors are coaxially mounted on three rods. This arrangement is known as Fabry-Perrot cavity. The mirrors have very high Q-value (~10000). The spherical mirrors are made using a 65 mm thick and 250 mm radius circular disk of aluminium. The radius of curvature of the mirrors is 800 mm. The lower frequency cut-off of the spectrometer is limited by Fresnel's condition.

$$\frac{a^2}{R\lambda} \geq 1$$

Where *a* is the radius and R is the radius of curvature of mirror. According to this condition, 3.8 GHz should be the lower frequency cut-off for our spectrometer. However, signals at as low frequency as 2447.8427 MHz have been observed.[6] The operating range of the spectrometer is ~2.5-20.0 GHz.

Chamber is seated on a 20″ diffusion pump (Vacuum Techniques, Bangalore, India). The pumping speed of the diffusion pump is 10,000 $l.s^{-1}$. Diffusion pump is backed up by a roots blower (Boc Edward, EH 250) and a beltless rotary pump (Boc Edward, E2M80). This overall arrangement of the backing pumps has a pumping speed of ~4000 $l.s^{-1}$. The whole arrangement can evacuate the cavity to $10^{-6}$ *torr* pressure. Diffusion pump produces enormous amount of heat. To keep the spectrometer at room temperature, a water cooling tower is installed which has a water circulation facility. To monitor the pressure inside the chamber, two types of pressure gauges are used, Penning gauge and Pirani gauge. Pirani gauge is capable of sensing pressure up to $1.0 \times 10^{-3}$ *torr* while Penning gauge can sense pressure up to $1.0 \times 10^{-6}$ *torr*. Pirani gauge is mounted at two places in the instrument; one at the top of the chamber and other just before the valve. The valve is used to barricade the

connection between chamber and pumps. Penning gauge is placed at the top of the chamber. The pressure is monitored using a pressure read out unit (VT-D2PP-01, Vacuum Techniques [P] Ltd. Bangalore).

Out of the two mirrors, one is fixed and the other is movable. Distance between the two mirrors can be varied from 630 *mm* to 730 *mm*. The movable mirror is attached to a fine pitch linear screw rod. The movement of the mirror is controlled by a stepper motor (103H8221-5041, Sanyo Denki, Japan). The linear screw rod has a pitch of 5 *mm*. It means, in full rotation (360°), the rod moves a distance of 5 *mm*. With the help of stepper motor, a full rotation can be carried out in 5000 steps which means that mirror moves by 1 micron in a single step. Thus, spacing between two mirrors can be controlled to a micron.

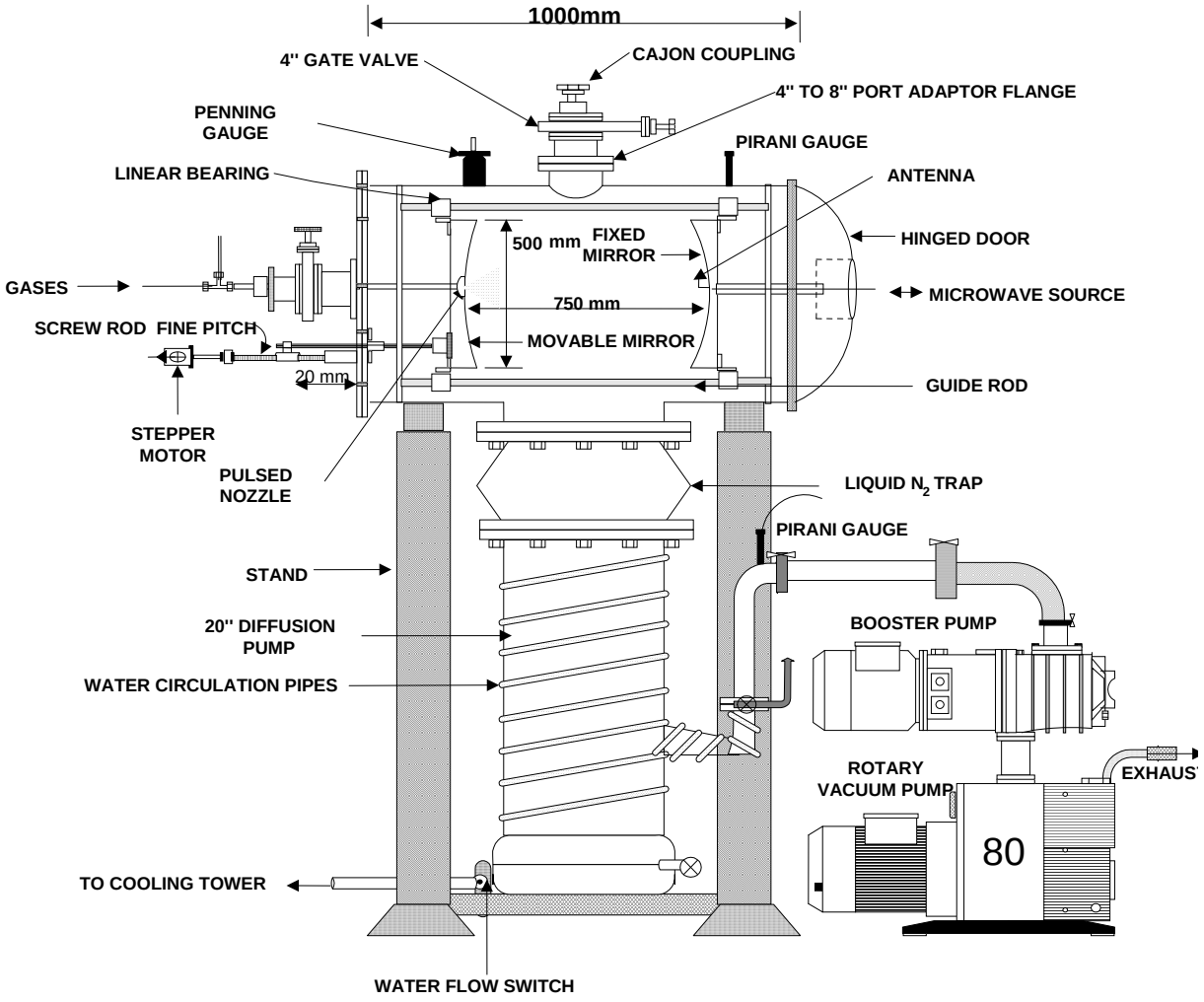


*Figure II. 1. Mechanical design of the PNFTMW spectrometer.*

At the centre of the movable mirror, there is a hole of 10 mm diameter. A general valve pulsed nozzle (General valve, USA, service 9) of 0.8 *mm* diameter, is placed at this hole. The outer end of the valve is connected with a stainless steel tube (0.25 inch outer diameter). We carry the sample through this tube to the valve and pulse it into the cavity by opening the valve for typically 1 ms. The pulse rate is controlled by a pulse driver (Micrologix, MSB-403). The other stationary mirror also has a hole at its centre. A female SMA connector, which is at the end of coaxial cable, is fitted in this hole. An L-shaped antenna is connected with the SMA male connector. Microwave radiation is transmitted and received using the same antenna. The operating range of the antenna roughly depends on the length the antenna (L) by following relationship.

$$L \approx \lambda/4$$

Using this approximation, we make antenna of different frequency range and 3 or 4 antennae are enough to cover the entire frequency range of our spectrometer.

## II.2.2. Electrical Design

Electric design of the spectrometer is shown in Figure II. 2. There are two purposes of the electronics; to generate the microwave pulse and to detect the microwave signal. The source of the microwave radiation is a signal generator (#1, in Figure II. 2, Agilent, MXG signal generator, N5183A). It can generate any frequency from 100 kHz to 32 GHz with a resolution of 0.01 Hz. The generated RF frequency ($\nu$) from signal generator with 13 dBm power is sent to a single-pole-double-throw (SPDT) switch (#7, Sierra Microwave, 0.5-26.5 SFD0526-00, isolation 60 dB). During the polarization cycle, the output of the SPDT switch is sent to a single side band mixer (SSBM, #5, Miteq, SMO-026LC1A) where it is mixed with the output of a 30 MHz function generator (#23, SRS, DS345), hereafter denoted by $\nu_1$. The upper band of the SSBM output, $\nu + \nu_1$, is amplified by a medium power amplifier (#6, Miteq, JS3-02002600-5-7A) with a gain of 24 dB. This output is directed to the other SPDT switch (#7′). Both SPDT switches (#7 and #7′) work synchronously and they are controlled by a delay generator (BNC-555). The delay generator produces two pulses of same time duration but opposite polarity and sends them to the two switches 7 and 7′.Typical microwave pulse length is of the order of microseconds resulting in a frequency bandwidth in

the range of MHz. The output of the SPDT switch is then directed to the directional coupler (#8, Narda, 1.7-26.5-4227-16). The antenna couples the signal with the cavity. This signal polarises the molecules. If the molecules absorb within the width of the signal, a transition occurs and the molecules emit ($\nu + \nu_1 + \Delta$) frequency coherently. $\Delta$ is the offset from the $\nu + \nu_1$ signal.

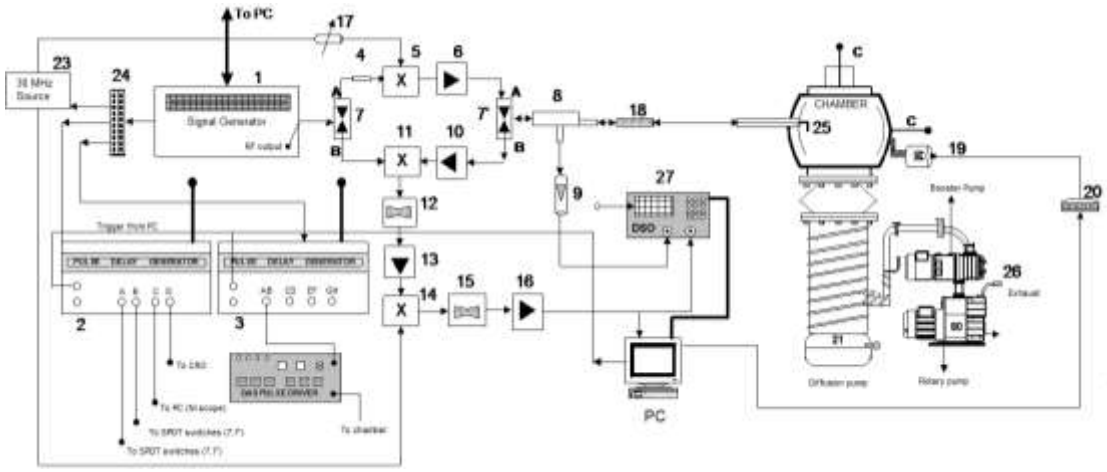


*Figure II. 2. Electrical design of the PN-FTMW spectrometer.*
*1, Signal generator ( Agilent, MXG signal generator, N5183A); 2, Delay generator (BNC-555); 3, Delay generator (SRS DG645); 4, Microwave attenuator (HP, 8493C, 3dB); 5, SSB mixer (Miteq,SMO-226LC1A); 6, Medium power amplifier (Miteq, JS3-02002600-5-7A); 7, MW SPDT switch (Sierra Microwave, 0.5-26.5 SFD0526-000); 8, Direction coupler (Narda, 1.7-26.5–4227–16); 9, Diode detector (Narda, 0.01-26.5–4507); 10, Low noise amplifier (Miteq, JS4-02002600-3-5P); 11, Image rejection mixer (Miteq, IRO-0226LC1A); 12, Band pass filter (Mini Circuits, BBP-30); 13, RF amplifier (Mini Circuits, ZFL-500LN); 14, RF mixer (Mini Circuits, ZAD-1); 15, Low pass filter (Mini Circuits, BLP-5); 16, RF amplifier (HD communication corp., HD 17153BB); 17, Attenuator (Mini Circuits, ZAFT-51020); 18, Blocking capacitor (HP, 11742A); 19, Stepper motor; 20, Motor driver; 21, Diffusion pump and 22,Rotary pump; 23, 30MHz function generator (Stanford Research System, DS345); 24, Distribution amplifier (Stanford Research System, FS710); 25, Antenna; 26, Exhaust; 27, Digital storage oscilloscope (Tektronix TDS 2022).*

The same antenna detects the signal which is then sent to the directional coupler. The coupler sends a fraction of the reflected signal's power (2.5 %) to a diode detector, output from which is sent to a digital storage oscilloscope (DSO, #27 Textronix TDS 2022). This signal is used to monitor the tuning of the cavity. The cavity should be tuned during the polarization of the molecules. If the distance between the two mirrors is half integral multiples of the wavelength of the radiation, cavity is said to be tuned. Figure II. 3 shows the DSO output when the cavity is in (i) not tuned (left side figure) and (ii) tuned condition (right side figure). As shown in the figure if the cavity is tuned there is a huge dip in the reflected signal due to

the formation of a standing wave inside the cavity. If cavity is not tuned, we move the movable mirror coaxially to adjust the distances between mirrors until a standing wave is formed inside the cavity. The mirror is moved using a stepper motor which is controlled by a stepper motor driver (Micrologix, embedded system ltd. MSB-403). Stepper motor is triggered by a PC.

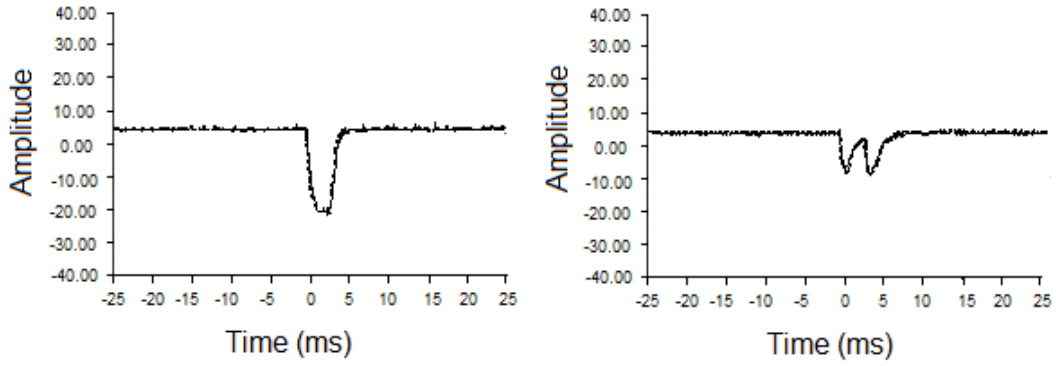


*Figure II. 3. Reflected signals on the oscilloscope.*
*Left side: when cavity is not tuned. Right side: when cavity is tuned.*

The other output of the direction coupler (97.5 % of the input signal) goes to a low noise amplifier (#10, Miteq, JS4-02002600-3-5P, noise 2.8 dB and gain 28 dB) via the SPDT switch. This amplified signal ($\nu + \nu_1 + \Delta$) mixes with the output of the signal generator ($\nu$) in an image rejection mixer (IRM, #11, Miteq, IRO,0226LC1A). Output from the IRM ($\nu_1 + \Delta$) is directed to a band pass filter (#12, Mini Circuits, BBP-30) and then to a low noise RF amplifier (#13, Mini circuits, ZFL-500LN). Then the signal is mixed with the output of the function generator ($\nu_1$) in an RF mixer (#14, Mini Circuits, ZAD-1), where it is down converted to $\Delta$. This signal $\Delta$ goes through a low pass filter (#15, mini Circuits, BLP-5) and further to the RF amplifier (#16, HD communication corp., HD 17153BB). This amplified signal goes to a digitizer and to the PC for digitization. NI scope card (National Instrument, PCI 5112) is installed in the PC for this purpose. The maximum sampling speed of the NI scope card is 100 MHz. The signal we digitize is usually of the bandwidth less than 1 MHz. We therefore, use a sampling speed of 5 MHz.

Digitized signal is Fourier transformed using a function inbuilt in LabView. In Figure II. 4, a rotational transition is shown in the time domain as well as in frequency domain.

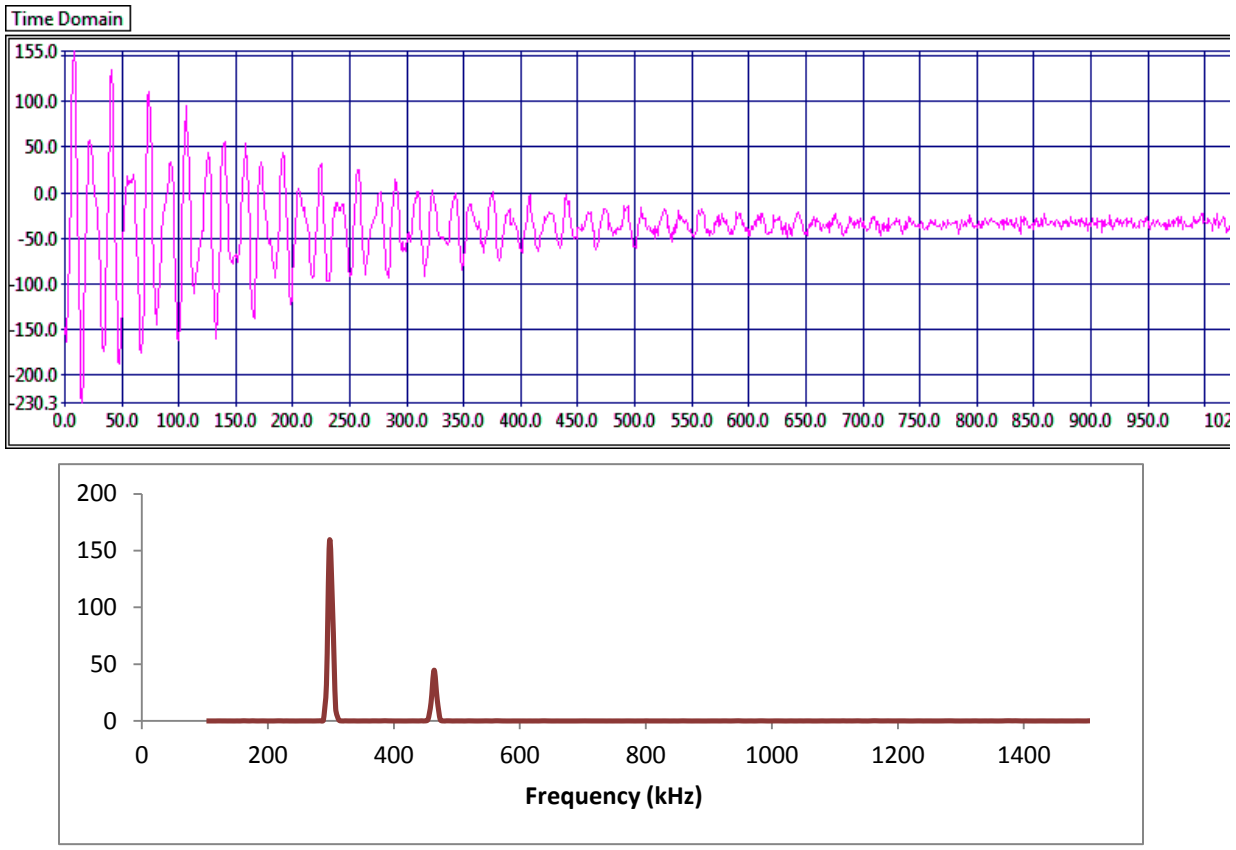


*Figure II. 4. Interface of LabView program for a signal in time domain and frequency domain*

### II.2.3. Time Sequence of the Pulses

The microwave pulses are controlled by a delay generator (BNC-555) and the sample gas pulse is controlled by another delay generator (DG-645). Pulse sequence for the experiments is given in Figure II. 5. First we send a microwave pulse inside the cavity. In general, time duration for the microwave pulse is in the range of 0.2-3.0 μs which depends on the strength of the electric dipole moment components of the molecules or complexes. After sending the microwave pulse, we introduce a delay of typically 10-40 μs to make sure that ringing from the cavity dies down. This delay is very important to observe the signal because peak to peak voltage of ringing from the cavity is around 6-8 V whereas, molecular signals strength is only few millivolts. Therefore, it would not be possible to observe a molecular signal with such a high background. This delay, which we term as ringing delay, is generated using one of the channels of the BNC-555 delay generator. This delay depends on the frequency range and it is found that longer delay (~35-40 μs) is needed in the low frequency range (< 6 GHz). After this a gas pulse of typically 1 ms time duration is sent to the cavity. The molecules or

complexes in the gas pulse are then polarised by a series of microwave pulses. There is a delay between the gas pulse and first of the microwave pulses (of the order of few tens of microseconds) which we call 'Start delay'. This delay is introduced by the processing time of the LabView program itself and is not controlled manually. The residence time of the pulsed gas inside the cavity is ~2 ms. A typical data acquisition time is 100 μs. Therefore, we can send multiple microwave pulses for a single gas pulse. The signal is extracted by subtracting the signal before sending the gas pulse from the signal of the 'single shot' experiment. The 'single shot' is defined as the whole process, starting from the first microwave pulse and ending with the polarization of the molecules by multiple microwave pulses. The experiment can be repeated for *n* number of shots which improves the signal to noise ratio.

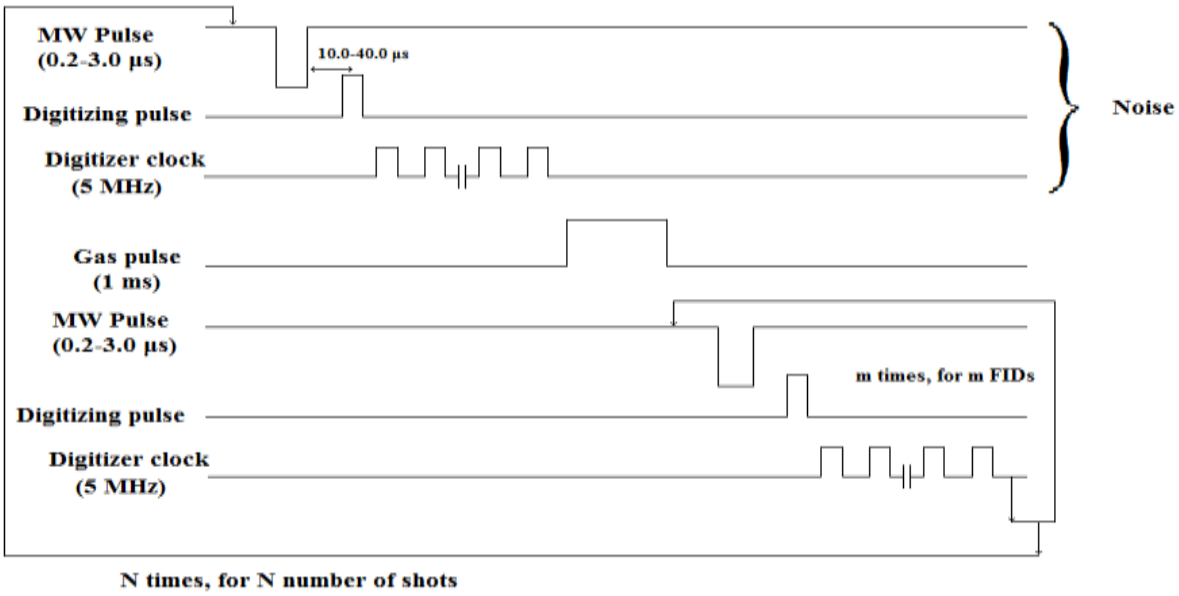


*Figure II. 5. Pulse sequence for PNFTMW spectrometer.*

## II.2.4. Software for the PNFTMW Spectrometer

Programs for our spectrometer are mainly based on LabView 7.1 software. LabView is a graphical programming language with a lot of user friendly options. LabView programs have two main parts; front panel and block diagram. Using the front panel the user can input the parameters and also monitor the real time data. The inbuilt controls available in the LabView help in the automation of the instrument. Block diagram is for the programmer to draw the

code. Programmer designs the front panel as well and decides what to interface on the front panel. The common extension for the LabView code is *.vi* and there are a lot of examples stored in the database of the program for the convenience of the users and programmers.

In our spectrometer, we control many units with the LabView program using a GPIB interface. To control different electronic instruments, different VIs are created. Moreover, programs for data acquisition are also written in LabView. By combining many small VIs a master code 'msb-403.vi' is written which is used for the experiments. A screen shot of the interface of the program is given in the Figure II. 6.

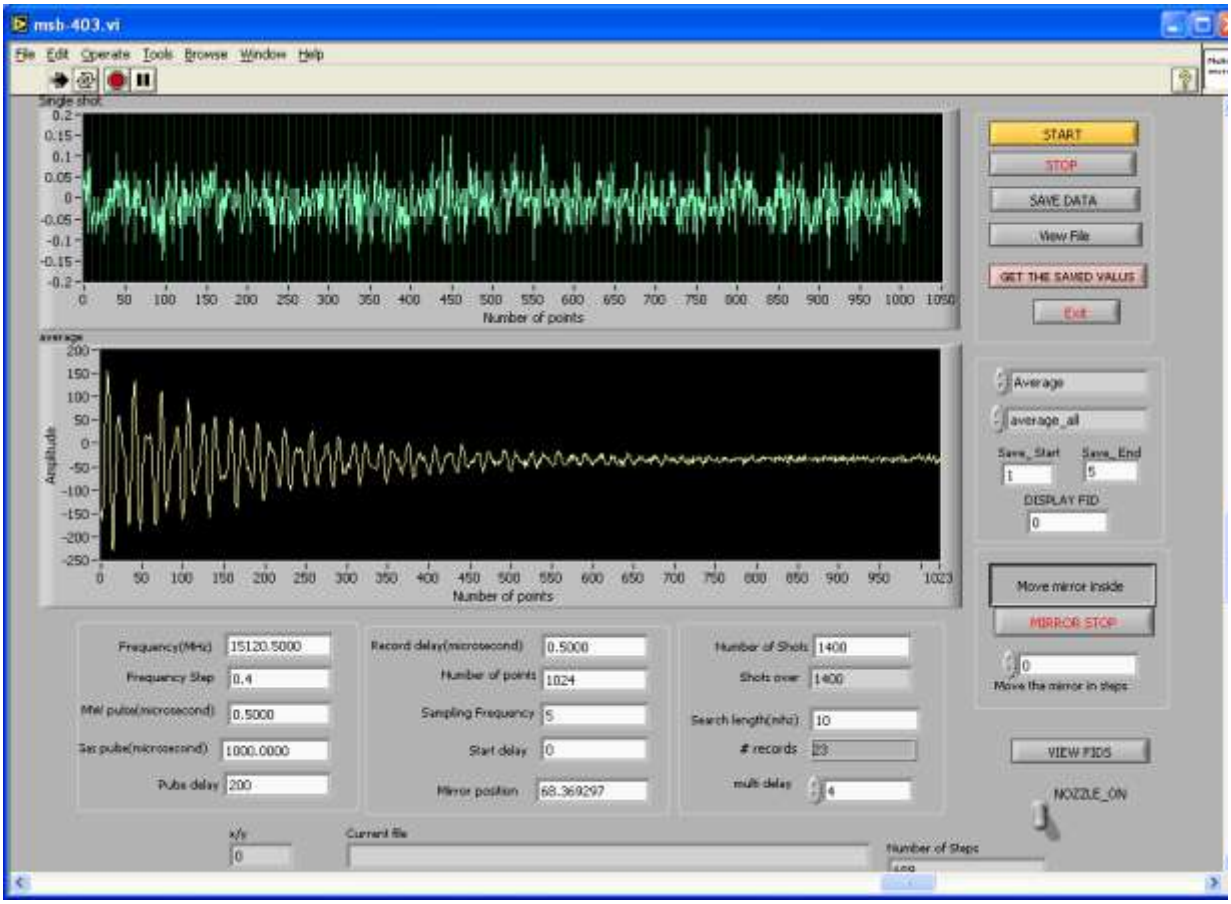


*Figure II. 6. Interface of the main LabView program which consists all information and control options.*

We also use some alternative methods to communicate with the electronic units. For example, the stepper motor is being controlled by the parallel port. To control the delay generator, we use RS-232 cable in combination with Hyperterminal program. There are some easy sets of commands which help in setting the microwave pulse width, delay between two

pulses, polarity of the pulses, external or internal triggering etc. All sets of commands can be found in the manual of the delay generator.

## II.3. Sample Preparation

We inject the sample inside the cavity through a pulsed valve. Argon or helium gases are used as carrier gases. If our sample is in liquid state, we bubble a small fraction of the carrier gas (1-2 %) through the liquid sample contained in a bubbler. A specially designed bubbler is used for this purpose. The carrier gas takes some of the sample molecules with it during the bubbling. In case of two liquid samples, two separate bubblers should be used for each sample. Before sending the carrier gases, containing the molecules from the two samples, to the cavity, we mix them at a four way junction. We control the flow of the gases by mass flow controllers (MKS, 1179). The mass flow controllers are controlled using a four channel control unit (MKS, Type-247). Now, the mixed sample is sent to the cavity from a back pressure of typically 1.0-1.5 atm through a pulsed nozzle of 0.8 mm diameter. Sample enters into the cavity when nozzle opens and then the expansion takes place. Collision between the molecules takes place in the high pressure region of the molecular beam (within a length of few nozzle diameters). Two body collision leads to cooling and three body collisions can lead to weakly bound complexes. The supersonic expansion leads to a very directional mass flow. In the supersonic molecular beam, translational degrees of freedom relax very fast and translational temperature of the molecules fall down to typically 0.02-0.03 K. However, vibrational and rotational degrees of freedom relax much slowly and vibrational and rotational temperatures of the molecules in the beam are typically 50-100 K and 2-3 K, respectively. In the molecular beams, the velocities of the molecules are more than the velocity of sound (in the local medium) and therefore it called as supersonic expansion.

## II.4. Quantum Chemical Calculations.

For the projects reported in this Thesis, the ab initio calculations were mainly performed to calculate the binding energy of the complexes under investigations and to get their rotational constants which were used to predict the rotational spectra. These calculations are discussed briefly in the following paragraphs.

## II.4.1. Binding Energy

Binding energy of a complex was calculated using the supermolecular approach. According to this approach, binding energy of a complex is given as:

$$B.E.(complex) = E(complex) - (E(monomer\ 1) + E(monomer\ 2) + \ldots)$$

Where B.E. stands for binding energy and E stands for the total electronic energy of the molecules or complex. There are different methods to calculate the total electronic energy. In this thesis, mainly post-HF and DFT methods have been used. DFT methods are comparatively faster than the post-HF ab initio methods. Moreover, the results for few of the complexes studied in this thesis, using long range corrected DFT level of theory, LC-wPBE[10] were found to be comparable to those obtained from the post-HF (MP2) level of theory. Proper selection of basis set for the calculation is very important. For most of the studies reported in this thesis, we used large basis sets like Pople's 6-311++G(d,p) and Dunning's aug-cc-PVTZ. Basis set superposition error (BSSE) happens when the basis set is smaller than optimum. BSSE was corrected using counterpoise (CP) method.[11] The counterpoise method is inbuilt in the Gaussain 09 software package.

## II.4.2. Rotational and Distortion Constants Calculation

Rotational constants for the optimized geometry of the complexes were extracted from the Gaussian calculations. In case of monomers, these calculated constants are usually very close to the experimental values. However, in case of floppier weakly bound complexes the potential energy surface is usually shallow. Therefore, the quantum chemical calculations are not so good in case of these complexes. Nonetheless, these calculations do help in the initial guess of geometries and work as an important aid in the experimental studies. Distortion constants for the complexes can also be obtained from Gaussian calculations[12] by using freq=vibrot[13] keyword. Chapter III and Chapter IV discuss the importance of calculated distortion constants for the HFIP monomer and HFIP•••$H_2O$ complex respectively.

## II.4.3. Anharmonic calculation

The main purpose behind performing expensive anharmonic calculation is to get the vibrationally averaged geometry. Normal optimization gives the equilibrium geometry for the molecules/complexes. For rigid and small molecules, the equilibrium geometry is closer

to the vibrationally averaged geometry. However, for complexes and floppy molecules, there is a significant difference between their equilibrium and vibrationally averaged geometries. Chapter IV of this thesis discusses more about the usefulness of anharmonic calculations. Freq=anharmonic[14] keyword is an inbuilt method in Gaussian 09 which was used for the calculation of the vibrationally averaged geometry.

## II.5. Atoms in Molecules Analysis

Atoms in molecules (AIM) theory was used to characterize the nature of bonds (both intermolecular and intramolecular). AIMAll[15] and Multiwfn[16] programs were used for AIM analysis. The AIM theory was developed by R. F. W. Bader.[17] The theory is based on the electron density topological analysis. Electron density can directly be calculated from the wavefunction. The electron density critical points arising from the AIM analysis give important information about the bonding in the molecules and complexes. These critical points are discussed in the next section.

### II.5.1. Critical Points

In AIM theory, electron density topology of the system under investigation, is analysed. In 3D space, one can write the Hessian for the electron density function. Hessian of a function (electron density in this case) is a matrix of its second derivatives with respect to all possible combination of coordinates. On diagonalization of Hessian matrix, three eigenvalues; $\lambda_1$, $\lambda_2$ and $\lambda_3$ are obtained. In this study, the convention $\lambda_1 \leq \lambda_2 \leq \lambda_3$ was used; some studies also use the reverse convention. These eigenvalues represent curvature of electron density in three perpendicular directions. Different critical points are classified on the basis of the rank (r) and signature (s) of the Hessian matrix and are represented as (r, s). Rank of the matrix is the number of its non-zero eigenvalues and signature is the algebraic sum of the signs of these eigenvalues.

**Nuclear Attractor (NA)**

Nuclear attractor (NA) is denoted as (3, -3) which means all three eigenvalues of the Hessian matrix are non-zero and curvature corresponding to these eigenvalues are maxima (negative sign) in all three directions. Nuclear attractors are the atoms constituting the molecules.

**Bond Critical Points (BCP)**

Bond critical point (BCP) is denoted as (3, -1) which means electron density along one of the direction is minimum (positive $\lambda_3$) and along the other two directions it is maximum (negative $\lambda_1$ and $\lambda_2$). The presence of BCP in between two atoms and presence of bond paths connecting it to the atoms denotes bonding interaction between the two. Bond critical points have been used extensively in the analysis of different types of weak intermolecular interactions.[18,19]

**Ring Critical Points (RCP)**

Ring critical point (RCP) is denoted by (3, +1) which means two eigenvalues ($\lambda_2$ and $\lambda_3$) have positive sign and $\lambda_1$ has negative sign. This type of critical point is present at the centre of molecular rings like benzene. Distance between BCP and RCP shows the stability of a bond. If an RCP appears very near to a BCP, it indicates that the bond represented by the BCP is unstable. This is because of the fact that $\lambda_2$ changes its sign (electron density curvature) at very short distance from the BCP to the RCP.

**Cage Critical Points (CCP)**

Cage critical point (CCP) is denoted by (3, +3) which means electron density is minima in all three direction. Cubane possesses a CCP.

In summary, all CPs are listed here with their properties;

| (r, s) | Sign of $\lambda_1$ | Sign of $\lambda_2$ | Sign of $\lambda_3$ | Critical points |
|---|---|---|---|---|
| (3, -3) | - | - | - | NA: Nuclear Attractor |
| (3, -1) | - | - | + | BCP: Bond Critical Point |
| (3, +1) | - | + | + | RCP: Ring Critical Point |
| (3, +3) | + | + | + | CCP: Cage Critical Point |

**Poincare-Hopf Relation**

This relationship links the number of non-degenerate CPs for a non periodic system. The relation among nuclear attractors (n), bond critical points (b), ring critical points (r) and cage critical points (c) is as follows

$$n - b + r - c = 1$$

Program uses this relationship as a constraint which helps in finding the missing CPs. This relationship has some limitations, for example, if one BCP and one RCP are missed during the calculation, the relationship is still satisfied but not correct. As stated in the book by Popelier[20] "*this rule can never prove the completeness of a set of CPs, it can only point out that it is inconsistent and therefore incomplete."*

## II.5.2. Laplacian of Electron Density

Laplacian of electron density ($\nabla^2\rho$) is the algebraic sum of all eigenvalues i.e.

$$\nabla^2\rho = \lambda_1 + \lambda_2 + \lambda_3$$

Sign of $\nabla^2\rho$ depends on the dominating eigenvalues. For example, in the case of a BCP, if $\lambda_3$ dominates over the summation of ($\lambda_1 + \lambda_2$), sign of $\nabla^2\rho$ will be negative. Large value of $\lambda_3$ indicates more electron density along bond path. In other words there is accumulation of the charge at BCP along the bond path which is a property of shared shell interactions (covalent bond). For closed shell interaction, $\nabla^2\rho$ values are positive and indicate the charge depletion along the bond path. Intermolecular interactions and ionic bonds fall under this category. This criterion is empirical.

## II.5.3. Ellipticity

Ellipticity ($\varepsilon$) is defined by the relation (($\lambda_1/\lambda_2$) -1) and its value measures the behaviour of electron density in the two perpendicular directions to the bond path. For acetylene, $\varepsilon = 0$ which represents the cylindrical symmetry of electron density around the bond.

## II.5.4. Mutual Penetration

Mutual penetration is defined as the summation of differences between bonded and non-bonded radii of atom A in acceptor part and atom X in donor part. For example, in the $H_3N$•••HF complex, A is nitrogen and X is hydrogen. Bonded radius for N and H are taken as their distances from the BCP present between N and H. Non-bonded radius of the nitrogen is the distance between N-atom to the 0.001 a.u. electron density surface from where interacting partner (X-) is approaching. This criterion is considered to be the necessary and sufficient criterion to confirm the presence of intermolecular bonding between two atoms.[19]

$$\text{Mutual penetration} = [r_A^0 - r_A] + [r_x^0 - r_x]$$

Here $r_A^0$ and $r_x^0$ are the non-bonded radii of acceptor and donor, respectively and $r_A$ and $r_x$ are the bonded radii of the acceptor and donor, respectively.

## II.5.5. Criteria for Bond Characterization

There are several criteria which can be used in differentiating the shared-shell interaction from the closed-shell interaction; one of which is an offshoot of the work done in this thesis. There is no sharp boundary between these two interactions and all the criteria are presented here are empirical. The properties used in these criteria are monitored at the intermolecular BCP and are as follows:

- Ratio of $|\lambda_1|/\lambda_3$: If the value of this ratio is greater than 1.00,[21] the interaction is considered as shared-shell interaction and if it is less than 0.25 it is considered as closed shell interaction. Intermediate types of bonds fall in the range 0.25-1.00.[22] This ratio is called $\eta$-index.

- Sign of $\nabla^2\rho$: As discussed earlier, positive value of the Laplacian indicates closed shell interaction and negative value indicates shared-shell interaction.[23]

- Total energy value (H): Cremer and Kraka[24] found some exceptions while using the sign of $\nabla^2\rho$ values and suggested that total energy (H) of electron density at the BCP should be used as a criterion for differentiating between the shared shell and closed shell interactions. The H value is the summation of potential (V) and kinetic (G) energies of the electron density at the BCP. Positive value of H means kinetic energy is more dominating than the potential energy at the BCP and such interactions are called closed shell interactions. Interactions with negative H-value at the BCP indicate the shared shell interaction.

- V/G ratio: If the ratio of potential energy to the kinetic energy at the BCP is less than one, it represents a closed shell interaction.[25] If this ratio is greater than two, it represents a shared shell interaction. For the intermediate types of bonds this ratio is in between 1 and 2.

## II.6. Natural Bond Orbital Analysis

Natural Bond Orbital (NBO) theory was developed by Weinhold.[26] NBO 6.0 software suite was used to perform this analysis. The analysis gives the second order perturbation energies (E(2) for the interactions between different orbitals. E(2) values for the interaction between the donor orbital and the acceptor orbital is often used in analysing the intermolecular interactions. Using Natural Resonance Theory (NRT),[27,28] which is a subset of NBO analysis, percent ionic and covalent characters of a bond can be calculated for the different resonance structures of a molecule/complex. It also calculates the percentage weightage of the different resonance structures. Using the NRT calculations, we have shown that there is bond conservation during complex formation, Chapter VI.

## II.7. References


1. T. J. Balle and W. H. Flygare, *Rev. Sci. Instrum.*, 1981, **52**, 33.

2. J.-U. Grabow, A. S. Pine, G. T. Fraser, F. J. Lovas, R. D. Suenram, T. Emilsson, E. Arunan, and H. S. Gutowsky, *J. Chem. Phys.*, 1995, **102**, 1181.

3. Y. Xu, W. Jäger, J. Djauhari, and M. C. L. Gerry, *J. Chem. Phys.*, 1995, **103**, 2827.

4. W. Jäger, Y. Xu, and M. C. L. Gerry, *J. Chem. Phys.*, 1993, **99**, 919.

5. G. G. Brown, B. C. Dian, K. O. Douglass, S. M. Geyer, S. T. Shipman, and B. H. Pate, *Rev. Sci. Instrum.*, 2008, **79**, 053103.

6. P. K. Mandal, *Ph. D. Dissertation, Indian Institute of Science*, 2005.

7. M. Goswami, *Ph. D. Dissertation, Indian Institute of Science*, 2009.

8. E. Arunan, A. P. Tiwari, P. K. Mandal, and P. C. Mathias, *Curr. Sci.*, 2002, **82**, 533–540.

9. D. Mani, *Ph. D. Dissertation, Indian Institute of Science*, 2013.

10. O. A. Vydrov and G. E. Scuseria, *J. Chem. Phys.*, 2006, **125**, 234109.

11. S. F. Boys and F. Bernardi, *Mol. Phys.*, 1970, **19**, 553–566.

12. Frisch, M. J.; Trucks, G. W.; Schlegel, H. B.; Scuseria, G. E.; Robb, M. A.; Cheeseman, J. R.; Scalmani, G.; Barone, V.; Mennucci, B.; Petersson, G. A.; Nakatsuji, H.; Caricato, M.; Li, X.; Hratchian, H. P.; Izmaylov, A. F.; Bloino, J.; Zheng, G.; Sonnenberg, J. L.; Hada, M.; Ehara, M.; Toyota, K.; Fukuda, R.; Hasegawa, J.; Ishida, M.; Nakajima, T.; Honda, Y.; Kitao, O.; Nakai, H.; Vreven, T.; Montgomery Jr., J. A.; Peralta, J. E.; Ogliaro, F.; Bearpark, M.; Heyd, J. J.; Brothers, E.; Kudin, K. N.; Staroverov, V. N.; Kobayashi, R.;

Normand, J.; Raghavachari, K.; Rendell, A.; Burant, J. C.; Iyengar, S. S.; Tomasi, J.; Cossi, M.; Rega, N.; Millam, J. M.; Klene, M.; Knox, J. E.; Cross, J. B.; Bakken, V.; Adamo, C.; Jaramillo, J.; Gomperts, R.; Stratmann, R. E.; Yazyev, O.; Austin, A. J.; Cammi, R.; Pomelli, C.; Ochterski, J. W.; Martin, R. L.; Morokuma, K.; Zakrzewski, V. G.; Voth, G. A.; Salvador, P.; Dannenberg, J. J.; Dapprich, S.; Daniels, A. D.; Farkas.O ; Foresman, J. B.; Ortiz, J. V; Cioslowski, J.; Fox, D. J. Gaussian 09 Revision C.01.

13. S. Califano, *Vibrational States*, Wiley, London, 1976.

14. C. Adamo, M. Cossi, N. Rega, and V. Baron, *Theoretical Biochemistry: Processes and Properties of Biological Systems, Theoretical and Computational Chemistry, Vol. 9*, Elsevier, New York.

15. *AIMAll (Version 13.11.04), Todd A. Keith, TK Gristmill Software, Overl. Park KS, USA, 2013*.

16. T. Lu and F. Chen, *J. Comput. Chem.*, 2012, **33**, 580–92.

17. R. F. W. Bader, *Atoms in Molecules: A Quantum Theory*, Clarendon Press, Oxford, 1990.

18. D. Mani and E. Arunan, *Phys. Chem. Chem. Phys.*, 2013, **15**, 14377–83.

19. U. Koch and P. L. A. Popelier, *J. Phys. Chem.*, 1995, **99**, 9747–9754.

20. P. L. A. Popelier, *Atoms in Molecules. An Introduction*, Pearson Education Ltd. Essex, England, 2000.

21. N. J. M. Amezaga, S. C. Pamies, M. Peruchena, N. M. Peruchena, and G. L. Sosa, *J. Phys. Chem. A*, 2010, **114**, 552–62.

22. A. Shahi and E. Arunan, *Phys. Chem. Chem. Phys.*, 2014, **16**, 22935-52.

23. R. F. W. Bader and H. Essen, *J. Chem. Phys.*, 1984, **80**, 1943–1960.

24. D. Cremer and E. Kraka, *Angew. Chemie Int. Ed. English*, 1984, **23**, 627–628.

25. E. Espinosa, I. Alkorta, J. Elguero, and E. Molins, *J. Chem. Phys.*, 2002, **117**, 5529.

26. A. E. Reed, L. A. Curtiss, and F. Weinhold, *Chem. Rev.*, 1988, **88**, 899–926.

27. E. D. Glendening and F. Weinhold, *J. Comput. Chem.*, 1998, **19**, 610–627.

28. E. D. Glendening and F. Weinhold, *J. Comput. Chem.*, 1998, **19**, 593–609.

# Chapter III. Microwave Spectrum of Hexafluoroisopropanol and Basic Chemistry of Molecules with Group $CF_3$-C-$CF_3$

## III.1. Introduction

Fluorinated alcohols are unique solvents and are used by biologists, polymer chemists, and organic chemists. Hexafluoroisopropanol (HFIP) is a protic solvent which can work as hydrogen bond donor as well as hydrogen bond acceptor. Its aqueous binary solution helps in stabilizing the α-helical structure of protein.[1] It has propensity to dissolve even polymers because of its strong hydrogen bond formation ability. The polymer should possess hydrogen bond acceptor groups. Hence, polymers like polythene terephthalate, polyamides etc[2] could be dissolve in HFIP. HFIP is a suitable solvent for rearrangements via zwitterionic intermediate, whereas $CH_3OH$ is not a suitable solvent in this case[3]. The HFIP molecule is an interesting molecule for spectroscopists as well. Conformational preference of HFIP molecule has been a subject of several studies. IR, Raman and Matrix isolation studies show that the molecule exists in two conformations antiperiplanar (AP) and synclinical (SC). The AP conformer has been found to be more stable than the SC conformer.[4–6] Both the conformers exists in $CCl_4$ solution as well as in $N_2$-matrix and CO-matrix. However, in these mediums the SC conformer was found to be more stable. In Ar-matrix, only AP conformer could be observed.[5] The relative intensity of the conformers depends on temperature also. These conformers exist because of the internal motion of the –OH group. Prototype molecule isopropanol also exists in two conformers due to the internal motion of its –OH group. However, for this molecule the SC conformer is more stable than the AP conformer.[6–8] Suhm's group has extensively[6] studied the effect of fluorination on isopropanol molecule using IR spectroscopy.

Our interest in HFIP was triggered by the fact that it is an exceptional solvent with potential of forming different types of hydrogen bonds with other hydrogen bond

acceptor/donor molecules. Therefore, we wanted to study hydrogen bonded complexes of HFIP with molecules like $H_2O$. However, we found that no rotational spectroscopic study on HFIP monomer was known. At the same time rotational spectra of other prototype molecules hexafluoroisobutene (HFIB)[9] and hexafluoroacetone imine[10] (HFA-IM) are known. The microwave spectroscopic studies showed that the rotational transitions of both the molecules appear as doublets. The reason for this splitting was found to be the counter rotation of the two $CF_3$ groups.

In this chapter, we report very first rotational spectroscopic study of the HFIP molecule. Along with the rotational spectroscopic studies, comparative studies of the HFIP with other prototype molecules which exhibit $CF_3$-C-$CF_3$ group have also been done.

## III.2. Experimental Methods

HFIP (≥99%) was bought from Aldrich. Its mono deuterated isotope (OD) was prepared by mixing it with $D_2O$ (99.9% by Cambridge Isotope Laboratory) in 1:1 molar ratio. Its double deuterated (CD-OD) isotopologue was purchased from Aldrich (99%). None of the purchased samples were further purified. All C-13 isotopologues were observed in natural abundance. The rotational spectrum was recorded using Pulsed Nozzle Fourier Transform Microwave (PNFTMW) Spectrometer.[11] Initial experiments were carried out using Ar as carrier gas. However, we observed that the HFIP signals were more intense while using helium as the carrier gas. Therefore, for further experiments, helium was used as the carrier gas. The flow rate of He was kept at 200 SCCM and 1% of it was flown through a bubbler containing HFIP sample. Carrier gas seeded with the HFIP molecules was expanded from a back pressure of 1.5 atm through the pulsed valve into the Fabry-Perot cavity where

supersonic expansion takes place. This expansion produces rotationally cold molecule with rotational temperature ≈ 3 K. Multiple free induction decays (FIDs) were recorded per gas pulse. At the sampling speed of 5 MHz, 256 points were collected for each FID during the search for rotational transitions. Once a signal was observed, it was further averaged with 512 or 1024 points to improve the resolution. Microwave pulse of 1.3 μs duration was found to be optimum for both the *b*- and *c*-type transitions.

## III.3. Theoretical Calculations

Ab initio calculations were performed using G09 suite of program[12]. Different possible conformers of HFIP were optimized at MP2/6-311++G(d,p) level. Frequency calculations were also performed for the optimized geometries at the same level. These calculations and earlier IR studies[6] show that the HFIP molecule has two minima, AP and SC. These two conformers originate due to the internal rotation of –OH group and the H1-C1-O1-H2 dihedral angle are 180° and 52° for AP and SC, respectively (Figure III. 1). Labeling of the atoms is shown in the Figure III. 1. Vibrational frequency calculations were done for both conformers. Frequencies corresponding to the different normal modes of vibration were found to be real for both the conformers which indicate that both the structures are true minima. Both the terminal $CF_3$ groups were eclipsed with respect to each other for the AP conformer and slightly staggered for the SC conformer. The dihedral angle F1-C2-C3-F6 for the SC conformer is 18.7°. Cartesian coordinates and calculated frequencies (without scaling) of both the conformer are given in supporting information (Table III. S. 1 and Table III. S. 2). Relaxed potential energy surface (PES) scan was performed for H1-C1-O1-H2 dihedral angle at MP2/6-311+G(d). AP conformer is more stable than SC by 5.02 kJ/mol, Figure III. 2. Two

identical structures minima corresponding to the SC conformer are present in the PES. These minimum points are separated by a small barrier of 1.30 kJ/mol (equivalent to 108.4 $cm^{-1}$), which is slightly less than the ZPE (109.5 $cm^{-1}$) of the corresponding vibrational motion. Saddle point for this barrier corresponds to the synperiplanar structure (H1-C1-O1-H2 dihedral angle is zero).

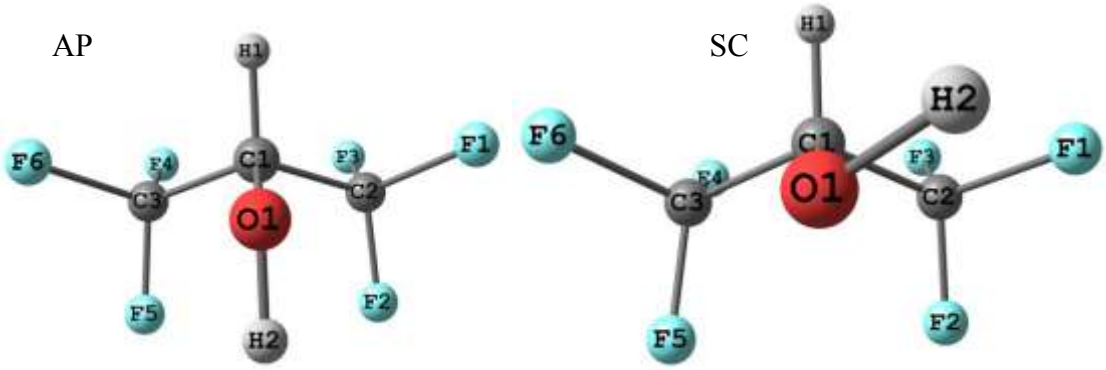


*Figure III. 1. Antiperiplanar (AP) and synclinical (SC) conformers of HFIP. Geometries were optimized at MP2/6-311++G(d,p) level.*

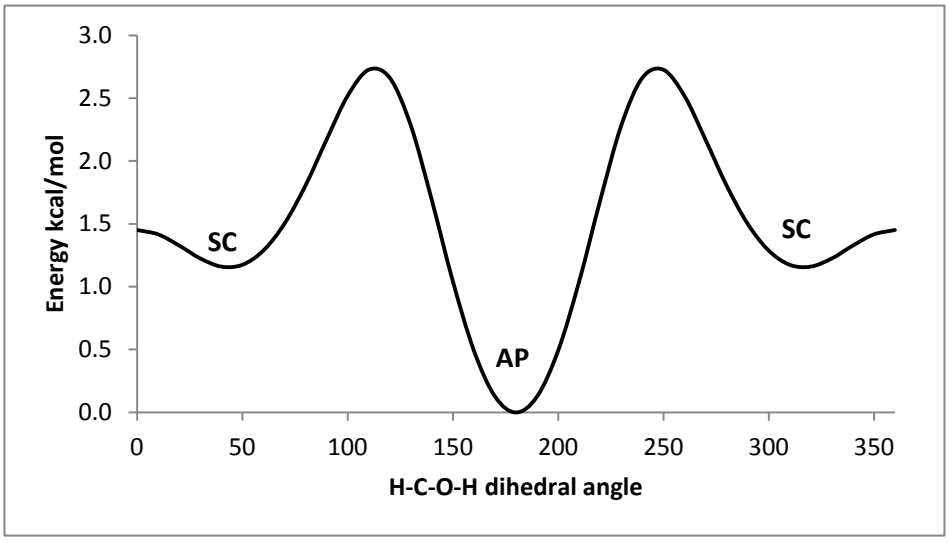


*Figure III. 2. Relaxed potential energy surface scan of OH internal motion for the HFIP molecule at MP2/6-311+G(d)level.*
*Variation of dihedral angle H1-C1-O1-H2 (x-axis) with relative energy (y-axis) has been presented.*

In the case of prototype molecules hexafluoroisobutene (HFIB)[9]and hexafluoroacetone imine (HFA-IM),[10] one more hindered torsional motion exists which causes splitting in the rotational transitions of these molecules, *vide infra*. Along with these molecules, some other prototype molecules which have $CF_3$-C-$CF_3$ group were also optimized at MP2/6-311++G(d,p). These molecules were collected to understand the reason behind splitting. Because of the presence of two $CF_3$ group, these systems should be treated as two dimensional double rotor problems. However, by the use of a symmetry coordinate, two rotor problems can be reduced to one rotor problem. In our case, F1-C2-C3-F6 dihedral angle was chosen as the symmetry coordinate and relaxed PES scan was performed for full rotation. After observing the non-periodic behavior of PES, we realized that substituent on the center C-atom was also playing significant role in deciding a particular conformer. Therefore, 2D-PES scan was performed for both the $CF_3$ internal rotors separately. The scan was performed with respect to the center C-atom's substituent for a 120° rotation. Other advantages of these scan were to compare the barrier heights, both small and large and also find out the most stable conformer, *vide infra*. Keeping computation cost in mind, a reasonably good level of theory B3LYP/6-311G* was selected to scan the coordinates for 1681 grid points (see Figure III. 5). Diagonal path to the 2D-scan graph mimics counter rotation of the two $CF_3$ groups. Orbital properties and their overlapping were observed using NBO 6.0[13] and Jmol[14] program for all molecules.

## III.4. Results and Discussion

Rotational constants for the AP and the SC conformers are very close to each other (Table III.2). These constants are for the optimized geometries at MP2/6-311++G(d,p) level. On the basis of predictions using these rotational constants, a search was started for a strong *b-type*

$4_{14} \leftarrow 3_{03}$ transition for the AP conformer, which was predicted at ~8465 MHz. The search was started at 8465 MHz with Ar as carrier gas. Within 10 MHz search, a transition was observed at 8473.8905 MHz. Next five signals were searched similarly on the basis of the predictions and were observed readily. These transitions were present at 9125.4651, 7059.1440, 10213.3467, 9526.6928 and 11161.5053 MHz and could be assigned to the $5_{05} \leftarrow 4_{14}$, $4_{04} \leftarrow 3_{13}$, $5_{15} \leftarrow 4_{04}$, $3_{21} \leftarrow 2_{12}$ and $6_{06} \leftarrow 5_{15}$, rotational transitions, respectively. All these signals depended on HFIP and were significantly stronger with He as the carrier gas. Ar is more polarizable than He. Therefore, Ar is more effective in forming complexes and thus reduces the concentration of the monomers. The above mentioned six transitions were fitted to a rigid rotor Hamiltonian. The rotational constants obtained from this tentative fitting were used for further predictions. In this way, eventually, a total of 111 transitions could be observed. One of these signals is shown in Figure III. 3.

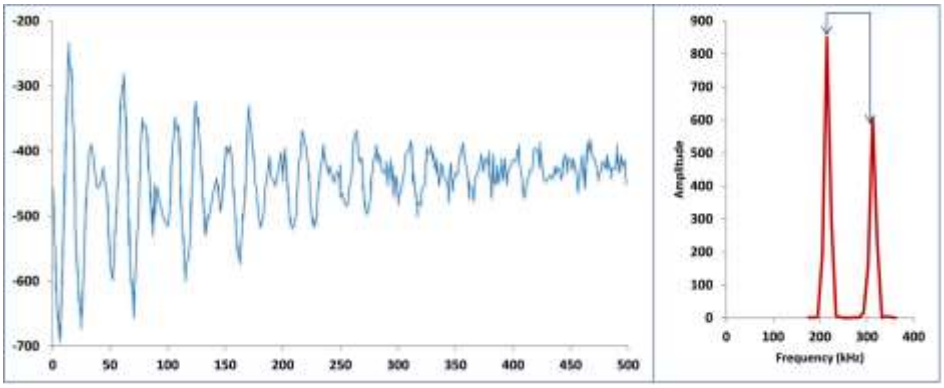


*Figure III. 3.A typical rotational transition for HFIP-monomer*

These transitions included both *b*- and *c-type* transitions of R and Q branches (Table III. 3). The observed transitions were fitted to Watson's S reduction Hamiltonian.[15] Programs used for the fitting were mainly SPFIT, [16,17] ASFIT,[18] and ASYM82[15] and as expected they produced the same results. The fitted rotational constants and distortion constants are listed in Table III.2. RMS deviation of the fit was 4 kHz. At this stage, it was not clear whether the observed progression is for the AP or the SC conformer. We were expecting the presence of other progressions corresponding to another conformer because of two reasons. First, IR, Raman and matrix isolation studies showed the presence of two conformers for HFIP and second, microwave study on prototype molecule isopropanol,[8,19] showed the presence two

isomers because of the internal motion of –OH group. Optimized geometry for the AP conformer has no *a-dipole* component. However, the SC conformer has finite dipole moment components along all the three (*a,b,c*) principal axes. Thus, for the SC conformer all the three types of transitions were expected. However, we could not observe any *a-type* transition even after performing long searches. These, searches were performed on the basis of ab initio rotational constants for both the AP and SC conformers. Absence of the *a-type* transitions suggested that experimentally observed spectra correspond to the AP conformer. However, another reason for not getting the *a-type* transitions for SC conformer could be a motion which averages out the *a-dipole* moment. Frequency calculations do predict one such motion. The barrier corresponding to such motion which averages out the a-dipole is 108.4 $cm^{-1}$. Energy required to cross this barrier is slightly less than the ZPE of the corresponding vibrational mode (109.5 $cm^{-1}$). The saddle point for this motion was synperiplanar structure, *vide supra*. While this may indicate that the observed spectra could be due to the SC conformer, more evidences favoring AP conformer are presented in the next paragraphs. Moreover, unlike the rotational spectra of the prototype HFIB and HFA-IM molecules, no doubling in rotational transitions of the HFIP molecule was observed. Reason behind this fact is discussed later.

*Table III. 1. Rotational transition frequencies for the AP conformer of HFIP are listed.*

| R-b type transitions | | | Q-b type transitions | | |
|---|---|---|---|---|---|
| $J, K_{-1}, K_{+1}$ <- $J, K_{-1}, K_{+1}$ | Frequency | Obs-Cal | $J, K_{-1}, K_{+1}$ <- $J, K_{-1}, K_{+1}$ | Frequency | Obs-Cal |
| 1, 1, 1 <- 0, 0, 0 | 3037.4637 | 0.0032 | 10, 4, 7 <- 10, 3, 8 | 7810.7660 | 0.0063 |
| 2, 1, 2 <- 1, 0, 1 | 4902.1380 | 0.0017 | 11, 4, 8 <- 11, 3, 9 | 7889.2270 | -0.0032 |
| 3, 0, 3 <- 2, 1, 2 | 4980.1636 | -0.0009 | 13, 3, 11 <- 13, 2, 12 | 7910.9312 | -0.0018 |
| 3, 1, 3 <- 2, 0, 2 | 6709.9531 | 0.0011 | 12, 4, 9 <- 12, 3, 10 | 8012.7315 | -0.0029 |
| 4, 0, 4 <- 3, 1, 3 | 7059.1440 | 0.0001 | 15, 2, 13 <- 15, 1, 14 | 8019.7668 | -0.0026 |
| 2, 2, 1 <- 1, 1, 0 | 7247.7030 | 0.0046 | 15, 3, 13 <- 15, 2, 14 | 9080.3805 | 0.0043 |
| 2, 2, 0 <- 1, 1, 1 | 7379.3140 | -0.0001 | 16, 4, 13 <- 16, 3, 14 | 9106.5263 | -0.0097 |
| 7, 2, 6 <- 6, 3, 3 | 8056.2860 | -0.0046 | 17, 4, 14 <- 17, 3, 15 | 9546.9948 | -0.0014 |
| 4, 1, 4 <- 3, 0, 3 | 8473.8905 | -0.0044 | 12, 5, 7 <- 12, 4, 8 | 9610.8610 | -0.0023 |
| 3, 2, 2 <- 2, 1, 1 | 9112.3672 | 0.0041 | 11, 5, 6 <- 11, 4, 7 | 9745.2899 | 0.0008 |
| 5, 0, 5 <- 4, 1, 4 | 9125.4651 | -0.0031 | 13, 5, 9 <- 13, 4, 10 | 9826.1295 | 0.0038 |
| 7, 2, 5 <- 6, 3, 4 | 9134.6363 | -0.0013 | 14, 5, 10 <- 14, 4, 11 | 9829.0117 | 0.0018 |
| 3, 2, 1 <- 2, 1, 2 | 9526.6928 | -0.0010 | 10, 5, 5 <- 10, 4, 6 | 9836.5750 | 0.0044 |
| 12, 6, 7 <- 11, 7, 4 | 9555.1948 | -0.0010 | 12, 5, 8 <- 12, 4, 9 | 9841.5585 | -0.0012 |
| 12, 6, 6 <- 11, 7, 5 | 9555.7447 | -0.0019 | 15, 5, 11 <- 15, 4, 12 | 9859.8783 | -0.0013 |
| 6, 1, 5 <- 5, 2, 4 | 9717.8613 | 0.0016 | 11, 5, 7 <- 11, 4, 8 | 9866.9440 | -0.0016 |
| 8, 2, 7 <- 7, 3, 4 | 9808.7553 | 0.0011 | 10, 5, 6 <- 10, 4, 7 | 9895.7021 | -0.0004 |
| 10, 4, 7 <- 9, 5, 4 | 10052.0152 | -0.0034 | 9, 5, 4 <- 9, 4, 5 | 9897.0826 | 0.0004 |
| 10, 4, 6 <- 9, 5, 5 | 10114.4290 | -0.0041 | 9, 5, 5 <- 9, 4, 6 | 9923.2200 | -0.0029 |
| 9, 3, 7 <- 8, 4, 4 | 10187.7490 | 0.0158 | 8, 5, 3 <- 8, 4, 4 | 9936.4800 | -0.0002 |
| 5, 1, 5 <- 4, 0, 4 | 10213.3467 | -0.0041 | 8, 5, 4 <- 8, 4, 5 | 9946.7705 | -0.0030 |
| 4, 2, 3 <- 3, 1, 2 | 10914.9394 | 0.0048 | 7, 5, 3 <- 7, 4, 4 | 9965.1802 | -0.0006 |
| 6, 0, 6 <- 5, 1, 5 | 11161.5053 | -0.0042 | 6, 5, 1 <- 6, 4, 2 | 9977.4400 | -0.0001 |
| 8, 2, 6 <- 7, 3, 5 | 11494.2363 | -0.0042 | 6, 5, 2 <- 6, 4, 3 | 9978.4076 | 0.0026 |
| 3, 3, 1 <- 2, 2, 0 | 11514.7876 | 0.0019 | 5, 5, 0 <- 5, 4, 1 | 9986.9165 | 0.0048 |
| 3, 3, 0 <- 2, 2, 1 | 11525.2593 | 0.0016 | 5, 5, 1 <- 5, 4, 2 | 9987.1125 | 0.0059 |
| 4, 2, 2 <- 3, 1, 3 | 11789.5221 | 0.0030 | 17, 5, 13 <- 17, 4, 14 | 10046.2949 | 0.0022 |
| 6, 1, 6 <- 5, 0, 5 | 11949.9311 | -0.0011 | 18, 4, 15 <- 18, 3, 16 | 10051.7417 | -0.0024 |
| 7, 1, 6 <- 6, 2, 5 | 12011.7074 | -0.0046 | 18, 5, 14 <- 18, 4, 15 | 10220.6673 | -0.0011 |
| 5, 2, 4 <- 4, 1, 3 | 12657.3443 | 0.0047 | 21, 5, 17 <- 21, 4, 18 | 11143.6080 | -0.0018 |
| 7, 0, 7 <- 6, 1, 6 | 13159.3272 | -0.0027 | 18, 6, 12 <- 18, 5, 13 | 11178.8705 | 0.0006 |
| 4, 3, 2 <- 3, 2, 1 | 13480.1583 | 0.0008 | 16, 6, 11 <- 16, 5, 12 | 11894.2363 | 0.0015 |
| 4, 3, 1 <- 3, 2, 2 | 13533.0925 | 0.0014 | 15, 6, 10 <- 15, 5, 11 | 11946.5814 | 0.0015 |
| 7, 1, 7 <- 6, 0, 6 | 13701.2685 | -0.0061 | 14, 6, 9 <- 14, 5, 10 | 11998.7516 | -0.0034 |
| 9, 2, 7 <- 8, 3, 6 | 13913.8562 | 0.0191 | 13, 6, 7 <- 13, 5, 8 | 12014.4102 | -0.0020 |
| 5, 2, 3 <- 4, 1, 4 | 14197.0979 | 0.0005 | 11, 6, 5 <- 11, 5, 6 | 12117.8300 | 0.0072 |
| 8, 1, 7 <- 7, 2, 6 | 14300.8539 | -0.0047 | 11, 6, 6 <- 11, 5, 7 | 12124.1070 | -0.0002 |
| 6, 2, 5 <- 5, 1, 4 | 14344.0340 | -0.0006 | 8, 6, 2 <- 8, 5, 3 | 12189.2087 | -0.0011 |
| 8, 0, 8 <- 7, 1, 7 | 15120.1191 | -0.0028 | 8, 6, 3 <- 8, 5, 4 | 12189.4432 | -0.0015 |
| 4, 4, 1 <- 3, 3, 0 | 15730.2270 | -0.0085 | 6, 6, 0 <- 6, 5, 1 | 12208.2040 | -0.0072 |
| 4, 4, 0 <- 3, 3, 1 | 15730.7660 | -0.0031 | 20, 7, 13 <- 20, 6, 14 | 13708.0022 | 0.0032 |
| Q-b type transitions | | | R-c type transitions | | |
| 6, 3, 3 <- 6, 2, 5 | 5771.3611 | 0.0014 | 1, 1, 0 <- 0, 0, 0 | 3159.1145 | -0.0014 |
| 9, 4, 5 <- 9, 3, 6 | 7378.2390 | 0.0020 | 2, 2, 0 <- 1, 1, 0 | 7257.6540 | -0.0047 |
| 8, 4, 4 <- 8, 3, 5 | 7541.1040 | -0.0006 | 2, 2, 1 <- 1, 1, 1 | 7369.3510 | -0.0028 |
| 6, 4, 2 <- 6, 3, 3 | 7710.9192 | 0.0032 | 3, 2, 1 <- 2, 1, 1 | 9161.7370 | 0.0090 |
| 21, 4, 17 <- 21, 3, 18 | 7713.0660 | 0.0043 | 4, 1, 3 <- 3, 0, 3 | 9686.8711 | -0.0036 |
| 5, 4, 1 <- 5, 3, 2 | 7745.9150 | -0.0015 | 4, 2, 2 <- 3, 1, 2 | 11060.1021 | 0.0018 |
| 7, 4, 4 <- 7, 3, 5 | 7746.3950 | 0.0012 | 3, 3, 0 <- 2, 2, 0 | 11515.2949 | -0.0025 |
| 8, 4, 5 <- 8, 3, 6 | 7748.9930 | -0.0015 | 3, 3, 1 <- 2, 2, 1 | 11524.7466 | 0.0007 |
| 6, 4, 3 <- 6, 3, 4 | 7751.8900 | -0.0022 | 4, 2, 3 <- 3, 1, 3 | 11644.3578 | 0.0044 |
| 12, 1, 11 <- 12, 0, 12 | 7758.0370 | 0.0015 | 5, 1, 4 <- 4, 0, 4 | 12023.9954 | -0.0041 |
| 5, 4, 2 <- 5, 3, 3 | 7759.8930 | 0.0033 | 5, 2, 3 <- 4, 1, 3 | 12984.1168 | -0.0008 |
| 4, 4, 0 <- 4, 3, 1 | 7763.4470 | 0.0084 | 4, 3, 1 <- 3, 2, 1 | 13483.7364 | 0.0102 |
| 4, 4, 1 <- 4, 3, 2 | 7766.9900 | 0.0044 | 4, 3, 2 <- 3, 2, 2 | 13529.5239 | 0.0015 |
| 9, 4, 6 <- 9, 3, 7 | 7767.3660 | -0.0005 | Q-c type transitions | | |
| | | | 9, 5, 5 <- 9, 4, 5 | 9896.2570 | 0.0011 |
| | | | 5, 5, 1 <- 5, 4, 1 | 9986.8900 | -0.0209 |

*Table III.2. Experimental and theoretical rotational and distortion constants for hexafluoroisopropanol are listed.*

| | Experimental | Calculated (ap) | Calculated (sc) |
|---|---|---|---|
| A/MHz | 2105.12166(18)[a] | 2098.76488 | 2102.51954 |
| B/MHz | 1053.99503(12) | 1053.29499 | 1054.01680 |
| C/MHz | 932.33959(13) | 931.98682 | 932.48540 |
| $D_J$/kHz | 0.05713(79) | 0.0522 | 0.0560 |
| $D_{JK}$/kHz | 0.50829(76) | 0.2635 | 0.2317 |
| $D_K$/kHz | -0.4592(41) | -0.2125 | -0.1833 |
| $d_1$/kHz | -0.00731(13) | -0.0068 | -0.0075 |
| $d_2$/kHz | 0.002357(59) | 0.0015 | 0.0017 |
| RMS (MHz) | 0.0048 | | |
| No. of transitions | 111 | | |
| Dipole Moment (a, b, c) Debye | a = 0<br>b > c ≠ 0 | 0.0, 0.6, 0.2 | 1.2, 1.5, 2.2 |

[a] *Number in parentheses are signal standard errors in unit of least significant figures.*

*Table III. 3. Rotational transition frequencies for HFIP-OD molecule are listed.*

| TRANSITION<br>J, $K_{-1}$, $K_{+1}$ <- J, $K_{-1}$, $K_{+1}$ | Type | Observed (MHz) | Obs-Calc (MHz) |
|---|---|---|---|
| 1, 1, 1 <- 0, 0, 0 | b | 2992.2562 | 0.0083 |
| 4, 0, 4 <- 3, 1, 3 | b | 7061.1912 | 0.0048 |
| 2, 2, 1 <- 1, 1, 0 | b | 7125.5320 | -0.0010 |
| 2, 2, 0 <- 1, 1, 0 | c | 7136.7565 | 0.0010 |
| 2, 2, 0 <- 1, 1, 1 | b | 7263.8851 | -0.0089 |
| 4, 1, 4 <- 3, 0, 3 | b | 8383.2581 | -0.0045 |
| 3, 2, 2 <- 2, 1, 1 | b | 8976.7290 | 0.0012 |
| 3, 2, 1 <- 2, 1, 1 | c | 9032.2717 | 0.0010 |
| 5, 1, 5 <- 4, 0, 4 | b | 10108.0501 | -0.0001 |
| 4, 2, 3 <- 3, 1, 2 | b | 10762.9521 | -0.0004 |
| 6, 0, 6 <- 5, 1, 5 | b | 11128.9483 | 0.0042 |
| 3, 3, 1 <- 2, 2, 0 | b | 11317.8825 | -0.0080 |
| 3, 3, 0 <- 2, 2, 1 | b | 11329.7461 | 0.0110 |
| 6, 1, 6 <- 5, 0, 5 | b | 11833.1368 | -0.0033 |
| 7, 1, 6 <- 6, 2, 5 | b | 12098.5827 | -0.0058 |
| 5, 2, 4 <- 4, 1, 3 | b | 12486.4826 | 0.0006 |
| 5, 2, 3 <- 4, 1, 3 | c | 12851.2217 | -0.0022 |
| 7, 0, 7 <- 6, 1, 6 | b | 13104.8094 | -0.0040 |
| 4, 3, 2 <- 3, 2, 1 | b | 13272.5893 | 0.0056 |
| 4, 3, 1 <- 3, 2, 1 | c | 13276.9191 | -0.0001 |
| 7, 1, 7 <- 6, 0, 6 | b | 13576.1680 | 0.0062 |
| 6, 2, 5 <- 5, 1, 4 | b | 14152.5965 | -0.0020 |
| 8, 1, 7 <- 7, 2, 6 | b | 14374.3448 | 0.0046 |
| 8, 0, 8 <- 7, 1, 7 | b | 15043.2703 | -0.0023 |
| 8, 1, 8 <- 7, 0, 7 | b | 15344.8770 | 0.0004 |
| 4, 4, 1 <- 3, 3, 0 | b | 15457.0527 | -0.0023 |

*Table III. 4. Rotational transition frequencies for HFIP-CD-OD molecule are listed.*

| TRANSITION | | Observed | Obs-Calc |
|---|---|---|---|
| J, $K_{-1}$, $K_{+1}$ <- J, $K_{-1}$, $K_{+1}$ | Type | (MHz) | (MHz) |
| 5, 0, 5 <- 4, 1, 4 | b | 9095.7415 | 0.0049 |
| 3, 1, 3 <- 2, 0, 2 | b | 6611.5240 | 0.0207 |
| 5, 1, 5 <- 4, 0, 4 | b | 10090.5135 | -0.0102 |
| 3, 2, 2 <- 2, 1, 1 | b | 8901.7330 | 0.0022 |
| 2, 2, 0 <- 1, 1, 1 | b | 7183.3315 | -0.0105 |
| 3, 3, 1 <- 2, 2, 0 | b | 11191.9822 | 0.0093 |
| 3, 3, 0 <- 2, 2, 1 | b | 11202.9940 | -0.0131 |
| 3, 3, 0 <- 2, 2, 0 | c | 11192.5486 | 0.0097 |
| 5, 2, 4 <- 4, 1, 3 | b | 12418.3510 | -0.0193 |
| 7, 1, 6 <- 6, 2, 5 | b | 12061.6020 | -0.0047 |
| 4, 4, 1 <- 3, 3, 0 | b | 15281.5220 | -0.0029 |
| 4, 4, 0 <- 3, 3, 1 | b | 15282.1090 | -0.0072 |
| 6, 0, 6 <- 5, 1, 5 | b | 11108.5685 | -0.0074 |
| 6, 1, 6 <- 5, 0, 5 | b | 11817.9070 | -0.0069 |
| 7, 0, 7 <- 6, 1, 6 | b | 13082.6790 | 0.0029 |
| 4, 3, 2 <- 3, 2, 1 | b | 13141.9180 | 0.0145 |
| 7, 1, 7 <- 6, 0, 6 | b | 13561.7000 | 0.0035 |
| 4, 3, 1 <- 3, 2, 2 | b | 13197.7002 | 0.0167 |
| 6, 2, 5 <- 5, 1, 4 | b | 14091.5100 | -0.0203 |
| 8, 1, 7 <- 7, 2, 6 | b | 14324.1020 | 0.0026 |
| 8, 0, 8 <- 7, 1, 7 | b | 15020.5585 | 0.0018 |
| 5, 3, 2 <- 4, 2, 2 | c | 15067.7800 | 0.0019 |
| 5, 3, 3 <- 4, 2, 2 | b | 15052.1390 | 0.0121 |
| 5, 3, 2 <- 4, 2, 3 | b | 15219.8900 | -0.0134 |
| 8, 1, 8 <- 7, 0, 7 | b | 15329.8850 | 0.0011 |
| 7, 2, 6 <- 6, 1, 5 | b | 15718.3540 | 0.0118 |
| 4, 1, 4 <- 3, 0, 3 | b | 8362.4050 | 0.0168 |
| 2, 2, 1 <- 1, 1, 0 | b | 7051.3020 | -0.0142 |

*Table III. 5. Rotational transition frequencies for HFIP-C-13 (center) molecule.*

| TRANSITION | | Observed | Obs-Calc |
|---|---|---|---|
| J, $K_{-1}$, $K_{+1}$ <- J, $K_{-1}$, $K_{+1}$ | Type | (MHz) | (MHz) |
| 6, 1, 6 <- 5, 0, 5 | b | 11940.649 | 0.007 |
| 5, 3, 2 <- 4, 2, 3 | b | 15538.606 | 0.003 |
| 4, 4, 1 <- 3, 3, 0 | b | 15693.337 | 0.000 |
| 3, 3, 1 <- 2, 2, 0 | b | 11488.268 | -0.001 |
| 3, 3, 0 <- 2, 2, 1 | b | 11498.776 | 0.007 |
| 5, 3, 3 <- 4, 2, 2 | b | 15378.841 | -0.003 |
| 8, 0, 8 <- 7, 1, 7 | b | 15113.683 | -0.003 |

| | | | |
|---|---|---|---|
| 8, 1, 8 <- 7, 0, 7 | b | 15466.534 | -0.000 |
| 7, 0, 7 <- 6, 1, 6 | b | 13154.473 | 0.000 |
| 4, 3, 1 <- 3, 2, 2 | b | 13505.644 | -0.002 |
| 4, 4, 0 <- 3, 3, 1 | b | 15693.87 | -0.003 |
| 6, 0, 6 <- 5, 1, 5 | b | 11158.3075 | -0.001 |
| 7, 1, 7 <- 6, 0, 6 | b | 13691.61 | 0.003 |
| 3, 1, 3 <- 2, 0, 2 | b | 6702.517 | -0.007 |
| 4, 2, 3 <- 3, 1, 2 | b | 10897.085 | -0.011 |
| 5, 0, 5 <- 4, 1, 4 | b | 9123.916 | 0.003 |
| 4, 3, 2 <- 3, 2, 1 | b | 13452.576 | 0.007 |

*Table III. 6. Rotational transition frequencies for HFIP-C-13 (side) molecule.*

| TRANSITION | | Observed | Obs-Calc |
|---|---|---|---|
| J, $K_{-1}$, $K_{+1}$ <- J, $K_{-1}$, $K_{+1}$ | Type | (MHz) | (MHz) |
| 4, 0, 4 <- 3, 1, 3 | b | 7030.303 | -0.012 |
| 5, 0, 5 <- 4, 1, 4 | b | 9090.973 | -0.001 |
| 6, 0, 6 <- 5, 1, 5 | b | 11121.912 | 0.014 |
| 4, 1, 4 <- 3, 0, 3 | b | 8454.937 | 0.001 |
| 5, 1, 5 <- 4, 0, 4 | b | 10189.076 | 0.010 |
| 6, 1, 6 <- 5, 0, 5 | b | 11919.964 | 0.000 |
| 3, 2, 2 <- 2, 1, 1 | b | 9103.778 | 0.011 |
| 5, 2, 4 <- 4, 1, 3 | b | 12638.658 | 0.002 |
| 4, 3, 2 <- 3, 2, 1 | b | 13470.693 | -0.000 |
| 4, 3, 1 <- 3, 2, 2 | b | 13522.800 | -0.004 |
| 4, 4, 1 <- 3, 3, 0 | b | 15726.622 | 0.004 |
| 4, 4, 0 <- 3, 3, 1 | b | 15727.138 | -0.001 |
| 7, 1, 7 <- 6, 0, 6 | b | 13665.221 | -0.006 |
| 3, 3, 0 <- 2, 2, 1 | b | 11521.676 | -0.003 |
| 3, 3, 1 <- 2, 2, 0 | b | 11511.368 | -0.002 |
| 8, 1, 8 <- 7, 0, 7 | b | 15434.177 | -0.003 |
| 8, 0, 8 <- 7, 1, 7 | b | 15071.107 | -0.001 |
| 5, 3, 2 <- 4, 2, 3 | b | 15549.502 | 0.002 |
| 3, 1, 3 <- 2, 0, 2 | b | 6696.157 | -0.016 |
| 4, 2, 3 <- 3, 1, 2 | b | 10901.114 | -0.003 |
| 6, 2, 5 <- 5, 1, 4 | b | 14320.749 | 0.003 |
| 5, 3, 3 <- 4, 2, 2 | b | 15392.621 | -0.002 |

Signal intensity also helped us in identifying the conformer. For the observed progression, *b-type* signals were always stronger than *c-type*. This observation was consistent with the calculated dipole moment of the AP conformer geometry for which the *b-dipole* component

(0.6 Debye) was larger than the *c-dipole* component (0.2 Debye). On the contrary, for the SC conformer, *c-dipole* component (2.1 Debye) was larger than both the *b-dipole* (1.8 Debye) and *a-dipole* (1.0 Debye) components. These findings strongly suggest that the observed rotational transitions correspond to the AP conformer.

*Table III. 7. Fitted rotational and distortion constants, RMS values and number of transitions for four different isotopologues of HFIP.*

| | $CF_3$-C(H)(OH)-$CF_3$ | $CF_3$-C(H)(OD)-$CF_3$ | $CF_3$-C(D)(OD)-$CF_3$ | $CF_3$-$^{13}$C(H)(OH)-$CF_3$ | $^{13}CF_3$-C(H)(OH)-$CF_3$ |
|---|---|---|---|---|---|
| A/MHz | 2105.12166(18) | 2066.6444(10) | 2042.0355(23) | 2099.9217(16) | 2105.0638(18) |
| B/MHz | 1053.99503(12) | 1052.74254(91) | 1046.7717(10) | 1053.43442(63) | 1050.43361(72) |
| C/MHz | 932.33959(13) | 925.60404(54) | 925.2142(10) | 931.88122(63) | 929.53229(60) |
| $D_J$/kHz | 0.05713(79) | 0.0552(55) | 0.0486(97) | 0.0492(57) | 0.0528(59) |
| $D_{JK}$/kHz | 0.50829(76) | 0.442(55) | 0.508(74) | 0.481(53) | 0.525(62) |
| $D_K$/kHz | -0.4592(41) | -0.483(71) | -0.54(11) | -0.460(60) | -0.411(74) |
| $d_1$/kHz | -0.00731(13) | -0.0089(37) | -0.00731 | -0.00731 | -0.00731 |
| $d_2$/kHz | 0.002357(59) | 0.0059(35) | 0.002357 | 0.002357 | 0.002357 |
| RMS | 0.0048 | 0.0056 | 0.013 | 0.0057 | 0.0076 |
| #N | 111 | 26 | 28 | 17 | 22 |

*a Numbers without parentheses are not included in fit. Monomer's values are used for that particular fitting.*

Since experimentally observed rotational constants were close to the calculated ones, predictions of spectra for the other isotopologues were easy. We took the difference between the experimental and calculated rotational constants of the parent molecule and assumed the same difference for the rotational constants of the other isotopologues. Rotational spectra for four different isotopologues, $CF_3$-C(H)(OD)-$CF_3$ or HFIP(OD), $CF_3$-C(D)(OD)-$CF_3$ or HFIP(CDOD), $CF_3$-$^{13}$C(H)(OH)-$CF_3$ or HFIP-13(center) and $^{13}CF_3$-C(H)(OH)-$CF_3$ or HFIP-13(side) could be observed experimentally. Observed transitions for HFIP(OD), HFIP(CDOD), HFIP-13(center) and HFIP-13(side) isotopologues are presented in Table III. 3, Table III. 4, Table III. 5 and Table III. 6, respectively. These transitions could be fitted within the experimental uncertainty. The rotational constants obtained from these fits are given in Table III. 7. We could observe only one set of rotational constants for the side C-13

carbon. The signals for the HFIP-13(side) isotopologue were more intense (approximately double) than the signals for the HFIP-13(center) isotopologue. This indicated that the side C atoms are identical which is in accordance to the ab initio results on the AP conformer. In the calculated structure the molecule exhibited a plane of symmetry containing H2-O1-C1-H1 atoms. However, both the side C atoms are different for the SC conformer in its equilibrium structure and there is no plane of symmetry. This fact again indicates that observed spectrum corresponds to the AP conformer. HFIP(OD) and HFIP(ODCD) isotopologues were comparatively easier to observe experimentally. Because of the presence of D-atom, transitions split into two or more lines. This is because of the hyperfine splitting due to D nucleus. However, the hyperfine splitting could not be resolved well and line centers were used in the fit.

With the help of Kraitchman analysis,[20] position of the isotopic substitution can be determined. The basic assumption of the theory is that the bond length of the molecule remains unchanged on isotopic substitution. This assumption is quite reasonable in the case of heavy atoms substitution in stable molecules. Kisiel's programs[18] were used for this analysis. Using rotational constants of the five isotopologues, Cartesian coordinates of the substituted atoms were determined. Along with direct bonded parameter, some non-bonded parameters were also measured. These parameters again supported the AP conformer, e.g. the distance between center of mass to H2 distance was equal to the calculated distance for AP conformer and significantly different for SC conformer (Table III. 8). Moreover, experimental H1-C1-H2 angle and C3-C1-H2-C2 dihedral angle were also close to calculated values of AP conformer. These are the strong evidences in support of AP conformer.

*Table III. 8. Results from Kraitchman's analysis for HFIP molecules, using the rotational constants of the different isotopologues.*

| Parameters | Experimental value | Calculated (AP) | Calculated (SC) |
|---|---|---|---|
| C1-C2 | 1.530(7) | 1.531 | 1.531 |
| C1-C3 | 1.530(7) | 1.531 | 1.527 |
| C1-H1 | 1.121(3) | 1.092 | 1.097 |
| C1-H2 | 1.935(3) | 1.930 | 1.930 |
| CM-H2 | 2.119(1) | 2.109 | 2.511 |
| | | | |
| C2-C1-C3 | 113.2(6) | 114.1 | 113.9 |
| H1-C1-C2 | 103.9(7) | 107.2 | 106.5 |
| H1-C1-C3 | 113.2(7) | 107.2 | 106.5 |
| H1-C1-H2 | 137.4(3) | 135.9 | 94.5 |
| | | | |
| C2-C1-H1-C3 | 123.2(8) | 122.8 | 121.9 |
| C3-C1-H2-C2 | 113.5(5) | 115.1 | 134.6 |

To examine the behavior of $CF_3$-C-$CF_3$ group, comparisons of HFIP with other prototype molecules, HFIB, HFA-IM, hexafluoroacetone (HFA), hexafluoroisobutane or HFI-CH3 ($CF_3$-C(H)($CH_3$)-$CF_3$) and hexafluoroisopropylamine or HFI-NH2 ($CF_3$-C(H)($NH_2$)-$CF_3$) have been done. Equilibrium geometries of these molecules are shown in Figure III. 4. Rotational constants were taken from the earlier works[9,10,21] and we fitted them back into the internal coordinates (Table III. 9). HFA monomer[22] did not show splitting in the rotational transitions. Also, the isotopic studies are not known for this molecule. Therefore, we used the calculated parameters for this molecule for the further analysis. The 2D-PES scan showed that two types of barriers exist for HFIB, HFA and HFA-IM (say; large and small). On the other hand, for the HFIP, HFI-CH3 and HFI-NH2 molecules only one (large) barrier was present. The large barriers, in all these molecules, are due to the $CF_3$ counter rotation which interconverts the staggered and the eclipse forms of these molecules (Figure III. 5). The smaller barrier is due to the restricted counter rotation of the two $CF_3$ groups present in these

molecules. Saddle points for the small barrier are marked in the figure by small green dots and are pointed by arrow. Compiled results are presented in Figure III. 6 and Table III. 10. Barrier heights can be extracted from these scanning calculations. The barrier heights corresponding to the staggered-eclipse interchange are very large and thus these should not be responsible for the doubling observed in the rotational spectra of HFIB and HFA-IM molecules. About small barrier, discussion has been done later. A representative one dimensional PES for all the molecules is shown in Figure III. 6. As discussed earlier, for some molecules the smaller barrier is not present. The Position 1in the PES represents saddle points for large barrier. Geometries at this saddle point, for all the molecules are shown in Figure III. S. 1 (a1-f1) of the supporting information which is given at the end of the chapter. In all these geometries, the two $CF_3$ groups were eclipsed. For most of the $CF_3$-C($sp^3$)-$CF_3$ type molecules, the most stable geometries are those in which the terminal $CF_3$ groups are eclipsed with respect to each other and are staggered with respect to the center carbon substituents (Figure III. 4 (d, e, f) or Figure III. S. 1 (d3, e3, f3)). The HFI-NH2 molecule is exception to this and the most stable structure for this molecule has slightly staggered $CF_3$ groups. For $CF_3$-C($sp^2$)-$CF_3$ group of molecules, the position 3 in Figure III. 6 correspond to the saddle points for the small barriers. The geometries corresponding to this point are given for all the molecules in Figure III. S. 1(a3, b3, c3). In these geometries both the $CF_3$ groups are eclipsed to each other as well as to the double bond. For molecules belonging to $CF_3$-C($sp^2$)-$CF_3$ type, equilibrium structures (position 2 or 4 in Figure III. 6) were slightly staggered (Figure III. 4 (a, b, c) and Figure III. S. 1(a2, b2, c2). At MP2/6-311++G(d,p) level of theory, cartesian coordinates of equilibrium geometries are given for all the molecules in Table III. S. 3.

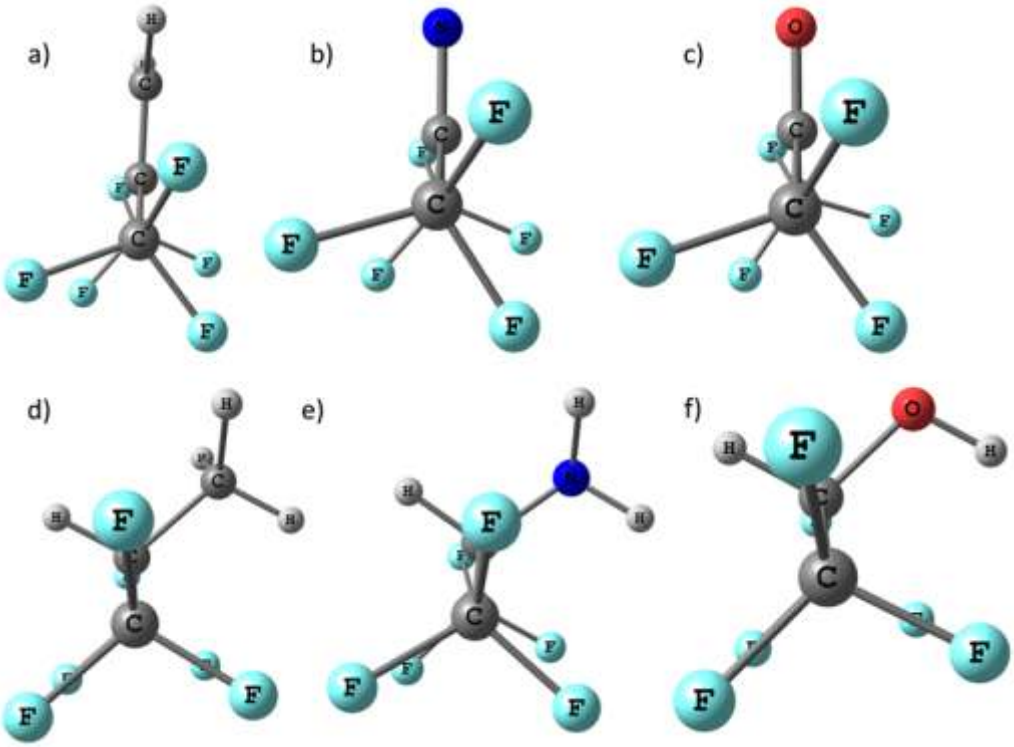


*Figure III. 4. Equilibrium geometries of the prototype molecules,*
*a) hexafluoroisobutene (HFIB), b) hexafluoroacetone imine (HFA-IM), c) hexafluoroacetone (HFA), d) hexafluoroisobutane (HFI-CH3), e) hexafluoroisopropylamine (HFI-NH2) and f) hexafluoroisopropanol (HFIP).*

*Table III. 9. Geometrical parameters obtained from the Kraitchman's analysis for HFIP, HFIB, HFA-IM and hexafluoropropane. For HFA ab initio calculated parameters are reported. All distances are in Å.*

| Parameters | Value (v=0) | Value(V=1) | Calculated |
|---|---|---|---|
| Hexafluoroisobutene (HFIB) | | | |
| C1-C2 | 1.465(2) | 1.462(3) | 1.507 |
| C1-C3 | 1.465(2) | 1.462(3) | 1.507 |
| C1-C4 | 1.339(4) | 1.340(4) | 1.337 |
| C2-C1-C3 | 121.0(2) | 121.0(3) | 116.7 |
| C2-C1-C4 | 116.1(12) | 119.5(2) | 121.6 |
| C3-C1-C4 | 122.9(12) | 119.5(2) | 121.6 |
| C2-C1-C4-C3 | 180(0) | 177.3(79) | 180.0 |
| Hexafluoroacetone Imine (HFA-IM) | | | |
| C1-C3 | 1.486(02) | 1.487(2) | 1.528 |
| C1-C2 | 1.490(29) | 1.478(2) | 1.525 |
| C1-N1 | 1.268(03) | 1.270(3) | 1.271 |
| C2-C1-C3 | 120.5(19) | 121.4(2) | 116.4 |
| N1-C1-C2 | 117.5(22) | 115.9(9) | 118.6 |
| N1-C1-C3 | 121.9(11) | 122.3(9) | 125 |
| C2-C1-N1-C3 | 177.5(116) | 172.8(40) | -179.0 |
| Hexafluoroacetone (HFA) | | | |
| C1-C2 | | | 1.547 |
| C1-C3 | | | 1.547 |
| C1-O1 | | | 1.203 |
| O1-C1-C2 | | | 121.8 |
| O1-C1-C3 | | | 121.8 |
| C2-C1-C3 | | | 116.4 |
| C1-C2-O1-C3 | | | 180.0 |

So far, we have characterized these molecules into two types, 'type I' with small barriers (e.g. HFIB, HFA and HFA-IM) and 'type II' without small barriers (e.g. HFIP, HFI-CH3 and HFI-NH2). Type I' and 'type II' will be used further as short hand notations. There were two important structural differences between type I and type II molecules. The first difference is that the two $CF_3$ groups are slightly staggered in type I molecules while these are eclipsed in type II molecules. The second difference is the hybridization of the middle carbon atom. Type I has center carbon in $sp^2$ hybridization and type II has center carbon in $sp^3$ hybridization. For the HFIP molecule, C-C bond lengths were 1.53 Å and angles at the centre carbon were close to tetrahedral angles which are typical features of the $sp^3$ C-atoms. However, in the HFIB and HFA-IM, C-C bond lengths were close to 1.47 Å and angles at the centre carbon were close to 120° which are typical of $sp^2$ carbon atom (Figure III. 4 and Table III. 9). Interestingly, HFA showed a longer C-C bond (1.55 Å) than expected, even though center C-atom was $sp^2$ hybridized and bond angles were close to 120°. Furthermore,

HFA did not show splitting in rotational spectrum even when small barrier is present and equilibrium geometry was slightly staggered. Overall, HFA was different from HFIB and HFA-IM in these aspects. Inspection of small barrier revealed the reason behind the presence/absence of doubling in the rotational transitions. For HFA, the height for the 'small barrier' was much more (0.91 kcal/mole) as compared to that for HFIB (0.32 kcal/mol) and HFA-IM (0.57 kcal/mole). Also, experimental splitting for HFIB is 10s of MHz[9] and for HFA-IM is 10s of kHz.[10] Resolving splitting below 5 kHz is not possible with the sensitivity of typical microwave spectrometers. The high barrier for the HFA molecule suggests that the splitting in case of this molecule should be of the order of 100s of Hz or less. In other words, because of this high barrier, tunneling was so small to be observed for this molecule. Moreover, there was a vibrational motion corresponding to counter motion of the $CF_3$ groups with frequencies 47, 59 and 60 $cm^{-1}$ for HFIB, HFA and HFA-IM respectively at the MP2/6-311++G(d,p). The ZPE corresponding to these motions are 0.06, 0.08 and 0.08 $cm^{-1}$ respectively. Thus, the small barriers were always larger than the ZPE corresponding to this vibrational mode for all the molecules. If the barrier height is less than ZPE, tunneling splitting cannot be observed since the motion will be free. To the best of our knowledge, microwave spectra of the HFA-IM and HFI-CH3 have not been studied till date. However, one laboratory is planning to study the rotational spectra of these molecules. Our prediction says that both molecules should not show doubling due to the counter rotation of the two $CF_3$ groups.

Ab initio calculations and experimental results showed that, slightly staggered conformer (skew conformer) was the equilibrium structure for HFIB. Now we will address this question, why skew conformer was global minimum for HFIB. For this purpose, NBO

calculations were performed for both the skew conformer (equilibrium geometry) and the eclipsed conformer (saddle point geometry). The overlapping between C1-C10 π-bonding orbitals and C2-F4 and C3-F9 antibonding orbitals was more in skew conformer than eclipsed conformer. The extent of overlapping between two orbitals (donor and acceptor) causes stabilization in the molecule and the corresponding stabilization energy can be extracted from the second order perturbation analysis in NBO basis. Since HFIB molecule shows overlapping between many orbitals, it was complicated to conclude about the conformational preference on the basis of extent of orbital overlapping for some specific MOs. However, we noticed that there were many orbital overlaps which led to more stabilization when eclipsed conformer changes to skew conformer. Also, some overlap between some other orbitals is lost during interchange. Note that the energy difference between both conformers was very small i.e. 1.34 kJ/mol. Finally, we decided to sum up all stabilization energies (second order perturbation energies) of a particular conformer. The total sums for the skew conformer and eclipsed conformer were 2713.95 and 2713.23 kJ/mol, respectively. Qualitatively, these values supported that the skew conformer is more stable than the eclipsed conformer. Of course, this is similar to the approach calculating the stabilization energy for weakly bound molecular complexes i.e. subtracting very large values to obtain a small difference. To the best of our knowledge, this approach is new, introduced first time to confirm the conformational preference. The electronic energy difference between two conformers was 1.34 kJ/mol and total stabilization energy difference was 0.67 kJ/mol. We were not expecting the exact matching between them because they were calculated by two different approaches.

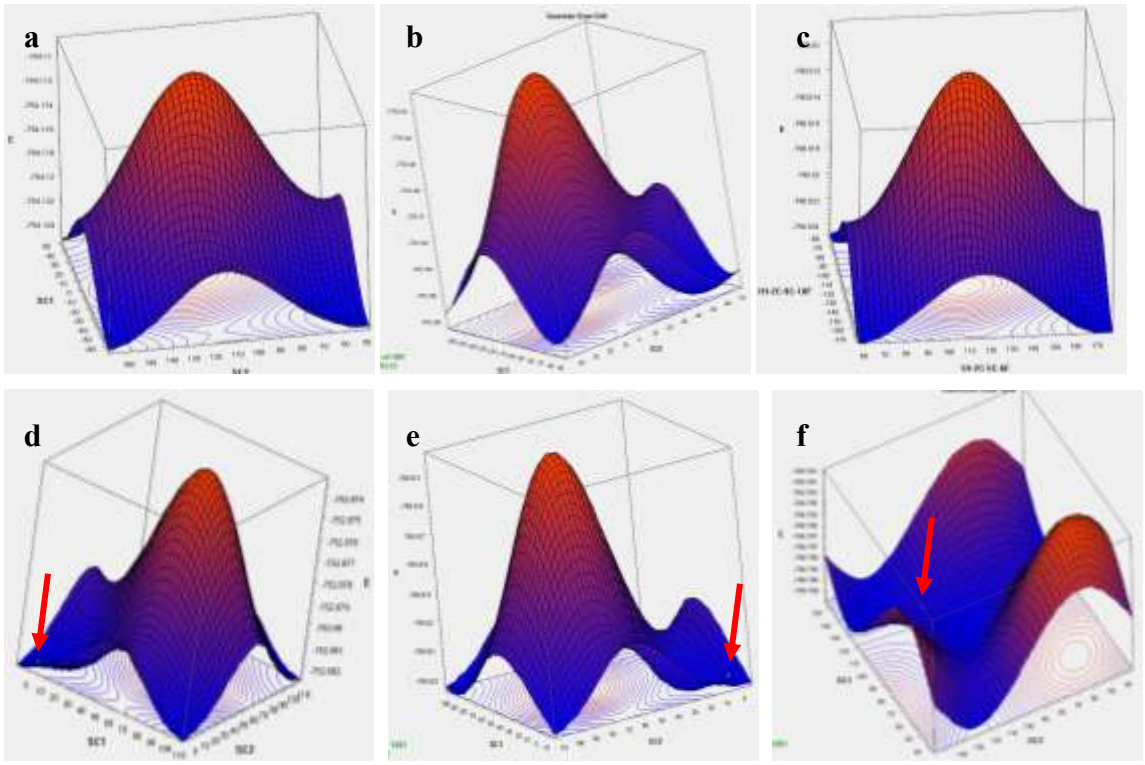


*Figure III. 5. 2D-PES scan for the $CF_3$ counter rotation,*
*a) hexafluoroisopropanol, b) hexafluoroisopropylamine, c) hexafluoroisobutane, d) hexafluoroisobutene, e) hexafluoroacetone imine and f) hexafluoroacetone molecules. In figure d, e and f, green dots (denoted by arrow) represent the small barrier and corresponding structures are saddle points.*

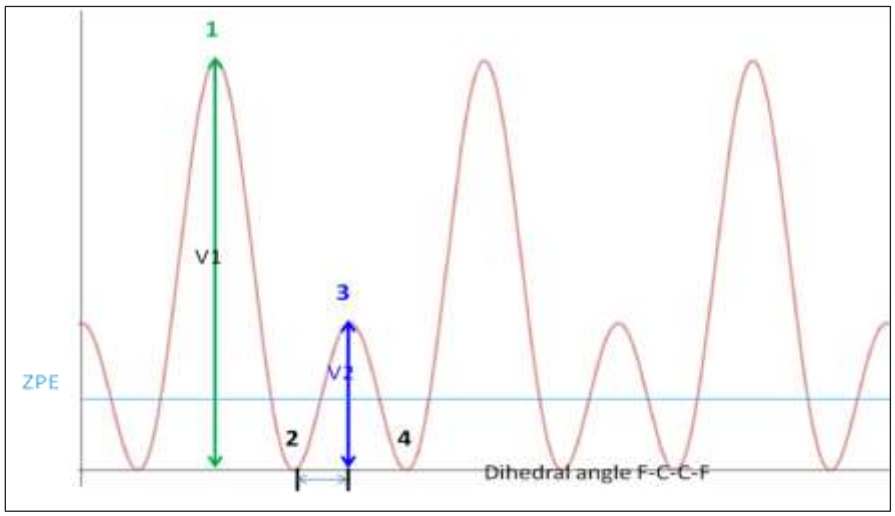


*Figure III. 6. Barrier for counter rotation of $CF_3$ groups.*
*The energy values for different positions are given in Table III. 10. Their structures are presented in Figure III. S. 1.*

*Table III. 10. Barrier height, angle and ZPE for all prototype molecules.*

| Properties | position | HFIB | HFA-IM | HFA | HFIP | HFI-CH3 | HFI-NH2 |
|---|---|---|---|---|---|---|---|
| Energy for large barrier (V1) (kJ/mol) | 1 | 25 | 21 | 15 | 43 | 45 | 47 |
| Energy for small barrier(V2) (kJ/mol) | 2 | 0 | 0 | 0 | 0 | 0 | 0 |
| | 3 | 0.22 | 0.78 | 1.56 | | | |
| | 4 | 0 | 0 | 0 | | | |
| Dihedral angle F-C-C=X | 1 | -30 | -42 | -52 | 0* | 0* | 25* |
| | 2 | 0 | 0 | 0 | | | |
| | 3 | 30 | 42 | 52 | | | |
| vibrational freq | $cm^{-1}$ | 30.54 | 23.79 | 36.78 | 21.83 | 25.72 | 39.69 |
| ZPE | kJ/mol | 0.18 | 0.14 | 0.22 | 0.13 | 0.15 | 0.24 |
| Experimental splitting | | 10s MHz | 10s kHz | Not observed | No barrier, no splitting | | |

**F-C-C-F dihedral angle. Numbers 1,2,3 and 4 are the position at PES scan of Figure III. 6.*

In the same way, we can also explain why AP conformer was more stable than SC. Orientation of lone pairs on O-atom were the important factor in deciding the more stable conformer. In the AP conformation, the lone pair on O-atom overlapped with C1-C2 and C1-C3 antibonding orbital with equal extent. Another lone pair of O-atom overlapped well with the C-H antibonding and O-H bonding MO overlapped with C-H antibonding MO. These two overlapping were the important reasons for AP conformer to be more stable than the SC conformer. Again, monitoring each overlapping and deciding on the basis of that, is a complicated procedure which can lead to an ambiguous result. The total second order perturbation energy sum for AP and SC conformers were 2557.41 and 2538.97 kJ/mol which predicts that AP was more stable than SC. However, electronic energy difference between two conformers is 5.02 kJ/mol.

## III.5. Conclusion

HFIP and its four isotopologues have been observed experimentally using PNFTMW spectrometer. Observed 111 transitions could be fitted well to Watson's S reduction

Hamiltonian within the experimental uncertainties. Rotational constants for AP and SC were close and it was challenging to prove that observed transitions corresponded to the AP conformer. Absence of *a-type* transitions and the fact that *b-type* transitions are stronger than the *c-type* of transitions provide some evidence in support of AP conformer as the experimental observed structure. With the help of different set of rotational constants, obtained from different isotopologues, structure of HFIP was determined. The obtained structure was another evidence for the AP conformer. In supersonic beam experiment, only antiperiplanar conformer was present. Because of the absence of small barrier, doubling in spectrum was not present. We performed 2D-PES scan for prototype molecules. This is a general effect of $CF_3$-C-$CF_3$ group: if center carbon atom is $sp^2$ hybridized, a small barrier will be there and rotational spectra will show splitting if conditions match. If center carbon was $sp^3$, there would be no small barrier and hence no splitting of rotational transitions will be present. HFIB, HFA-IM and HFA, all exhibited small barrier but splitting could be observed only for HFIB and HFA-IM. HFA has small barrier but barrier height is significantly larger than the other two molecules and we suspect that splitting is too small to be observed using a typical microwave spectrometer. With the help of NBO calculations, reasons for a particular conformational preference can be explained. Total second order perturbation energy for a molecule can give an idea about the conformational preference, a new approach proposed here. We hope that this approach can be generalized and used extensively.

## III.6. Supporting Information

In supporting information, coordinates and normal mode vibrational frequencies are given for the AP and the SC conformer (Table III. S. 1 and Table III. S. 2). Along with this, different

structures of all the prototype molecules corresponding to the different positions in Figure III. 6, are shown (Figure III. S. 1). Coordinates of the prototype of the molecules are also given (Table III. S. 3).

## III.7. Future Work

During experiments we observed some signals which could not be fit in the monomer pattern. These unassigned lines may be from HFIP-dimer or any other possible oligomer of HFIP. The unassigned lines are given in appendix II. Microwave spectra of HFA-IM and HFA-CH3 need to be measured to confirm the predictions.

**In Addition:** On the referee's suggestion, following paragraphs are added.

The following points explain the absence of SC conformer,

- Geometrical parameters from the Kraitchman's analysis of the isotopic data. (see table III.8).
- Calculated energy (see page 51).
- Barrier of PES scan (see figure III.2).
- The b-type signals were stronger than the c-type signals.
- Absence of a-type dipole moment (see page 55).

From the previous study (Barnes at al. *J. Chem. Soc. Faraday Trans. 2*, 68, 1642, 1972), difference in the enthalpy of formation between two conformers is calculated as 4.6 kJ/mol on the basis of signal intensities. We calculated the population ratio of both conformers using Boltzmann distribution under thermal equilibrium condition at 300 K (before expansion) and 3 K (after expansion). The population of AP to SC ratio is 6.3 and $1.2x10^{80}$ at 300 K and 3 K respectively. This indicates the absence of SC conformer in molecular beam. The large amplitude motion (219 $cm^{-1}$) appeared as the responsible motion for SC to AP exchange. Large amplitude motions and internal rotations take part in the equilibration of different conformers.

## III.8. References


1. D. Hong, M. Hoshino, R. Kuboi, and Y. Goto, *J. Am. Chem. Soc.*, 1999, **121**, 8427–8433.

2. J. Cazes, *Encyclopedia of Chromatography, Volume 2*, Taylor & Francis, 2005.

3. M. Burdisso, R. Gandolfi, L. Toma, R. Obertib, and R. Oberti, *Tetrahedron*, 1991, **47**, 6725–6736.

4. S. J. Cyvin, J. Brunvoll, and M. Perttilä, *J. Mol. Struct.*, 1973, **17**, 17–21.

5. A. J. Barnes and J. Murto, *J. Chem. Soc. Faraday Trans. 2*, 1972, **68**, 1642.

6. H. Schaal, T. Häber, and M. A. Suhm, *J. Phys. Chem. A*, 2000, **104**, 265–274.

7. E. Hirota and Y. Kawashima, *J. Mol. Spectrosc.*, 2001, **207**, 243–253.

8. S. Kondo and E. Hirota, *J. Mol. Spectrosc.*, 1970, **34**, 97–107.

9. G. S. Grubbs, S. E. Novick, W. C. Pringle, J. Laane, E. J. Ocola, S. A. Cooke, G. S. G. Ii, J. Esther, and A. H. Road, *J. Phys. Chem. A*, 2012, **116**, 8169–8175.

10. D. A. Obenchain, D. J. Frohman, G. S. Grubbs II, B. E. Long, W. C. Pringle, and S. E. Novick, *Talk TC04, 67th Int. Symp. Mol. Spectrosc. Ohio State Univ. Columbus, OH.*, 2012.

11. E. Arunan, A. P. Tiwari, P. K. Mandal, and P. C. Mathias, *Curr. Sci.*, 2002, **82**, 533–540.

12 Frisch, M. J.; Trucks, G. W.; Schlegel, H. B.; Scuseria, G. E.; Robb, M. A.; Cheeseman, J. R.; Scalmani, G.; Barone, V.; Mennucci, B.; Petersson, G. A.; Nakatsuji, H.; Caricato, M.; Li, X.; Hratchian, H. P.; Izmaylov, A. F.; Bloino, J.; Zheng, G.; Sonnenberg, J. L.; Hada, M.; Ehara, M.; Toyota, K.; Fukuda, R.; Hasegawa, J.; Ishida, M.; Nakajima, T.; Honda, Y.; Kitao, O.; Nakai, H.; Vreven, T.; Montgomery Jr., J. A.; Peralta, J. E.; Ogliaro,

F.; Bearpark, M.; Heyd, J. J.; Brothers, E.; Kudin, K. N.; Staroverov, V. N.; Kobayashi, R.; Normand, J.; Raghavachari, K.; Rendell, A.; Burant, J. C.; Iyengar, S. S.; Tomasi, J.; Cossi, M.; Rega, N.; Millam, J. M.; Klene, M.; Knox, J. E.; Cross, J. B.; Bakken, V.; Adamo, C.; Jaramillo, J.; Gomperts, R.; Stratmann, R. E.; Yazyev, O.; Austin, A. J.; Cammi, R.; Pomelli, C.; Ochterski, J. W.; Martin, R. L.; Morokuma, K.; Zakrzewski, V. G.; Voth, G. A.; Salvador, P.; Dannenberg, J. J.; Dapprich, S.; Daniels, A. D.; Farkas, O.; Foresman, J. B.; Ortiz, J. V; Cioslowski, J.; Fox, D. J. Gaussian~09 Revision C.01.

13. E. D. Glendening, J. K. Badenhoop, A. E. Reed, J. E. Carpenter, J. A. Bohmann, C. M. Morales, C. R. Landis, and F. Weinhold, *NBO6.0*, 2006.

14. *Jmol: an open-source Java viewer for chemical structures in 3D.*, http://www.jmol.org/.

15. J. K. G. Watson, in Vibrational Spectra and Structure, ed. J. R. Durig, Elsevier, Amsterdam, 1977, vol. 6, p. 1. We thank G. T. Fraser for providing us with the programme ASYM82 by A. G. Maki which was used in the fitting. Ankit Jain added a feature that enables the programme to remove one line from the fitting at a time and compare the rms deviation with the full fitting. The feature aids in identifying a wrong assignment.

16. H. M. Pickett, *J. Mol. Spectrosc.*, 1991, **148**, 371–377.

17. H. M. Pickett, *SPFIT/SPCAT*, http://spec.jpl.nasa.gov/ftp/pub/calpgm.

18. Z. Kisiel, *PROSPE – Programs for Rotational Spectroscopy*, http://info.ifpan.edu.pl/~kisiel/prospe.htm.

19. E. Hirota, *J. Phys. Chem.*, 1979, **83**, 1457–1465.

20. W. Gordy and R. L. Cook, *Microwave Molecular Spectra. 2nd ed.*, New York: Wiley Interscience, 1984.

21. M. Onda, K. Tsuda, and E. Sakamoto, *J. Mol. Struct.*, 2006, **780-781**, 222–224.

22. J.-U. Grabow, N. Heineking, and W. Stahl, *Z. Naturforsch*, 1991, **46a**, 229–232.

# *Supporting Information*

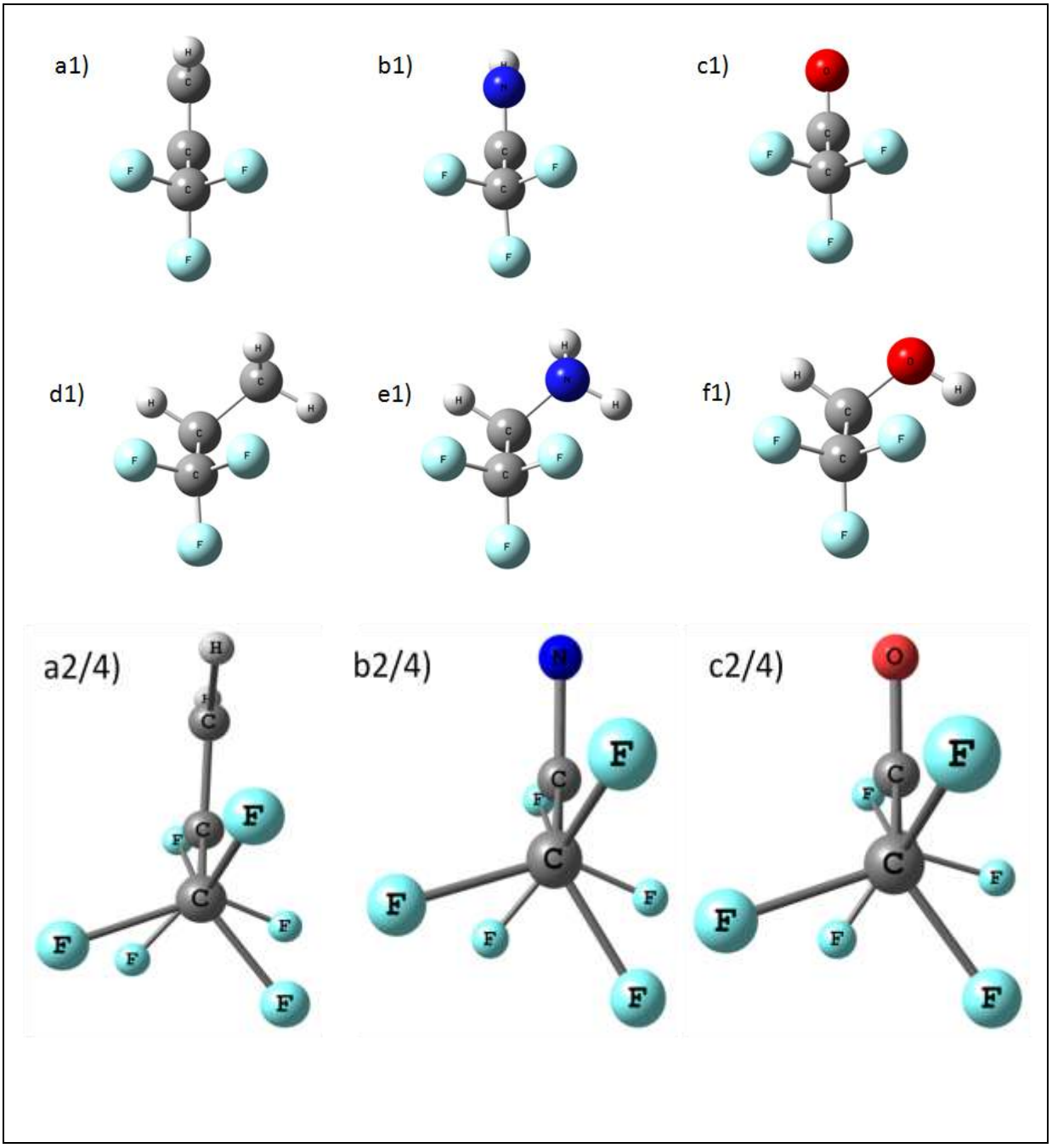

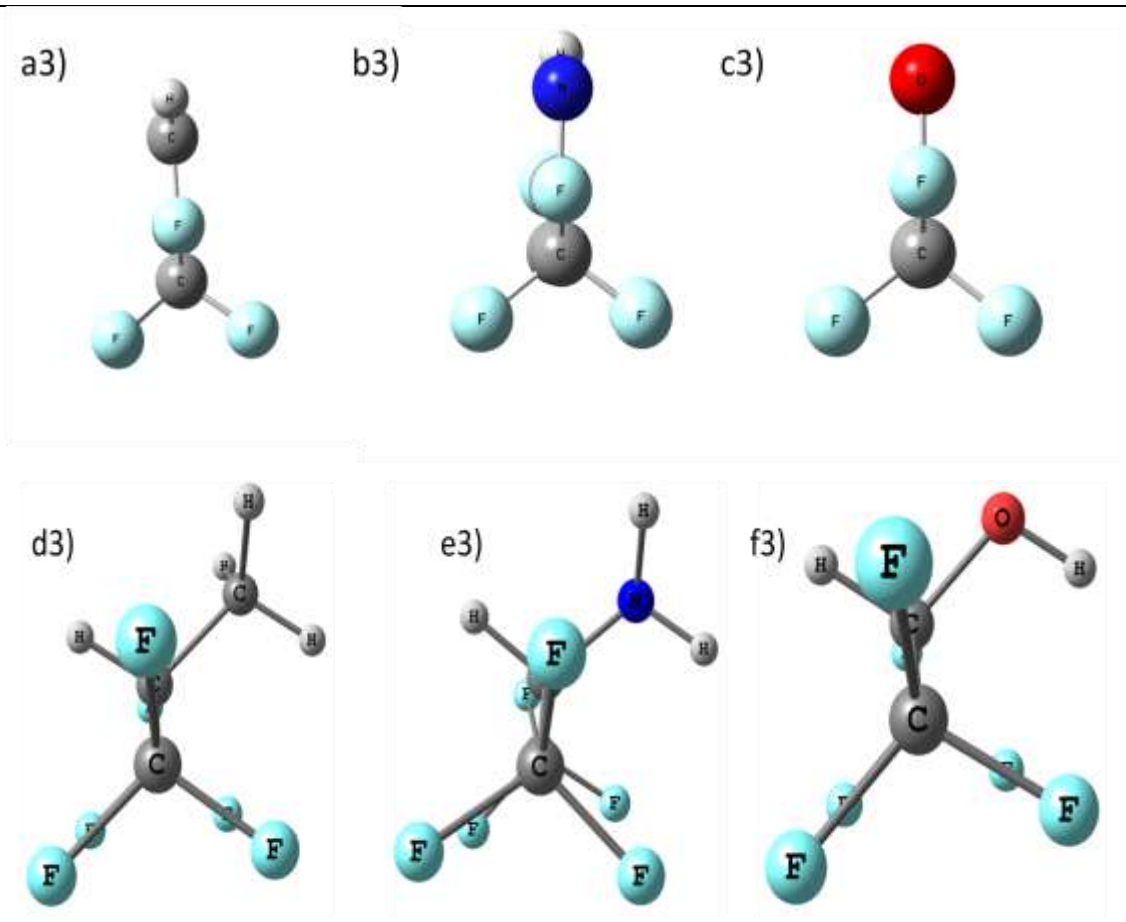


*Figure III. S. 1. Figures for the different positions in Figure III. 6 (see main text) for all prototype molecules.. All the structures are picked up from the minima and maxima position of 2D-PES scan.*

*Table III. S. 1. Geometrical parameters in Cartesian form for SC and AP conformers. Distances are given in Å.*

| | SC Conformer | | |
|---|---|---|---|
| C | -0.08486 | 0.580644 | -0.51067 |
| C | 1.235386 | -0.10812 | -0.15374 |
| C | -1.32623 | -0.22022 | -0.12041 |
| O | -0.19312 | 1.813967 | 0.143819 |
| H | -0.10386 | 0.670938 | -1.60364 |
| H | 0.476422 | 2.403579 | -0.21761 |
| F | 2.240758 | 0.747293 | -0.44243 |
| F | 1.325156 | -0.41927 | 1.137364 |
| F | 1.428748 | -1.21569 | -0.87669 |
| F | -1.27464 | -1.45504 | -0.64074 |
| F | -1.46349 | -0.32565 | 1.200172 |
| F | -2.41588 | 0.386331 | -0.60789 |
| | AP Conformer | | |
| C | -0.00719 | 0.55787 | -0.45868 |
| C | 1.277781 | -0.15084 | -0.02077 |
| C | -1.29135 | -0.17946 | -0.06819 |
| O | -0.03084 | 1.867637 | 0.032268 |
| H | 0.012282 | 0.61632 | -1.54913 |
| H | -0.04816 | 1.824597 | 0.996255 |
| F | 2.33557 | 0.52124 | -0.48751 |
| F | 1.373685 | -0.18288 | 1.319974 |
| F | 1.350212 | -1.40458 | -0.47618 |
| F | -1.319 | -1.43431 | -0.52545 |
| F | -1.43592 | -0.21418 | 1.268118 |
| F | -2.3459 | 0.469099 | -0.57392 |

*Table III. S. 2. Calculated vibrational frequencies and their intensities at MP2/6-311++G** level for SC and AP conformers.*

| # | Frequency for SC | intensity | Frequency for AP | intensity |
|---|---|---|---|---|
| 1 | 38.2 | 0.2 | 36.8 | 0.1 |
| 2 | 96.4 | 1.9 | 100.7 | 0.3 |
| 3 | 163.8 | 2.7 | 170.8 | 1.0 |
| 4 | 219.9 | 119.7 | 238.3 | 7.3 |
| 5 | 236.1 | 3.4 | 252.2 | 0.9 |
| 6 | 264.3 | 14.0 | 296.6 | 11.6 |
| 7 | 301.5 | 2.3 | 333.0 | 0.5 |
| 8 | 335.1 | 0.6 | 348.4 | 14.8 |
| 9 | 357.6 | 2.5 | 396.3 | 104.2 |

| | | | | |
|---|---|---|---|---|
| 10 | 469.5 | 3.2 | 468.1 | 9.4 |
| 11 | 523.1 | 10.4 | 522.1 | 8.2 |
| 12 | 541.9 | 4.6 | 538.5 | 4.5 |
| 13 | 558.1 | 1.2 | 560.2 | 5.1 |
| 14 | 618.0 | 0.6 | 617.8 | 1.8 |
| 15 | 690.3 | 44.3 | 695.9 | 57.2 |
| 16 | 743.6 | 21.1 | 746.2 | 11.5 |
| 17 | 865.1 | 35.8 | 850.6 | 41.5 |
| 18 | 911.8 | 53.5 | 916.3 | 59.4 |
| 19 | 1126.3 | 178.7 | 1130.6 | 160.9 |
| 20 | 1162.1 | 111.6 | 1139.8 | 115.8 |
| 21 | 1183.3 | 51.6 | 1201.7 | 30.5 |
| 22 | 1219.4 | 424.3 | 1225.3 | 343.0 |
| 23 | 1236.6 | 235.7 | 1259.5 | 333.9 |
| 24 | 1270.5 | 172.2 | 1293.7 | 99.5 |
| 25 | 1328.0 | 44.0 | 1297.2 | 190.5 |
| 26 | 1339.0 | 250.3 | 1340.9 | 151.5 |
| 27 | 1423.6 | 49.8 | 1429.7 | 129.2 |
| 28 | 1475.6 | 70.3 | 1451.1 | 2.9 |
| 29 | 3104.3 | 8.7 | 3163.7 | 3.1 |
| 30 | 3882.6 | 81.7 | 3845.6 | 70.6 |

*Table III. S. 3. Geometrical parameter in Cartesian coordinate format for prototype molecules at MP2/6-311++G(d,p). HFIP, HFIB , HFA-IM, HFA , HFI-NH2 and HFI-CH3.*

| HFIP | x(Å) | y(Å) | z(Å) |
|---|---|---|---|
| C | -0.007193 | 0.55787 | -0.458678 |
| C | 1.277781 | -0.150844 | -0.02077 |
| C | -1.291352 | -0.179458 | -0.068188 |
| O | -0.030843 | 1.867637 | 0.032268 |
| H | 0.012282 | 0.61632 | -1.549126 |
| H | -0.048156 | 1.824597 | 0.996255 |
| F | 2.33557 | 0.52124 | -0.487512 |
| F | 1.373685 | -0.182881 | 1.319974 |
| F | 1.350212 | -1.404582 | -0.476183 |
| F | -1.318997 | -1.434311 | -0.525448 |
| F | -1.435921 | -0.214175 | 1.268118 |
| F | -2.345901 | 0.469099 | -0.573915 |
| | | | |
| HFIB | | | |
| C | -0.000011 | 0.677323 | -0.000016 |

| | | | |
|---|---|---|---|
| C | 1.282915 | -0.112811 | 0.002523 |
| C | -1.282902 | -0.112871 | -0.002538 |
| F | 2.327164 | 0.647174 | 0.36501 |
| F | 1.215884 | -1.149327 | 0.851238 |
| F | 1.550063 | -0.604939 | -1.218574 |
| F | -1.215712 | -1.149615 | -0.850904 |
| F | -1.550239 | -0.604578 | 1.218714 |
| F | -2.32709 | 0.647022 | -0.36544 |
| C | -0.000074 | 2.014093 | -0.000025 |
| H | -0.931167 | 2.566931 | -0.028287 |
| H | 0.930962 | 2.567027 | 0.028236 |

HFA-IM

| | | | |
|---|---|---|---|
| C | -0.000746 | 0.701028 | -0.014785 |
| C | -1.307441 | -0.085903 | -0.006659 |
| C | 1.28634 | -0.121447 | -0.000306 |
| F | -2.312017 | 0.628623 | -0.495664 |
| F | -1.187518 | -1.206633 | -0.734948 |
| F | -1.610047 | -0.441535 | 1.251462 |
| F | 1.208007 | -1.126604 | 0.875637 |
| F | 1.533479 | -0.631467 | -1.212359 |
| F | 2.326435 | 0.652889 | 0.339315 |
| N | -0.054959 | 1.971083 | -0.014326 |
| H | 0.890735 | 2.362891 | 0.019802 |

HFA

| | | | |
|---|---|---|---|
| C | -0.000003 | 0.717848 | -0.000045 |
| C | 1.314897 | -0.097747 | 0.004333 |
| C | -1.314884 | -0.097765 | -0.004324 |
| F | 2.317317 | 0.64405 | 0.454829 |
| F | 1.196032 | -1.184023 | 0.775143 |
| F | 1.59259 | -0.487978 | -1.246308 |
| F | -1.196036 | -1.184083 | -0.775076 |
| F | -1.592594 | -0.487856 | 1.246352 |
| F | -2.317306 | 0.644002 | -0.454884 |
| O | -0.00001 | 1.921123 | -0.000036 |

HFI-NH2

| | | | |
|---|---|---|---|
| C | -0.001519 | 0.538544 | -0.511876 |
| C | 1.270617 | -0.170346 | -0.036007 |
| C | -1.283131 | -0.150929 | -0.044763 |
| H | 0.00335 | 0.470462 | -1.603572 |
| F | 2.341362 | 0.539205 | -0.444673 |

| | | | |
|---|---|---|---|
| F | 1.327365 | -0.247841 | 1.302353 |
| F | 1.397995 | -1.40451 | -0.53391 |
| F | -1.250559 | -1.473708 | -0.255443 |
| F | -1.489692 | 0.051792 | 1.266671 |
| F | -2.335566 | 0.340289 | -0.706925 |
| N | -0.073641 | 1.926688 | -0.116806 |
| H | 0.656905 | 2.467297 | -0.564791 |
| H | 0.021279 | 2.024777 | 0.889227 |

HFI-CH3

| | | | |
|---|---|---|---|
| 6 | -0.000017 | 0.525213 | -0.505032 |
| 6 | 1.26997 | -0.172372 | -0.039224 |
| 6 | -1.269989 | -0.172378 | -0.039232 |
| 1 | -0.000016 | 0.448755 | -1.596786 |
| 9 | 2.341993 | 0.461107 | -0.555022 |
| 9 | 1.398865 | -0.1546 | 1.295843 |
| 9 | 1.336264 | -1.44867 | -0.4397 |
| 9 | -1.336531 | -1.4485 | -0.440272 |
| 9 | -1.398519 | -0.15518 | 1.295886 |
| 9 | -2.34204 | 0.461483 | -0.554462 |
| 6 | -0.000009 | 1.993786 | -0.070209 |
| 1 | -0.885757 | 2.496556 | -0.460378 |
| 1 | -0.000239 | 2.072017 | 1.018884 |
| 1 | 0.885989 | 2.496418 | -0.459988 |

# Chapter IV. Microwave Spectrum of Strongly Hydrogen Bonded Hexafluoroisopropanol•••Water Complex.

## IV.1. Introduction

It is unquestionable that hydrogen bonding is most important among all the known weak interactions. In daily life, aliphatic alcohols play important role by forming hydrogen bonds e.g. water ($H_2O$), methanol ($CH_3OH$) and ethanol ($C_2H_5OH$) are the first three "alcohols" having entirely different effect on human body. In recent years it has been found that fluorinated aliphatic alcohols possess unique properties. The titled fluorinated aliphatic alcohol, hexafluoroisopropanol (HFIP) is one of the important solvents for organic chemistry, polymer chemistry and biology. The aqueous solution of HFIP and other fluoroalcohols help in stabilizing α-helical structure of protein and peptide.[1] Interestingly, it is the only solvent which can dissolve polythene terephthalate, a hard-to-dissolve polymer.[2] HFIP can work as a suitable solvent for rearrangement via zwitterionic intermediate, whereas $CH_3OH$ fails to do that for certain reactions.[3] In aqueous solution, interaction is complex and depends on the mole fraction of HFIP.[4] We are interested to study the interaction between HFIP and water in gas phase using microwave spectroscopy and this is the main objective of this work. FTIR-ATR, IR, Raman, X-ray diffraction, small angle neutron scattering, NMR, mass and molecular simulation studies have been done to investigate the interaction between HFIP and water in the condensed phase.[5,4] Moreover, as discussed in Chapter III, we have studied HFIP monomer using microwave spectroscopy. Rotational spectra of the monomer and its five isotopologues confirmed that the molecule exists only in antiperiplanar (AP) form in supersonic expansion.[6]

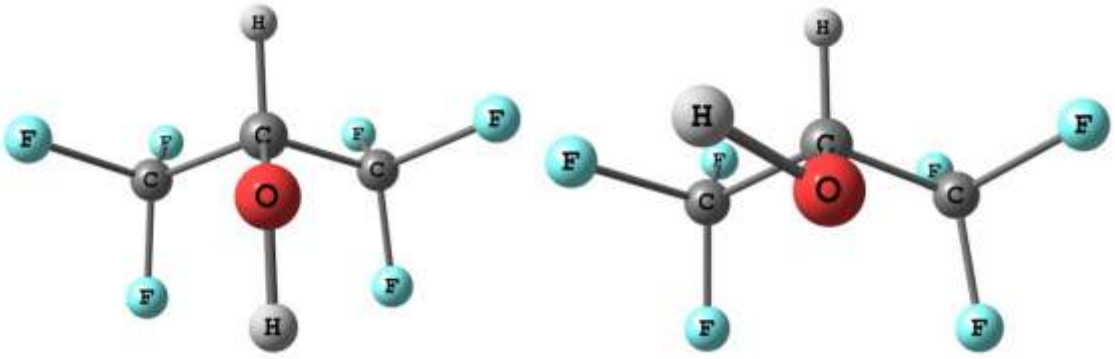

*Figure IV. 1. Two conformers of HFIP; antiperiplanar (left side) and synclinical (right side).*

It is important to understand the monomer unit well before starting the discussion about the complex. In this paragraph, structural properties of the HFIP monomer are discussed. The

other unit, water, is well known and its structure is well established. Conformational preference of HFIP is very interesting. IR, Raman and Matrix isolation studies show that molecule exist in two conformation; antiperiplanar (AP) and synclinical (SC) (Figure IV. 1). In gas phase, AP conformer is more stable than synclinical (SC).[7–9] In CO and $N_2$ matrices, both the conformers of HFIP have been observed. However, in argon matrix, only AP conformer could be observed.[8] Relative intensity of these conformers varies with temperature. These conformers exists due to an internal motion of the –OH group. The energy difference between these two conformers is 5.02 kJ/mol but there is a barrier of 11.29 kJ/mol height for the AP to SC interchange. Prototype molecule, isopropanol, also exists in two isomers because of –OH internal rotation. However, for this molecule the SC conformer is more stable than AP.[9,11,12] Examination of the effect of fluorination on isopropanol molecule has been done by Suhm's group, extensively[9]. Other prototype molecules Hexafluoroisobutene (HFIB)[13] and Hexafluoroacetone imine[14] (HFA-IM) shows doublet in rotational spectrum because of the counter motion of opposite $CF_3$ groups. However, HFIP did not show signature of splitting. These patterns and the reasons behind them have been discussed in Chapter III.

In this chapter, rotational spectra of HFIP•••$H_2O$ complex have been discussed. Moreover, results from theoretical analysis, like ab initio, DFT, AIM and NBO, have also been given.

## IV.2. Computational and Experimental Details

### IV.2.1. Computational Details

Ab initio calculations have been used for the structure optimization of different possible geometries of the title complex using G09 suite of program.[15] Mainly, long range corrected DFT level theory, LC-wPBE with 6-311++G(d,p) basis set was selected for these calculation.[16] Apart from this, MP2/6-311++G(d,p) and other theories (e.g. B2PLYP, CAM-B3LYP, wB97XD at 6-311++G(d,p)[17–19] were also used. From these calculations, rotational constants were extracted which helped in predicting rotational frequencies for experimental guidance. After collecting the experimental transitions, semi-rigid rotor Watson's asymmetric Hamiltonian was used to fit the transitions. [20] There are several programs coded by different groups for fitting. In this work mainly ASFIT and SPFIT programs have been

used to fit the transitions.[21–23] Calculation of the distortion constants for a molecule or complex was done using FREQ=VIBROT keyword which is inbuilt in G09 program. To get the vibrationally averaged geometry, anharmonic calculation was performed using FREQ=ANHARMONIC keyword. We analyzed the electrostatic potential of HFIP and water to guess the initial geometries (Figure IV. 2). Position of the surface maxima and minima of electrostatic potential (ESP) at the periphery of the molecule (i.e. at 0.001 a.u. surface) could be located with the help of Multiwfn program.[24,25] This analysis has been done for both the monomer units i.e. HFIP and water. In Figure IV. 2, pink spheres represent surface minima (labeled from 13 to 20 for HFIP and 6 for water) and yellow spheres are the position of surface maxima (labeled from 21 to 25 for HFIP and 4 and 5 for water). ESP values of these extemum points are given in kJ/mol in Table IV. S. 1 and Table IV. S. 2 with the same labeling as in Figure IV. 2. The largest values are starred in the tables. Coordinates of the molecular graph of HFIP and water in same the frame are given in Table IV. S. 3 and Table IV. S. 4. The minima positions (pink spheres) are nucleophilic sites of the molecule and maxima positions (yellow spheres) are electrophilic sites of the molecule. For bond characterization, AIM theory has been used.[26] There are different criteria for the characterization of weak interactions as discussed in Chapter VI. For AIM analysis, wavefunction was generated using Gaussian checkpoint files. AIMAll program has been used to perform the AIM analysis.[27] To determine the orbital overlaps between bonded atoms, Natural Bond Orbital (NBO) theory have been used. It was performed using NBO 6.0 software.[28]

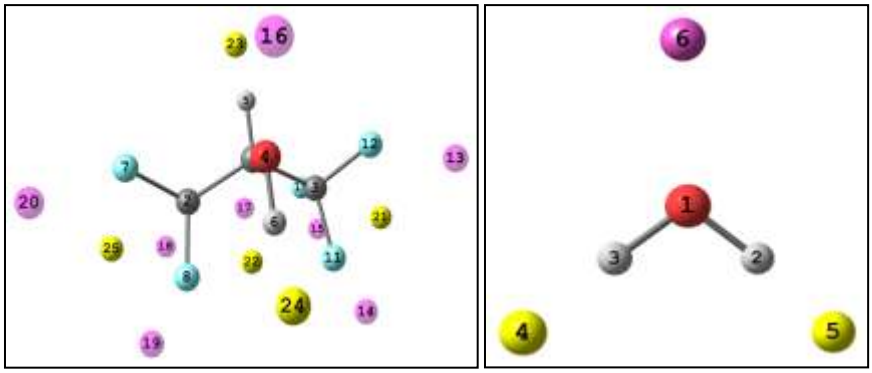


*Figure IV. 2. ESP minima (pink spheres) and maxima (yellow spheres) are shown.*

## IV.2.2. Experimental Details

### IV.2.2.1. Sample Preparation

HFIP (≥99%) was bought from Aldrich and was used without further purification. The mono deuterated isotope of water (HOD) was prepared by mixing $D_2O$ (99.9% bought from Cambridge Isotope Laboratory) and $H_2O$ in 1:1 molar ratio. Helium gas was used as carrier gas since signal was more intense in helium than in argon gas. Two separate bubblers were used, one for the HFIP and the other for $H_2O$. Small fraction of the carrier gas was flown through these bubblers; ~1% through the HFIP bubbler and ~2% through the $H_2O$ bubbler.

### IV.2.2.2. Rotational Spectra

Home built Pulsed Nozzle Fourier Transform Microwave Spectrometer (PNFTMW) [29] was used to collect the rotational spectrum. The carrier gas containing the HFIP and $H_2O$ molecules was expanded through the pulsed valve into a Fabry-Perot cavity. The pressure inside the cavity was 1.1 x $10^{-6}$ mbar. Carrier gas pressure behind the nozzle was 1.5 bar. Expansion from 1.5 bar to 1.1 x $10^{-6}$ mbar produced rotationally cold molecules with rotational temperature ≈ 3 K. Multiple free induction decays (FIDs) were recorded per gas pulse. Microwave pulse of 1.0 μs duration was found to be optimum for both the *b-type* and *c-type* transitions.

## IV.3. Results and Discussions

## IV.3.1. Structure optimization

The ESP calculations have often been useful in identifying the site of possible interactions in the HFIP molecule.[30,31] The ESP extrema in the HFIP molecule were located using Multiwfn software and are shown in Figure IV. 2. The ESP values corresponding to these extremum points are given in Table IV. S. 1 and Table IV. S. 2. Initial geometries for the optimization of HFIP•••$H_2O$ complex were considered in such a way that electrophilic site of HFIP interacts with nucleophilic site of $H_2O$ and vice versa. However, there are many such possible combinations which lead to different structures. In the guess geometries, AP and SC both conformers of HFIP were taken into account. All these structures converged to three

minima at B3LYP/6-31G* and are shown in (Figure IV. 3a, 3b and 3c). These structures were used as initial structures for the calculations at higher level MP2/6-311++G** level of theory. Structures shown in Figure IV. 3a and IV. 3b converged to the structures shown in Figure IV. 4a and IV. 4b respectively. The third structure was not a minimum at MP2 level. The structures were confirmed to be minima by getting all the real vibrational frequencies. Structures shown in Figure IV. 3a and IV. 4a have an important structural difference, first one has a plane of symmetry while the latter does not. The structures shown in Figure IV. 3b or Figure IV. 4b show complexes with SC conformer of HFIP. During the monomer study we had found that the SC conformer does not exist in supersonic expansion. Therefore, the complexes, shown in Figure IV. 3b and IV. 4b were not considered further. However, binding energy for this complex was greater than that of HFIP(AP)•••water and hydrogen bond distance is 1.8 Å (Table IV. 1). Both values indicated a very strong hydrogen bonding between HFIP(SC) and water. We expect that this complex might be observed in the experiments carried out at room temperature or in matrix isolation. During literature survey, we came across another structure which was identified from a molecular dynamics study (structure 2 of Figure IV. 5).[32] This structure also has HFIP in the AP form. This structure has two hydrogen bonds leading to a cyclic structure. In this structure, the C-H group of HFIP forms a C-H•••O hydrogen bond with oxygen of water and the O-H group in $H_2O$ forms O-H•••O hydrogen bond with O of HFIP (Figure IV. 5b). However, both the hydrogen bonds are bent in this structure and it is less stable than Structure 1. Finally two minima, shown in Figure IV. 5, were considered as guess geometries for the prediction of microwave spectra. 'Structure 1' and 'structure 2' will be used further as short hand notation for these two lowest energy conformers. Though complexes were optimized at many different level but a long range corrected DFT method, LC-wPBE/6-311++G(d,p), has been found reasonably good after comparing with experimental results, *vide infra*. Results presented throughout the article are at this level unless otherwise mentioned. From rotational spectroscopic point of view, we expect to observed all three *a*-, *b*- and *c-type* of transitions for both the structures, since for these none of the dipole moment component is zero. Moreover, calculated rotational constants for both structures 1 and 2 are quite close to each other (Table IV. 1).

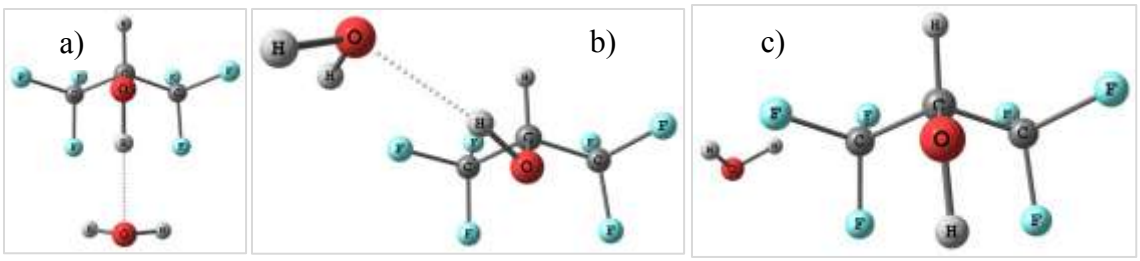


*Figure IV. 3. Three minima for the HFIP•••$H_2O$ complex, obtained at B3LYP/6-31G* level.*

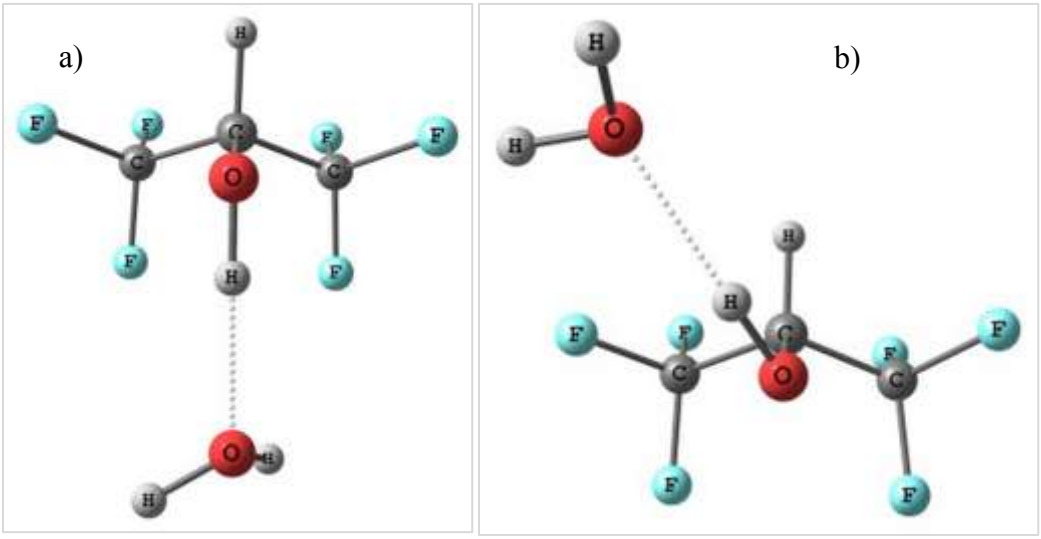


*Figure IV. 4. Two minima for the HFIP•••$H_2O$ complex, obtained at MP2/6-311++G** level.*

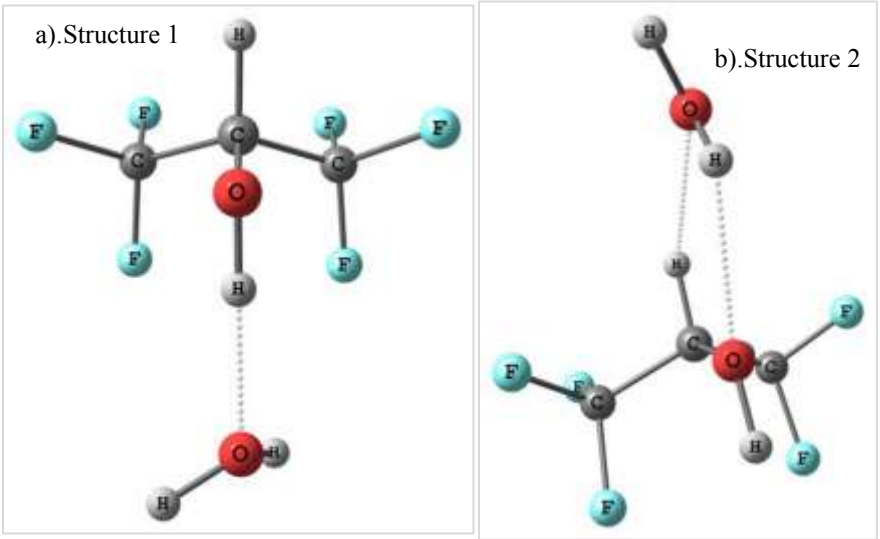


*Figure IV. 5. Two minima for the HFIP•••$H_2O$ complex obtained at LC-wPBE/6-311++G** level.*

*Table IV. 1. Binding energy, rotational constants, dipole moment and hydrogen bond length of the structures shown in Figure IV. 4a, 4b and 3b, at different level of theory.*

| | **Structure 1 (4a)** | **Structure 2 (4b)** | **Structure 3* (3b)** |
|---|---|---|---|
| **Binding Energy** (BSSE corrected) in kJ/mol | | | |
| B3LYP/6-31G(d) | -33.9[#] | -12.1 | -38.4 |
| LC-wPBE/6-311++G(d,p) | -31.8 | -17.5 | -36.8 |
| MP2/6-311++G(d,p) | -28.8 | -18.0 | -34.3 |
| **Rotational Constants** ( in MHz) at LC-wPBE/6-311++G(d,p) | | | |
| A | 1148.0 | 1249.6 | 1053.5 |
| B | 986.9 | 845.9 | 980.6 |
| C | 709.2 | 636.4 | 676.2 |
| **Dipole Moment components** (in Debye) at LC-wPBE/6-311++G(d,p) | | | |
| $\mu_a$ | 0.5 | 1.9 | 5.6 |
| $\mu_b$ | 1.8 | 0.2 | 1.8 |
| $\mu_c$ | 1.6 | 1.6 | 1.5 |
| Hydrogen bond length (in Å) | | | |
| O•••H distances | 1.78 | 2.23, 2.28 | 1.80 |

*[*] this structure is for HFIP(SC)•••$H_2O$ comple, [#] this binding energy correspond to the symmetrical structure.*

## IV.3.2. Rotational Spectra and Analysis

Rotational transitions were searched on the basis of the predictions for Structure 1 since it is the most stable structure. The early searches were made for the selected *b-type* of transitions e.g. $5_{1,5}$, → $6_{0,6}$, $5_{0,5}$ → $6_{1,6}$, $6_{1,6}$ →$7_{0,7}$, $6_{0,6}$ → $7_{1,7}$ etc. Rotational transitions could be observed within 10-20 MHz range of predictions which implied that the predictions were quite good. After getting few transitions, they were fitted to rotational Hamiltonian and it was easy to predict the other corresponding transitions. We got one progression of 46 transitions (Table IV. 2). Out of these 46, there were 35 *b-type* and 11 *c-type* transitions. These transitions could be fitted with a semi-rigid rotor Watson's S-reduction asymmetric Hamiltonian within experimental uncertainties (Table IV. 3). The RMS deviation for the fitting was 4.1 kHz. With the help of well fitted rotational and distortion constants, *a-type* transitions were predicted and searched. However, none of them could be found. We also considered the possibilities of splitting in *a-type* transitions because of some hindered rotation or tunneling motion and performed long range searches for that. These searches did not yield any transitions. Reason behind the absence of *a-type* signals is discussed later in details. Dipole moment components of structure 1 and structure 2 are presented in table 1. During experiments, it has been observed that *b-type* transitions were always more intense than *c-type* transitions. This observation was consistent with calculated dipole moment

components of structure 1 while the trend is reverse for structure 2 i.e. *c-dipole* moment (1.6 Debye) is more than *b-dipole* (0.2 Debye). Therefore, on the basis of signal intensity, structure 1 is likely to be experimentally observed structure. More evidences for this observation will be provided in next paragraphs.

*Table IV. 2. Observed rotational transitions for the hexafluoroisopropanol•••water complex.*

| J, $K_{-1}$, $K_{+1}$ <- J, $K_{-1}$, $K_{+1}$ | Type | Observed (MHz) | Obs-Calc (MHz) |
|---|---|---|---|
| 2, 0, 2 <- 1, 1, 1 | b | 3062.6515 | -0.0029 |
| 2, 1, 2 <- 1, 0, 1 | b | 3250.3360 | 0.0080 |
| 3, 0, 3 <- 2, 1, 2 | b | 4556.3460 | 0.0031 |
| 3, 1, 3 <- 2, 0, 2 | b | 4607.4975 | 0.0089 |
| 4, 0, 4 <- 3, 1, 3 | b | 5987.3295 | -0.0025 |
| 4, 1, 4 <- 3, 0, 3 | b | 5996.9975 | -0.0008 |
| 5, 0, 5 <- 4, 1, 4 | b | 7401.5900 | -0.0005 |
| 5, 1, 5 <- 4, 0, 4 | b | 7403.1100 | -0.0069 |
| 5, 2, 4 <- 4, 1, 3 | b | 8139.8660 | 0.0052 |
| 5, 2, 3 <- 4, 3, 2 | b | 8434.5610 | 0.0015 |
| 4, 4, 1 <- 3, 3, 0 | b | 8760.1525 | -0.0008 |
| 4, 4, 0 <- 3, 3, 0 | c | 8799.4635 | -0.0050 |
| 6, 0, 6 <- 5, 1, 5 | b | 8812.6180 | 0.0044 |
| 6, 1, 6 <- 5, 0, 5 | b | 8812.8320 | -0.0001 |
| 4, 4, 1 <- 3, 3, 1 | c | 8852.7780 | -0.0031 |
| 4, 3, 1 <- 3, 2, 2 | b | 8988.1890 | -0.0072 |
| 5, 3, 3 <- 4, 2, 2 | b | 9126.4780 | -0.0030 |
| 6, 1, 5 <- 5, 2, 4 | b | 9507.5520 | -0.0004 |
| 6, 2, 5 <- 5, 1, 4 | b | 9521.1735 | -0.0104 |
| 6, 2, 4 <- 5, 3, 3 | b | 10103.4265 | 0.0029 |
| 7, 0, 7 <- 6, 1, 6 | b | 10223.1295 | -0.0038 |
| 7, 1, 7 <- 6, 0, 6 | b | 10223.1685 | 0.0058 |
| 5, 4, 2 <- 4, 3, 1 | b | 10257.7875 | 0.0013 |
| 5, 3, 2 <- 4, 2, 2 | c | 10264.5755 | -0.0022 |
| 6, 3, 4 <- 5, 2, 3 | b | 10354.0435 | 0.0022 |
| 5, 2, 3 <- 4, 1, 3 | c | 10397.9045 | -0.0002 |
| 5, 1, 4 <- 4, 0, 4 | c | 10516.2925 | 0.0016 |
| 5, 4, 1 <- 4, 3, 1 | c | 10523.6245 | -0.0001 |
| 5, 2, 4 <- 4, 1, 4 | c | 10526.5365 | 0.0058 |
| 5, 3, 3 <- 4, 2, 3 | c | 10539.2920 | 0.0022 |
| 5, 4, 2 <- 4, 3, 2 | c | 10715.2270 | 0.0041 |
| 7, 1, 6 <- 6, 2, 5 | b | 10922.3905 | -0.0010 |
| 7, 2, 6 <- 6, 1, 5 | b | 10924.7730 | -0.0064 |
| 5, 5, 1 <- 4, 4, 0 | b | 11066.9635 | 0.0009 |
| 5, 5, 0 <- 4, 4, 0 | c | 11081.8605 | 0.0032 |
| 5, 5, 1 <- 4, 4, 1 | c | 11106.2760 | -0.0018 |
| 5, 5, 0 <- 4, 4, 1 | b | 11121.1725 | 0.0000 |
| 8, 0, 8 <- 7, 1, 7 | b | 11633.5880 | 0.0019 |
| 8, 1, 8 <- 7, 0, 7 | b | 11633.5880 | -0.0019 |
| 7, 3, 4 <- 6, 4, 3 | b | 12015.0996 | 0.0000 |
| 8, 1, 7 <- 7, 2, 6 | b | 12333.2535 | 0.0002 |
| 8, 2, 7 <- 7, 1, 6 | b | 12333.6345 | 0.0016 |
| 9, 0, 9 <- 8, 1, 8 | b | 13044.0270 | 0.0005 |
| 9, 1, 9 <- 8, 0, 8 | b | 13044.0270 | 0.0001 |
| 10, 0, 10 <- 9, 1, 9 | b | 14454.4560 | 0.0002 |
| 10, 1, 10 <- 9, 0, 9 | b | 14454.4560 | 0.0001 |

*Table IV. 3. Experimental rotational and distortion constants, and their comparison with calculated rotational and distortion constants for structure 1 and structure 2.*

| | **Experimental** | **Calculated Structure 1** | **Calculated Structure 2** |
|---|---|---|---|
| A/MHz | 1134.53898(77) | 1147.98533 | 1053.47733 |
| B/MHz | 989.67594(44) | 986.88906 | 980.62909 |
| C/MHz | 705.26602(20) | 709.22576 | 676.23923 |
| $D_J$/kHz | -0.0876(51) | -0.0291 | 0.5969 |
| $D_{JK}$/kHz | 2.230(39) | 1.541 | -2.0501 |
| $D_K$/kHz | -1.805(29) | -1.202 | 2.8820 |
| $d_1$/kHz | 0.0092(27) | 0.0015 | -0.2418 |
| $d_2$/kHz | -0.0738(18) | -0.0502 | 0.0315 |
| RMS (MHz) | 0.0041 | -- | -- |
| No. of transitions | 46(*b*- & *c-type* only) | | |

As the rotational constants for both of the guess geometries were close, the agreement between observed and predicted distortion constants is important. Search for the rotational transitions of Structure 2 were also performed but no transitions could be found.

The experimental rotational constants were close to the structure 1 as well as structure 2 and it was difficult to confirm whether observed progression corresponds to structure 1 or structure 2. Inspection of experimental and calculated distortion constants helped in assigning the structure. Structure 1 has the same sign and magnitude (in order) of the experimental distortion constants (Table IV. 3) whereas structure 2 has opposite signs. Therefore, structure 1 showed closeness to the experimentally observed rotational and distortion constants. This is another support in favor of structure 1 along with the earlier mentioned signal intensity trend.

In order to get more structural information, two isotopologues of the complex, HFIP•••$D_2O$ and HFIP•••HOD, have been considered. Rotational spectrum predictions of the isotopologues were done by comparing the theoretical and experimental rotational constants of the parent complex, and we assumed that similar difference should be there in the rotational constants for the isotopologues (Table IV. 7). In this way, we predicted the rotational constants of the isotopologues on the basis of structure 1. On the basis of prediction, we first searched for HFIP•••$D_2O$ complex since both HFIP and $D_2O$ were available in their pure form. Therefore, spectrum could be observed easily. A total of 30 transitions, mostly *b-type* transitions were observed for the HFIP•••$D_2O$ complex (Table IV. 4). Two rotational transitions, corresponding to the HFIP•••$D_2O$ isotopologues, are shown in Figure IV. 6. The presented signals are at frequency 7178.7880 and 7179.0490 MHz and are assigned as $4_{14} \rightarrow 5_{05}$ and $4_{04} \rightarrow 5_{15}$ respectively for HFIP•••$D_2O$.

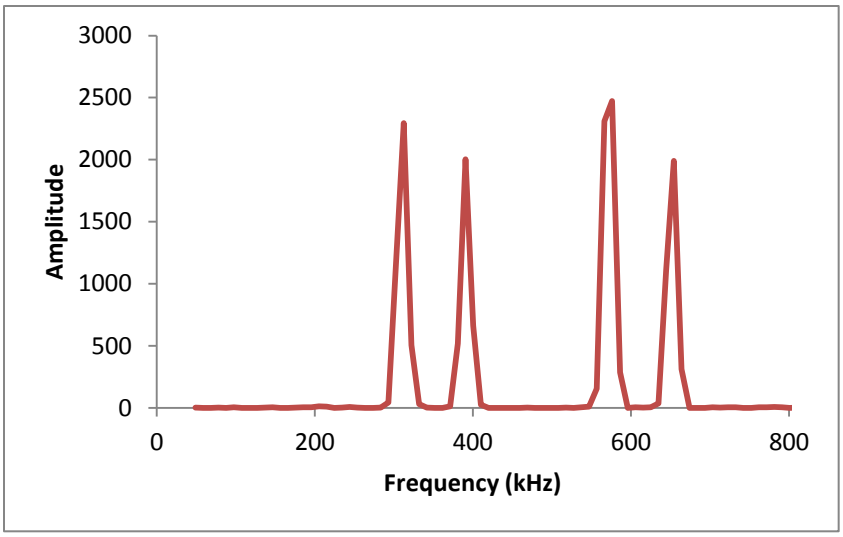


*Figure IV. 6. A sample spectrum of HFIP•••$D_2O$ complex. This figure contains two transitions. First and second peaks are the two Doppler components of the one of the signals. Similarly third and fourth are the two Doppler components of the other signal. The molecular frequencies corresponding to these signal are 7179.049 MHz and 7178.788 MHz.*

Next, we started searching for another isotopologue HFIP•••HOD and could observe 36 transitions (Table IV. 5). Among these 36, 31 were b-dipole and 5 were c-dipole transitions. Splitting in rotational transitions because of deuterium quadruple moment have been seen in some signals. However, these were insufficient to assign and measure the quadruple coupling constant. Line center were used in the fit. Transitions of both the isotopologues could be fitted using a rotational Hamiltonian. The experimental rotational constants and distortion constants for both the isotopologues are given in Table IV. 6. The RMS values for these fits were 3.5 and 4.2 kHz for HFIP•••$D_2O$ and HFIP•••HOD isotopologues, respectively. The *b-type* transitions were stronger than *c-type* transitions for both the isotopologues. For the HFIP•••HOD complex, value of the distortion constant $d_1$ was taken as that for the parent and was kept constant during the fit. If we included $d_1$ in fit, uncertainty became larger than the absolute value.

*Table IV. 4. Observed rotational transitions for the HFIP•••$D_2O$ complex.*

| J, $K_{-1}$, $K_{+1}$ <- J, $K_{-1}$, $K_{+1}$ | Type | Observed (MHz) | Obs-Calc (MHz) |
|---|---|---|---|
| 4, 0, 4 <- 3, 1, 3 | b | 5810.5170 | -0.0016 |
| 4, 1, 4 <- 3, 0, 3 | b | 5813.0460 | 0.0010 |
| 5, 0, 5 <- 4, 1, 4 | b | 7178.7880 | -0.0010 |
| 5, 1, 5 <- 4, 0, 4 | b | 7179.0490 | -0.0005 |
| 5, 2, 4 <- 4, 1, 3 | b | 7874.8170 | 0.0069 |
| 6, 0, 6 <- 5, 1, 5 | b | 8546.1100 | -0.0051 |

| | | | |
|---|---|---|---|
| 6, 1, 6 <- 5, 0, 5 | b | 8546.1390 | -0.0004 |
| 6, 1, 5 <- 5, 2, 4 | b | 9230.7850 | -0.0027 |
| 6, 2, 5 <- 5, 1, 4 | b | 9233.1410 | 0.0003 |
| 7, 0, 7 <- 6, 1, 6 | b | 9913.3510 | 0.0023 |
| 7, 1, 7 <- 6, 0, 6 | b | 9913.3510 | 0.0001 |
| 8, 0, 8 <- 7, 1, 7 | b | 11280.5705 | 0.0009 |
| 8, 1, 8 <- 7, 0, 7 | b | 11280.5705 | 0.0007 |
| 7, 2, 5 <- 6, 3, 4 | b | 11281.7270 | 0.0030 |
| 7, 3, 5 <- 6, 2, 4 | b | 11293.4195 | -0.0023 |
| 5, 3, 2 <- 4, 2, 2 | c | 10083.8165 | 0.0017 |
| 5, 5, 0 <- 4, 4, 1 | b | 10621.2490 | 0.0046 |
| 7, 1, 6 <- 6, 2, 5 | b | 10598.5855 | 0.0040 |
| 7, 2, 6 <- 6, 1, 5 | b | 10598.8510 | 0.0014 |
| 5, 5, 1 <- 4, 4, 0 | b | 10499.0430 | -0.0003 |
| 5, 1, 4 <- 4, 2, 3 | b | 7857.0490 | -0.0022 |
| 6, 6, 0 <- 5, 5, 1 | b | 12739.5975 | -0.0037 |
| 4, 4, 0 <- 3, 3, 1 | b | 8528.5805 | -0.0061 |
| 9, 0, 9 <- 8, 1, 8 | b | 12647.7785 | -0.0008 |
| 9, 1, 9 <- 8, 0, 8 | b | 12647.7785 | -0.0008 |
| 8, 2, 6 <- 7, 3, 5 | b | 12651.9490 | -0.0068 |
| 8, 3, 6 <- 7, 2, 5 | b | 12653.5610 | 0.0024 |
| 6, 6, 1 <- 5, 5, 0 | b | 12679.7318 | 0.0028 |
| 9, 1, 8 <- 8, 2, 7 | b | 13332.7780 | 0.0019 |
| 9, 2, 8 <- 8, 1, 7 | b | 13332.7780 | -0.0008 |

*Table IV. 5. Observed rotational transitions for the HFIP•••HOD complex.*

| J, $K_{-1}$, $K_{+1}$ <- J, $K_{-1}$, $K_{+1}$ | Type | Observed (MHz) | Obs-Calc (MHz) |
|---|---|---|---|
| 6, 0, 6 <- 5, 1, 5 | b | 8706.6000 | -0.0009 |
| 6, 1, 6 <- 5, 0, 5 | b | 8706.7025 | -0.0031 |
| 8, 0, 8 <- 7, 1, 7 | b | 11493.3855 | 0.0019 |
| 8, 1, 8 <- 7, 0, 7 | b | 11493.3855 | 0.0006 |
| 4, 4, 1 <- 3, 3, 1 | c | 8684.1000 | 0.0038 |
| 7, 0, 7 <- 6, 1, 6 | b | 10100.0100 | 0.0001 |
| 7, 1, 7 <- 6, 0, 6 | b | 10100.0100 | -0.0121 |
| 7, 1, 6 <- 6, 2, 5 | b | 10792.2780 | 0.0028 |
| 5, 5, 0 <- 4, 4, 0 | c | 10858.0510 | 0.0002 |
| 5, 5, 0 <- 4, 4, 1 | b | 10909.5245 | 0.0027 |
| 6, 2, 5 <- 5, 1, 4 | b | 9404.1610 | 0.0034 |
| 4, 4, 0 <- 3, 3, 1 | b | 8735.5610 | -0.0062 |
| 4, 0, 4 <- 3, 1, 3 | b | 5917.0530 | -0.0002 |
| 4, 1, 4 <- 3, 0, 3 | b | 5923.2175 | 0.0042 |
| 5, 0, 5 <- 4, 1, 4 | b | 7312.9070 | 0.0022 |
| 6, 3, 4 <- 5, 2, 3 | b | 10187.6340 | -0.0005 |

| | | | |
|---|---|---|---|
| 7, 2, 6 <- 6, 1, 5 | b | 10793.4310 | 0.0067 |
| 5, 5, 1 <- 4, 4, 0 | b | 10836.4875 | 0.0038 |
| 5, 5, 1 <- 4, 4, 1 | c | 10887.9485 | -0.0062 |
| 5, 2, 4 <- 4, 1, 3 | b | 8030.5025 | -0.0001 |
| 6, 1, 5 <- 5, 2, 4 | b | 9396.5805 | 0.0006 |
| 9, 1, 9 <- 8, 0, 8 | b | 12886.7470 | 0.0016 |
| 9, 0, 9 <- 8, 1, 8 | b | 12886.7470 | 0.0018 |
| 10, 1, 10 <- 9, 0, 9 | b | 14280.0900 | -0.0026 |
| 10, 0, 10 <- 9, 1, 9 | b | 14280.0900 | -0.0026 |
| 11, 0, 11 <- 10, 1, 10 | b | 15673.4240 | 0.0024 |
| 11, 1, 11 <- 10, 0, 10 | b | 15673.4240 | 0.0024 |
| 10, 3, 8 <- 9, 2, 7 | b | 15665.6685 | 0.0024 |
| 10, 1, 9 <- 9, 2, 8 | b | 14972.0880 | -0.0008 |
| 10, 2, 9 <- 9, 1, 8 | b | 14972.0880 | -0.0033 |
| 7, 7, 1 <- 6, 6, 0 | b | 15308.1415 | -0.0023 |
| 7, 7, 0 <- 6, 6, 0 | c | 15311.2610 | -0.0075 |
| 7, 7, 1 <- 6, 6, 1 | c | 15316.5590 | 0.0066 |
| 7, 7, 0 <- 6, 6, 1 | b | 15319.6805 | 0.0033 |
| 9, 2, 7 <- 8, 3, 6 | b | 14272.7320 | -0.0031 |
| 9, 3, 7 <- 8, 2, 6 | b | 14273.8295 | -0.0006 |

*Table IV. 6. Rotational and distortion constants for the different isotopologues.*

| | HFIP•••$H_2O$ | HFIP•••$D_2O$ | HFIP•••HOD |
|---|---|---|---|
| A /MHz | 1134.53898(77) | 1075.1262(10) | 1110.15554(67) |
| B /MHz | 989.67594(44) | 983.0710(16) | 986.0420(17) |
| C /MHz | 705.26602(20) | 683.64615(22) | 696.72950(21) |
| $D_J$ /kHz | -0.0876(51) | -0.148(25) | -0.1737(74) |
| $D_{JK}$ /kHz | 2.230(39) | 2.43(16) | 3.526(89) |
| $D_K$ /kHz | -1.805(29) | -1.91(14) | -2.977(86) |
| $d_1$ /kHz | 0.0092(27) | 0.029(11) | [0.0092] |
| $d_2$ /kHz | -0.0738(18) | -0.0861(57) | -0.1214(39) |
| RMS /MHz | 0.0041 | 0.0035 | 0.0042 |
| No of transitions | 46 | 30 | 33 |

*Value in square brackets is directly taken from parent complex and kept constants during fix.*

*Table IV. 7. Differences between experimental and theoretical rotational constants for the different isotopologues are given in MHz*

| | Experiment | Structure 1 | Cal-Exp | Structure 2 | Cal-Exp |
|---|---|---|---|---|---|
| HFIP---$H_2O$ | 1134.53898 | 1147.98 | 13 | 1053.32 | -81 |
| | 989.67594 | 986.89 | -3 | 980.76 | -9 |
| | 705.26602 | 709.23 | 4 | 676.1 | -29 |
| HFIP---HOD | 1110.15554 | 1123.34 | 13 | 1031.45 | -79 |
| | 986.042 | 983.08 | -3 | 979.95 | -6 |
| | 696.7295 | 700.83 | 4 | 666.98 | -30 |
| HFIP---$D_2O$ | 1075.1262 | 1090.89 | 16 | 1000.28 | -75 |
| | 983.071 | 981.97 | -1 | 973.35 | -10 |
| | 683.64615 | 688.1 | 4 | 651.5 | -32 |

Using Kraitchmann's analysis, positions of the isotopic substitutions were located which helped in determining many important structural parameters for the complex. It was found that the distance between center of mass (CM) and H1 was closer to that in structure 1 than structure 2. Similarly, the distance between center of mass and H2 was found to be closer to that in structure 1 than structure 2 (Table IV. 8) and Figure IV. 7). These two distances clearly indicated that the experimentally observed structure is structure 1.

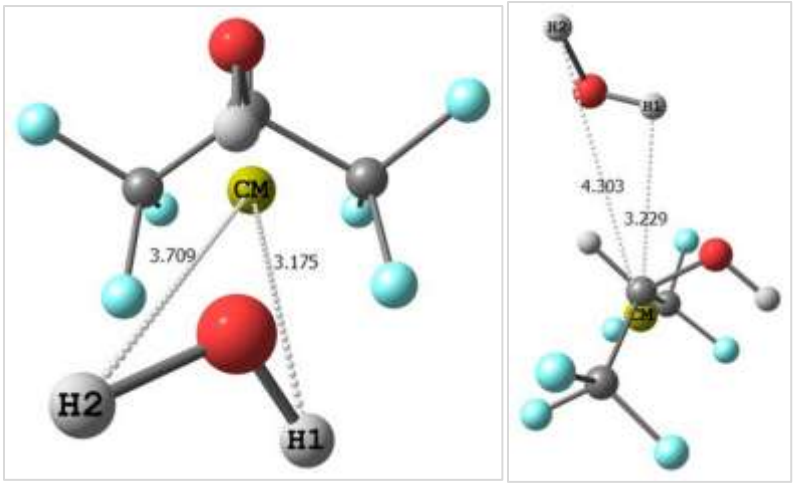


*Figure IV. 7. Distances between substituted atoms (H1 and H2) and centre of mass (CM) at LC-wPBE/6-311++G**.*
*See table 8 for comparison with Kraitchmann's analysis.*

*Table IV. 8. Parameters for the HFIP•••$H_2O$ complex from Kraitchman's analysis and ab initio calculations. .*

| Distances | Kraitchman's analysis(Å) | Structure 1 (Å) | Structure 2 (Å) |
|---|---|---|---|
| CM-H1 | 3.19588(83) | 3.175 | 3.229 |
| CM-H2 | 3.88827(70) | 3.709 | 4.303 |

**CM stands for center of mass and H1 and H2 are the hydrogen of water molecule in complex.*

In the structure 1 both the hydrogen are not equivalent according to the high level ab initio calculations. If this was true, we should have observed two sets of progression for the HFIP•••HOD isotopologue corresponding to the two different hydrogen atoms. However, experimentally, we observed only one progression which suggests that the two water hydrogen atoms are equivalent and the vibrationally averaged structure of the HFIP•••$H_2O$ complex has a plane of symmetry. The only possible motion which can make the structure symmetric, on an average, was motion of $H_2O$ about its $C_{2V}$. Relaxed potential energy scan of the $H_2O$ molecule about its $C_{2V}$ axis has been performed at LC-wPBE/6-311++G(d,p) level of theory (Figure IV. 8). The dihedral angle C2-C1-O2-H4 was chosen for the scan and the selected range was -30° to 30°. The corresponding vibrational frequency for the normal mode similar to this motion was 74 $cm^{-1}$ at LC-wPBE/6-311++G(d,p) level of theory. The zero point energy (ZPE) 0.46 kJ/mol for this normal mode vibrational motion was higher than barrier obtained from scan, 0.25 kJ/mol. It suggests that this motion is free and both the hydrogen atoms are equivalent in the zero-point dynamic structure of the complex. This also explained the absence of *a-type* of transition. Since due to this free motion, *a-dipole* averages out. All these observation are also supporting the presence of structure 1 experimentally instead of structure 2.

The above analysis suggests that there is an effective plane of symmetry and the two hydrogen atoms in $H_2O$ are equivalent. This contradicts the results from Kraitchmann's analysis. However, it is worth remembering that H/D substitution, especially in floppy complexes can lead to significant changes in vibrationally averaged structure. For rigid system, we observed the effectiveness of Kraitchmann's analysis in previous chapter. The

parameters for the HFIP monomer, obtained from this analysis and ab initio calculation, were in good agreement.

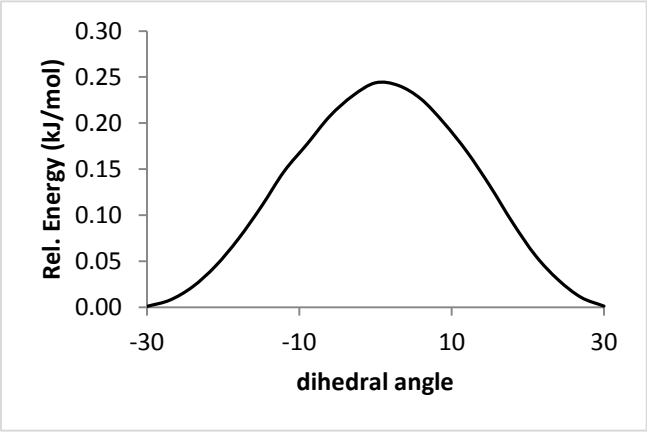


*Figure IV. 8. Relaxed PES scan of C2-C1-O2-H4 dihedral angle at LC-wPBE/6-311++G(d,p) level.*

Next question arises, how can we reduce the mismatching of experimental and calculated rotational constants? Results from ab initio optimized geometry should not be compared to experimental values. This is because the ab initio calculations give equilibrium geometry but in the real world, a molecule vibrates at even 0 K. Calculation of vibrationally averaged geometry can reduce the difference between experimental and calculated rotational constants. We have performed anharmonic calculations to get the vibrationally averaged geometry and compared it with equilibrium geometry. First comparison has been done for the rotational constants. In this case, rotational constants were underestimated in vibrationally averaged geometry and overestimated in equilibrium geometry (Table IV. 9). From this table, it was difficult to conclude about the usefulness of the vibrationally averaged geometry. But we found that, vibrationally averaged geometry supporting experimental observations more than equilibrium geometry. One important experimental observation from this work is that both hydrogen of water molecule were identical in the titled complex and also this was a point of controversy with Kraitchmann's analysis. In equilibrium geometry, the distances between center of mass (CM) to H1 and H2 were 3.175 and 3.709 Å respectively. However, in vibrationally averaged geometry, these distances are 3.414 and 3.655 Å. Water's both hydrogen can be identical if these distances became equal. It is clear that, in later case, distances were very close to their mean whereas in equilibrium geometry, distances were far away from their mean. We understand that, calculated distances cannot be so accurate (third

place of decimal) and using it so precisely may or may not be acceptable. It has been used because we wanted to compare two distances precisely. The complete parameter of vibrationally averaged geometry and its comparison with equilibrium geometry in internal coordinate and in Cartesian coordinate are presented in Table IV. S. 9.

*Table IV. 9. Comparison among rotational constant of experimental, vibrationally averaged and equilibrium geometry.*

| | Experimental | Vib.Av.Geom | Exp - Vib | Eqbm.Geom | Exp - Eqbm | Eqbm-Vib |
|---|---|---|---|---|---|---|
| A/MHz | 1134.53898 | 1124.2 | 10.3 | 1146.6 | -12.0 | 22.3 |
| B/MHz | 989.67594 | 983.4 | 6.2 | 987.9 | 1.8 | 4.5 |
| C/MHz | 705.26602 | 697.0 | 8.3 | 709.0 | -3.7 | 12.0 |

## IV.3.3. AIM and NBO analysis

For structure 1, calculated hydrogen bond length was very short, 1.8 Å and it can be considered as a very strong O•••H-O hydrogen bond. In AIM theory[26], characterization of hydrogen bond (closed-shell interaction) from the shared-shell interaction (covalent bond) can be done on the basis of different properties e.g. sign of Laplacian of electron density[33], V/G ratio[34], H-values[35] and $|\lambda_1|/\lambda_3$ ratio[36] (see Chapter 2 for details). For structure 1, Laplacian has a positive sign (+0.12252 a.u.), V/G ratio is 0.9964, H-value is 0.0001 a.u. and $|\lambda_1|/\lambda_3$ ratio is 0.24 (see Chapter VI for details of criteria). All these values indicated that it is a very strong closed-shell interaction and mostly lies at the boundary between shared-shell and closed-shell interaction.

Usually, in the case of hydrogen bonds, electron density and binding energies are linearly correlated. The electron density value at BCP is 0.035 a.u. for O•••H-O hydrogen bond in HFIP•••$H_2O$ complex. It is 0.024 a.u. for O•••H-O hydrogen bond in water dimer. These numbers indicate that the O-H•••O hydrogen bonding in HFIP•••$H_2O$ complex is stronger than that in water dimer. Water dimer is a simple example of O•••H-O interaction and information about the complex are well established using different theories and experiments. Qualitatively, HFIP•••water complex should be stronger than the water dimer because of two electron withdrawing groups, $CF_3$ make the OH hydrogen more acidic (electrophilic). For structure 2, two BCPs were found and their values are given in Figure IV. 9. Structure 1 which has only one intermolecular hydrogen bond BCP is even more stable than structure 2 even though this structure has two hydrogen bond BCPs. The sum of the electron densities values at these two BCPs of structure 2 is less than the electron density value at the hydrogen

bond BCP of structure 1. In the structure 1, there are three more unexpected BCPs, one between two fluorine atoms and two similar BCPs between two different F and O. Similarly in the structure 2, one unexpected F-F BCP is present. These can be considered as the artifact of the AIM calculation since there was no such overlapping observed between connecting atoms by NBO analysis. It is well known that the deviation from 180° of O•••H-O hydrogen bond angle results in weakening of the hydrogen bond.[37] In structure 1, O•••H-O bond angle was 180° while in structure 2, it was 123°. Another C-H•••O hydrogen bond angle was 125°. Non linear hydrogen bond angles of structure 2 were another reason for the less stability of this complex. NBO shows that there is extensive orbital overlapping or charge transfer from the lone pair of oxygen of water molecule to the O-H antibonding of HFIP. The complex is stabilized by 87.78 kJ/mol due to this charge transfer. In structure 2, overlapping of Oxygen's lone pair of water with C-H(σ*) of HFIP stabilizes the complex by 7.52 kJ/mol and second overlapping of Oxygen's lone pair of HFIP with O-H(σ*) of HFIP stabilizes the complex by 3.68 kJ/mol. These values clearly indicate that hydrogen bond in structure 1 is more stable.

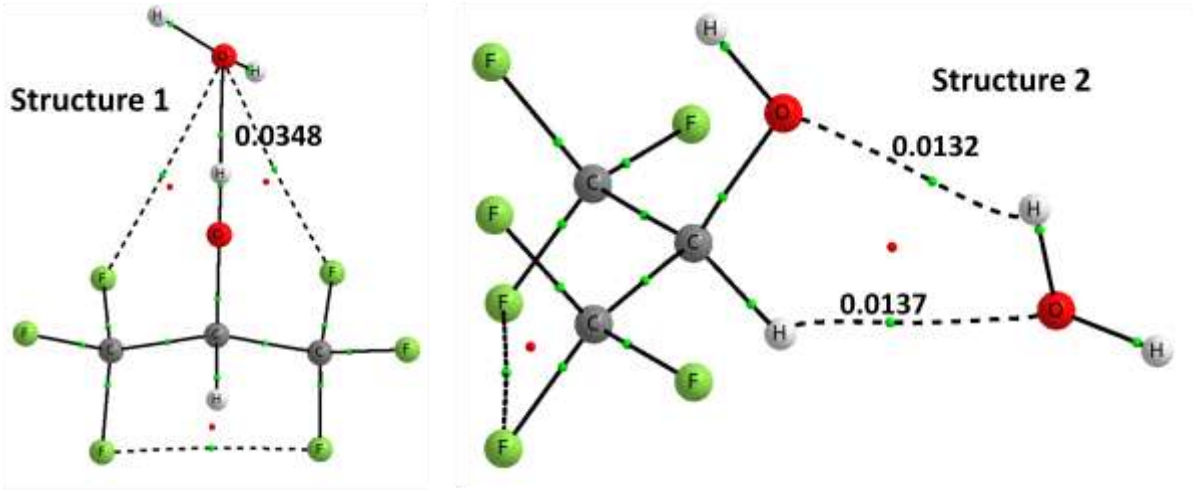


*Figure IV. 9. AIM analysis of the structure 1 (left) and structure 2 (right).*

*Table IV. 10. Comparison of experimental and calculated rotational constants(MHz) and distortion constants(kHz).*

| | Experiment | MP2 | mp2=full | b2plyp | B2plypd | LC-wPBE | CAM-B3LYP | wB97XD | #MP2/6-31G(d)* |
|---|---|---|---|---|---|---|---|---|---|
| a | 1134.53898(77) | 1148.3 | 1151.0 | 1142.9 | 1170.2 | 1148.0 | 1164.7 | 1165.4 | 1187.6 |
| b | 989.67594(44) | 986.2 | 988.5 | 977.9 | 979.8 | 986.9 | 982.9 | 977.3 | 985.9 |
| c | 705.26602(20) | 710.5 | 712.4 | 704.9 | 719.3 | 709.2 | 715.2 | 714.1 | 734.6 |
| D J | -0.0876(51) | -0.007 | -0.007 | 0.005 | -0.004 | -0.029 | 0.010 | -0.010 | -0.056 |
| D JK | 2.230(39) | 1.144 | 1.135 | 1.116 | 1.007 | 1.542 | 1.018 | 1.142 | 1.680 |
| D K | -1.805(29) | -0.869 | -0.864 | -0.795 | -0.800 | -1.203 | -0.756 | -0.865 | -1.478 |
| d 1 | 0.0092(27) | -0.003 | -0.003 | -0.004 | 0.001 | 0.002 | -0.005 | -0.0001 | -0.003 |
| d 2 | -0.0738(18) | -0.038 | -0.038 | -0.037 | -0.030 | -0.050 | -0.033 | -0.035 | -0.050 |

*# At this level, structure is symmetric same as shown in figure 3a. Basis set used for the calculations is 6-311++G(d,p) except last column.*

After collecting all experimental information, comparing these results with theory may be fruitful for the community. Rotational and distortion constants at the different level of theory are listed in Table IV. 10. At LC-wPBE level of theory, calculated constants are close to the experimental values. MP2 values were also reliable. Interestingly, performing calculation at MP2 level and low basis set (6-31G(d)) gave a structure which has a plane of symmetry. In other words, both the hydrogen atoms of the water molecules are identical at this level which is true according to our experimental observation.

## IV.4. Conclusion

The most stable structure (structure 1) of HFIP•••water complex was determined using PNFTMW spectrometer. Monomer HFIP exists in the form of two conformers, AP and SC. The AP conformer is more stable than the SC conformer. Ab initio calculation predicted two structures for the complex. The rotational constants for both the structures are close and it was always challenging to provide proper evidences in favor of experimentally observed structure. To confirm the geometry, three isotopologues, HFIP•••$H_2O$, HFIP•••$D_2O$ and HFIP•••HOD, were studied and fitted well within the experimental uncertainties. Absences of *a-type* transition, more intensity of *b-type* transition over *c-type* transition were some of the strong experimental evidences which supported structure 1. Absence of *a-type* transitions can be explained on the basis of the internal rotation of water along its $C_{2V}$ axis. The barrier for this motion was lower than the ZPE of corresponding normal mode vibration. This free

motion also explains that both of the hydrogen atoms of water are identical in the complex. Furthermore, Kraitchmann's analysis also supported that the observed structure is structure 1. The experimentally observed structure (Structure 1) has a very strong hydrogen bond as confirmed on the basis of AIM and NBO analysis. HFIP•••water complex is even stronger than water dimer. The LC-wPBE/6-311++G** method works better than many other methods for this complex.

## IV.5. Supporting Information

The values of ESP minima and maxima are given for HFIP and water along with their coordinated at LC-wPBE level of theory. Coordinates for the HFIP•••water complex are also given for different possible structure at MP2.6-311++G** and LC-wPBE/6-311++G** level of theory. Finally, coordinates of the vibrationally averaged geometry are given for the different structures of HFIP•••water complex at LC-wPBE level of theory.

## IV.6. References


1. M. Rosenblatt, N. V Beaudette, and G. D. Fasman, *Proc. Natl. Acad. Sci. U. S. A.*, 1980, **77**, 3983–7.

2. D. Hong, M. Hoshino, R. Kuboi, and Y. Goto, *J. Am. Chem. Soc.*, 1999, **121**, 8427–8433.

3. M. Burdisso, R. Gandolfi, L. Toma, R. Obertib, and R. Oberti, *Tetrahedron*, 1991, **47**, 6725–6736.

4. K. Yoshida and T. Yamaguchi, *Chem. Phys.*, 2003, **119**, 6132–6142.

5. B. Czarnik-Matusewicz, S. Pilorz, L.-P. Zhang, and Y. Wu, *J. Mol. Struct.*, 2008, **883-884**, 195–202.

6. A. Shahi and E. Arunan, *Talk number RK16, 68th Int. Symp. Mol. Spectrosc.*, 2013.

7. S. J. Cyvin, J. Brunvoll, and M. Perttilä, *J. Mol. Struct.*, 1973, **17**, 17–21.

8. A. J. Barnes and J. Murto, *J. Chem. Soc. Faraday Trans. 2*, 1972, **68**, 1642.

9. H. Schaal, T. Häber, and M. A. Suhm, *J. Phys. Chem. A*, 2000, **104**, 265–274.

10. D. R. Truax, H. Wieser, P. N. Lewis, and R. S. Roche, *J. Am. Chem. Soc.*, 1974, **96**, 2327–2338.

11. E. Hirota and Y. Kawashima, *J. Mol. Spectrosc.*, 2001, **207**, 243–253.

12. S. Kondo and E. Hirota, *J. Mol. Spectrosc.*, 1970, **34**, 97–107.

13. G. S. Grubbs, S. E. Novick, W. C. Pringle, J. Laane, E. J. Ocola, S. A. Cooke, G. S. G. Ii, J. Esther, and A. H. Road, *J. Phys. Chem. A*, 2012, **116**, 8169–8175.

14. D. A. Obenchain, D. J. Frohman, G. S. Grubbs II, B. E. Long, W. C. Pringle, and S. E. Novick, *Talk TC04, 67th Int. Symp. Mol. Spectrosc. Ohio State Univ. Columbus, OH.*, 2012.

15. Frisch, M. J.; Trucks, G. W.; Schlegel, H. B.; Scuseria, G. E.; Robb, M. A.; Cheeseman, J. R.; Scalmani, G.; Barone, V.; Mennucci, B.; Petersson, G. A.; Nakatsuji, H.; Caricato, M.; Li, X.; Hratchian, H. P.; Izmaylov, A. F.; Bloino, J.; Zheng, G.; Sonnenberg, J. L.; Hada, M.; Ehara, M.; Toyota, K.; Fukuda, R.; Hasegawa, J.; Ishida, M.; Nakajima, T.; Honda, Y.; Kitao, O.; Nakai, H.; Vreven, T.; Montgomery Jr., J. A.; Peralta, J. E.; Ogliaro, F.; Bearpark, M.; Heyd, J. J.; Brothers, E.; Kudin, K. N.; Staroverov, V. N.; Kobayashi, R.; Normand, J.; Raghavachari, K.; Rendell, A.; Burant, J. C.; Iyengar, S. S.; Tomasi, J.; Cossi, M.; Rega, N.; Millam, J. M.; Klene, M.; Knox, J. E.; Cross, J. B.; Bakken, V.; Adamo, C.; Jaramillo, J.; Gomperts, R.; Stratmann, R. E.; Yazyev, O.; Austin, A. J.; Cammi, R.; Pomelli, C.; Ochterski, J. W.; Martin, R. L.; Morokuma, K.; Zakrzewski, V. G.; Voth, G. A.; Salvador, P.; Dannenberg, J. J.; Dapprich, S.; Daniels, A. D.; Farkas, O.; Foresman, J. B.; Ortiz, J. V; Cioslowski, J.; Fox, D. J. Gaussian 09 Revision C.01.

16. O. A. Vydrov and G. E. Scuseria, *J. Chem. Phys.*, 2006, **125**, 234109.

17. J.-D. Chai and M. Head-Gordon, *Phys. Chem. Chem. Phys.*, 2008, **10**, 6615–20.

18. S. Grimme, *J. Chem. Phys.*, 2006, **124**, 034108.

19. J.-D. Chai and M. Head-Gordon, *Phys. Chem. Chem. Phys.*, 2008, **10**, 6615–6620.

20. W. Gordy and R. L. Cook, *Microwave Molecular Spectra. 2nd ed.*, New York: Wiley Interscience, 1984.

21. H. M. Pickett, *J. Mol. Spectrosc.*, 1991, **148**, 371–377.

22. Z. Kisiel, *PROSPE - Programs for ROtational SPEctroscopy*, http://info.ifpan.edu.pl/~kisiel/prospe.htm.

23. Z. Kisiel, in *Spectroscopy from Space SE - 6*, eds. J. Demaison, K. Sarka, and E. Cohen, Springer Netherlands, 2001, vol. 20, pp. 91–106.

24. T. Lu and F. Chen, *J. Comput. Chem.*, 2012, **33**, 580–92.

25. T. Lu and F. Chen, *J. Mol. Graph. Model.*, 2012, **38**, 314–23.

26. R. F. W. Bader, *Atoms in Molecules: A Quantum Theory*, Oxford University Press, Oxford, 1990.

27. *AIMAll (Version 13.11.04), Todd A. Keith, TK Gristmill Software, Overl. Park KS, USA, 2013*.

28. E. D. Glendening, J. K. Badenhoop, A. E. Reed, J. E. Carpenter, J. A. Bohmann, C. M. Morales, C. R. Landis, and F. Weinhold, *NBO6.0*, 2006.

29. E. Arunan, S. Dev, and P. K. Mandal, *Appl. Spectrosc. Rev.*, 2004, **39**, 131–181.

30. S. R. Gadre and P. K. Bhadane, *J. Chem. Phys.*, 1997, **107**, 5625–26.

31. P. Politzer and J. S. Murray, *Chemphyschem*, 2013, **14**, 278–94.

32. T. Yamaguchi, S. Imura, T. Kai, and K. Yoshida, *Zeitschrift für Naturforsch. A*, 2013, **68a**, 145–151.

33. R. F. W. Bader and H. Essen, *J. Chem. Phys.*, 1984, **80**, 1943–1960.

34. E. Espinosa, I. Alkorta, J. Elguero, and E. Molins, *J. Chem. Phys.*, 2002, **117**, 5529.

35. D. Cremer and E. Kraka, *Angew. Chemie Int. Ed. English*, 1984, **23**, 627–628.

36. N. J. M. Amezaga, S. C. Pamies, M. Peruchena, N. M. Peruchena, and G. L. Sosa, *J. Phys. Chem. A*, 2010, **114**, 552–62.

37. E. Arunan, G. R. Desiraju, R. a. Klein, J. Sadlej, S. Scheiner, I. Alkorta, D. C. Clary, R. H. Crabtree, J. J. Dannenberg, P. Hobza, H. G. Kjaergaard, A. C. Legon, B. Mennucci, and D. J. Nesbitt, *Pure Appl. Chem.*, 2011, **83**, 1619–1636.

# *Supporting Information*

*Table IV. S. 1. ESP maxima and minima for HFIP at LC-wPBE/6-311++G**. Starred points are the extreme values in the set of maxima or minima.*

HFIP maxima and minima values

Number of surface minima: 8

| | # (label) | kJ/mol | X (Å) | Y (Å) | Z (Å) |
|---|---|---|---|---|---|
| | 13 | -27.17 | -3.91 | 0.66 | -0.15 |
| | 14 | -23.41 | -2.25 | -0.97 | 2.36 |
| | 15 | -25.50 | -1.94 | -2.76 | 0.46 |
| * | 16 | -78.17 | -0.05 | 3.33 | -1.23 |
| | 17 | -28.84 | -0.07 | -2.63 | -0.22 |
| | 18 | -25.50 | 1.97 | -2.76 | 0.44 |
| | 19 | -23.41 | 2.25 | -0.96 | 2.37 |
| | 20 | -27.17 | 3.87 | 0.81 | -0.10 |

Number of surface maxima: 5

| | | | | | |
|---|---|---|---|---|---|
| | 21 | 62.7 | -2.90 | -0.93 | 0.56 |
| | 22 | 84.02 | 0.03 | -1.37 | 1.10 |
| | 23 | 149.64 | 0.05 | 0.15 | -2.88 |
| * | 24 | 235.75 | -0.07 | 2.28 | 1.90 |
| | 25 | 62.28 | 2.92 | -0.91 | 0.55 |

*Table IV. S. 2. ESP maxima and minima for water at LC-wPBE/6-311++G**. Starred points are the extreme values in the set of maxima or minima.*

Water maxima and minima values

Number of surface minima: 1

| | Number | | | | |
|---|---|---|---|---|---|
| * | 6 | -160.51 | -0.05 | 1.96 | 0.05 |

Number of surface maxima: 2

| | | | | | |
|---|---|---|---|---|---|
| * | 4 | 191.86 | -1.68 | -1.25 | 0.03 |
| | 5 | 191.44 | 1.62 | -1.31 | -0.04 |

*Table IV. S. 3. Coordinate of HFIP at LC-wPBE/6-311++G***

| Coordinate of the HFIP molecule | | | |
|---|---|---|---|
| Atoms | X (Å) | Y (Å) | Z (Å) |
| C | 0.00 | 0.52 | -0.53 |
| C | 1.29 | -0.15 | -0.04 |
| C | -1.29 | -0.15 | -0.04 |
| O | 0.00 | 1.86 | -0.18 |
| H | 0.00 | 0.46 | -1.62 |
| H | 0.00 | 1.95 | 0.78 |
| F | 2.34 | 0.44 | -0.61 |
| F | 1.42 | -0.02 | 1.29 |
| F | 1.33 | -1.45 | -0.34 |
| F | -1.33 | -1.45 | -0.34 |
| F | -1.42 | -0.02 | 1.29 |
| F | -2.34 | 0.44 | -0.61 |

*Table IV. S. 4. Coordinate of the water molecule at LC-wPBE/6-311++G***

| Coordinate of water molecule | | | |
|---|---|---|---|
| Atoms | X (Å) | Y (Å) | Z (Å) |
| O | 0.00 | 0.12 | 0.00 |
| H | 0.76 | -0.46 | 0.00 |
| H | -0.76 | -0.46 | 0.00 |

*Table IV. S. 5. Coordinate of the HFIP(AP)---water complex for structure 1 ( Figure IV. 4a) at MP2/6-311++G***

| Structure 3a at MP2/6-311++G** AP---water | | | |
|---|---|---|---|
| Atoms | X (Å) | Y (Å) | Z (Å) |
| C | -0.05 | -0.30 | 0.80 |
| C | -1.34 | -0.35 | -0.02 |
| C | 1.20 | -0.66 | 0.00 |
| O | 0.10 | 0.93 | 1.43 |
| H | -0.15 | -1.06 | 1.58 |
| H | 0.22 | 1.63 | 0.76 |
| F | -2.38 | -0.05 | 0.77 |

| | | | |
|---|---|---|---|
| F | -1.33 | 0.53 | -1.03 |
| F | -1.56 | -1.57 | -0.53 |
| F | 1.10 | -1.87 | -0.59 |
| F | 1.45 | 0.24 | -0.97 |
| F | 2.26 | -0.69 | 0.80 |
| O | 0.48 | 3.02 | -0.35 |
| H | -0.28 | 3.56 | -0.59 |
| H | 0.88 | 2.78 | -1.19 |

*Table IV. S. 6. Coordinate of the HFIP(SC)---water complex for structure 2 (Figure IV. 4b) at MP2/6-311++G***

| Atoms | X (Å) | Y (Å) | Z (Å) |
|---|---|---|---|
| C | -0.11 | -0.35 | -0.13 |
| C | -0.49 | 1.12 | 0.04 |
| C | 1.40 | -0.60 | -0.12 |
| O | -0.66 | -1.12 | 0.89 |
| H | -0.46 | -0.65 | -1.13 |
| H | -1.55 | -1.38 | 0.59 |
| F | -1.84 | 1.21 | 0.09 |
| F | -0.01 | 1.66 | 1.15 |
| F | -0.09 | 1.87 | -1.00 |
| F | 2.03 | 0.17 | -1.02 |
| F | 1.94 | -0.36 | 1.08 |
| F | 1.64 | -1.88 | -0.43 |
| O | -3.08 | -1.48 | -0.40 |
| H | -3.63 | -0.69 | -0.33 |
| H | -3.70 | -2.21 | -0.40 |

*Table IV. S. 7. Coordinate of the HFIP(AP)---water complex for structure 1 (Figure IV. 5a) at LC-wPBE/6-311++G***

| Atoms | X (Å) | Y (Å) | Z (Å) |
|---|---|---|---|
| C | -0.03 | -0.30 | 0.80 |
| C | -1.32 | -0.43 | -0.01 |
| C | 1.24 | -0.59 | -0.01 |
| O | 0.05 | 0.93 | 1.42 |
| H | -0.08 | -1.06 | 1.58 |
| H | 0.12 | 1.66 | 0.76 |

| | | | |
|---|---|---|---|
| F | -2.37 | -0.18 | 0.77 |
| F | -1.36 | 0.43 | -1.04 |
| F | -1.47 | -1.66 | -0.51 |
| F | 1.20 | -1.78 | -0.61 |
| F | 1.46 | 0.34 | -0.95 |
| F | 2.30 | -0.58 | 0.81 |
| O | 0.27 | 3.05 | -0.35 |
| H | -0.51 | 3.58 | -0.54 |
| H | 0.66 | 2.82 | -1.20 |

*Table IV. S. 8. Coordinate of HFIP(AP)•••water complex for structure 2 (Figure IV. 5b) at LC-wPBE/6-311++G***

| Atoms | X (Å) | Y (Å) | Z (Å) |
|---|---|---|---|
| C | -0.28 | -0.18 | 0.03 |
| C | -0.26 | 1.34 | -0.09 |
| C | 1.10 | -0.84 | -0.09 |
| O | -0.87 | -0.55 | 1.24 |
| H | -0.91 | -0.57 | -0.77 |
| H | -0.34 | -0.24 | 1.97 |
| F | -1.51 | 1.81 | -0.06 |
| F | 0.40 | 1.90 | 0.95 |
| F | 0.32 | 1.76 | -1.21 |
| F | 1.72 | -0.52 | -1.23 |
| F | 1.90 | -0.49 | 0.93 |
| F | 0.96 | -2.17 | -0.06 |
| O | -2.84 | -1.74 | -0.48 |
| H | -3.79 | -1.79 | -0.60 |
| H | -2.69 | -1.59 | 0.46 |

*Table IV. S. 9. Cartesian coordinate and internal coordinate of HFIP•••water complex for vibrationally averaged geometry and equilibrium geometry at LC-wPBE/6-311++G**.*

| Reference Geometry or Equilibrium Geometry | | | | | parameter | | |
|---|---|---|---|---|---|---|---|
| Center | Atomic | Coordinates | (Angstroms) | | parameter | Vib. Av. Geom. | Equb.Geom. |
| Number | Number | X | Y | Z | R(1-2) | 1.538 | 1.532 |
| | | | | | R(1-3) | 1.538 | 1.532 |
| 1 | 6 | -0.01898 | -0.2955 | 0.801654 | R(1-4) | 1.382 | 1.378 |
| 2 | 6 | -1.30652 | -0.45953 | -0.01279 | R(1-5) | 1.101 | 1.093 |
| 3 | 6 | 1.25347 | -0.56932 | -0.00593 | R(2-7) | 1.337 | 1.336 |
| 4 | 8 | 0.039863 | 0.937324 | 1.41456 | R(2-8) | 1.344 | 1.344 |

| | | | | | | | |
|---|---|---|---|---|---|---|---|
| 5 | 1 | -0.05591 | -1.06242 | 1.57985 | R(2-9) | 1.337 | 1.337 |
| 6 | 1 | 0.095774 | 1.662438 | 0.759191 | R(3-10) | 1.337 | 1.336 |
| 7 | 9 | -2.36094 | -0.20096 | 0.765122 | R(3-11) | 1.346 | 1.346 |
| 8 | 9 | -1.35626 | 0.389544 | -1.05312 | R(3-12) | 1.337 | 1.335 |
| 9 | 9 | -1.44778 | -1.70021 | -0.49064 | R(4-6) | 0.976 | 0.979 |
| 10 | 9 | 1.22975 | -1.75719 | -0.61679 | R(13-14) | 0.9 | 0.96 |
| 11 | 9 | 1.454217 | 0.370932 | -0.94839 | R(13-15) | 0.952 | 0.961 |
| 12 | 9 | 2.311353 | -0.54839 | 0.807688 | R(6-13) | 1.813 | 1.784 |
| 13 | 8 | 0.199225 | 3.056412 | -0.3491 | A(2-1-3) | 113.5 | 113.5 |
| 14 | 1 | -0.58887 | 3.571171 | -0.53778 | A(2-1-4) | 111.4 | 111.6 |
| 15 | 1 | 0.595453 | 2.841485 | -1.19737 | A(2-1-5) | 106.1 | 106 |
| | | | | | A(1-2-7) | 109.5 | 109.5 |
| | Vibrationally averaged geometry | | | | A(1-2-8) | 112 | 112 |
| Center | Atomic | Coordinates | (Angstroms) | | A(1-2-9) | 112.4 | 112.2 |
| Number | Number | X | Y | Z | A(3-1-4) | 110.9 | 111 |
| | | | | | A(3-1-5) | 106.2 | 106.1 |
| 1 | 6 | -0.01462 | -0.29852 | 0.802987 | A(1-3-10) | 112.7 | 112.7 |
| 2 | 6 | -1.3082 | -0.45947 | -0.01348 | A(1-3-11) | 111.7 | 111.6 |
| 3 | 6 | 1.261208 | -0.58459 | -0.00671 | A(1-3-12) | 109.5 | 109.5 |
| 4 | 8 | 0.05092 | 0.943876 | 1.404604 | A(4-1-5) | 108.3 | 108.2 |
| 5 | 1 | -0.05519 | -1.06388 | 1.593426 | A(1-4-6) | 112.1 | 111.6 |
| 6 | 1 | 0.088209 | 1.667176 | 0.750275 | A(7-2-8) | 107.3 | 107.4 |
| 7 | 9 | -2.36271 | -0.1995 | 0.765803 | A(7-2-9) | 107.6 | 107.7 |
| 8 | 9 | -1.3577 | 0.39197 | -1.0516 | A(8-2-9) | 107.8 | 107.8 |
| 9 | 9 | -1.45556 | -1.69876 | -0.4943 | A(10-3-11) | 107.7 | 107.7 |
| 10 | 9 | 1.234604 | -1.77831 | -0.60793 | A(10-3-12) | 107.8 | 107.9 |
| 11 | 9 | 1.466775 | 0.347265 | -0.9557 | A(11-3-12) | 107.2 | 107.3 |
| 12 | 9 | 2.321139 | -0.56136 | 0.807714 | A(4-6-13) | 174.9 | 176.4 |
| 13 | 8 | 0.148836 | 3.11468 | -0.34021 | A(14-13-15) | 107.5 | 106.6 |
| 14 | 1 | -0.59463 | 3.481742 | -0.68978 | A(14-13-6) | 122.1 | 119.6 |
| 15 | 1 | 0.810246 | 3.099392 | -1.0249 | A(15-13-6) | 116.3 | 113.4 |

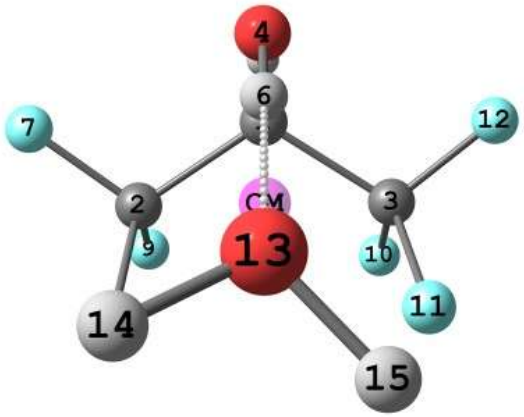


Reference molecule for the geometrical parameter.

# Chapter V. Hydrogen Bond and van der Waals Radii

## V.1. Introduction

The van der Waals (vdW) radius is one of the easiest ways of confirming the weak interaction and it is extensively used for intermolecular and intramolecular interactions. In general, two atoms are considered to be bonded or interacting if the distance between them is shorter than the summation of their vdW radii. There are many other well established theoretical and experimental methods to determine the non-covalent interactions. However, these methods are difficult to apply quickly to determine the weak interaction and vdW radii method is still the most popular criteria. Pauling's seminal book[1] introduces various types of bonding e.g. covalent, ionic, metallic, hydrogen as well as vdWinteractions. He also defined the radii corresponding to these interactions like covalent radii, ionic radii, metallic radii and vdW radii but did not define hydrogen bond radii. There must be several good reasons behind this. One of the reasons could be using X-ray crystallographic data in which locating H-atom was not possible accurately. Pauling proposed a table for the vdW radii of the atoms on the basis of contact distances observed by experiments. Later, it has been revised by many groups, using the same or different methods.[2–9] The most popular table, used by the scientific community for the vdW radii is from Bondi's work.[2]However, Bondi,in his paper itself, clearly mentioned that "*It cannot be overemphasized that the van der Waals radii of this paper have been selected for the calculation of volumes. They may not always be suitable for the calculation of contact, distances in crystals."* The basic assumption for calculating the vdW radii was that "the effective shapes of atoms are spherical". Other important observation made by Bondi is; radii remain unchanged in different environment except for light atoms and radii are additive. In short, the 'vdW radius of an atom is constant'. There are at least three assumptions involved; 1) state of hybridization and

the substituent should not affect the radii of atoms, 2) atoms will be spherical and therefore, distance between them should not depend on the approac angle and 3) radii are additive which means distance between the two interacting atoms A and H (A•••H) would be equal to the average of the corresponding homoatomic contacts, A•••A and H•••H.[10] We look at the validity of all these assumptions closely in this work. However, the largest database for crystal structures 'Cambridge Crystallographic Data Center' (CCDC) still uses the Bondi's radii for the confirmation of hydrogen bond.[11]

In another instance, Pauling mentioned that hydrogen occupies no space in hydrogen bonded complexes. The reason was given as follows: in complex, hydrogen has no electron and act as a bare nucleus, it can be treated as proton (radius 0.66 fm)[12] which is insignificant in comparison to the typical intermolecular distances in molecules.[1] Buckingham and Fowler also concluded similarly, stating that hydrogen atom immersed in the vdW sphere of the heavy atoms A and D for the A•••H-D complex.[13] Influenced by these two works, confirmation of hydrogen bonding in A•••H-D was done by comparing the experimental distance between the two heavy atoms (A, D) and the sum of their vdW radii. If the sum of the vdW radii of heavy atoms is more than the experimentally observed distances between the heavy atoms, they are considered to be bonded through hydrogen. Perhaps, the reason behind using this rule was again the lack of information (location) about H-atom from X-ray crystallography. However, location of heavy atoms can be probed well by X-ray crystallography.

Our group has defined 'hydrogen bond radii' for various hydrogen bond donors.[14–16] Based on the result from about 100 complexes, it was suggested that the use of a single vdW radius for hydrogen and acceptor atom, in determining the presence or absence of hydrogen bond, should be discontinued. For different donor molecules DH, hydrogen bond radius was found to be

different from different D. Therefore, using a single radius for hydrogen (or any light atoms) in all kind of complexes is just not acceptable. This issue has been noticed many times.[14,15,17,18]

The next issue we would like to address is the shape of hydrogen in the hydrogen bonded complexes. The non-spherical atoms are known for long.[19] Bondi mentioned about the pear shape of the atoms without citing any references.[2] Bondi states "*...all atoms have been treated as spheres and spherical segments, although it is well known that many are more nearly pear-shaped.*" There are many unanswered questions in his article about the anisotropy of the atoms.

In fact, the shape of the H atom in an A•••H-D hydrogen bonded complex depends on both donor and acceptor part, let us call it the 'environment' to represent it collectively. Moreover, hybridization of D-atom also affects the hydrogen bond radii.[2] Anisotropy in the shape of H atoms bonded to oxygen by a single bond is less than that in the shape of hydrogen bonded to oxygen with a double bond. The difference in the anisotropy is more prominent in the perpendicular direction to the bond.[2] The objective of this Chapter is to find the changes in the shape of hydrogen atom before and after complex formation as we have learned that hydrogen bond radius changes with environment. Using the word 'radii' is itself misleading and directly indicating the assumption of spherical shape of atoms. What is the shape of hydrogen? How it changes with different donors and acceptors? These are the major questions addressed in the present work. This study may be useful to the organic chemists, crystallographers, biologists and software developers who use the contact distance as a criterion to confirm the presence of hydrogen bond. Throughout the study, we focus particularly on the shape of the hydrogen atom and hydrogen bond radii for monomer H-D and for complex A•••H-D. This compilation also covers extensively the literature available on this topic till date.

## V.2. Earlier Work: Estimation of Radii and Shape of Hydrogen

In his famous book, *The Elements,* Emsley[12] mentioned about the vdW radius as "the face that the atom presents to the world beyond the molecule". The correct representation of radius is rather important. First of all, we would like to distinguish vdW radii of hydrogen from hydrogen bond radii. General meaning of the radii is hydrogen bond radii throughout this chapter. A large number of works have been done on the hydrogen bond radii and anisotropy of the atom. However, most of these are based on the crystal structural database.

In general, three atoms participate in the formation of a hydrogen bond represented as A•••H-D. A is an acceptor which is mostly electron rich region of the molecule e.g. A can be an atom (Ar), an atom, of a molecule, with a lone pair (e.g. N of $NH_3$) or electron rich regions of the molecules (like π-electrons of $C_2H_2$). It can also be a source of a single electron ($CH_3$) or σ-electrons ($H_2$). H-atom is covalently bonded to D and D-H is called the hydrogen bond donor. D can be any atom (F, Cl or Br) or any group (OH, SH, NC, CCH or CN) which is more electronegative than hydrogen. The three dots in the A•••H-D notation denote the intermolecular bond between H and A. The old definition of hydrogen bonding suggested that A and D should be highly electronegative atoms (F, N, O). However, now a large number of complexesare known in which D and A are not N/F/O. Examples of such complexes are those bound with interactions like C-H•••O and C-H•••π. To the best of our knowledge, the first work on the hydrogen bond radii was done by Wallwork in 1962.[20] The objective of the work was the estimation of hydrogen bond distances from crystal structure information which were less in number at that time. Wallwork collected D••••A distances in the D-H•••A contacts and assumed it to be the sum of hydrogen bond radii for D-H and van der Waals radii for A,

$$r_{D\cdots A} = r_H\,(DH) + r_v\,(A)$$

Though he could generate a set of hydrogen bond radii for several DH molecules, he could not find any pattern. This work was soon forgotten and crystallographers continued to use van der Waals radii of D and A to decide about hydrogen bond between D-H and A.

Gadre and Bhadane[21] took the next step towards determining the hydrogen bond radii. They used theoretical and experimental H•••A distances, in a series of F-H•••A complexes, rather than F••••A distances. With theory, locating the hydrogen atoms is never a problem. Hence they wrote the H•••A distance as,

$$r_{H\cdots A} = r_v\,(H) + r_v\,(A)$$

They called $r_v$ (H) as the van der Waals radii of the hydrogen atoms and $r_v$ (A) as the van der Waals radii of A. However, instead of using the standard van der Waals radii for A, they determined the same using electrostatic potential for A. This work concluded that the van der Waals radius of the hydrogen for HF as donor was 0.47 Å which is much less than standard van der Waals radius of hydrogen (1.2 Å).

Mandal and Arunan[14] extended this analysis to HCl/HBr/HCN. They defined the differences between the hydrogen bond distance $r_{H\cdots A}$ and $r_{esp}$ (A) as the 'hydrogen bond radius'.

$$r_{H\cdots A} = r_v\,(H) + r_v\,(A)$$

Here $r_v$ (A) was the same value calculated using electrostatic potential in Gadre and Bhadane's work. Experimental data for several complexes were used to get $r_{H\cdots A}$ distance i.e. hydrogen bond distance for each donor molecule, HD (like HF, HCl, HBr, HCN). All data were plotted as

shown in the Figure V. 1 (right side). In this plot, on X-axis, $r_v$ (A) distance is shown and on Y-axis, the difference between hydrogen bond length and $r_v$ (A) is shown. As a result of fitting, there are different values for different donor molecule. For example 0.55(07), 0.74(08), 0.80(11) and 0.93(07) Å are the respective hydrogen bond radii for the HF, HCl, HBr and HCN donor molecules. Furthermore, they noted a correlation between these hydrogen bond radii (Y-axis) and the dipole moments of the HD (left side of Figure V. 1). Good correlation was observed and it helped in calculation of hydrogen bond radii for HI (0.90 Å). Intercept of the fitted line on Y-axis indicates a molecule with zero dipole moment. This intercept (1.1 Å) was interpreted as van der Waals radius of hydrogen and this was close to the value given by Pauling as well as Bondi (1.2 Å).(references)

Arunan et al.[15] have further extended the above study by introducing more number of donors but the obtained fitted line was not able to reproduce the van der Waals radii. Non-linear fitted line intersects the Y-axis at 1.4 Å which is larger than the standard vdW radii of hydrogen (left side Figure V. 2). Then AIM theory was used for the further calculation and results were promising. In this study, the acceptor radius was considered as the distance from acceptor to the intermolecular bond critical point (BCP), denoted by $r_{A\cdots BCP}$ (A) whereas the hydrogen bond radius was the distance from H-atom to the same intermolecular BCP denoted by $r_v$ (H).

$$r_{H\cdots A} = r_v(DH) + r_{A\cdots BCP}(A)$$

The hydrogen bond radii found from this analysis, were 0.65(07), 0.78(09), 0.81(11), 0.78(08), 0.97(13), 0.85(08) and 0.92(07) Å for HF, HCl, HBr, $H_2O$, $H_2S$, HCN and $C_2H_2$ donor molecules, respectively. The hydrogen bond radius of a particular donor was obtained by averaging all $r_v$ (H) distances for different acceptors. These radii when plotted against dipole

moment, showed better correlation. The fitted line gave vdW radii as 1.1 Å, very close to 1.2 Å (right side of Figure V. 2). About one hundred complexes were selected for the calculation of the hydrogen bond radius of the mentioned donors. Using crystal structural database and microwave spectroscopic data, the hydrogen bond radii of OH, NH and acidic CH groups were determined in another work.[22]

According to Koch and Popelier[23], one of the necessary and sufficient criteria to confirm the hydrogen bond is positive penetration between the interacting atoms. Positive penetration mean when the sum of the non-bonded radii of H and A is greater than the sum of the bonded radii of H and A.

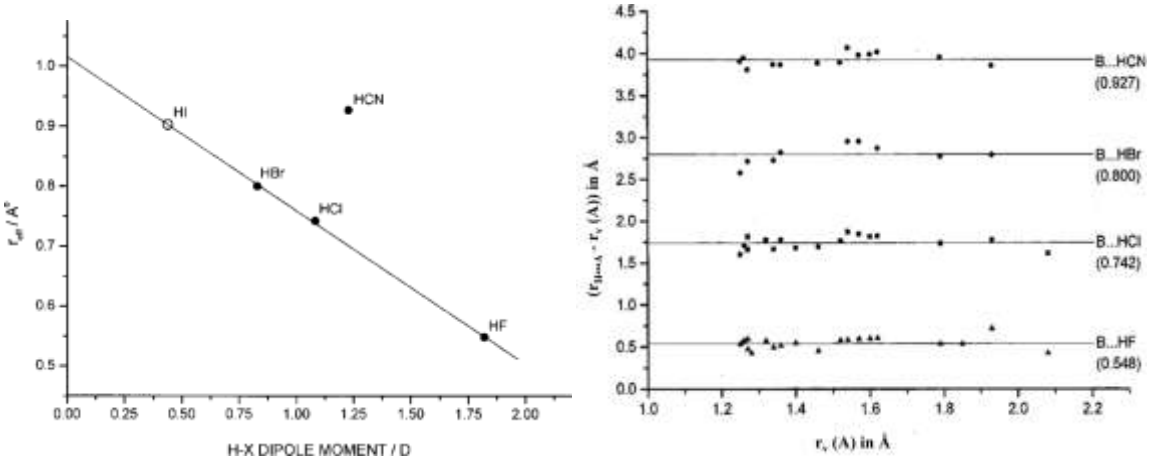


*Figure V. 1. Correlation of hydrogen bond radii with dipole moment (left side). Hydrogen bond radii values for different molecule (right side).*
*In the left side figure, on Y-axis, the values $r_{eff}$ is the hydrogen bond radius (given in small brackets in right side figure). These figures are reproduced with permission of the publisher.*

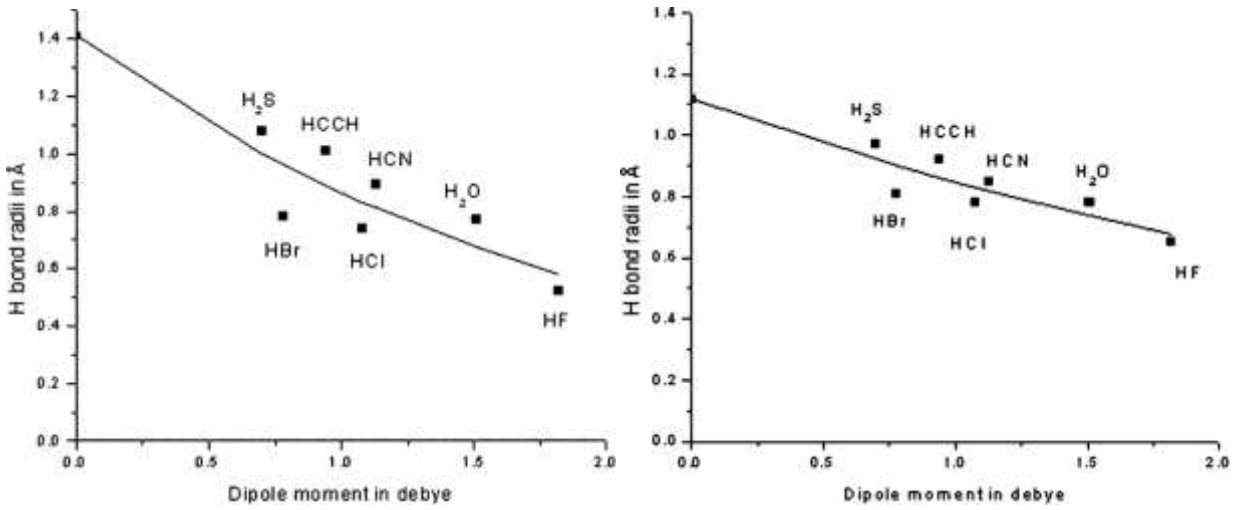


*Figure V. 2. Correlation between hydrogen bond radii (calculated by MESP value) with dipole moment (left side).*
*In the right side figure, correlation between hydrogen bond radii (calculated by AIM) with dipole moment. These figures are reproduced with permission of the publisher.*

The variation of hydrogen bond radii for various donor D-H was explained by Klein[18] using the electron density at the BCP. He pointed out that the electron density values at BCP vary widely for various DH. Typically four types of interactions have been monitored in the study, O•••H-O, O•••H-N, N•••H-N and O•••H-C. Modified vdW atomic radii for hydrogen, nitrogen and oxygen are given at different electron density contour plot (Table 1 of reference[18]). Since our work focuses on the hydrogen, therefore only data related to hydrogen are presented in Table V. 1. For a complex D-H•••A, value of electron density at the BCP of H•••A bond decided the choice of electron density contour value used for the calculation of radii. For example, Klein suggested that vdW radius corresponding to 0.005 a.u. contour plot should be used for X-H•••O and X-H•••N interactions where X= N or O. These radii are 0.98 Å, 1.46 Å and 1.33 Å for hydrogen, nitrogen and oxygen respectively. Therefore, maximum hydrogen bond distances for H•••N- and H•••O- can be 2.44 Å and 2.31 Å. On the other hand, for weak hydrogen bond, such as C-H•••O or C-H•••N the appropriate vdW atomic radii correspond to 0.002 a.u. electron density contour. Radii are 1.18 Å, 1.66 Å and 1.50 Å for hydrogen, nitrogen and oxygen

respectively. Note that the van der Waals radius of hydrogen is 1.2 Å, proposed by Pauling[1] and Bondi[2] and for the weak interaction cases (C-H•••O or C-H•••N), hydrogen bond radius is almost equal to the van der Waals radius (1.2 Å). This is an important point to emphasis that van der Waals radius is suitable for weak hydrogen bonds and not for the strong hydrogen bond. This analysis may also be useful in determining the intramolecular interaction. Theoretically, there are no straightforward methods to calculate intramolecular binding energy. AIM theory can predict the intramolecular bonding by showing the presence of BCP at the expected position. For 1,2-ethanediol, AIM results indicate that there is no intramolecular hydrogen bond (there is no BCP). However, infrared spectroscopy suggests the presence of an intramolecular hydrogen bond. Interestingly, in this molecule the H•••O distance is less than the sum of the van der Waals radii for H and O. However, it is more than the sum of 'hydrogen bond radii' for O-H and O. However, O-H•••O angle is not linear. Hence the conclusion from hydrogen bond radii may be incorrect in this case. Another study, where the CH•••π interactions were monitored on the basis of contact distance, showed the usefulness of hydrogen bond radii. The details of both the studies have been given in the section 5.3.4.

*Table V. 1. van der Waals radii (in Å) for hydrogen atoms at different electron density contour plot.*

| Electron density | 0.001 | 0.002 | 0.005 | 0.010 |
|---|---|---|---|---|
| Bader work[24] | 1.52 | 1.34 | -- | -- |
| Klein work[18] | 1.34 | 1.18 | 0.98 | 0.82 |

Bondi himself has mentioned about non-spherical 'peer-shaped' atoms in 1966 itself. Independently, Nyburg and Batsanov have done enormous amount of work to determine the vdW radii and shape of atoms. Nyburg published a paper titled "Polar Flattening: Non-Spherical Effective Shapes of Atoms in Crystals" in 1979.[19] Crystal structure database was used for the structural searches. Anisotropy in the F, Cl, Br, I, N and H had been found and parameters

related to the anisotropy are given in Table V. 2. Distance along the bond, a, is larger than the distance perpendicular to the bond, b. Authors produced two major factors for the reason behind polar flattening; electron density profile and bond polarizability. In a previous work, Nyburg measured the anisotropy in the fluorine atom.[25] In summary, fluorine-atom in $F_2$ molecules was considered as the semi-spheroid with major radii of 1.34 and 1.55 Å. In this work, the author assumed that molecular multipole interactions are the reason behind this anisotropy. About a decade ago, 'polar flattening' has been interpreted as 'σ-hole' by Politzer.[26] In subsequent works,[8,27] Nyburg revised the vdW radii for H, N, O, F, S, Cl, Se, Br and I atoms which were bonded to carbon. He found non-spherical shape of S, Cl, Se, Br, I.[8] The shapes of the atoms were spheroid with the shortest distance in the direction of bond pole, termed as 'polar flattening'. In this study, N and O were showing spherical shape. Author's second objective was to observe the reason for anisotropy, whether it was influenced by environment (lattice) or by directly bonded atom to the targeted atom. Finally, he concluded that shortest distance was influenced by the atom directly bonded to it. This is the same conclusion given by Wallwork in 1962 *(vide supra)*.[20] Also, work has been done on the hydrogen directly bonded to the carbon (both $sp^2$ and $sp^3$). Hydrogen was of spheroid shape with shortest radii towards the bond pole (polar flattening).[27] This article presented that C($sp^2$) bonded hydrogen atoms have less radii than the C($sp^3$) bonded hydrogen atoms and concluded that the effective radii of hydrogen depends on the state of hybridization of the C-atom**.**

*Table V. 2. Least-squares fit of shortest non-bonded interatomic distance.*

| Atom | System | a(Å) | b(Å) | References |
|---|---|---|---|---|
| F | X-F•••F-X | 1.54 | 1.34 | a |
| Cl | Cl-Cl•••Cl-Cl | 1.90 | 1.67 | b |
| Cl | C-Cl•••Cl-C | 1.75 | 1.69 | c |
| Br | Br-Br•••Br-Br | 2.01 | 1.64 | d |
| I | I-I•••I-I | 2.16 | 1.76 | e |
| N | $RCN^{-}$•••$Y^{+}$ | 1.69 | 1.42 | f |
| H | H-H•••H-H | 1.53 | 1.31 | g |
| H | H-H•••H-H | 1.78 | 1.45 | h |

*X = halogens, (a) Nyburg & Szymafiski (1968). (b) Collin (1956). (c) Sakurai, Sundaralingam & Jeffrey (1963). (d) Vonnegut & Warren (1963). (e) Kitaigorodskii, Khotsyanova & Struchkov (1953). (f) Andersen, Klewe & Thom (1967). (g) Calculated from data given by Etters, Danilowicz & England (1975). (h) Calculated from data given by Kochanski (1973). This table is reproduced with permission of the publisher.*

Batsanov[28] has determined the vdW radius of hydrogen for HF, HCl, HBr, OH, SH, HB and HAl on the basis of gas phase data and HCl, HBr, HI, $CH_4$ and $H_2S$ on the basis of solid phase data. Another objective of this study was to compare the effects of phase (solid and gas) on the radii. In solid state, the average vdW radii for hydrogen were 0.75, 0.86 and 0.96 for HCl, HBr and HI, respectively. The vdW radii of hydrogen for $CH_4$ and $H_2S$ in the longitudinal direction of bonds were 1.04 and 1.01 Å. It is interesting to know that these values are close to the 'hydrogen bond radii' for these molecules as determined by our laboratory. In the gas phase, to measure the vdW radius of hydrogen in $H_2$ molecule, electronic polarisabilty anisotropy data were used which gives the information about volume and radii. The vdW radius for the hydrogen along the longitudinal direction (bond pole) is 1.52 Å. In gas phase study for Rg•••HX complex (where Rg= rare gases atom and X = F, Cl, I, O, S, B, Al), hydrogen bond distances and angles were used for the calculation of the radii along longitudinal bond. If acceptor was deviated from the linearity, radii values increased e.g. Ar•••HF complex, hydrogen radii is 0.987 Å at 127° angle, which is 0.135 Å longer than the value at 180°. The details are presented in Table V. 3. It appears from this study that, radii become smaller when there is increment of positive charge on the hydrogen atom. The vdW radii for C-H hydrogen increases in the order C($sp$) < C($sp^2$) < C($sp^3$). The difference in the hydrogen vdW radii between gas and solid state cannot be generalized (Table V. 4). For the hydrogen halides, it was concluded that in solid phase hydrogen

is more electropositive because of environment and therefore there was a decrement in radii in the solid phase. Another very important outcome of this article was that hydrogen vdW radii correlated well with the bond polarity (electronegativity difference between H and covalently bonded atom) presented in Figure V. 4. An important observation which is not mentioned in the original article is at zero polarity, a vdW radius is around 1.2 Å, (intersection at Y-axis) which is vdW radius of hydrogen (Figure V. 4).

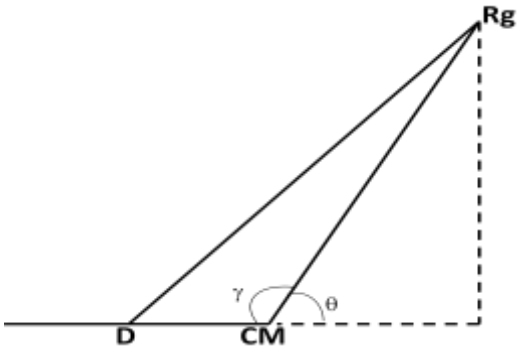


*Figure V. 3. Structural parameters of Rg•••HD complex.*
*This is a reference figure for Table V. 3, adopted from reference[28].*

*Table V. 3. The van der Waals radii of H and anisotropy in the shape of hydrogen for Rg•••HD.*

| Rg•••HD | $Rg•••HD_{cm}$ | γ° | Δγ | d (Rg•••H) | Rγ(H) | $R_l$(H) | $R_l$ (H) (Avg) |
|---|---|---|---|---|---|---|---|
| Ar•••HF | 3.5096[a] | 127 | 0.135 | 2.917 | 0.987 | 0.852 | 0.82 |
| Kr•••HF | 3.6105[a] | 130 | 0.12 | 2.988 | 0.905 | 0.785 | |
| Ar•••HCl | 3.9795[a] | 123 | 0.155 | 3.160 | 1.249 | 1.094 | 1.04 |
| Kr•••HCl | 4.0822[a] | 128 | 0.13 | 3.200 | 1.190 | 1.060 | |
| Xe•••HCl | 4.2457[a] | 133 | 0.11 | 3.300 | 1.089 | 0.979 | |
| Ar•••HBr | 4.1331[a] | 121 | 0.165 | 3.237 | 1.308 | 1.143 | 1.12 |
| Kr•••HBr | 4.2431[a] | 126 | 0.14 | 3.262 | 1.232 | 1.092 | |
| Ne•••HO | 3.6894[b] | 180 | 0 | 2.767 | 1.163 | 1.163 | 0.94 |
| Ar•••HO | 3.7049[b] | 180 | 0 | 2.782 | 0.868 | 0.868 | |
| Kr•••HO | 3.7827[b] | 180 | 0 | 2.860 | 0.796 | 0.796 | |
| Ne•••HS | 4.2097[b] | 180 | 0 | 2.901 | 1.185 | 1.185 | 1.03 |
| Ar•••HS | 4.2093[b] | 180 | 0 | 2.900 | 0.974 | 0.974 | |
| Kr•••HS | 4.2771[b] | 180 | 0 | 2.968 | 0.941 | 0.941 | |
| Ar•••HB | 3.70[C] | 90 | 0.25 | 3.53 | 1.64 | 1.39 | 1.39 |
| Ar•••HAl | 3.86[C] | 97 | 0.24 | 3.71 | 1.77 | 1.53 | 1.53 |

*Ref a =[29], Ref b =[30], ref c = [31]. Where D is F, Cl, Br, O, S, B, Al. Rg is rare gas and Rg•••HDcm is the distance between Rg and centre of mass of HD. γ value is presented in Figure V. 3. This table is reproduced with permission of the publisher.*

*Table V. 4. Comparison of gas and solid phase vdW radii.*

| Group | HO | HCl | HBr | $CH_4$ | $H_2$ |
|---|---|---|---|---|---|
| Solid | 0.90 | 0.75 | 0.86 | 1.04 | 1.52 |
| Gas-phase | 0.92 | 1.02 | 1.12 | 1.01 | 1.52 |

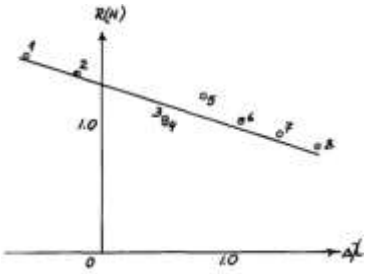


*Figure V. 4. Dependence R(H) in the Rg•••HA molecules on the electronegativity difference. Electronegativity difference $\Delta\chi = \chi(A) - \chi(H)$: 1. HA1, 2. HB, 3. HC, 4. HS, 5. HBr, 6. HC1, 7. HO, 8. HF. This figure is reproduced with permission of the publisher.*

Estimations of the vdW radii have been done by Batsanov for atoms using different data and methods e.g. determination of vdW radii of metal using bond distances,[4] thermodynamics determination of vdW radii,[5] vdW radii from spectroscopic data,[7] vdW radii of elements from the data of structural inorganic chemistry,[6] Compilation of vdW radii has also been done in some review articles.[3,9]

Natural steric analysis, a theory based on Natural Bond Orbital[32] also presented the anisotropy in H-atom[33]. It is worth mentioning here the work by Benoit and Marx[34], on the dependence of the shape of proton/hydrogen on hydrogen bond length. In other words, investigation has been done that showed how the changes in the distance between acceptor and donor affect the real space shape of the proton in the hydrogen bond. Study has been done on ice sample of 16 water molecules which led to thirteen different densities spanning hydrogen bond length from 2.85 to 2.17 Å. At 2.85 Å distances which corresponds to the equilibrium geometry, hydrogen possess disk like geometry (oblate) in complex.

Recently, Dean[35] suggested to include the anisotropy of the atoms and several important aspects of vdW radii in undergraduate text books. We are discussing two important aspects of vdW radii in this work; anisotropy and effect of the directly bonded atom on radii. To the best of our knowledge, the names such as snub-nosed[36], disk like structure or oblate like structure[34], polar flattening[19], pear-shaped have been given so far to address anisotropy in atoms..[2]

In addition, there is a report which shows reverse results to this anisotropy.[37] According to this study, hydrogen has shorter distance on side-on contact (along the bond pole) and longer distance on the head-on contact (perpendicular to the bond). Basically, the shape the hydrogen appeared as prolate, instead of oblate. This study was done on the inorganic crystals. In the organic crystals the shape of the hydrogen was oblate. There were some environmental forces (unknown to author!) which dominate over the responsible forces (unknown to author!) for anisotropy. It was concluded that when such ambiguity arises, one should not consider anisotropy in atoms. However, according to the results present is this study, the atoms are not spherical and anisotropy in the shape of the atoms should not be neglected.

## V.3. Ab initio Methods: Shape of Hydrogen

### V.3.1. Computational Method

The structure optimization of molecules and complexes have been done using MP2/6-311++G(d,p) level of theory. G09 suite program was used for the calculations[38]. In order to confirm the minima, frequency calculations have been performed at the same level of theory. Presence of the all real frequencies suggested that the optimized structures correspond to true minima. Our main objective for these calculations was to consider isolated molecules which are unperturbed by lattice or solvent interaction. Quantum calculations for isolated molecules are

very good for the prediction of different gas phase experimental values. Later, wavefunctions were generated from the optimized geometries at the same level. These wavefunction were used for the Atoms in Molecules (AIM) analysis.[39,40] AIMALL program has been used for the AIM calculations[41]. AIM theory defines the properties of an atom inside the molecules. Electron density plays an important role in determining and predicting the properties of the molecules. In this work, electron density profile of hydrogen atoms has been chosen to determine the anisotropy in it.

H-F, H-Cl, H-Br, $H_2O$, $H_2S$, $NH_3$, HNC, $CH_4$, HCCH and HCN monomers have been considered. These are the popular donors (H-D) for the H-bonded complexes. $CH_4$ or $NH_3$ rarely works as donor but for comparison purpose they are included in the list. Only two cases are known where ammonia works as donor in the gas phase, $(NH_3)_2$ and $C_6H_6$•••$NH_3$ complex[42–45] and perhaps no experimentally observed complexes for $CH_4$. But theoretically $H_3C$-H•••$OH_2$ complex exists as a minimum (not a global minimum).[46] Matrix isolation experiment is a tool which can trap local minima of a complex. It may be possible to observe this complex in such experiments. In any complex, the H-atom being surrounded by two atoms, A and D and therefore its property depends on both. Treating hydrogen as identical and using a single vdW radii for all hydrogen bond complexes do not appear to be reasonable as pointed out many times.[14–16] For example, in the complex $NH_3$•••HF, hydrogen atoms shape and radii will be different from the complex $NH_3$•••HCl. Therefore, we need to introduce the concept of two distances rather than one radius.

## V.3.2. Evaluation and Determination of the Shape in Monomer

To determine the anisotropy, electron density contours have been plotted for three different values 0.02, 0.005 and 0.002 a.u. (Figure V. 5) for all molecules. These contour plots (2D) were

enough informative for linear molecules but not for non-linear molecules, 3D surface plots should be considered because of non-symmetry along the H-D bond. In this work, only 2D contour plot have been considered for all molecules. Value 0.02 a.u. should be used for very strong H-bonded complexes like N•••H-F and 0.002 a.u. for very weak hydrogen bond like O•••H-C. Other values 0.005 a.u. can be used for intermediate type of bonding and most of the complexes fall in this region. Part of this idea is taken from the work of Klein.[18] Roughly an intermolecular bonding with binding energy (BE) more than 25 kJ/mole comes under very strong bond and below 8 kJ/mole comes under weak H-bonding. It is important to point out that there is no sharp boundary between different types of complexes. There are several other parameters in AIM theory which can characterize the strength like values of electron density at (BCP) and the ratio of potential to kinetic energy of the electron density at BCP (for details, see Chapter VI). For $H_2O$ and $H_2S$, molecular plane has been chosen for plotting contours. Inner contour correspond to the 0.02 a.u. electron density, Outer contour for 0.002 a.u. and middle one is for 0.005 a.u. (Figure V. 5). Interatomic surface is denoted by dashed line and after this region, effect of D-atom dominates.

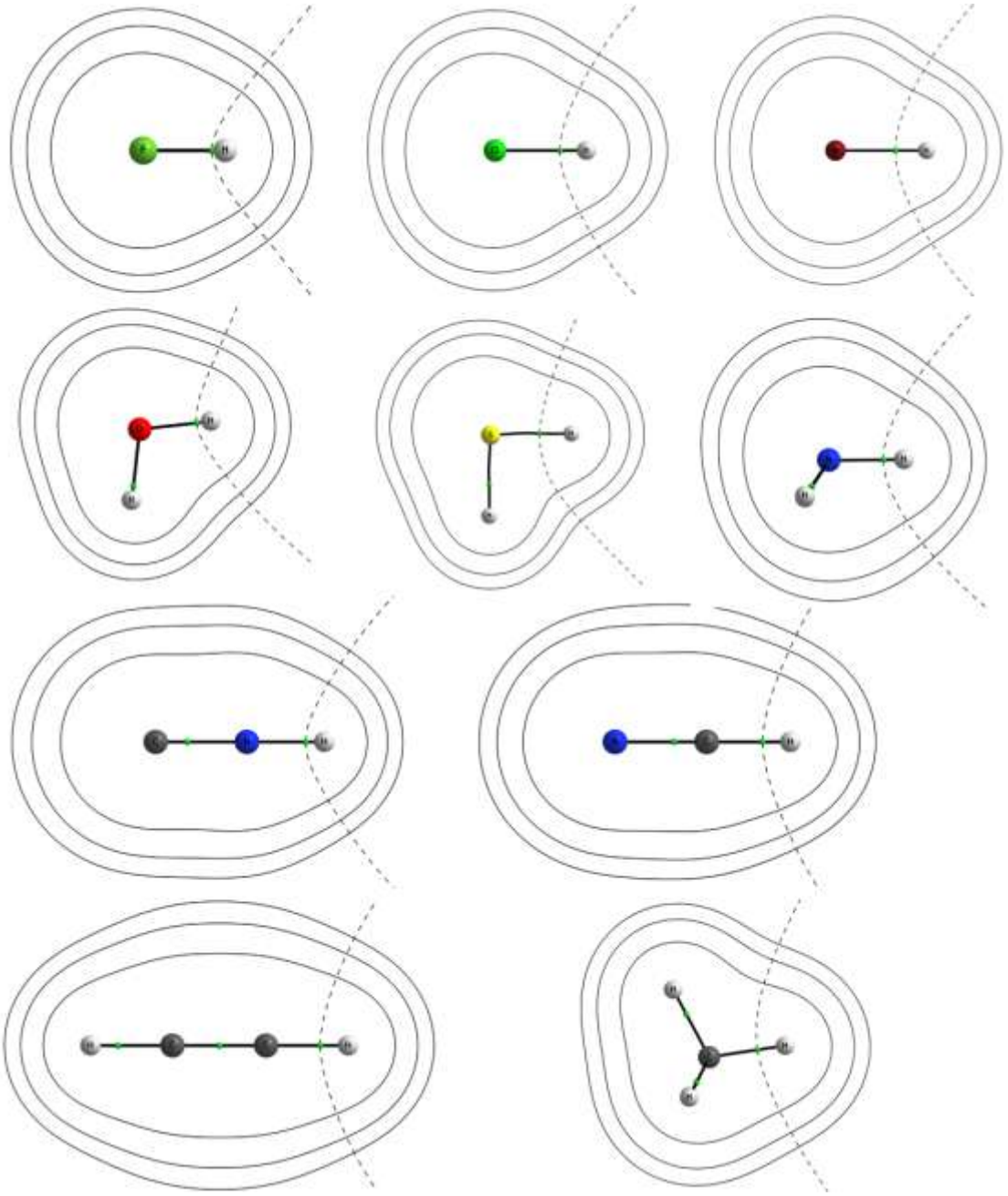

*Figure V. 5. Contour plots of total electron density at the 0.02, 0.005, and 0.002 a.u. (inwards to outwards).*
*Green dot in between the two atoms is bond critical point. Dashed line denotes interatomic surface. Molecules from left to right: HF, HCl, HBr, $H_2O$, $H_2S$, $NH_3$, HNC, HCN, HCCH, $CH_4$.*

As per the new hydrogen bond definition,[47] for a conventional hydrogen bonding, A•••H-D angle should not be less than 110°. The recommendation and accompanying report do not give any justification for this cut off.[47] The interatomic line shown in Figure V. 5 does give a

justification for such cut off. This will be discussed in the appendix A in more details. In this study, contour points are collected only for 110-180° angle range for all molecules (Figure V. 6). Left side figure is a sample figure to demonstrate the distances and angle and right side figure is real one. For ease, we have selected the ∠ A-H-R denoted as angle 'θ', as one of the variables. Ranges between 0-70° were considered for this angle. Another variable is distance (r) between H and contour points at angle θ . Next objective is to fit the coordinate (r, θ) in such a function which has less number of parameters and constrain. We have made several attempts to fit them in trigonometric, exponential, logarithmic functions. But to get a proper fit, many constrains had to be imposed and therefore we looked for some other approach. After changing the (r, θ) to cartesian coordinate, we were able to fit them in to an ellipse equation (right side of Figure V. 6). Fitted graphs for all the molecules are given in Figure V. 7.

$$X^2/a^2 + Y^2/b^2 = 1$$

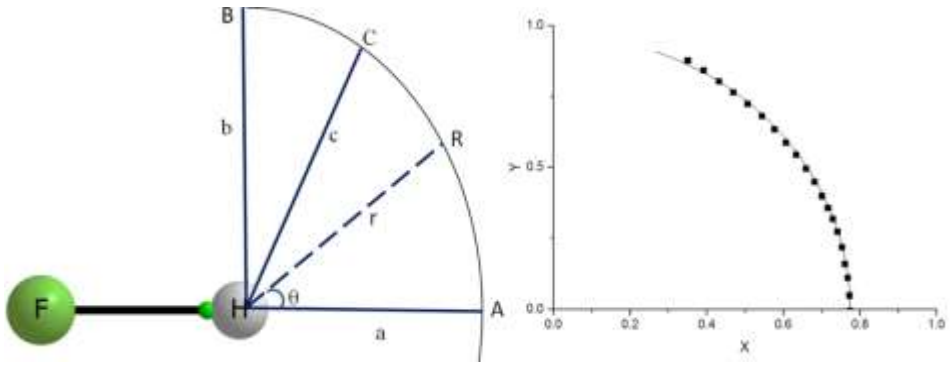


*Figure V. 6. Shape of hydrogen in HF monomer.*
*Left side: a is the distance between H atom and a particular contour point A when ∠F-H-A =180°. b is the distance between H atom B when ∠F-H-B =90°. c is the distance between H atom C when ∠F-H-C =110°. r is the distance from H-atom to R at angle θ and was treated as a variable. Right Side: Contour plot at 0.005 a.u. is shown for HF molecule. Data points were extracted from contour at 0.005 a.u. electron density in the range θ = 0-70°. In this case semi-minor axis a = 0.774 Å (fixed), semi-major axis b = 0.966 Å (fitted) and flattening factor g = 20 %.*

*Table V. 5. Anisotropy in hydrogen for different molecules and complexes.*

| | 0.02 (Strong) | | | | 0.005 (moderate) | | | | 0.002 (Weak) | | | |
|---|---|---|---|---|---|---|---|---|---|---|---|---|
| Monomer | a | b | c | g% | a | b | c | g% | a | b | c | g% |
| HF | 0.53 | 0.67 | 0.65 | 21 | 0.77 | 0.97 | 0.94 | 21 | 0.97 | 1.15 | 1.12 | 16 |
| HCl | 0.58 | 0.71 | 0.69 | 18 | 0.90 | 1.03 | 1.01 | 13 | 1.12 | 1.25 | 1.23 | 10 |
| HBr | 0.61 | 0.73 | 0.71 | 16 | 0.93 | 1.06 | 1.04 | 12 | 1.16 | 1.28 | 1.26 | 9 |
| HOH | 0.57 | 0.67 | 0.66 | 15 | 0.85 | 0.97 | 0.95 | 12 | 1.06 | 1.16 | 1.15 | 9 |
| HSH | 0.64 | 0.73 | 0.72 | 12 | 0.97 | 1.06 | 1.05 | 8 | 1.20 | 1.27 | 1.26 | 6 |
| HNH2 | 0.61 | 0.72 | 0.70 | 15 | 0.90 | 1.05 | 1.03 | 14 | 1.10 | 1.27 | 1.25 | 13 |
| HNC | 0.55 | 0.66 | 0.64 | 17 | 0.82 | 0.95 | 0.93 | 14 | 1.02 | 1.15 | 1.13 | 11 |
| HCH3 | 0.67 | 0.76 | 0.75 | 12 | 0.99 | 1.09 | 1.08 | 9 | 1.21 | 1.32 | 1.31 | 8 |
| HCN | 0.60 | 0.72 | 0.70 | 17 | 0.89 | 1.03 | 1.01 | 14 | 1.09 | 1.25 | 1.23 | 13 |
| HCCH | 0.61 | 0.73 | 0.71 | 16 | 0.90 | 1.05 | 1.03 | 14 | 1.11 | 1.27 | 1.25 | 13 |
| Complex | BCP-H distance | | | | | | | | | | | |
| FH---Ar | 0.93 | 1.43 | 1.33 | 35 | | | | | | | | |
| FH---NH3 | 0.52 | 1.02 | 0.88 | 49 | | | | | | | | |

Where, $X = a\cos(\theta)$ and $Y = b\sin(\theta)$. The distances *a* and *b* are the parameters termed as semi-minor and semi-major radius ($a < b$) respectively. The value of *b* is obtained from the extrapolation of the curve up to 90°. At θ=0° and 90°, value of r represent *a* and *b,* respectively. Traditionally, *a* is called hydrogen bond radii which we have discussed in previous sections. The main focus of this section is to find out the shape of hydrogen, therefore at this juncture, *a*-value has been kept constant during the fit. Varying *a*-values in the fit gives the same result but increases the number of parameter unnecessarily. Also, in large number of studies, presented in last section, mainly *a*-values have been given importance. Results from Arunan et al.[15] and Klein[18] are the most appropriate from our point of view. At the end, we have only one parameter to fit i.e. *b.* As we have learned that, roughly beyond 70°, effect of D-atom dominates in the total electron density. Therefore, in Table V. 5, '*c*' values are also presented. But for the calculation of *c*-value and g-value, there is a need of *b*-value. Uncertainty was in the third place of decimal. The extent of anisotropy can be measured in terms of g-value which is defined as (1-*a*/*b*)*100% and called flattening factor of the ellipse. If the value of g is zero, it represents the isotropic or

spherical structure of the H-atom. It is clear from Table V. 5, g-values vary between 6-21% roughly. This range includes the effect of monomers only. Effects of acceptors along with donors are also presented in Table V. 5. If we move away from the nucleus towards the outer contours, g-value decreases. In other words, shape of the atom changes and tends towards being sphere. Moving downwards or leftwards to the periodic table, g-value for the H atom in HD molecules decreases in general. This is mainly because of the change in electronegativity of the D-atom of the H-D molecule. We have seen the effect of bond polarity and dipole moment on the hydrogen bond radius in previous discussed work.[14,15,28] These works showed the effect of electronegativity or bond polarity on the 'shape of hydrogen'. Hybridization also causes change in g-value. There is less g-values for the H bonded to $sp^3$ C-atom ($CH_4$) than the H bonded to sp hybridized C-atom (HCN and HCCH) and the same is true for the hydrogen bonded with N-atom with single and double bond in $NH_3$ and HNC molecules, respectively (Table V. 5). Average of g-values at 0.02, 0.005 and 0.002 a.u. is 16%, 13% and 11% for strong, moderate and weak intermolecular interactions, respectively. Note that the effect of acceptor is not taken in to account yet. In most of the work, contour corresponds to the 0.001 a.u. electron density, considered as van der Waals periphery and assumed to be circular with single radii. There is lesser but significant amount of anisotropy even for 0.001 a.u. (not presented in the Table V. 5). On the basis of angle A•••H-D and strength of the complex, anisotropy in the hydrogen shape can be predicated quickly but roughly.

| Molecule | 0.02 | 0.005 | 0.002 |
|---|---|---|---|
| HF | 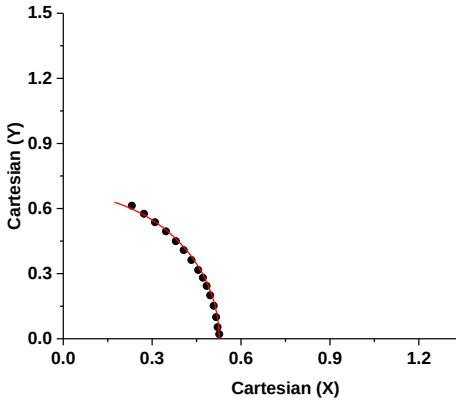 | 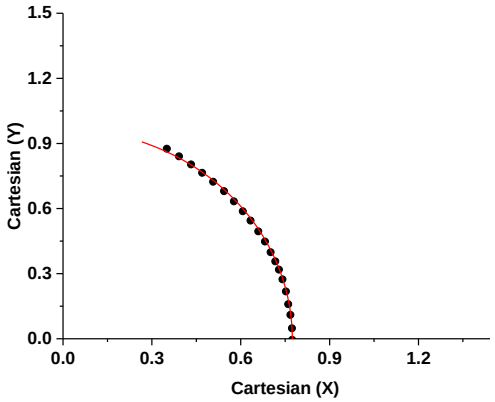 | 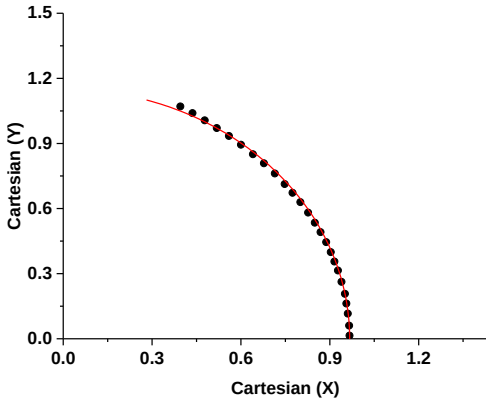 |
| HCl | 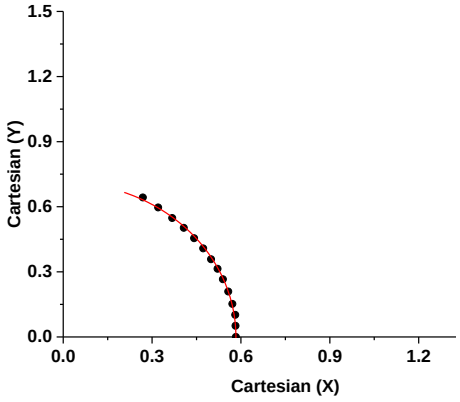 | 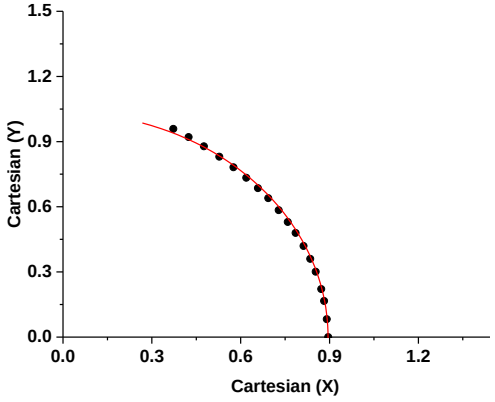 | 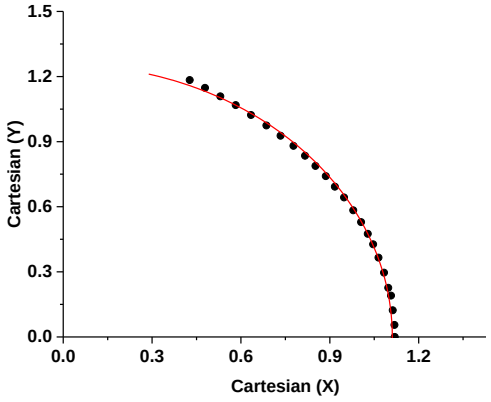 |

| Molecule | 0.02 | 0.005 | 0.002 |
|---|---|---|---|
| HBr | 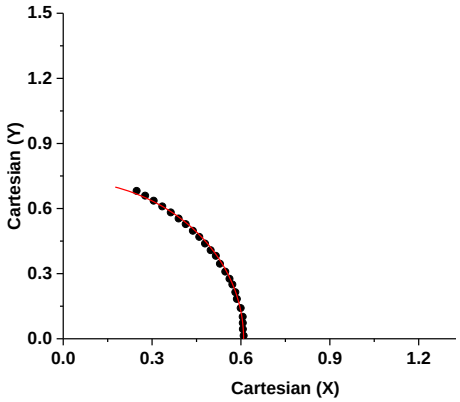 | 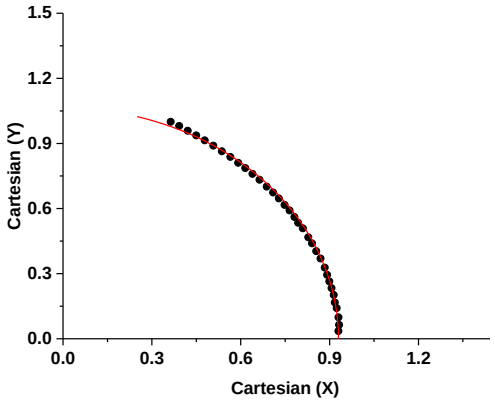 | 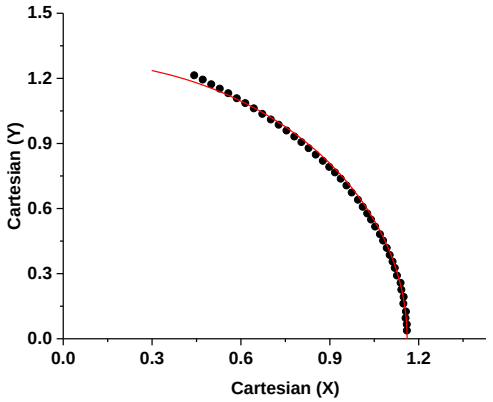 |
| $H_2O$ | 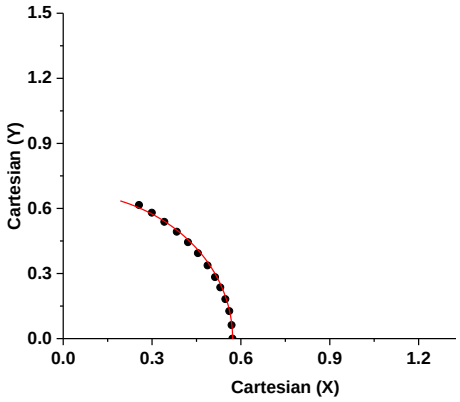 | 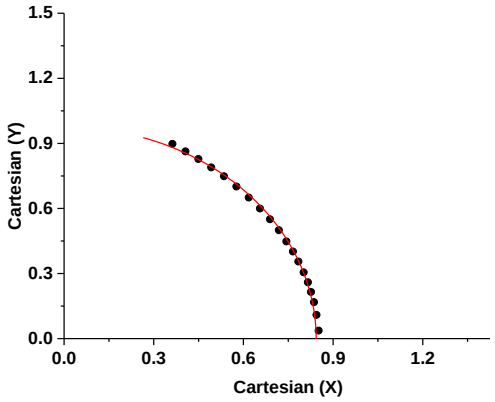 | 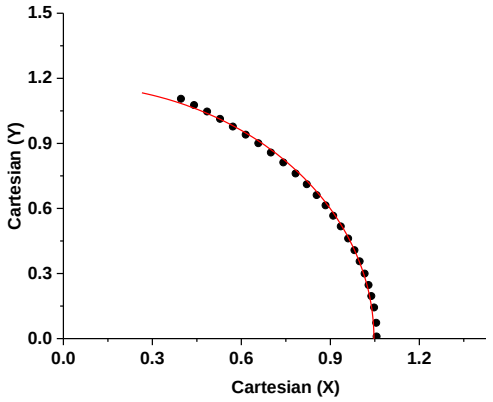 |

| Molecule | 0.02 | 0.005 | 0.002 |
|---|---|---|---|
| $H_2S$ | 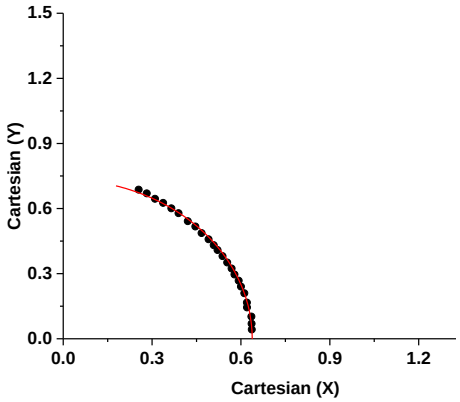 | 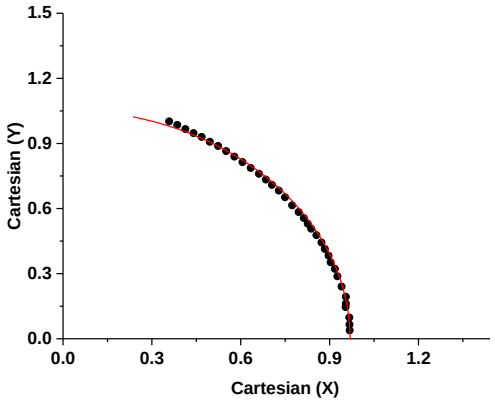 | 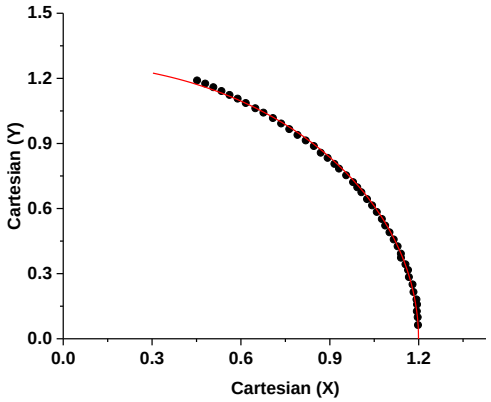 |
| HNC | 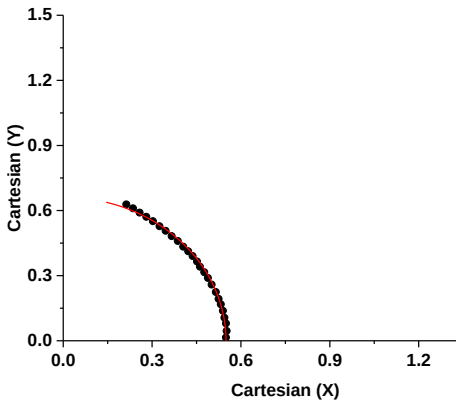 | 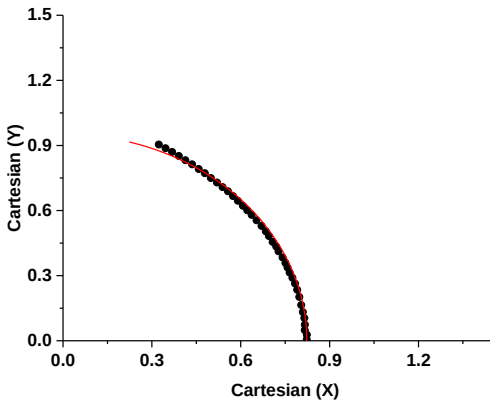 | 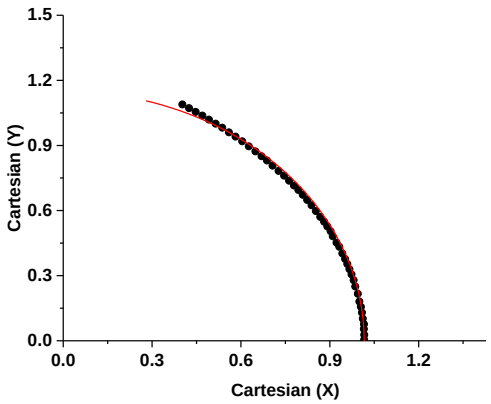 |

| Molecule | 0.02 | 0.005 | 0.002 |
|---|---|---|---|
| $NH_3$ | 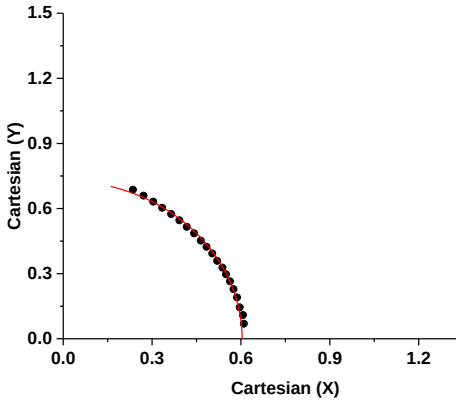 | 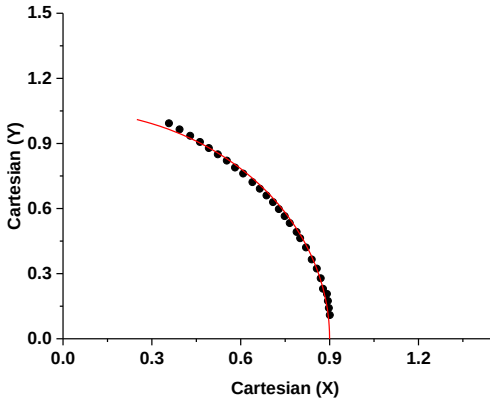 | 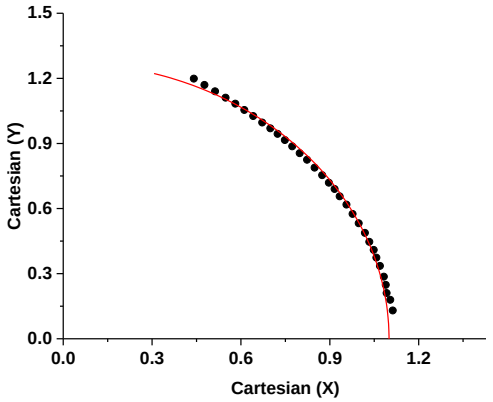 |
| HCN | 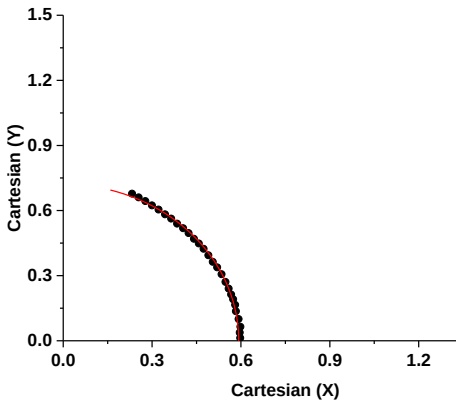 | 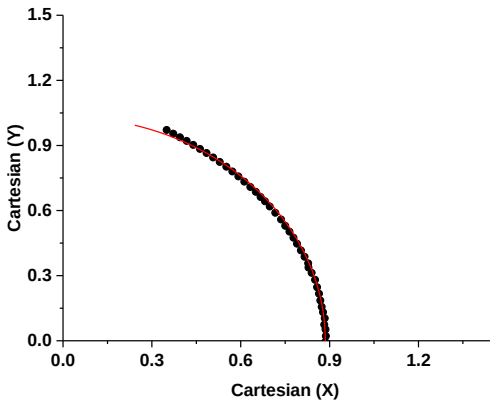 | 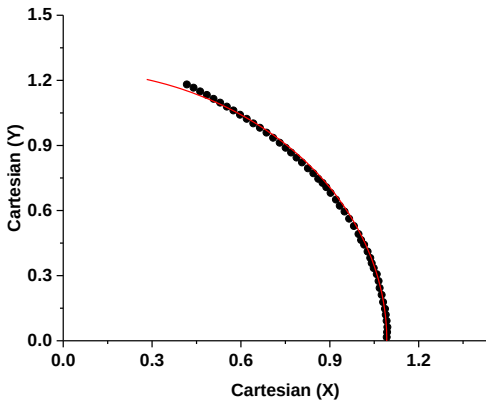 |

| Molecule | 0.02 | 0.005 | 0.002 |
|---|---|---|---|
| HCCH | 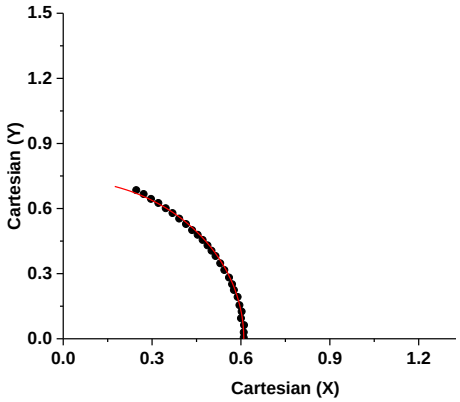 | 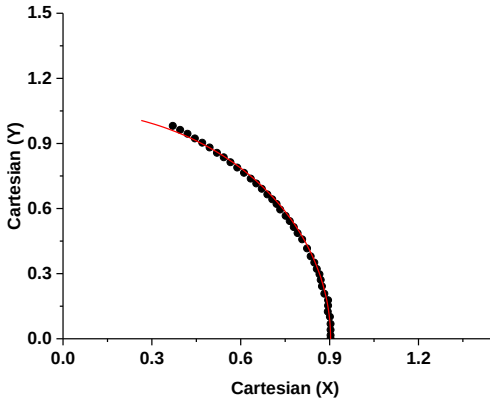 | 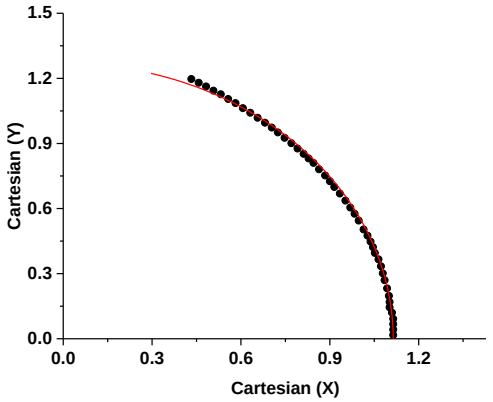 |
| CH4 | 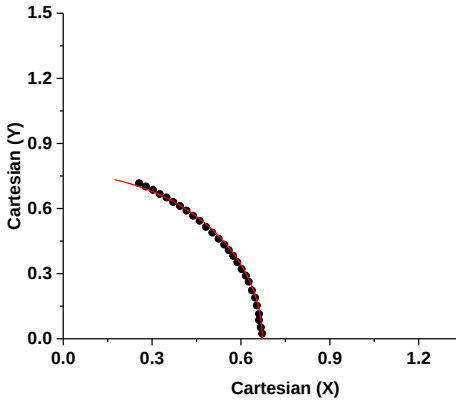 | 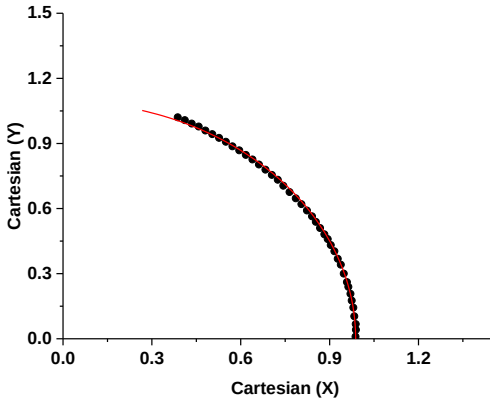 | 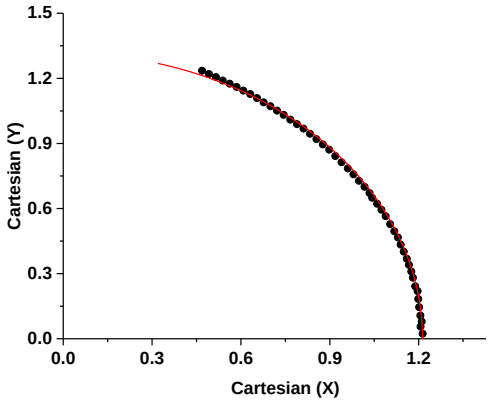 |

| **Complexes** | **0.02** |
|---|---|
| Ar•••HF | 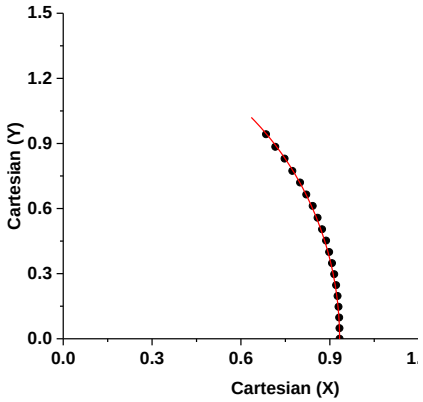 |
| $NH_3$•••HF | 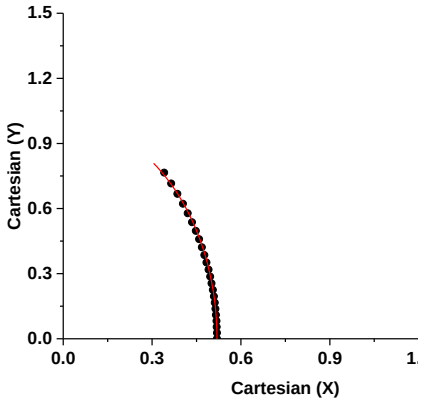 |



*Figure V. 7. Graphs of all molecules at 0.02, 0.005 and 0.002 a.u. contours.*

### V.3.3. The Shape of Hydrogen in a complex

In this part we analyze the effect of acceptor A on the hydrogen bond radius in complex A•••H-D. Hydrogen atom also affects the radius of acceptor A. Here we only focus on former case. Two models have been chosen for this purpose. In the first model, the changes in H-bond radius has been observed by optimizing the F-H•••Ar complex at different hydrogen bond angles from 110° to 180° with the step size of 3°. Relaxed scan, inbuilt method in G09, has been performed for the angle scanning. In the relaxed scan, all geometrical parameters vary during optimization except the angle selected for scanning. In this way, we mimic the real dynamics of the system. Further, AIM analysis has been done for each scanned structures. In this case, distance between H-atom and intermolecular bond critical point (BCP) is taken as variable 'r'. These BCPs are present at the bond path joining H and Ar and by definition, BCP are the limit of the H atomic basin in the direction of acceptor. Ar-atom is working as acceptor and bonding mainly occurs via dispersion and dipole-induced dipole interaction. Coordinates r and θ were fitted in the equation of ellipse after changing it to cartesian form. For this fit, both parameters *a* and *b* were derived (Table V. 5). In all the cases uncertainties were at the third place of decimal. Interestingly, g-value becomes almost two times higher than the g-value of HF monomer for 0.002 a.u. electron density. In the second model, acceptor is a source of an electron pair i.e. $NH_3$. A similar PES scan was performed for $NH_3$•••H-F complex as for Ar•••H-F complex. The g-value is more for $NH_3$ complex (49 %) than Ar complex (35 %). One important point to be noted here is that effect of donor (D) on *b*-value or *c*-values is less than the effect of the acceptor. However, effect of donor on *a*-value is more than the effect of acceptor. This conclusion is given on the basis of two complexes. First, $NH_3$•••H-F which comes under very strongly bonded category and

therefore the *a-, b-, c*-values are compared with the *a-, b-, c*-values of 0.02 a.u. electron density contour for HF monomer. Second, Ar•••H-F complex which comes under weak complex and therefore, data compared with 0.002 a.u. contour values of HF monomer.

Considering water as acceptor in the model leads to complications as it has two non-equivalent lone pairs of electrons. It is generally considered that the orientations of these lone pairs determine the A•••H-D angle which is non-linear in most of the $H_2O$•••H-D complexes. However, the situation is more complicated as the donor of H appears to influence the location of the lone pair (see Chapter VI). However, an extensive study about the effect of oxygen's lone pair on the linearity of a complex can be found in the review[48] by Legon where examples are taken from the experimental results. The non-linearity of A•••H-D angle because of the orientation of oxygen's two lone pair is completely a different issue from the objective of the present work. Therefore, selection of $NH_3$ avoided this complication since it has one lone pair along the $C_{3V}$ axis of the molecule.

### V.3.4. CCDC: Shape of Hydrogen

Shape of the hydrogen can also be determined by obtaining r and θ from the crystal structures. The CCDC database11 was used for the crystal structure searches. Two interactions C(H)2N•••H-N and C(H)2N•••H-O were searched in this work. The acceptor A was a primary amine and bonding through its lone pair to the H-atom of donor. As usual, θ was the N•••H-D hydrogen bond angle but r was the distance between N and H. Therefore, in this case, we are not expecting any quantitative explanation of the shape of hydrogen-atom. In this case, r includes the effect of both acceptor and donor on anisotropy and there is no way to separate them. It is worth mentioning that the analysis here is based on the statistics and it may not be applicable to specific example. Specifically, Isostar49 program was used to see hydrogen bonding. Using information from Isostar, queries were submitted to program Conquest50 for structural search. Isostar is a graphical way to visualize all interaction simultaneously (Figure V. 8). The information, we extracted from Isostar, was mainly the

range of hydrogen bond length which was optimized to reduce the number of unwanted structures. Unwanted structures contained other interactions which would affect the value of r and θ. In Figure V. 8, maximum information (r, θ) were collected from dense area which showing N•••H-(N/O) interactions. The interactions with N-H group of primary amine are unwanted structures which are showing some randomness also. With these good ranges, queries were submitted for structural search to Conquest program. In this way, unwanted structures can be avoided in conquest program too. Of course, the number of hits will reduce but the observed data were sufficient for this study (Table V. 6).

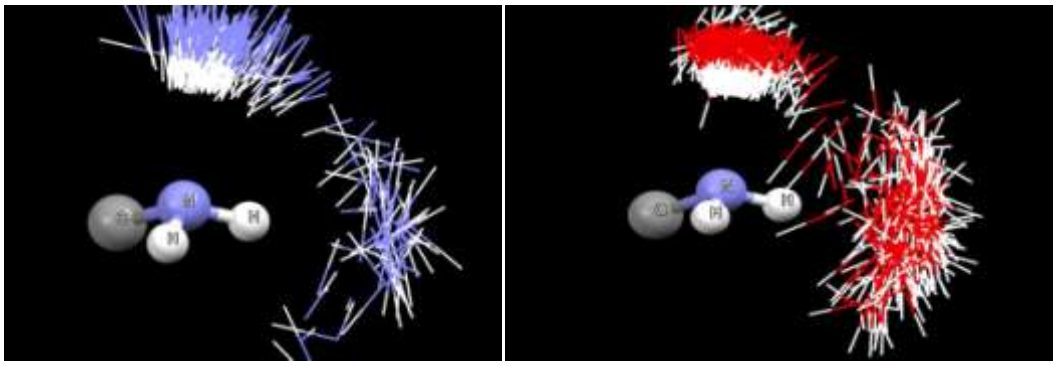

*Figure V. 8. Visualization of all interactions simultaneously with the help if Isostar program. Violet, red and white sticks represent N, O and H atoms respectively.*

Other criteria applied for the searches are as follows; R factor ≤ 0.05, no disordered data, no errors data, no polymeric data, no ionic data, no powder structure data and only organic structures. Along with these criteria, N•••H distances are limited to the range 1.6-2.5 Å for both interactions, $C(H)_2N$•••H-N and $C(H)_2N$•••H-O. Queries were submitted for 110-180° range of N•••H-X angle at the step size of 10°. For each angle, there is a corresponding distance and average of all distances has been taken for the particular angle range. Therefore, two variables are θ, which is mean of the angle range, and r, which is the average of all distances within the angle range (Table V. 6). For convenience in fitting, complementary angle of θ was selected and used hereafter. Fitting and analysis of the data have been done similar to previous section. The (r, θ) coordinates were fitted to the equation of ellipse. The fitted parameters semi-major axis (*b*) and semi minor axis (*a*), axis at angle 70° (*c*) and flattening factor g are presented in Table V. 6. Qualitatively, *a* and *c* are show the angular dependence of radii, similar to the result of previous section. Note that a and c are the

distances between H and A and they include the anisotropy of both H and A. Therefore, these values cannot be compared to results presented in earlier sections. Graphs for fitted data are shown in Figure V. 9. Acceptors in both the cases are the same and one can assume the same effect of anisotropy on H-atom. On this basis, the g-value (flattening) is more for N•••H-O interaction, as expected on the basis of previous analysis. This is because of the fact that electronegativity of oxygen is more than nitrogen. Also, *a*-value is smaller for N•••H-O interaction because of the larger electronegativity of O-atom, compared to N-atom.

*Table V. 6. Anisotropy in hydrogen from CCDC database.*

| | | | N•••H-N | | N•••H-O | |
|---|---|---|---|---|---|---|
| Angle Range | Mean | θ | Average Distance | no. of hits | Average Distance | no. of hits |
| 170-180 | 175 | 5 | 2.239 | 186 | 1.951 | 304 |
| 160-170 | 165 | 15 | 2.273 | 368 | 2.013 | 349 |
| 150-160 | 155 | 25 | 2.302 | 260 | 2.257 | 179 |
| 140-150 | 145 | 35 | 2.351 | 159 | 2.171 | 123 |
| 130-140 | 135 | 45 | 2.364 | 74 | 2.284 | 114 |
| 120-130 | 125 | 55 | 2.300* | 33 | 2.321 | 100 |
| Fitted Value | | | | | | |
| a | | | 2.253 (11) | | 2.031(56) | |
| b | | | 2.526 (42) | | 2.596(181) | |
| c | | | 2.489 | | 2.505 | |
| g% | | | 11 | | 22 | |

**this value excluded from fit.*

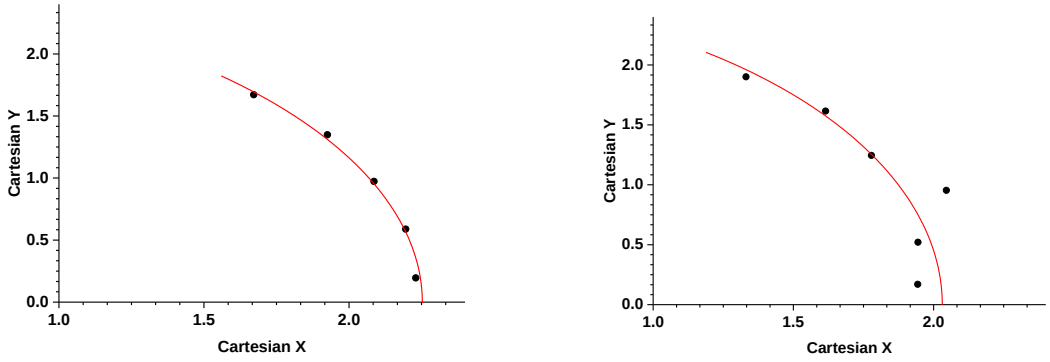


*Figure V. 9. CCDC data fitting for the collective anisotropy of H and N.*
*Left side figure is for N•••H-N interaction and right side is for N•••H-O interaction.*

## V.3.5. Gas Phase Study: Shape of Hydrogen

Structural determination from the microwave spectroscopy provides the most reliable information till date for gas phase molecules or complexes. In this study, data have been collected from different experimental studies and compared them with present work. Sometime D-H-A angle and H•••A distance were not available in the references. These parameters are derived from other information given in the experimental studies. Since this work focuses on the radii of hydrogen atom only, radii of the other atoms are collected from the previous work, if needed.[15] Also, we are not considering the anisotropy in H-atom because of acceptors. For different complexes A•••H-D, hydrogen bond radii have been taken from present work (Table V. 5). Angular dependence on hydrogen bond radius is also included for all examples, though it is less significant in most of the cases, because angles were close to 180° (Table V. 7). There is a good agreement between experimental (column 2) values and the predicted values from this work (column 7).

*Table V. 7. Comparisons with experimental structural parameter.*

| | Experimental parameters | | Ref [15] | This work | | |
|---|---|---|---|---|---|---|
| | A•••H distance | A•••H-D Angle | A-Radius | H-radius | rho of contour | Sum of radii |
| $NH_3$---HBr | 2.0* | 148 | 1.3 | 0.6 | 0.02 | 1.9 |
| $NH_3$---HCN | 2.2 | 164 | 1.3 | 0.9 | 0.005 | 2.2 |
| $NH_3$---HCCH | 2.4 | 164 | 1.3 | 0.9 | 0.005 | 2.2 |
| $CH_3$(HO)---HCl | 1.9 | 172 | 1.2 | 0.6 | 0.02 | 1.8 |
| Oxirane---HF | 1.7* | 170 | 1.2 | 0.5 | 0.02 | 1.7 |
| Oxirane---HCl | 1.8* | 170 | 1.2 | 0.6 | 0.02 | 1.8 |
| Oxirane---HBr | 1.9* | 170 | 1.2 | 0.6 | 0.02 | 1.8 |

**Derived information from available experimental information.*

As mentioned in section 5.2, Batsanov[28] discussed the anisotropy in hydrogen shape of hydrogen atom in Rg•••H-D complexes using experimental data available.[29–31] Our results are in qualitative agreement with his results (Table V. 8). However, Batsanov considered the effect of both Rg and H-D on the anisotropy. Our work has focused on only the donor HD.

*Table V. 8. Comparisons with the experimental structure for Rg•••HD complexes.*

| | | | Batsanov Work[28] | | | This Work | | |
|---|---|---|---|---|---|---|---|---|
| Rg•••HD | γ° | d (Rg•••H) | $R_l$(H) | $R_\gamma$(H) | $\Delta R_\gamma$ | a | *c*(γ) | Δ(*c*-*a*) |
| Ar•••HF | 127 | 2.917 | 0.852 | 0.987 | 0.135 | 0.97 | 1.07 | 0.10 |
| Kr•••HF | 130 | 2.988 | 0.785 | 0.905 | 0.12 | 0.97 | 1.06 | 0.09 |
| Ar•••HCl | 123 | 3.16 | 1.094 | 1.249 | 0.155 | 1.12 | 1.21 | 0.09 |
| Kr•••HCl | 128 | 3.2 | 1.06 | 1.19 | 0.13 | 1.12 | 1.20 | 0.08 |
| Xe•••HCl | 133 | 3.3 | 0.979 | 1.089 | 0.11 | 1.12 | 1.18 | 0.06 |
| Ar•••HBr | 121 | 3.237 | 1.143 | 1.308 | 0.165 | 1.16 | 1.24 | 0.08 |
| Kr•••HBr | 126 | 3.262 | 1.092 | 1.232 | 0.14 | 1.16 | 1.23 | 0.07 |
| Ne•••OH | 180 | 2.767 | 1.163 | 1.163 | 0 | 1.06 | 1.06 | 0 |
| Ar•••OH | 180 | 2.782 | 0.868 | 0.868 | 0 | 1.06 | 1.06 | 0 |
| Kr•••OH | 180 | 2.86 | 0.796 | 0.796 | 0 | 1.06 | 1.06 | 0 |
| Ne•••SH | 180 | 2.901 | 1.185 | 1.185 | 0 | 1.20 | 1.20 | 0 |
| Ar•••SH | 180 | 2.9 | 0.974 | 0.974 | 0 | 1.20 | 1.20 | 0 |
| Kr•••SH | 180 | 2.968 | 0.941 | 0.941 | 0 | 1.20 | 1.20 | 0 |

*Descriptions for part of the term are given in Table V. 3. a is hydrogen bond radius along bond, c(γ) is the hydrogen bond radius at angle γ and Δ (c-a) is the difference between them which indicates anisotropy.*

Finally, we discuss an example which shows the usefulness of the hydrogen bond radii over van der Waals radii of hydrogen. This is the example of 1,2-ethanediol conformer where intramolecular interaction O•••H-O is debated. The reported hydrogen bond distance is 2.2 Å and angle is 110°.[51,18] We have repeated the calculation for this molecule to get the structural parameter at MP2/6-311++G** level of theory. The hydrogen bond distance is 2.32 Å and angle is 109° from the calculation. This is a medium type of bonding (based on hydrogen bond distance) and therefore hydrogen bond radius of $H_2O$ corresponding to 0.005 a.u. contour plot is taken (Table V. 5). The molecule water is the closest donor example in our study which have O-H donor group similar to 1,2-ethanediol and therefore, radius of the hydrogen is taken at 0.005 a.u. electron density from water molecule. The hydrogen bond radii are 0.85 and 0.95 Å at the hydrogen bond angle 180° and 110° respectively (Table V. 5). From previous work,[15] the radius of oxygen as acceptor is 1.27 Å. Using these distances, summation of hydrogen bond radius (at 110°) and acceptor radius is equal to the 2.22 Å, very close to the calculated distance. Whereas, using hydrogen bond distance 0.85 Å at 180° gives 2.12 Å, less than the calculated distance.

The distance between O- and H- is less than the sum of van der Waals radii and so on intramolecular bond is proposed. Chopera et al.[52] showed that the concerned distance is longer than the sum of H-bond radii for OH and O-atom and hence, there is no intramolecular H-bond. The work reported here shows that this distance will be within the accepted values of H-bond when angular dependence is taken into account.

## V.4. Conclusions

A comprehensive work on the angular dependence of hydrogen bond radii is presented. H-F, H-Cl, H-Br, $H_2O$, $H_2S$, $NH_3$, HNC, $CH_4$, HCCH and HCN monomers and $NH_3$•••HF and Ar•••HF complexes were chosen for the study at MP2/6-311++G** level of theory. With the help of electron density contour plot from AIM theory, shape of the hydrogen atoms came out as spheroid after fitting. Only 110-180° range of hydrogen bond angle was selected for study. Flattening factor (g-value) represents anisotropy in the shape of hydrogen atom. The g-values change under certain conditions; 1) increases when moving from outer contour (0.002 a.u.) to inner contour (0.02 a.u.), 2) decreases when going downwards or leftwards in the periodic table, 3) increases when hydrogen attached to different hybridized carbon atom in the order ($sp^3 > sp^2 > sp$) and same with nitrogen attachment and 4) increases because of acceptor presence. The change in g-values can be explained with the help of charge on hydrogen atom or dipole moment of donor part. Crystal structure data and experimental data qualitatively agree with the above observations. Finally, with the help of an example, 1,2-ethanediol, usefulness of angular dependence hydrogen bond radii is shown.

We would like to suggest that it might be prudent not to use van der Waals radius of hydrogen for all type of complexes and recommended the use of hydrogen bond radii instead. Moreover, the angular dependence should be taken in to account and the short and long radii reported for various D-H donor are recommended. These two facts are often ignored by crystallographers, biologists and other chemists who confirm weak interactions on the basis of contact distance. Depending on the donor part, values of hydrogen bond radius along bond path changes and also depending on the angle, values of hydrogen bond radius around the hydrogen changes. Finally, acceptors also affect the radii, significantly.

## V.5. Supporting Information

In this section, coordinate of all the molecules, investigated for the hydrogen bond radii are presented at MP2/6-311++G** level of theory.

## V.6. References


1. L. Pauling, The Nature of the Chemical Bond and the Structure of Molecules and Crystals; An Introduction to Modern Structural Chemistry, Cornell University Press, Ithaca, New York, 1960.

2. A. Bondi, J. Phys. Chem., 1964, **68**, 441–451.

3. S. Batsanov, Inorg. Mater., 2001, **37**, 871–885.

4. S. S. S. Batsanov, J. Mol. Struct., 1999, **468**, 151–159.

5. S. S. Batsanov, J. Mol. Struct., 2011, **990**, 63–66.

6. S. S. Batsanov, Russ. Chem. Bull., 1995, **44**, 18–23.

7. S. S. Batsanov and A. Scientific, Russ. Chem. Bull., 1994, **43**, 1300–1304.

8. S. Nyburg and C. Faerman, Acta Crystallogr. Sect. B …, 1985, **B41**, 274–279.

9. S. S. Batsanov, Russ. J. Inorg. Chem., 1991, **36**, 3015–3037.

10. S. S. Batsanov, J. Chem. Soc. Dalt. Trans., 1998, 1541–1546.

11. F. H. Allen, Acta Crystallogr. Sect. B Struct. Sci., 2002, **58**, 380–388.

12. J. Emsley, The Elements, Clarendon Press, Oxford, Third Ed., 1998.

13. A. D. Buckingham and P. W. Fowler, Can. J. Chem., 1985, **63**, 2018.

14. P. K. Mandal and E. Arunan, J. Chem. Phys., 2001, **114**, 3880.

15. B. Raghavendra, P. K. Mandal, and E. Arunan, Phys. Chem. Chem. Phys., 2006, **8**, 5276.

16. B. Lakshmi, A. G. Samuelson, K. V. J. Jose, S. R. Gadre, E. Arunan, and P. Chemistry, Database, 2005, 371–377.

17. B. Lakshmi, A. G. Samuelson, K. V. J. Jose, S. R. Gadre, and E. Arunan, New J. Chem., 2005, **29**, 371–377.

18. R. A. Klein, Chem. Phys. Lett., 2006, **425**, 128–133.

19. S. C. Nyburg, Acta Crystallogr. Sect. A, 1979, **35**, 641–645.

20. S. C. Wallwork, Acta Crystallogr., 1962, **15**, 758–759.

21. S. R. Gadre and P. K. Bhadane, J. Chem. Phys., 1997, **107**, 5625–26.

22. B. Lakshmi, A. G. Samuelson, K. V. J. Jose, S. R. Gadre, E. Arunan, and P. Chemistry, Database, 2005, 371–377.

23. U. Koch and P. L. A. Popelier, J. Phys. Chem. Chem., 1995, **99**, 9747–9754.

24. R. F. W. Bader, M. T. Carroll, J. R. Cheeseman, and C. Chang, J. Am. Chem. Soc., 1987, **109**, 7968–7979.

25. S. C. Nyburg and J. T. Szymanski, Chem. Commun., 1968, 669–671.

26. P. Politzer, J. S. Murray, and T. Clark, Phys. Chem. Chem. Phys., 2013, **15**, 11178–89.

27. S. C. Nyburg, C. H. Faerman, and L. Prasad, Acta Crystallogr. Sect. B Struct. Sci., 1987, **43**, 106–110.

28. S. Batsanov, Struct. Chem., 1999, **10**, 395–400.

29. M. R. Keenan, J. Chem. Phys., 1981, **74**, 2133.

30. C. C. Carter and T. a Miller, J. Chem. Phys., 1997, **107**, 3447.

31. E. Hwang and P. J. Dagdigian, J. Phys. Chem., 1995, **99**, 3430–3437.

32. A. E. Reed, L. A. Curtiss, and F. Weinhold, Chem. Rev., 1988, **88**, 899–926.

33. J. K. Badenhoop and F. Weinhold, J. Chem. Phys., 1997, **107**, 5422.

34. M. Benoit and D. Marx, Chemphyschem, 2005, **6**, 1738–41.

35. P. a. W. Dean, J. Chem. Educ., 2014, **91**, 154–157.

36. A. Legon, Angew. Chemie Int. Ed., 1999, **38**, 2686–2714.

37. W. H. Baur, Acta Crystallogr. Sect. B Struct. Sci., 1992, **48**, 745–746.

38. Frisch, M. J.; Trucks, G. W.; Schlegel, H. B.; Scuseria, G. E.; Robb, M. A.; Cheeseman, J. R.; Scalmani, G.; Barone, V.; Mennucci, B.; Petersson, G. A.; Nakatsuji, H.; Caricato, M.; Li, X.; Hratchian, H. P.; Izmaylov, A. F.; Bloino, J.; Zheng, G.; Sonnenberg, J. L.; Hada, M.; Ehara, M.; Toyota, K.; Fukuda, R.; Hasegawa, J.; Ishida, M.; Nakajima, T.; Honda, Y.; Kitao, O.; Nakai, H.; Vreven, T.; Montgomery Jr., J. A.; Peralta, J. E.; Ogliaro, F.; Bearpark, M.; Heyd, J. J.; Brothers, E.; Kudin, K. N.; Staroverov, V. N.; Kobayashi, R.; Normand, J.; Raghavachari, K.; Rendell, A.; Burant, J. C.; Iyengar, S. S.; Tomasi, J.; Cossi, M.; Rega, N.; Millam, J. M.; Klene, M.; Knox, J. E.; Cross, J. B.; Bakken, V.; Adamo, C.; Jaramillo, J.; Gomperts, R.; Stratmann, R. E.; Yazyev, O.; Austin, A. J.; Cammi, R.; Pomelli, C.; Ochterski, J. W.; Martin, R. L.; Morokuma, K.; Zakrzewski, V. G.; Voth, G. A.; Salvador, P.; Dannenberg, J. J.; Dapprich, S.; Daniels, A. D.; Farkas, O.; Foresman, J. B.; Ortiz, J. V; Cioslowski, J.; Fox, D. J. Gaussian 09 Revision C.01.

39. R. F. W. Bader, Atoms in Molecules: A Quantum Theory, Oxford University Press, Oxford, 1990.

40. P. L. A. Popelier, Atoms in Molecules. An Introduction, Pearson Education Ltd. Essex, England, 2000.

41. AIMAll (Version 13.11.04), Todd A. Keith, TK Gristmill Software, Overl. Park KS, USA, 2013.

42. D. D. Nelson, W. Klemperer, G. T. Fraser, F. J. Lovas, and R. D. Suenram, J. Chem. Phys., 1987, **87**, 6364.

43. D. D. Nelson, G. T. Fraser, and W. Klemperer, J. Chem. Phys., 1985, **83**, 6201.

44. J. W. I. van Bladel, A. van der Avoird, P. E. S. Wormer, and R. J. Saykally, J. Chem. Phys., 1992, **97**, 4750.

45. D. A. Rodham, S. Suzuki, R. D. Suenram, F. J. Lovas, S. Dasgupta, W. A. Goddard, and G. A. Blake, Nature, 1993, **362**, 735–737.

46. B. Raghavendra and E. Arunan, Chem. Phys. Lett., 2008, **467**, 37–40.

47. E. Arunan, G. R. Desiraju, R. a. Klein, J. Sadlej, S. Scheiner, I. Alkorta, D. C. Clary, R. H. Crabtree, J. J. Dannenberg, P. Hobza, H. G. Kjaergaard, A. C. Legon, B. Mennucci, and D. J. Nesbitt, Pure Appl. Chem., 2011, **83**, 1619–1636.

48. A. Legon and D. Millen, Chem. Soc. Rev., 1987, **16**, 467–498.

49. I. Bruno, J. Cole, J. M. Lommerse, R. S. Rowland, R. Taylor, and M. Verdonk, J. Comput. Aided. Mol. Des., 1997, **11**, 525–537.

50. I. J. Bruno, J. C. Cole, P. R. Edgington, M. Kessler, C. F. Macrae, P. McCabe, J. Pearson, and R. Taylor, Acta Crystallogr. Sect. B Struct. Sci., 2002, **58**, 389–397.

51. R. A. Klein, J. Comput. Chem., 2002, **23**, 585–99.

52. D. Chopra, T. N. Guru, E. Arunan, and R. A. Klein, J. Mol. Struct., 2010, **964**, 126–133.

# *Supporting Information*

*Table V. S. 1. Coordinates of the optimized geometry for all molecules under investigation at, MP2/6-311++G** level of theory are given.*

| Molecule | X (Å) | Y (Å) | Z (Å) |
|---|---|---|---|
| HF | | | |
| H | 0.0000 | 0.0000 | -1.0139 |
| F | 0.0000 | 0.0000 | -0.0972 |
| | | | |
| HCl | | | |
| H | 0.0000 | 0.0000 | -1.1922 |
| Cl | 0.0000 | 0.0000 | 0.0810 |
| | | | |
| HBr | | | |
| H | 0.0000 | 0.0000 | -1.3732 |
| Br | 0.0000 | 0.0000 | 0.0392 |
| | | | |
| $H_2O$ | | | |
| O | 0.6468 | 0.0000 | -1.4743 |
| H | 0.6468 | 0.7533 | -0.8799 |
| H | 0.6468 | -0.7533 | -0.8799 |
| | | | |
| $H_2S$ | | | |
| S | 0.6468 | 0.0000 | -1.6951 |
| H | 0.6468 | 0.9598 | -0.7695 |
| H | 0.6468 | -0.9598 | -0.7695 |
| | | | |
| HNC | | | |
| H | 0.0000 | 0.0000 | 1.4356 |
| N | 0.0000 | 0.0000 | 0.4349 |
| C | 0.0000 | 0.0000 | -0.7466 |

| Molecule | X (Å) | Y (Å) | Z (Å) |
|---|---|---|---|
| $NH_3$ | | | |
| N | 0.0000 | 0.0000 | -0.1117 |
| H | -0.7936 | -0.5085 | 0.2608 |
| H | 0.8373 | -0.4328 | 0.2608 |
| H | -0.0437 | 0.9416 | 0.2607 |
| | | | |
| HCN | | | |
| H | -0.1149 | 0.0000 | -1.2831 |
| C | -0.1149 | 0.0000 | -0.2151 |
| N | -0.1149 | 0.0000 | 0.9563 |
| | | | |
| $C_2H_2$ | | | |
| C | -0.2875 | 0.0000 | -2.2612 |
| C | -0.2875 | 0.0000 | -1.0449 |
| H | -0.2875 | 0.0000 | 0.0197 |
| H | -0.2875 | 0.0000 | -3.3258 |
| | | | |
| $CH_4$ | | | |
| C | 0.0000 | 0.0000 | 0.0000 |
| H | 0.6294 | 0.6294 | 0.6294 |
| H | -0.6294 | -0.6294 | 0.6294 |
| H | 0.6294 | -0.6294 | -0.6294 |
| H | -0.6294 | 0.6294 | -0.6294 |

# Chapter VI. Hydrogen Bonding, Halogen Bonding and Lithium Bonding: An Atoms in Molecules and Natural Bond Orbital Perspective Towards Conservation of Total Bond Order, Inter- and Intra-molecular

*Accepted as a perspective article in Physical Chemistry Chemical Physics, volume 16, 22935-52,* **2014.**

## VI.1. Introduction

Due to the unquestionable importance of hydrogen bonding to life as we know it, there have been an enormous interest in it, with several books being published in the last five decades[1–7]. Hydrogen bonding perhaps belongs to the general non-covalent interactions which are significantly weaker than a typical chemical bond (presumed to be covalent bond)[8,9]. Though, characterization, classification, properties and usefulness of these weak interactions have been actively investigated in the last two decades, such weak interactions are not new. A flavour of such interactions was given by Benesi and Hildebrand[10] as chargetransfer bonds first and later Mulliken[11] termed, complexes formed by weak interaction as electron donor-acceptor complexes and classified as outer and inner type complexes on the basis of strength of intermolecular interaction. The unique position of hydrogen in the periodic table, naturally led to studies on lithium bonding [12] and halogen bonding [13]. Legon [13], in his recent review used pre-reactive complexes which are mostly Mulliken's outer type complexes and described the rules for predicting the angular geometry for hydrogen and halogen bonds. The term 'Halogen bond' was used by Hassel in his Nobel lecture[14]. Recently it has been shown that halogen bonds can be orthogonal to hydrogen bonds in biomolecules (DNA), both playing crucial roles. [15]

Our group had earlier looked at a few selected D-X•••A complexes with DX = FH, FCl or FLi and A being four diverse acceptors, $H_2O$ with a lone pairs, $C_2H_4$ with a $\pi$ pair, $CH_3$ with an unpaired electron and $H_2$ with a $\sigma$ pair of electrons[16]. All these complexes had linear D-X•••A geometry. Many of the electron density topological properties calculated using Atoms in Molecules theory[17], suggested by Koch and Popelier [18] for C-H•••O hydrogen bonding, were comparable for the three different interactions. There was a strong correlation between electron density at the X•••A bond critical point and the interactions energy, though the four acceptors were very different. However, it was noted that the slopes of these correlation plots were very similar for X = H and Cl (263 and 277 respectively) and that for X = Li was distinctly different (769). The sign of the Laplacian indicated that all are closed-shell (non-covalent) interactions. We were curious to see if this trend is general or if it was only applicable for the limited set of complexes chosen for the study. Since our work, detailed AIM theoretical analysis has been reported for halogen bonding [19] and lithium bonding[20].

Our main objective in this work is to take a comprehensive look at all these three interactions with a large number of examples and identify similarities and differences.

Though, the term non-covalent interaction has gained popularity [8], there have been discussions about the extent of covalent contribution to hydrogen bonding from the early days[1–7]. Hydrogen bonding has contributions from electrostatics, polarization, dispersion forces, and charge-transfer covalency to varying extents. The covalent contribution to hydrogen bonding was confirmed by NMR[21] and Compton scattering[22] experiments, published around the same time in 1999 and is now generally accepted. The recent IUPAC recommendation on the definition of hydrogen bonding emphasizes on the 'evidence for bond formation'[23] and Grabowski has reviewed 'the covalency in hydrogen bonding'[24]. Even more recently, visualisation of hydrogen bonding has been made possible by non-contact atomic force microscopy[25]. Hydrogen bonding was initially assumed to be 'simple electrostatic interaction' between two dipoles leading Huggins to suggest the term 'hydrogen bridge'[26]. Hydrogen bonding is still described as 'just electrostatic interaction between two dipoles' in some sources.[27] Unwillingness to accept the term 'hydrogen bond' appears to come out of the conviction that a chemical bond has to be covalent (shared-shell interaction). It is surprising as 'ionic bonding' (closed-shell interaction) is always taught along with 'covalent bonding' starting from high school chemistry.

Both AIM[28,17] and NBO[29] theoretical methods have been extensively used to investigate hydrogen bonds, halogen bonds and lithium bonds. Several criteria based on AIM have been suggested to distinguish between closed-shell and shared-shell interactions. These criteria have been examined comprehensively in this work for H/Cl/Li-bonding. Our results clearly indicate that the complexes with X = H and Cl are very similar with the nature of interaction varying from closed-shell (ionic/electrostatic) to shared-shell (covalency). All D-Li•••A complexes have mostly closed-shell interactions with a very small non-zero covalent contribution. This comprehensive study has revealed one important conclusion to us. It is time now to think about a conservation of a total bond order that includes covalency and ionicity in both inter- and intra-molecular bonding. Conservation of bond order is a concept that has been around from the time of Pauling.[7] Detailed comparison between what is proposed here and some results from earlier work is given towards the end of this manuscript.

## VI.2. Computational Details

All the 100 complexes investigated in this work can be written in short as D-X•••A, representing the bond donor group X-D and an acceptor group A which has lone pair(s) of electrons ($H_2O$, $NH_3$), σ-electrons ($H_2$), π-electrons ($C_2H_4$,$C_2H_2$) or unpaired electron ($CH_3$). In the donor part X-D, D = CN, NC, CCH, H, F, Cl, Br or OH and X = H, Li or Cl. Out of these 100 complexes, 40, 35 and 25 are the examples of lithium, hydrogen and chlorine bonding respectively. All the structures were optimized at MP2(full)[30] (second-order Møller-Plesset perturbation theory) level of theory which does not assume a frozen core. The Dunning[31] basis set used for this level of theory is aug-cc-pvtz (augmented correlation-consistent polarized valence triple-zeta basis set). In our experience, MP2(full)/aug-cc-PVTZ level of calculations offer the right balance in terms of both reliability and speed considering the large number of complexes investigated. Calculations have been performed using Gaussian09 and Gaussian03 suite of programs[32]. Frequency calculations were performed at the same level of theory and basis set for all complexes in order to confirm that the obtained structures correspond to true energy minima. The binding energy of the complex is calculated as the difference between complex energy and the sum of the monomers energies i.e. supermolecule approach. For the correction of interaction energy from the inherent basis set superposition error (BSSE), counterpoise (CP) method[33] was used for all complexes.

The atoms in molecules (AIM) theory[17] has been used to analyze the topology of all the optimized complexes with the help of AIMAll[34] and AIM2000[35] programs. Natural resonance theory (NRT)[36], an inbuilt function in NBO6.0[37] program has been used to calculate the fraction of covalency and ionicity for X-D and A•••X bond.

## VI.3. Results and Discussion

The BSSE corrected binding energies and geometrical parameters of all the systems at MP2(full)/aug-cc-pVTZ are presented in Table VI. 1, where *d(A•••X)* and *d(X-D)* define the bond lengths between A and X and X and D, respectively. The X bond angle has been

denoted as $\theta(A\bullet\bullet\bullet X\text{-}D)$. All the distances are in Å and energies in kJ/mol. The bond elongation represents the increase in bond length of X-D after complex formation. The complexes considered in this work could have other minima but this work focuses on the 'X-bonded' structures having $\theta$ close to 180°. Structure of all complexes is presented with atom labeled in Figure VI. 1. Cartesian coordinates of all hundred figures and vibrational frequency are tabulated in Table VI. S. 1-6 of the supporting information.

## VI.3.1. Structure: Generalized Legon-Millen Rule for Angular Geometry

Legon and Millen suggested rules for predicting the angular geometry of A•••H-D hydrogen bonded complexes[13]. Their rules were suggested for hydrogen bonded complexes with lone pair (Rule 1) or π pair of electrons (Rule 2) as hydrogen bond acceptors. A close inspection of the results in Table VI. 1 indicates that these are applicable for all the complexes investigated in this work. However, Table VI. 1 summarizes typical structural parameters reported in the literature focusing on the A•••X-D. Indeed, when A is $NH_3$, $C_2H_4$, $C_2H_2$, $H_2$ or $CH_3$, the two distances and one angle are sufficient to see if Legon-Millen rules work. It may be noted that the acceptors have been expanded to include σ bonded and unpaired electrons as well. One can anticipate complications for hydrogen bonded complexes with $H_2O$ as acceptor as discussed below.

Water has two lone pairs of electrons which are commonly mistaken to be degenerate arising from $sp^3$ hybridization of the O atom. However, an isolated $H_2O$ molecule should obey the symmetry rules for $C_{2v}$ point group and has two non-degenerate orbitals, one in the plane of $H_2O$ and one perpendicular to the plane. Hence DX could approach O atom in two directions. One is perpendicular to the plane of $H_2O$ the X•••O line making an angle of 90° with the $C_2$ axis of $H_2O$ and the other is along the $C_2$ axis in the direction opposite to the two H atoms. Thus, in principle, complexes involving $H_2O$ as acceptors could have two geometrical isomers. However, as of now there is no experimental or theoretical evidence for this and only one structure has been found for these complexes which have $H_2O$ as acceptor. A close examination of the direction in which DX approaches $H_2O$ indicates that they have no obvious relations to the lone pair directionality in the monomer. The angle between D-X line and $C_2$ axis of $H_2O$ varies widely. For example, in $H_2O$•••HCN it is 180° but in $H_2O$•••$H_2O$ it is 118° (See in Table VI. 1). Interestingly, all the $H_2O$•••LiD complexes

have this angle as 180° except for $H_2O$•••LiCl. One could conclude that $H_2O$•••HCN and $H_2O$•••LiD structures are dominated by electrostatics and the two dipoles have aligned in a head to tail fashion. However, as shown later, NBO analysis does show partial covalency in all complexes including Li-bonded ones.

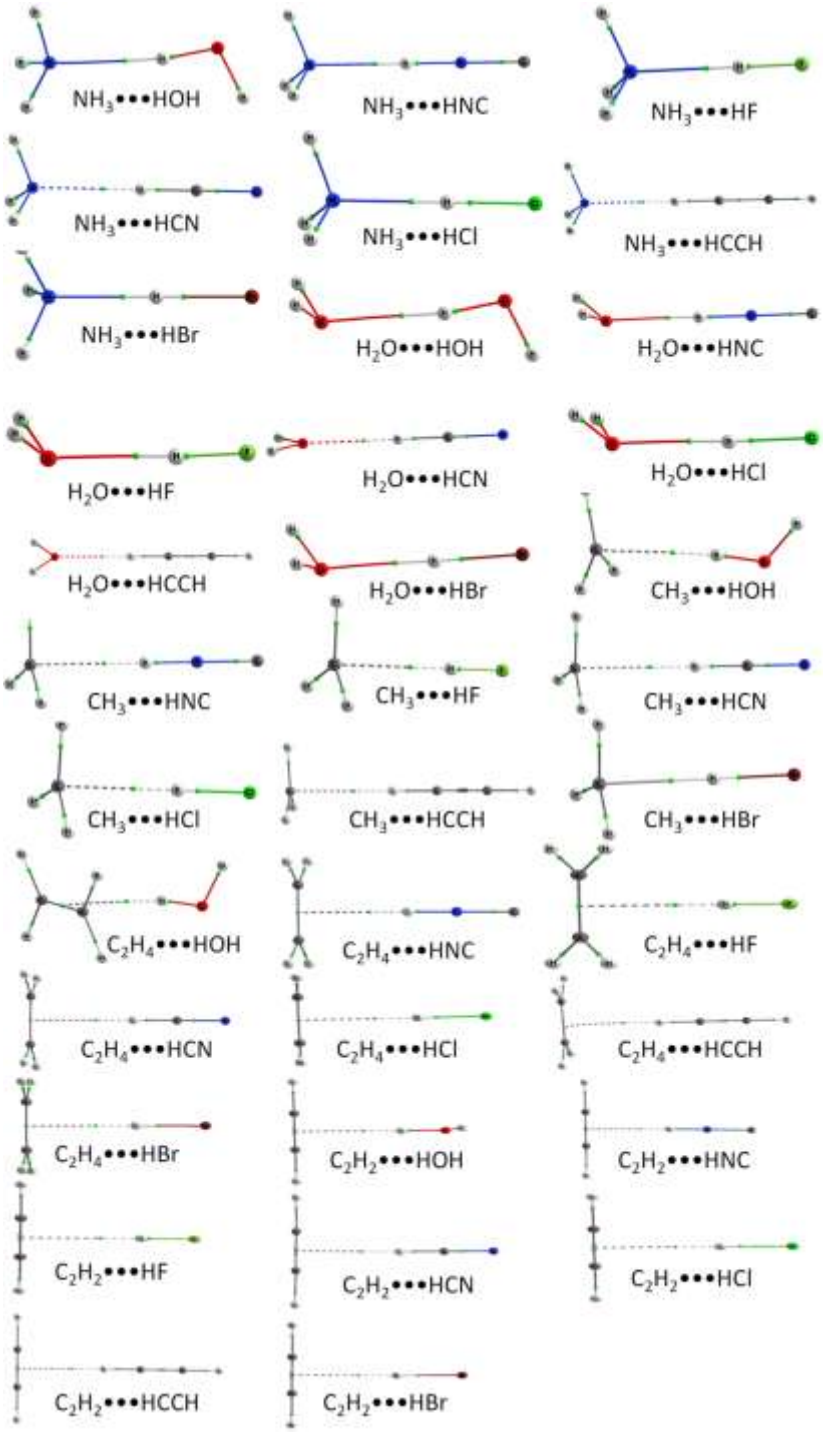

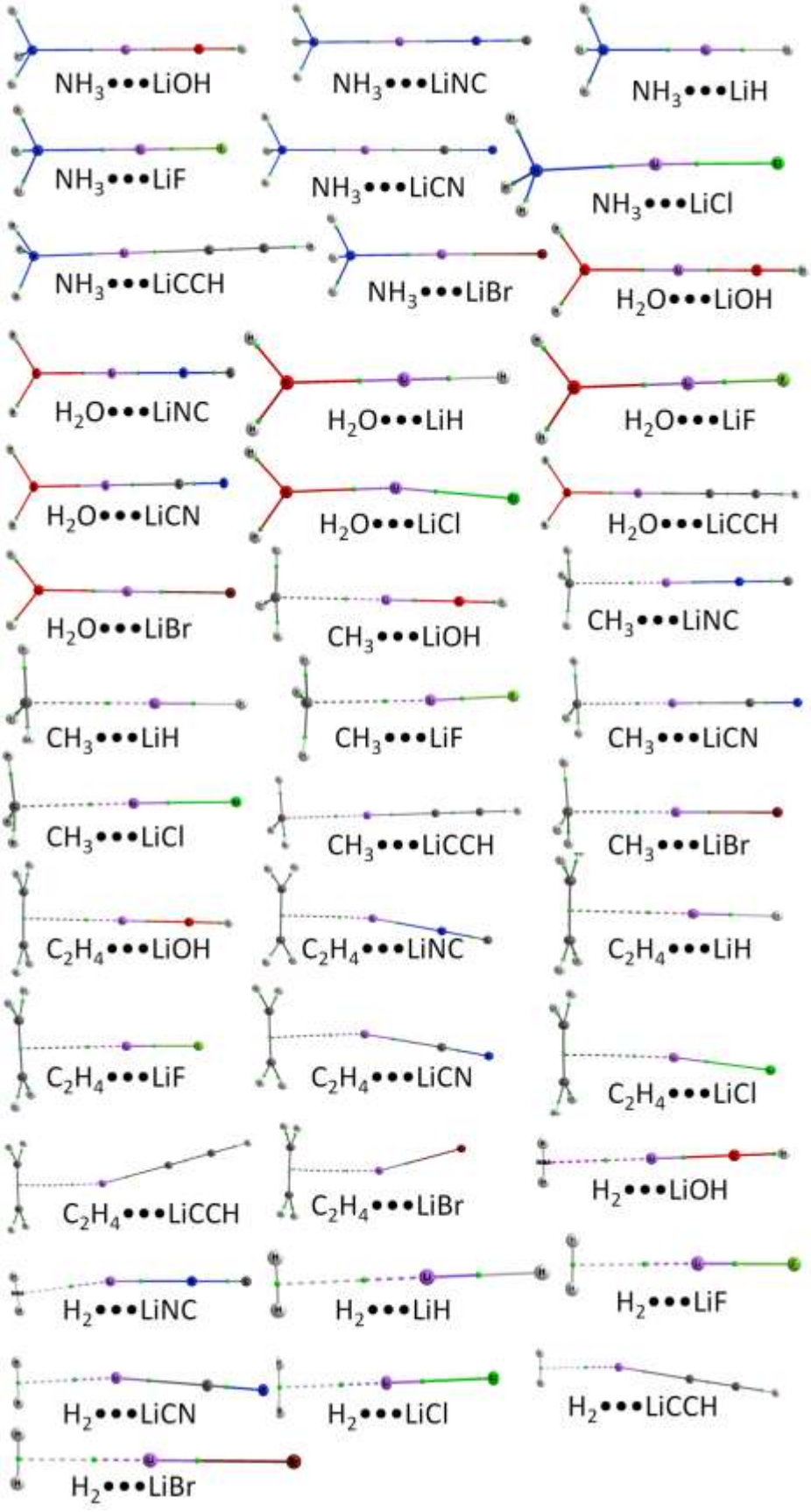
NH3•••LiOH
NH3•••LiNC
NH3•••LiH
NH3•••LiF
NH3•••LiCN
NH3•••LiCl
NH3•••LiCCH
NH3•••LiBr
H2O•••LiOH
H2O•••LiNC
H2O•••LiH
H2O•••LiF
H2O•••LiCN
H2O•••LiCl
H2O•••LiCCH
H2O•••LiBr
CH3•••LiOH
CH3•••LiNC
CH3•••LiH
CH3•••LiF
CH3•••LiCN
CH3•••LiCl
CH3•••LiCCH
CH3•••LiBr
C2H4•••LiOH
C2H4•••LiNC
C2H4•••LiH
C2H4•••LiF
C2H4•••LiCN
C2H4•••LiCl
C2H4•••LiCCH
C2H4•••LiBr
H2•••LiOH
H2•••LiNC
H2•••LiH
H2•••LiF
H2•••LiCN
H2•••LiCl
H2•••LiCCH
H2•••LiBr

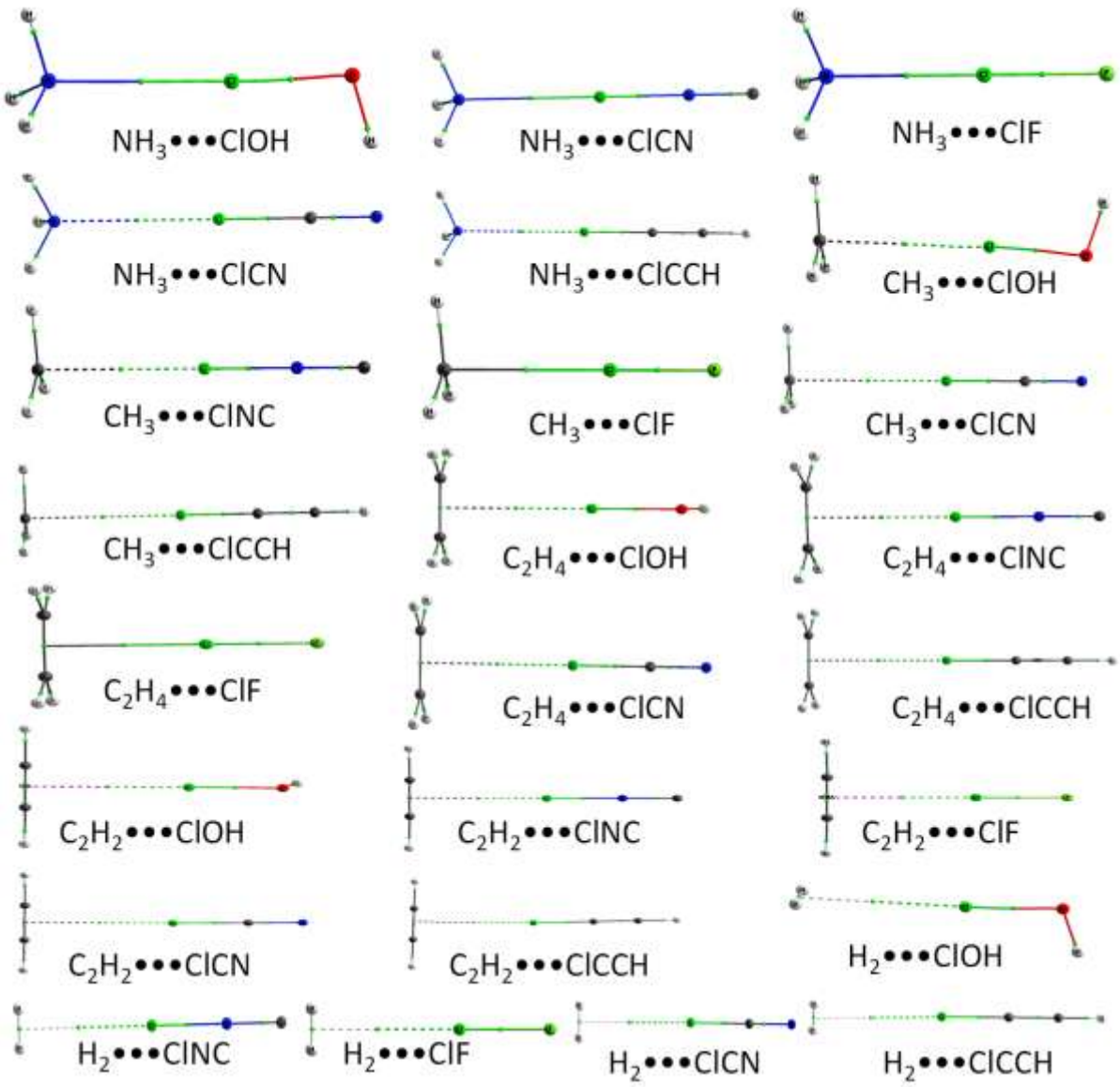


Figure VI. 1. Structure of all complexes in order of hydrogen-bonding, lithium-bonding and chlorine- bonding. Between two atoms, green dot represents the bond critical point, BCP (see section VI.3.4 for details). Dotted lines denote intermolecular bond and at some places, it is shown by solid line (especially in case of $NH_3$) because of software limitations. Bond between two elements is drawn using their element colour and dividing point is BCP.

*Table VI. 1. Important structural, spectroscopic and energetic properties of the X-bonded complexes.*

| Complexes | d(A•••X) | d(X-D) | θ(A•••X-D)# | Frequency shift | Bond Elongation | Energy (BSSE) |
|---|---|---|---|---|---|---|
| | | | Lithium Bond | | | |
| $CH_3$•••LiCN | 2.36 | 1.92 | 179.6 | 38 | 0.01 | 29.37 |
| $CH_3$•••LiNC | 2.35 | 1.78 | 179.8 | -4 | 0.01 | 29.16 |
| $CH_3$•••LiBr | 2.32 | 2.18 | 179.9 | -30 | 0.01 | 28.49 |
| $CH_3$•••LiCl | 2.36 | 2.04 | 179 | -20 | 0.01 | 27.74 |
| $CH_3$•••LiCCH | 2.38 | 1.9 | 179.9 | -20 | 0.01 | 25.94 |
| $CH_3$•••LiH | 2.39 | 1.59 | 177.9 | 30 | 0.01 | 24.06 |
| $CH_3$•••LiF | 2.37 | 1.59 | 178.3 | 1 | 0.01 | 23.14 |
| $CH_3$•••LiOH | 2.41 | 1.59 | 180 | 5 | 0.01 | 21.67 |
| | | | | | | |
| $H_2O$•••LiCN | 1.89 | 1.93 | 180 | -22 | 0.02 | 79.41 |
| $H_2O$ •••LiNC | 1.89 | 1.79 | 180 | -53 | 0.03 | 79.16 |
| $H_2O$ •••LiBr | 1.88 | 2.19 | 180 | -107 | 0.03 | 77.45 |
| $H_2O$ •••LiCl | 1.89 | 2.05 | 172.4 (170) | -76 | 0.03 | 75.77 |
| $H_2O$ •••LiCCH | 1.9 | 1.92 | 180 | -66 | 0.03 | 72.26 |
| $H_2O$ •••LiH | 1.9 | 1.61 | 180 | 63 | 0.02 | 68.99 |
| $H_2O$ •••LiF | 1.91 | 1.6 | 180 | -19 | 0.02 | 66.73 |
| $H_2O$ •••LiOH | 1.92 | 1.61 | 180 | 3 | 0.02 | 62.89 |
| | | | | | | |
| $NH_3$•••LiCN | 2.02 | 1.94 | 180 | -17 | 0.03 | 95.02 |
| $NH_3$•••LiNC | 2.02 | 1.8 | 179.8 | -31 | 0.03 | 94.89 |
| $NH_3$•••LiBr | 2 | 2.2 | 179.3 | -99 | 0.03 | 93.43 |
| $NH_3$•••LiCl | 2.02 | 2.06 | 176.5 | -63 | 0.03 | 91.42 |
| $NH_3$•••LiCCH | 2.04 | 1.92 | 180 | -55 | 0.03 | 87.15 |
| $NH_3$•••LiH | 2.03 | 1.62 | 179.9 | 42 | 0.03 | 83.05 |
| $NH_3$•••LiF | 2.03 | 1.61 | 179.8 | -7 | 0.02 | 80.71 |
| $NH_3$•••LiOH | 2.05 | 1.61 | 180 | 11 | 0.03 | 76.69 |
| | | | | | | |
| $H_2$•••LiCN | 2.06 | 1.91 | 173.3 | 31 | 0 | 11.72 |
| $H_2$•••LiNC | 2.04 | 1.77 | 172.4 | -19 | 0 | 11.59 |
| $H_2$•••LiBr | 2 | 2.17 | 179.8 | -49 | 0 | 11.38 |
| $H_2$•••LiCl | 2.03 | 2.03 | 176.8 | -25 | 0 | 11.17 |
| $H_2$•••LiCCH | 2.07 | 1.89 | 170.2 | -25 | 0.01 | 10.46 |
| $H_2$•••LiH | 2.08 | 1.59 | 179.8 | 5 | 0 | 9.2 |
| $H_2$•••LiF | 2.06 | 1.58 | 179.2 | -10 | 0 | 9.04 |
| $H_2$•••LiOH | 2.08 | 1.59 | 180 | -7 | 0 | 8.91 |
| | | | | | | |
| $C_2H_4$•••LiCN | 2.32 | 1.92 | 168.2 | 33 | 0.01 | 42.84 |
| $C_2H_4$•••LiNC | 2.31 | 1.78 | 171.6 | -6 | 0.01 | 42.97 |
| $C_2H_4$•••LiBr | 2.28 | 2.18 | 163.9 | -51 | 0.01 | 42.43 |
| $C_2H_4$•••LiCl | 2.31 | 2.04 | 174 | -31 | 0.01 | 41.17 |

| | | | | | | |
|---|---|---|---|---|---|---|
| $C_2H_4$•••LiCCH | 2.33 | 1.9 | 165.8 | -26 | 0.01 | 38.53 |
| $C_2H_4$•••LiH | 2.35 | 1.6 | 180 | 40 | 0.01 | 35.19 |
| $C_2H_4$•••LiF | 2.34 | 1.59 | 178.5 | 0 | 0.01 | 34.43 |
| $C_2H_4$•••LiOH | 2.36 | 1.6 | 180 | 11 | 0.01 | 33.1 |
| | | | Hydrogen Bond | | | |
| $CH_3$•••HBr | 2 | 1.42 | 180 | 250 | 0.02 | 8.7 |
| $CH_3$•••HCl | 2.12 | 1.28 | 179.9 | 107 | 0.01 | 9.54 |
| $CH_3$•••HF | 2.12 | 0.93 | 179.9 | 117 | 0.01 | 12.55 |
| $CH_3$•••HNC | 2.23 | 1 | 180 | 169 | 0.01 | 11.84 |
| $CH_3$•••HCN | 2.44 | 1.06 | 179.9 | 1 | 0 | 6.32 |
| $CH_3$•••HOH | 2.34 | 0.96 | 174.3 | 46 | 0 | 3.14 |
| $CH_3$•••HCCH | 2.47 | 1.06 | 180 | 5 | 0 | 6.53 |
| $H_2O$ •••HBr | 1.82 | 1.42 | 179.8 (133) | 195 | 0.02 | 18.54 |
| $H_2O$ •••HCl | 1.81 | 1.29 | 178.7 (133) | 171 | 0.02 | 22.55 |
| $H_2O$ •••HF | 1.69 | 0.94 | 178 (132) | 329 | 0.02 | 35.77 |
| $H_2O$•••HNC | 1.79 | 1.01 | 179.3 (147) | 346 | 0.02 | 34.14 |
| $H_2O$ •••HCN | 2.02 | 1.06 | 179.7 (180) | 52 | 0 | 20.42 |
| $H_2O$ •••HOH | 1.93 | 0.97 | 172.4 (118) | 106 | 0.01 | 19.79 |
| $H_2O$ •••HCCH | 2.13 | 1.06 | 180 (180) | 4 | 0 | 11.09 |
| $NH_3$•••HBr | 1.66 | 1.47 | 180 | 808 | 0.07 | 35.94 |
| $NH_3$•••HCl | 1.72 | 1.32 | 180 | 640 | 0.05 | 39.08 |
| $NH_3$•••HF | 1.68 | 0.95 | 179.9 | 703 | 0.04 | 54.43 |
| $NH_3$•••HNC | 1.8 | 1.03 | 180 | 673 | 0.04 | 48.66 |
| $NH_3$•••HCN | 2.09 | 1.07 | 180 | 182 | 0.01 | 25.98 |
| $NH_3$•••HOH | 1.95 | 0.97 | 171.1 | 238 | 0.01 | 26.48 |
| $NH_3$•••HCCH | 2.19 | 1.06 | 180 | 53 | 0.01 | 14.02 |
| $C_2H_4$•••HBr | 2.21 | 1.41 | 179.5 | 88 | 0.01 | 11.67 |
| $C_2H_4$•••HCl | 2.23 | 1.28 | 180 | 62 | 0.01 | 13.68 |
| $C_2H_4$•••HF | 2.09 | 0.93 | 179.5 | 169 | 0.01 | 19.2 |
| $C_2H_4$•••HNC | 2.24 | 1 | 179.3 | 212 | 0.01 | 18.07 |
| $C_2H_4$•••HCN | 2.46 | 1.06 | 179.4 | 23 | 0 | 9.79 |
| $C_2H_4$•••HOH | 2.33 | 0.96 | 169.8 | 52 | 0 | 10.63 |
| $C_2H_4$•••HCCH | 2.51 | 1.06 | 178.1 | 163 | 0 | 5.69 |
| $C_2H_2$•••HBr | 2.25 | 1.41 | 179.5 | 53 | 0.01 | 11.13 |
| $C_2H_2$•••HCl | 2.24 | 1.28 | 179.6 | 28 | 0.01 | 12.89 |
| $C_2H_2$•••HF | 2.11 | 0.93 | 179.4 | 124 | 0.01 | 18.16 |
| $C_2H_2$•••HNC | 2.22 | 1 | 179.2 | 183 | 0.01 | 17.66 |
| $C_2H_2$•••HCN | 2.44 | 1.06 | 179.2 | 10 | 0 | 9.87 |

| | | | | | | |
|---|---|---|---|---|---|---|
| $C_2H_2$•••HOH | 2.32 | 0.96 | 178.9 | 36 | 0 | 10.59 |
| $C_2H_2$•••HCCH | 2.5 | 1.06 | 179.5 | 7 | 0 | 10.59 |
| | | | Chlorine Bond | | | |
| $CH_3$•••ClF | 2.62 | 1.64 | 180 | -123 | 0.02 | 13.51 |
| $CH_3$•••ClCN | 3.24 | 1.63 | 179.9 | -32 | 0 | 5.4 |
| $CH_3$•••ClNC | 2.93 | 1.63 | 180 | 27 | 0.01 | 8.58 |
| $CH_3$•••ClCCH | 3.3 | 1.63 | 179.9 | 3 | 0 | 3.72 |
| $CH_3$•••ClOH | 2.97 | 1.7 | 176.7 | -35 | 0.01 | 6.11 |
| $NH_3$•••ClF | 2.21 | 1.71 | 180 | 201 | 0.09 | 53.35 |
| $NH_3$•••ClCN | 2.93 | 1.63 | 180 | -20 | 0 | 17.45 |
| $NH_3$•••ClNC | 2.61 | 1.64 | 180 | 67 | 0.02 | 28.45 |
| $NH_3$•••ClCCH | 3.04 | 1.64 | 180 | 10 | 0 | 10.42 |
| $NH_3$•••ClOH | 2.61 | 1.72 | 177.1 | 65 | 0.03 | 18.62 |
| $C_2H_2$•••ClF | 2.69 | 1.66 | 179.9 | 91 | 0.03 | 18.66 |
| $C_2H_2$•••ClCN | 3.2 | 1.63 | 179.3 | -27 | 0 | 9 |
| $C_2H_2$•••ClNC | 2.96 | 1.63 | 179.8 | 25 | 0.01 | 13.22 |
| $C_2H_2$•••ClCCH | 3.26 | 1.63 | 179.1 | 5 | 0 | 6.61 |
| $C_2H_2$•••ClOH | 2.96 | 1.7 | 177.9 | 30 | 0.02 | 10.13 |
| $C_2H_4$•••ClF | 2.46 | 1.69 | 180 | 182 | 0.06 | 28.58 |
| $C_2H_4$•••ClCN | 3.19 | 1.63 | 179.9 | -24 | 0 | 9.46 |
| $C_2H_4$•••ClNC | 2.9 | 1.63 | 180 | 40 | 0.01 | 14.9 |
| $C_2H_4$•••ClCCH | 3.24 | 1.63 | 179.9 | 7 | 0 | 7.03 |
| $C_2H_4$•••ClOH | 2.86 | 1.71 | 177.2 | 48 | 0.02 | 12.09 |
| $H_2$•••ClF | 2.66 | 1.64 | 179.8 | 28 | 0.01 | 3.77 |
| $H_2$•••ClCN | 3.08 | 1.63 | 179.6 | -32 | 0 | 1.88 |
| $H_2$•••ClNC | 2.87 | 1.62 | 180 | 3 | 0 | 2.8 |
| $H_2$•••ClCCH | 3.12 | 1.63 | 179 | 1 | 0 | 1.55 |
| $H_2$•••ClOH | 2.89 | 1.69 | 177.3 | 6 | 0.01 | 2.26 |

*All the distances are in Å , angles are in degree and energies in kJ/mol.**

Despite the complexity pointed above, all these complexes have O•••HD nearly linear. Most of the complexes have $\theta$ near 180° though some have smaller values, the lowest being 164° among the complexes investigated. Hence, we propose a small modification of Legon-Millen rule that is applicable for geometries of all the X-bonded complexes: *The equilibrium angular geometry of an X-bonded complex A•••X-D can be predicted by assuming that the*

*bond axis of the X-D is collinear with the line connecting A and X, with A being an atom or a bond centre, electrons of which are the acceptors of X- bond from XD.* We expect this rule to be applicable when there is one dominant acceptor site in A. Legon and Millen's third rule suggests that a lone pair succeeds over a π pair when either of them could be the acceptor. Though, all the acceptors chosen in our study have only one dominant site, we note that the binding energy increases in the order σ < π < unpaired < lone pair, broadly in agreement with the third rule. We further note that there can be unusual acceptors, such as $CH_4$[38] in which the acceptor site may be an electron rich region in the tetrahedron face center which cannot be thought of as a simple σ or π bonded pair of electrons. Even in this case, the O-H•••C is linear.

A closer inspection of Table VI. 1 reveals some interesting observations. For D = OH, the $\theta(A\bullet\bullet\bullet X\text{-}D)$ = 180° for all A•••LiOH complexes. However, for A•••ClOH complexes, it is about 177° and for A•••HOH complexes it varies from 170-179. The difference appears to be due to possible secondary interactions for ClOH and $H_2O$, both of which are bent whereas LiOH is linear. The linear geometry of Li-OH donor moiety is because of the more ionic nature of Li-O bond while the corresponding bonds in H-OH and Cl-OH donor moieties have significant covalent nature. The atoms in molecule (AIM) theoretical analysis supports this observation (*vide infra*). In general, when $\theta$ is below 180°, it is suggestive of some long range secondary interactions. For example, $\theta$ for $C_2H_4$•••Li-D complexes vary from 164° for D = Br to 180° for D = H. Except for D = H, all other complexes are somewhat bent indicative of some attractive interaction between D and $C_2H_4$.

## VI.3.2. Structure: The A•••X Distance

In the earlier days, for a hydrogen bonded complex D-H•••A, the distance between D and A was expected to be less than the sum of van der Waals radii of D and A.[4–7] It has now been well established that such conclusions may only be applicable to strong hydrogen bonds. The use of van der Waals radii to conclude about hydrogen bonding has not been recommended in the recent IUPAC definition.[23] In recent years, the H•••A distance in DH•••A has been interpreted as the sum of hydrogen bond radii for DH and A.[39–42] We focus on the A•••X distance in the X bonded complexes in this section.

We group all the complexes investigated in this work in to two cases. Case I has the complexes having same donors (DX) with varying acceptors and case II has the complexes having same acceptors (A) with varying donors. The distances between A and X, *d(A•••X)*, for X = H/Cl varied for both cases, when either A or D was varied. These are broadly consistent with the hydrogen bond radii[39–42] and chlorine bond radii[43] recommended for various DX and A. For X = Li, the *d(A•••X)* distances are almost constant for case II. These could be thought of as the sum of Lithium bond radii for LiD and A. As A has been kept constant and the A•••D distances do not vary much, it is clear that the lithium bond radii are very similar for all LiD. It should clearly be due to the fact that all LiD have ionic bonds and the radii of Li in these molecules would be close to the ionic radii of $Li^+$. Indeed the AIM calculations reported later confirm this. For case I complexes, A•••Li distances vary and it is clearly due to the variation in the A radii. Another important difference is noted between H/Cl bonded complexes and the Li bonded complexes. For the latter the Li atom is nearly equidistant from both A and D whereas for all the H/Cl bonded complexes investigated in this work D-X is shorter than X•••A. (Table VI. 1).

### VI.3.3. Stabilization Energy for D-X•••A Complexes

The stabilization energies for all the X-bonded complexes have been given in Table VI. 1. Not surprisingly, it is observed that interaction energy is almost constant for the case II complexes for X = Li. There have been several reports earlier pointing out that the lithium bond is stronger than hydrogen bond[16,20,44–49] and we observe the same trend. There have been relatively fewer studies comparing H-, Cl- and Li-bonded complexes. Our results indicate that Li-bond is stronger than Cl-bond as well. The larger dipole moment of LiD molecules in comparison to HD and ClD molecules is primarily responsible for this difference.

For case I complexes in general, the stabilization energies for all three types of bonding decrease in the order A = $NH_3$ > $H_2O$ > $C_2H_4$ > $C_2H_2$ > $CH_3$ > $H_2$. As pointed out in the previous section, this reconfirms the strength of acceptors as, lone pair > $\pi$ pair > unpaired electron > $\sigma$ bonded pair. For case II when the A is kept fixed and DX varies, hydrogen and chlorine bonding show similar behaviour. The order for D is F > NC > Cl > Br > OH > CN > CCH for hydrogen bonding with some exceptions and F > NC > OH > CN > CCH for

chlorine bonding without exceptions (Table 1). For the diatomic hydrogen halide donors, HF, HCl and HBr, the binding energy correlates well with the dipole moment of the donors, 1.82 D, 1.08 D and 0.82 D, respectively. However, dipole moment trends cannot explain the trends in stabilization energy for other DH. For example, the dipole moment of HCN and HNC are both close to 3.0 D but A•••HNC complexes are twice as stable as A•••HCN complexes. Interestingly, the binding energy correlated better with the charge on H atom in these cases. For example, the charge on H atom in HCN is 0.24 but that in HNC is 0.57. The A•••HCCH complexes are very close in stability to A•••HCN complexes. The charge on H atom in HCCH is 0.17 though the molecular dipole moment is zero (See Table VI. 8). Clearly, the charge on H in DH is more important and at best one can think about bond dipoles for polyatomic donors. We note that the stabilization energies for Cl-bonded complexes follow similar trend.

As already mentioned, Li-bonding is more stable than H/Cl bonding for the same D and A. Moreover, we note that the stabilization energies of DLi•••A varies dramatically when A changes from $H_2$ (9.9 – 11.7 kJ $mol^{-1}$) to $H_2O$ (76.7 – 95.0 kJ $mol^{-1}$). For the same A, the stabilization energy decreases in the order CN > NC > Br > Cl > CCH > H > F > OH. Note that CN tops the list here whereas for H/Cl bonding, it appeared towards the bottom of the list. This trend is in general similar to the trend observed in dipole moment of DLi. The values of dipole moments in Debye are Li-CN(9.5) > Li-NC(8.7) > Li-Br(7.4) > Li-Cl(7.3) > Li-CCH(6.2) > Li-H(5.9) > Li-F(6.5) > Li-OH(4.7). The available experimental dipole moments[50] are in reasonable agreement with the calculated dipole moments.

It is worth reemphasizing a comparison between hydrogen bonds and lithium bonds. For A•••LiD (D = F/Cl/Br) the trend for binding energy is A•••Li-Br > A•••Li-Cl > A•••Li-F and for A•••HD, there is a reverse trend i.e. A•••H-F > A•••H-Cl > A•••H-Br. However in both cases, the dipole moment follows the same trend. The HD molecules are covalent and the dipole moment increases with the electronegativity difference between H and D. The LiD molecules are all ionic and the charge on Li is nearly the same for all D and the dipole moment increases as the Li-D distance increases in the order LiBr>LiCl>LiF. However, we caution the reader that, description of these complexes as simple dipole-dipole interactions would be incomplete if not incorrect. Two dipoles can arrange in two ways: linear or anti parallel and if the interaction is pure electrostatic, linear arrangement should be the global

minimum.[27] Neither hydrogen bonded complexes such as HF dimer nor lithium bonded complexes such as LiF dimer have linear global minimum.[51]

Elongation in H-D bond length and red shift in H-D frequency on complex formation are well known characteristics of hydrogen bounded complexes, [1–7] though now there are some examples for blue-shifting hydrogen bonds.[23] However, for DCl•••A and DLi•••A complexes, the D-X stretching can get mixed with some other modes in A. Such mode mixing between vibrations in donor and acceptor can cause apparent red- and blue-shifting and so, for chlorine- and lithium bonded complexes, frequency shift is not a useful measure.[16] In the examples included in this investigation, most lithium bonded complexes show a small blue-shift and all hydrogen bonded complexes show red-shift. The chlorine bonded complexes show red- or blue-shifts (Table VI. 1).

## VI.3.4. Atoms in Molecules (AIM) Theoretical Analysis and Koch and Popelier Criteria

Bader's AIM theory has been successfully applied to study the properties of conventional and non-conventional Hydrogen bonds, halogen bonds and lithium bonds. The comparison between hydrogen and halogen bond has been done extensively. [16,19,52–54] Carroll and Bader[55,56] initially proposed several criteria based on electron density topology. Koch and Popelier[18] provided a good summary listing out eight criteria for C-H•••O hydrogen bonds. We begin our discussion by examining these criteria for all the H/Cl/Li bonded complexes investigated here. The sign of Laplacian is used to distinguish closed-shell and shared-shell interaction by Koch and Popelier[18] following the work by Bader.[56] This has been shown to be ambiguous and several other criteria have been proposed by Cremer and Kraka[57], Espinoza[58] and Amezaga et al.[19] These are also considered in our discussion.

### VI.3.4.1. Topology

The presence of a bond critical point (BCP) and bond path between X and A is the first criterion and this is satisfied in all 100 complexes. For most of the cases, the bond paths are linear. Figure VI. 1 shows the optimized structures and electron density critical points for all hundred complexes.

### VI.3.4.2. Electron Density at the Bond Critical Point.

The values of electron density at all BCPs are relatively low in comparison to that for a covalent bond, which is to be expected. The reported range for C-H•••O hydrogen bond by Koch and Popelier[18] is 0.002-0.034 a.u. and it can be compared to results for Li-bond, 0.0142-0.0274 a.u.[20] and for Cl-bond, 0.02-0.06 a.u.[19]. These values do depend on the range of examples included in these studies and also to some extent the level of theory and basis sets used.[59] In the present study, the ranges are 0.0102-0.0642 a.u., 0.0098 - 0.0320 a.u. and 0.0042-0.0687 a.u. for H-bond, Li-bond and Cl-bond respectively (Table VI. 4).The upper limit in our study is larger compared to that recommended by Koch and Popelier as our work has considered a wide range of donors and acceptors. In general, $NH_3$ as acceptor leads to the upper limit quoted above. The $NH_3$•••Cl-F complex has the highest value of electron density at BCP, 0.0687 a.u. and it is comparable to earlier work[19].

It has been well established that there is a strong correlation between the electron density at BCP and the bond energy. As mentioned earlier, this work began with a main objective of verifying our earlier results on a few selected complexes.[16] Indeed, this work covering 100 complexes not only confirms the linear relationship but also the distinctly different slope for Li- bonded complexes in comparison to H/Cl- bonded complexes.[16] The correlation coefficients are 0.97, 0.96 and 0.88 for lithium, chlorine and hydrogen bonding respectively and the corresponding slopes are 3271, 777 and 776. (Note that Reference 16 had the binding energy in kcal $mol^{-1}$ and so the slopes were correspondingly smaller) The results are presented in Figure VI. 2 and Table VI. 2. Our results are consistent with published reports on similar complexes[19,20] and a comprehensive summary is given in Table VI. 3.

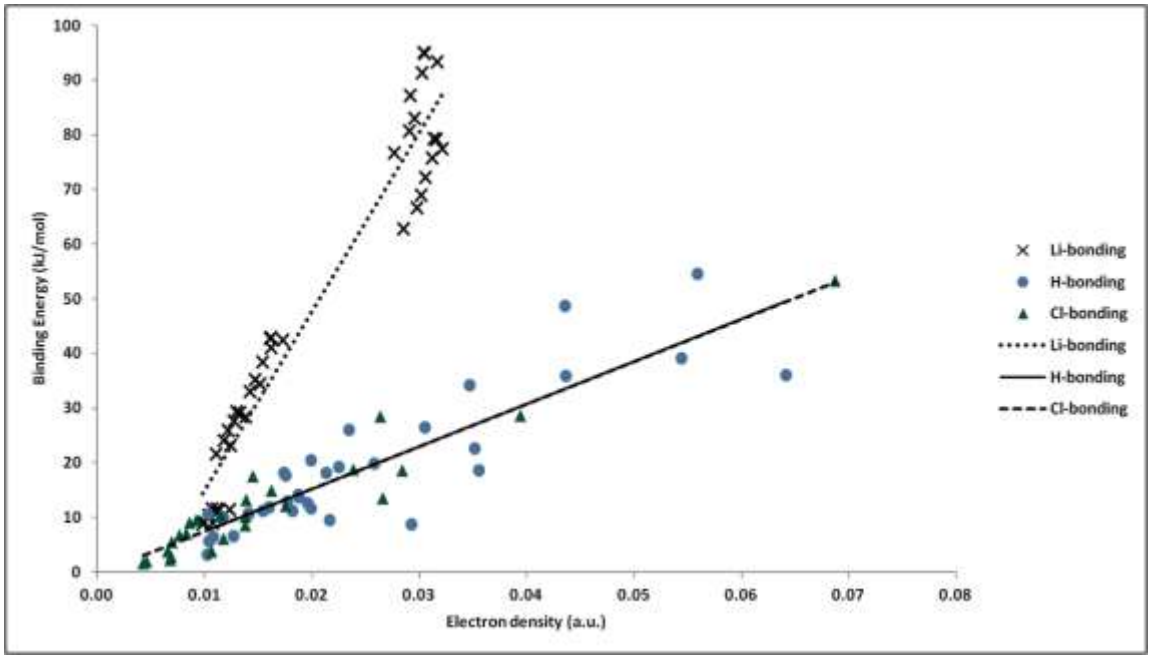


*Figure VI. 2. Correlation plots for binding energy and electron density for H-/Cl- and Li-bonding. Lines show the best linear fit.*

*Table VI. 2. Correlation coefficient (CC), slope and intercept for the all complexes, case I and case II type of complexes.*

| Complex | Li-Bonding | | | H-Bonding | | | Cl-bonding | | |
|---|---|---|---|---|---|---|---|---|---|
| | CC | Slope | Intercept | CC | Slope | intercept | CC | slope | intercept |
| Overall | 0.97 | 3271 | -17.6 | 0.88 | 777 | -0.4 | 0.96 | 776 | -0.3 |
| | | | (CASE-I) | Same Donor (X-D) , Different acceptor | | | | | |
| A•••X-F | 0.97 | 3150 | -18.2 | 0.99 | 1037 | -5.7 | 0.99 | 849 | -5.2 |
| A•••X-Cl | 0.97 | 3337 | -18.2 | 0.97 | 748 | -2.5 | XXX | | |
| A•••X-Br | 0.97 | 3416 | -22.5 | 0.95 | 566 | -1.7 | XXX | | |
| A•••X-CN | 0.97 | 3424 | -17.7 | 0.99 | 1425 | -7.6 | 1 | 1577 | -5.2 |
| A•••X-NC | 0.97 | 3445 | -19 | 0.99 | 1189 | -4.6 | 0.98 | 1337 | -7 |
| A•••X-CCH | 0.97 | 3225 | -16 | 0.78 | 903 | -2.8 | 0.98 | 1259 | -3.7 |
| A•••X-OH | 0.97 | 3150 | -18.2 | 0.99 | 987 | -4.4 | 0.98 | 748 | -1.8 |
| A•••X-H | 0.97 | 3057 | -14.5 | XXX | | | XXX | | |
| | | | (CASE-II) | Same acceptor (A) , Different Donor | | | | | |
| $CH_3$ •••X-D | 0.86 | 2928 | -10.3 | 0.53 | 257 | 3.9 | 0.98 | 458 | 1.4 |
| $NH_3$•••X-D | 0.88 | 5080 | -63.2 | 0.76 | 601 | 9.9 | 0.97 | 706 | 4.5 |
| $H_2O$•••X-D | 0.95 | 5093 | -83 | 0.78 | 692 | 2.4 | XXX | | |
| $C_2H_4$•••X-D | 0.89 | 3767 | -19.9 | 0.82 | 865 | -1.5 | 0.98 | 660 | 2.4 |
| $C_2H_2$•••X-D | XXX | | | 0.75 | 671 | 2.3 | 0.96 | 698 | 2.1 |
| $H_2$•••X-D | 0.68 | 1002 | -0.3 | XXX | | | 0.97 | 335 | 0.2 |

*This result from correlation plot of binding energy with electron density.*

*Table VI. 3. Comparison of slope from other studies and present work.*

| | Comparison of slopes from different studies | | | |
|---|---|---|---|---|
| Level of theory | Li-bonding | H-bonding | Cl-bonding | References$ |
| MP2(full)/aug-cc-PVTZ | 3271(-17.6)* | 777(-0.4) | 776(-0.3) | This work |
| MP2(full)/aug-cc-PVTZ | 2951(-9.1) | 1001(-3.8) | 855(-3.8) | [16] |
| B3LYP/6-311++G(d,p) | ---- | 911(-2.9) | 1623(-21.9) | [19] |
| MP2/6-311G++(d,p) | 2435(11.9)/5316(-47.8) | 717(-4.5)/708(-1.1) | ---- | [20] |

**In parentheses, intercept are presented. $references are from main text.*

The correlation coefficient for hydrogen bonded complexes mentioned above is relatively lower than that for Cl/Li bonded complexes. It may be noted that Koch and Popelier had concluded in their work that[18] "linear correlation is excellent as long as the acceptor atom remains unchanged within the set.". As they already had the donor fixed as C-H, their results imply that the correlation will be good for similar donors and acceptors. Considering this, the correlation we have found for the range of donors and acceptors appear to be quite reasonable. In any case, several fits were tried for case I (donors constant) and case II (acceptors constant) complexes. The correlation coefficients and their corresponding slopes and intercepts for all sets (case I and II) are given in Table VI. 2. We note that the correlations are excellent for case I complexes for all three bonding. For case II, correlations are much better for Cl-bonding than Li-bonding and H-bonding. We note that in general keeping the donor fixed produces better correlation. Our conclusion is in agreement with the results of Li Bian [60] "*proton donor is more important than proton acceptor in hydrogen bond formation.*"

Another interesting fact came out when we plotted binding energy vs electron density at BCPs for typical type of ionic and covalent bonds in DX along with the X•••A bonds. For this analysis, the donors were restricted to be diatomics i.e D was F/Cl/Br only. The results are shown in Figure VI. 3. Extrapolation of the plot for Li-bonding leads towards the ionic bond (D-Li) while H-/Cl-bond lead towards covalent bonds (D-H/D-Cl). This analogy was expected when the slopes in such a plot for ionic (LiD) and covalent (HD and ClD) molecules were determined. Hydrogen bonding has been thought of as a link between covalent bonding and van der Waals interactions for long. In particular electron density at the BCP has been used to describe 'hydrogen bonding without borders' by Parthasarathi et al. who investigated a range of 'hydrogen bonded complexes'.[61] Our comparison of H/Cl/Li-bonded complexes and the covalent/ionic molecules, clearly show that such 'bonding without

borders' can be extended to all inter- and intra-molecular bonding. Clearly, one can think about a conservation of bond order, that includes covalency and ionicity, *vide infra*.

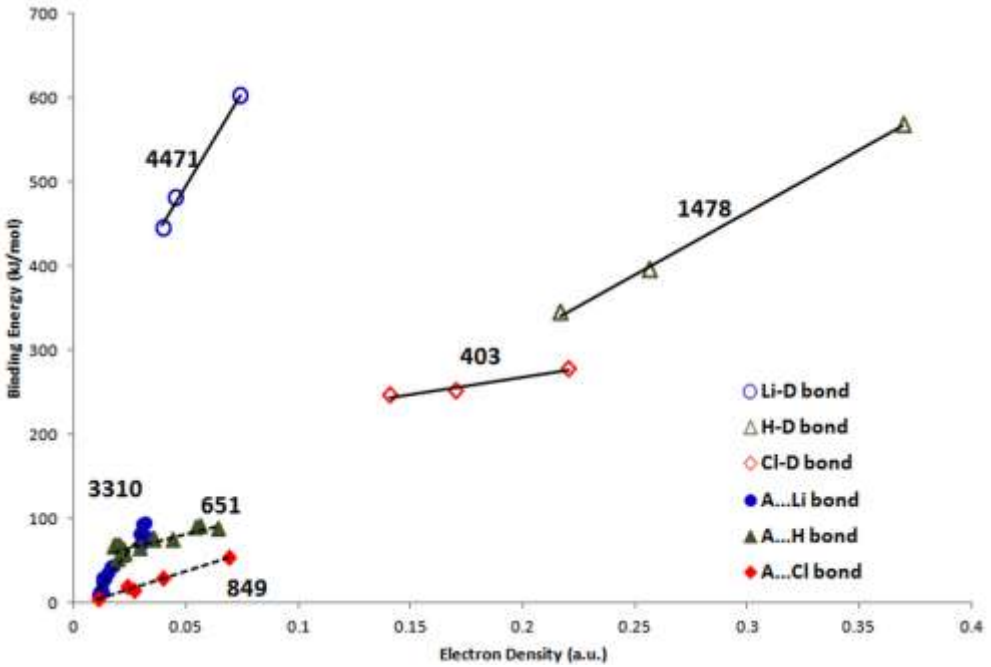


*Figure VI. 3. Comparison of electron density vs. binding energy plots for H-, Cl-and Li-bonding with typical intramolecular bonds. Slopes of the best fit lines are shown.*

### VI.3.4.3. The Laplacian of the Charge Density at the Bond Critical Point

As mentioned earlier, the sign of the Laplacian of electron density at the BCP, $\nabla^2\rho(r)$, has been used to differentiate shared-shell (covalent) and closed-shell (ionic, non-covalent, van der Waals etc…) interactions. If it is negative, there is electron accumulation in between the two atoms indicative of shared-shell, covalent, interaction. If it is positive, there is charge depletion between the two atoms indicative of closed-shell interactions. For typical hydrogen bonded systems, $\nabla^2\rho(r)$ are positive. It is indeed positive for ionic and typical intermolecular bonds [62]. For example, previously reported ranges in $\nabla^2\rho(r)$ for Li-bond[20], H-bond[18] and Cl-bond[19] are 0.06-0.21 a.u., 0.024-0.139a.u. and 0.04-0.14 a.u. respectively. The values of $\nabla^2\rho(r)$ at BCP for Li-, H- and Cl-bonding are given in Table VI. 4, and ranges for these bonding are 0.0527-0.2584 a.u., 0.0284-0.1050 a.u. and 0.0183-0.1422 a.u. respectively. For comparison, $\nabla^2\rho(r)$ values at the BCP of X-D bonds are 0.676, -2.849 and -0.173 for Li-OH, H-OH and Cl-OH monomers respectively. Li-O bond in Li-OH molecule is

ionic and $\nabla^2\rho(r)$ has a large positive value whereas the Cl-O and H-O bond in ClOH and $H_2O$ are covalent and $\nabla^2\rho(r)$ have negative values. Indeed, this difference in the nature of bonding does affect the structure and Li-OH is a linear molecule while $H_2O$ and ClOH are bent having a V-shape.

Cremer and Kraka[57] have showed that the characterization of bond on the basis of Laplacian of electron density can lead to erroneous conclusions. For instance, they have shown that the $\nabla^2\rho(r)$ is positive for some strongly covalent double/triple bonds, as in CO. They suggested considering the potential, $V(r_c)$, kinetic, $G(r_c)$, and total, $H(r_c)$, electron energy densities at BCP. We denote these as V, G and H from now on. For shared-shell interaction, the potential energy dominates, $|V| > G$ and H is negative, whereas for closed-shell interaction the kinetic energy dominates, $|V| < G$ and H is positive. Another similar criterion was proposed by Espinoza[58] on the basis of the ratio $|V|/G$. For closed-shell interaction, $|V|/G < 1$ and for shared-shell interaction, $|V|/G > 2$. Interaction is taken as intermediate type if the ratio falls between these two limits. There is no sharp boundary between the two types of bond. Some strongly bound complexes have $|V|/G$ value greater than 1.00 and it is taken as evidence for partial covalent nature. For the 100 examples chosen in our study, both these criteria were examined. Hydrogen bonded complexes fall in the closed-shell or intermediate region (See Table VI. 4, Figure VI. 5 and Table VI. 4). Chlorine bonded complexes fall mostly in the closed-shell interaction regions except for the three ClF complexes. All the lithium bonded complexes have closed-shell interaction irrespective of the criterion used. For lithium bonded complexes, the total energy H is positive in every case and $|V|/G$ ratios is close to and smaller than 1.00 (Figure VI. 5 and Table VI. 4). Clearly, hydrogen bonding and chlorine bonding are similar but lithium bonding has distinct characteristics. Correlations between binding energy, electron density at the BCP and mutual penetration also lead to the same conclusions (*vide infra*). Comparison of the weak interaction and strong interaction (ionic and covalent bond) has been done for above mentioned properties in Figure VI. 6.

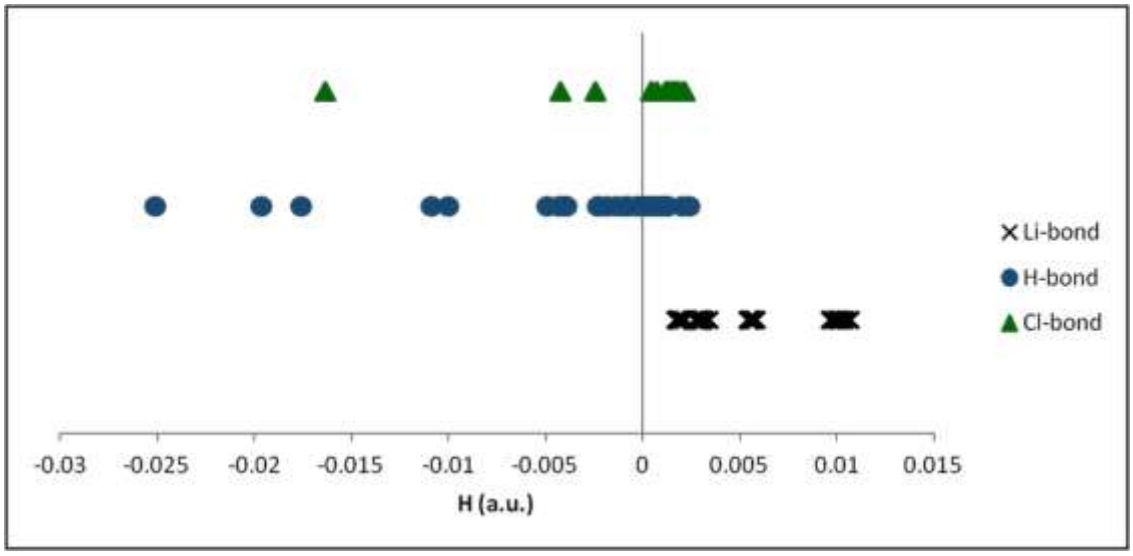


*Figure VI. 4. Plot of total energy density at BCP, H (in atomic units), for H-, Cl- and Li-bonds. (See Figure VI. 6 for data on ionic and covalent bonds).*

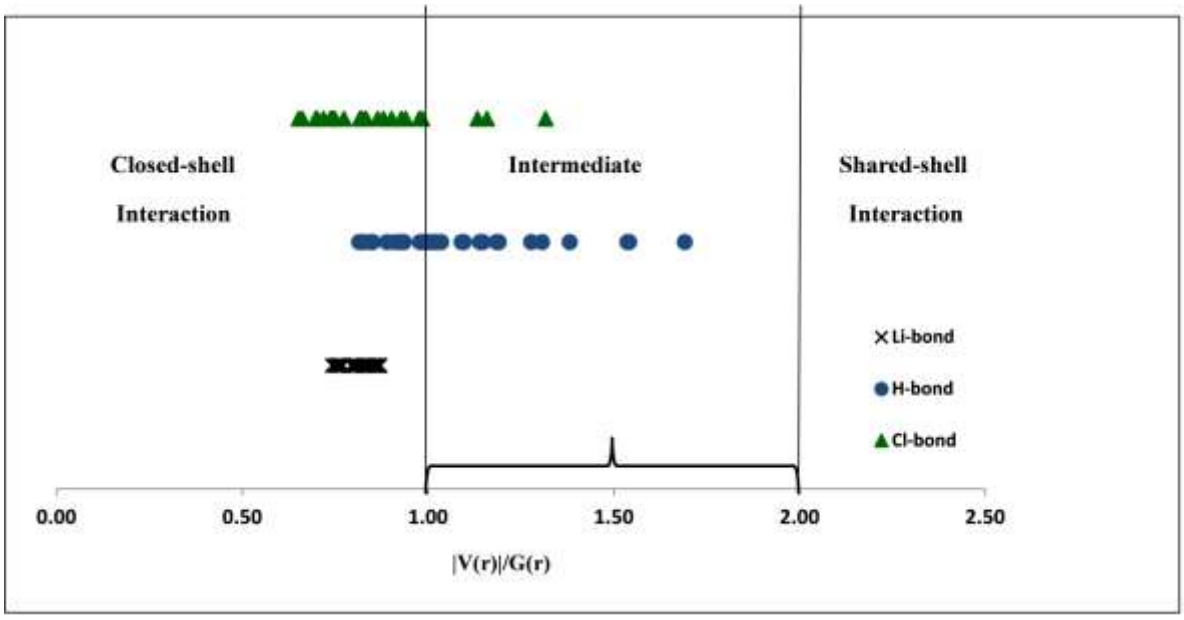


*Figure VI. 5. Plot of |V|/G ratio for the characterization of bonding.*

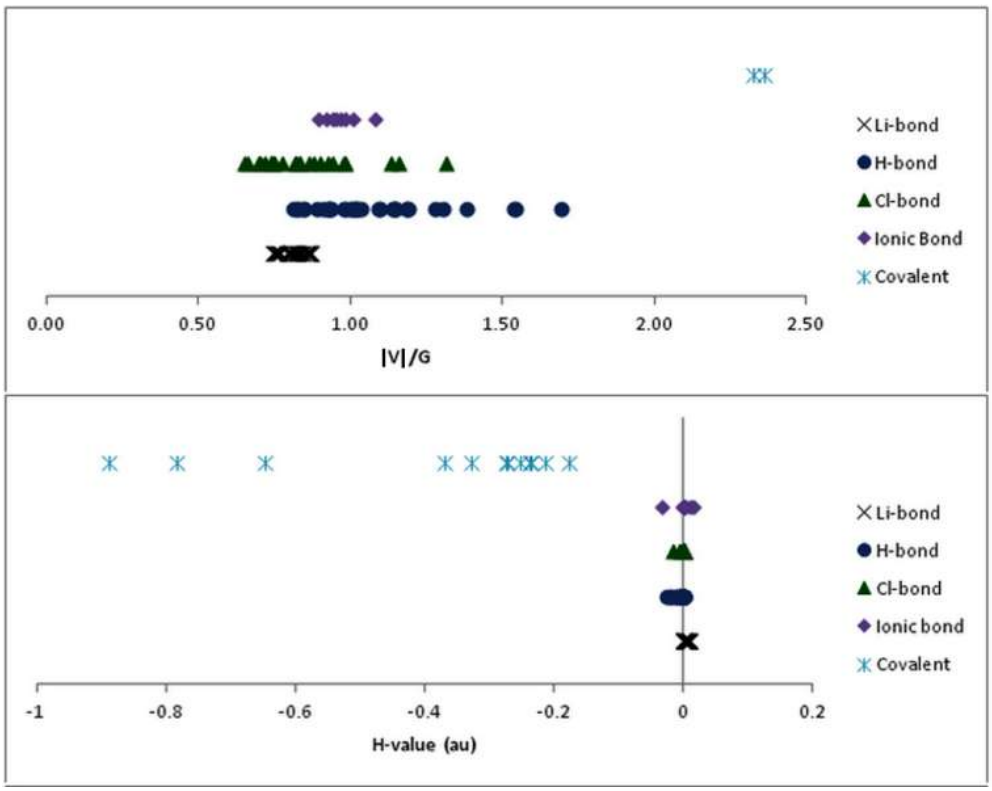


*Figure VI. 6. Criteria for interactions on the basis of |V|/G values, H values. These figures include ionic and covalent bond position.*

*Table VI. 4. Electron density topological and energies properties from atoms in molecules calculations.*

| | ρ | $\nabla^2\rho$ | ε | V(r) | G(r) | H | \|V(r)\|/G(r) | λ1 | λ2 | λ3 | λ1/λ3 |
|---|---|---|---|---|---|---|---|---|---|---|---|
| Lithium bond | | | | | | | | | | | |
| $CH_3$•••LiCN | 0.0129 | 0.0604 | 0.000 | -0.012 | 0.013 | 0.002 | 0.87 | -0.017 | -0.017 | 0.095 | 0.181 |
| $CH_3$•••LiNC | 0.0132 | 0.0617 | 0.001 | -0.012 | 0.014 | 0.002 | 0.87 | -0.017 | -0.017 | 0.097 | 0.181 |
| $CH_3$•••LiBr | 0.0138 | 0.0660 | 0.003 | -0.013 | 0.015 | 0.002 | 0.87 | -0.019 | -0.018 | 0.103 | 0.180 |
| $CH_3$•••LiCl | 0.0127 | 0.0629 | 0.004 | -0.011 | 0.014 | 0.002 | 0.84 | -0.017 | -0.017 | 0.097 | 0.177 |
| $CH_3$•••LiCCH | 0.0122 | 0.0578 | 0.001 | -0.011 | 0.013 | 0.002 | 0.85 | -0.016 | -0.016 | 0.090 | 0.179 |
| $CH_3$•••LiH | 0.0117 | 0.0567 | 0.000 | -0.010 | 0.012 | 0.002 | 0.84 | -0.016 | -0.016 | 0.088 | 0.177 |
| $CH_3$•••LiF | 0.0123 | 0.0570 | 0.004 | -0.011 | 0.013 | 0.002 | 0.87 | -0.016 | -0.016 | 0.089 | 0.181 |
| $CH_3$•••LiOH | 0.0110 | 0.0527 | 0.000 | -0.010 | 0.011 | 0.002 | 0.84 | -0.014 | -0.014 | 0.081 | 0.174 |
| | | | | | | | | | | | |
| $H_2O$ •••LiCN | 0.0313 | 0.2479 | 0.077 | -0.042 | 0.052 | 0.010 | 0.80 | -0.064 | -0.060 | 0.372 | 0.173 |
| $H_2O$ •••LiNC | 0.0315 | 0.2493 | 0.077 | -0.042 | 0.052 | 0.010 | 0.81 | -0.065 | -0.060 | 0.374 | 0.173 |
| $H_2O$ •••LiBr | 0.0320 | 0.2584 | 0.077 | -0.043 | 0.054 | 0.011 | 0.80 | -0.066 | -0.062 | 0.386 | 0.172 |
| $H_2O$ •••LiCl | 0.0311 | 0.2496 | 0.076 | -0.042 | 0.052 | 0.010 | 0.80 | -0.064 | -0.060 | 0.373 | 0.172 |
| $H_2O$•••LiCCH | 0.0305 | 0.2413 | 0.076 | -0.040 | 0.050 | 0.010 | 0.80 | -0.063 | -0.058 | 0.362 | 0.173 |
| $H_2O$•••LiH | 0.0301 | 0.2408 | 0.077 | -0.040 | 0.050 | 0.010 | 0.80 | -0.062 | -0.058 | 0.361 | 0.172 |
| $H_2O$•••LiF | 0.0297 | 0.2346 | 0.077 | -0.039 | 0.049 | 0.010 | 0.80 | -0.060 | -0.056 | 0.351 | 0.171 |
| $H_2O$•••LiOH | 0.0285 | 0.2253 | 0.075 | -0.037 | 0.047 | 0.010 | 0.79 | -0.057 | -0.053 | 0.336 | 0.170 |
| | | | | | | | | | | | |
| $NH_3$•••LiCN | 0.0304 | 0.1850 | 0.000 | -0.035 | 0.041 | 0.006 | 0.87 | -0.053 | -0.053 | 0.291 | 0.182 |
| $NH_3$•••LiNC | 0.0304 | 0.1849 | 0.000 | -0.035 | 0.041 | 0.005 | 0.87 | -0.053 | -0.053 | 0.291 | 0.182 |

| | | | | | | | | | | | |
|---|---|---|---|---|---|---|---|---|---|---|---|
| $NH_3$•••LiBr | 0.0316 | 0.1959 | 0.000 | -0.037 | 0.043 | 0.006 | 0.87 | -0.056 | -0.056 | 0.307 | 0.181 |
| $NH_3$•••LiCl | 0.0302 | 0.1863 | 0.001 | -0.035 | 0.041 | 0.006 | 0.86 | -0.053 | -0.053 | 0.292 | 0.181 |
| $NH_3$•••LiCCH | 0.0291 | 0.1762 | 0.000 | -0.033 | 0.039 | 0.005 | 0.86 | -0.051 | -0.051 | 0.277 | 0.182 |
| $NH_3$•••LiH | 0.0295 | 0.1814 | 0.000 | -0.034 | 0.040 | 0.006 | 0.86 | -0.052 | -0.052 | 0.285 | 0.182 |
| $NH_3$•••LiF | 0.0290 | 0.1767 | 0.000 | -0.033 | 0.039 | 0.005 | 0.86 | -0.050 | -0.050 | 0.277 | 0.181 |
| $NH_3$•••LiOH | 0.0276 | 0.1686 | 0.000 | -0.031 | 0.037 | 0.005 | 0.85 | -0.047 | -0.047 | 0.263 | 0.179 |
| | | | | | | | | | | | |
| $H_2$•••LiCN | 0.0106 | 0.0611 | 0.099 | -0.009 | 0.012 | 0.003 | 0.75 | -0.017 | -0.015 | 0.093 | 0.181 |
| $H_2$•••LiNC | 0.0111 | 0.0632 | 0.102 | -0.010 | 0.013 | 0.003 | 0.76 | -0.018 | -0.016 | 0.097 | 0.182 |
| $H_2$•••LiBr | 0.0123 | 0.0716 | 0.106 | -0.011 | 0.015 | 0.003 | 0.77 | -0.020 | -0.018 | 0.109 | 0.181 |
| $H_2$•••LiCl | 0.0112 | 0.0649 | 0.102 | -0.010 | 0.013 | 0.003 | 0.76 | -0.018 | -0.016 | 0.099 | 0.180 |
| $H_2$•••LiCCH | 0.0103 | 0.0599 | 0.100 | -0.009 | 0.012 | 0.003 | 0.75 | -0.016 | -0.015 | 0.091 | 0.179 |
| $H_2$•••LiH | 0.0099 | 0.0582 | 0.096 | -0.009 | 0.012 | 0.003 | 0.74 | -0.016 | -0.014 | 0.088 | 0.178 |
| $H_2$•••LiF | 0.0107 | 0.0599 | 0.102 | -0.009 | 0.012 | 0.003 | 0.77 | -0.017 | -0.015 | 0.092 | 0.182 |
| $H_2$•••LiOH | 0.0098 | 0.0568 | 0.102 | -0.009 | 0.011 | 0.003 | 0.75 | -0.015 | -0.014 | 0.085 | 0.176 |
| | | | | | | | | | | | |
| $C_2H_4$•••LiCN | 0.0160 | 0.0765 | 0.365 | -0.013 | 0.016 | 0.003 | 0.83 | -0.022 | -0.016 | 0.115 | 0.192 |
| $C_2H_4$•••LiNC | 0.0162 | 0.0768 | 0.367 | -0.014 | 0.016 | 0.003 | 0.83 | -0.022 | -0.016 | 0.115 | 0.192 |
| $C_2H_4$•••LiBr | 0.0172 | 0.0840 | 0.380 | -0.015 | 0.018 | 0.003 | 0.83 | -0.024 | -0.017 | 0.125 | 0.191 |
| $C_2H_4$•••LiCl | 0.0161 | 0.0778 | 0.368 | -0.014 | 0.017 | 0.003 | 0.82 | -0.022 | -0.016 | 0.116 | 0.190 |
| $C_2H_4$•••LiCCH | 0.0153 | 0.0742 | 0.364 | -0.013 | 0.016 | 0.003 | 0.82 | -0.021 | -0.015 | 0.111 | 0.190 |
| $C_2H_4$•••LiH | 0.0147 | 0.0708 | 0.350 | -0.012 | 0.015 | 0.003 | 0.81 | -0.020 | -0.015 | 0.106 | 0.191 |
| $C_2H_4$•••LiF | 0.0151 | 0.0715 | 0.362 | -0.013 | 0.015 | 0.003 | 0.82 | -0.020 | -0.015 | 0.107 | 0.191 |
| $C_2H_4$•••LiOH | 0.0142 | 0.0690 | 0.367 | -0.012 | 0.014 | 0.003 | 0.81 | -0.019 | -0.014 | 0.102 | 0.186 |
| | | | | | Hydrogen Bond | | | | | | |
| $CH_3$•••HBr | 0.0292 | 0.0448 | 0.000 | -0.021 | 0.016 | -0.005 | 1.31 | -0.035 | -0.035 | 0.115 | 0.306 |
| $CH_3$•••HCl | 0.0216 | 0.0406 | 0.002 | -0.015 | 0.013 | -0.002 | 1.19 | -0.024 | -0.024 | 0.089 | 0.273 |
| $CH_3$•••HF | 0.0196 | 0.0386 | 0.001 | -0.014 | 0.012 | -0.002 | 1.19 | -0.023 | -0.023 | 0.086 | 0.275 |
| $CH_3$•••HNC | 0.0160 | 0.0362 | 0.001 | -0.011 | 0.010 | -0.001 | 1.09 | -0.018 | -0.018 | 0.072 | 0.248 |
| $CH_3$•••HCN | 0.0108 | 0.0285 | 0.004 | -0.006 | 0.007 | 0.000 | 0.93 | -0.010 | -0.010 | 0.049 | 0.211 |
| $CH_3$•••HOH | 0.0127 | 0.0326 | 0.054 | -0.008 | 0.008 | 0.000 | 1.00 | -0.013 | -0.013 | 0.058 | 0.227 |
| $CH_3$•••HCCH | 0.0102 | 0.0284 | 0.004 | -0.006 | 0.007 | 0.001 | 0.91 | -0.010 | -0.009 | 0.047 | 0.201 |
| | | | | | | | | | | | |
| $H_2O$•••HBr | 0.0355 | 0.0957 | 0.042 | -0.032 | 0.028 | -0.004 | 1.15 | -0.057 | -0.055 | 0.208 | 0.276 |
| $H_2O$•••HCl | 0.0351 | 0.0957 | 0.041 | -0.032 | 0.028 | -0.004 | 1.14 | -0.057 | -0.055 | 0.208 | 0.276 |
| $H_2O$•••HF | 0.0436 | 0.1050 | 0.036 | -0.046 | 0.036 | -0.010 | 1.28 | -0.083 | -0.080 | 0.267 | 0.309 |
| $H_2O$•••HNC | 0.0347 | 0.1005 | 0.051 | -0.034 | 0.030 | -0.004 | 1.15 | -0.060 | -0.057 | 0.217 | 0.276 |
| $H_2O$•••HCN | 0.0199 | 0.0790 | 0.077 | -0.016 | 0.018 | 0.002 | 0.89 | -0.028 | -0.026 | 0.133 | 0.210 |
| $H_2O$•••HOH | 0.0258 | 0.0843 | 0.026 | -0.023 | 0.022 | -0.001 | 1.03 | -0.039 | -0.038 | 0.161 | 0.242 |
| $H_2O$•••HCCH | 0.0154 | 0.0642 | 0.079 | -0.011 | 0.014 | 0.002 | 0.82 | -0.020 | -0.018 | 0.102 | 0.193 |
| | | | | | | | | | | | |
| $NH_3$•••HBr | 0.0642 | 0.0450 | 0.000 | -0.062 | 0.036 | -0.025 | 1.69 | -0.116 | -0.116 | 0.277 | 0.419 |
| $NH_3$•••HCl | 0.0544 | 0.0598 | 0.000 | -0.050 | 0.033 | -0.018 | 1.54 | -0.093 | -0.093 | 0.247 | 0.379 |
| $NH_3$•••HF | 0.0559 | 0.0681 | 0.000 | -0.056 | 0.037 | -0.020 | 1.54 | -0.103 | -0.103 | 0.275 | 0.376 |
| $NH_3$•••HNC | 0.0436 | 0.0710 | 0.000 | -0.040 | 0.029 | -0.011 | 1.38 | -0.072 | -0.072 | 0.215 | 0.335 |
| $NH_3$•••HCN | 0.0235 | 0.0649 | 0.000 | -0.017 | 0.016 | 0.000 | 1.01 | -0.030 | -0.030 | 0.126 | 0.242 |
| $NH_3$•••HOH | 0.0305 | 0.0702 | 0.013 | -0.025 | 0.022 | -0.004 | 1.18 | -0.045 | -0.044 | 0.159 | 0.282 |
| $NH_3$•••HCCH | 0.0187 | 0.0573 | 0.000 | -0.012 | 0.013 | 0.001 | 0.92 | -0.022 | -0.022 | 0.102 | 0.220 |
| | | | | | | | | | | | |
| $C_2H_4$•••HBr | 0.0199 | 0.0440 | 0.470 | -0.012 | 0.011 | 0.000 | 1.02 | -0.022 | -0.015 | 0.082 | 0.275 |

| | | | | | | | | | | | |
|---|---|---|---|---|---|---|---|---|---|---|---|
| $C_2H_4$•••HCl | 0.0188 | 0.0419 | 0.457 | -0.011 | 0.011 | 0.000 | 1.02 | -0.021 | -0.015 | 0.078 | 0.273 |
| $C_2H_4$•••HF | 0.0225 | 0.0454 | 0.424 | -0.015 | 0.013 | -0.002 | 1.14 | -0.029 | -0.020 | 0.094 | 0.304 |
| $C_2H_4$•••HNC | 0.0174 | 0.0408 | 0.425 | -0.011 | 0.010 | 0.000 | 1.01 | -0.020 | -0.014 | 0.075 | 0.269 |
| $C_2H_4$•••HCN | 0.0116 | 0.0317 | 0.422 | -0.006 | 0.007 | 0.001 | 0.85 | -0.012 | -0.008 | 0.051 | 0.225 |
| $C_2H_4$•••HOH | 0.0141 | 0.0373 | 0.471 | -0.008 | 0.009 | 0.001 | 0.93 | -0.015 | -0.010 | 0.063 | 0.244 |
| $C_2H_4$•••HCCH | 0.0104 | 0.0298 | 0.421 | -0.005 | 0.006 | 0.001 | 0.82 | -0.010 | -0.007 | 0.047 | 0.213 |
| | | | | | | | | | | | |
| $C_2H_2$•••HBr | 0.0182 | 0.0465 | 0.342 | -0.011 | 0.011 | 0.000 | 0.98 | -0.019 | -0.014 | 0.080 | 0.241 |
| $C_2H_2$•••HCl | 0.0177 | 0.0454 | 0.336 | -0.011 | 0.011 | 0.000 | 0.98 | -0.019 | -0.014 | 0.079 | 0.243 |
| $C_2H_2$•••HF | 0.0213 | 0.0502 | 0.307 | -0.015 | 0.014 | -0.001 | 1.10 | -0.026 | -0.020 | 0.096 | 0.272 |
| $C_2H_2$•••HNC | 0.0176 | 0.0465 | 0.309 | -0.012 | 0.012 | 0.000 | 1.00 | -0.020 | -0.015 | 0.082 | 0.245 |
| $C_2H_2$•••HCN | 0.0117 | 0.0356 | 0.315 | -0.007 | 0.008 | 0.001 | 0.84 | -0.011 | -0.009 | 0.056 | 0.206 |
| $C_2H_2$•••HOH | 0.0141 | 0.0409 | 0.340 | -0.009 | 0.010 | 0.001 | 0.93 | -0.015 | -0.011 | 0.067 | 0.224 |
| $C_2H_2$•••HCCH | 0.0103 | 0.0326 | 0.320 | -0.006 | 0.007 | 0.001 | 0.81 | -0.010 | -0.007 | 0.050 | 0.195 |
| Chlorine bond | | | | | | | | | | | |
| $CH_3$•••ClF | 0.0266 | 0.0641 | 0.000 | -0.021 | 0.019 | -0.002 | 1.13 | -0.020 | -0.020 | 0.104 | 0.192 |
| $CH_3$•••ClCN | 0.0069 | 0.0265 | 0.000 | -0.004 | 0.005 | 0.001 | 0.74 | -0.004 | -0.004 | 0.035 | 0.121 |
| $CH_3$•••ClNC | 0.0138 | 0.0424 | 0.000 | -0.009 | 0.010 | 0.001 | 0.93 | -0.009 | -0.009 | 0.061 | 0.153 |
| $CH_3$•••ClCCH | 0.0065 | 0.0231 | 0.010 | -0.004 | 0.005 | 0.001 | 0.75 | -0.004 | -0.004 | 0.031 | 0.124 |
| $CH_3$•••ClOH | 0.0117 | 0.0419 | 0.073 | -0.008 | 0.009 | 0.001 | 0.86 | -0.007 | -0.007 | 0.056 | 0.131 |
| | | | | | | | | | | | |
| $NH_3$•••ClF | 0.0687 | 0.1422 | 0.000 | -0.068 | 0.052 | -0.016 | 1.32 | -0.071 | -0.071 | 0.284 | 0.250 |
| $NH_3$•••ClCN | 0.0145 | 0.0545 | 0.000 | -0.009 | 0.012 | 0.002 | 0.82 | -0.011 | -0.011 | 0.077 | 0.145 |
| $NH_3$•••ClNC | 0.0263 | 0.1006 | 0.000 | -0.022 | 0.024 | 0.001 | 0.94 | -0.022 | -0.022 | 0.144 | 0.150 |
| $NH_3$•••ClCCH | 0.0115 | 0.0443 | 0.000 | -0.007 | 0.009 | 0.002 | 0.77 | -0.008 | -0.008 | 0.061 | 0.136 |
| $NH_3$•••ClOH | 0.0284 | 0.0951 | 0.019 | -0.023 | 0.023 | 0.000 | 0.98 | -0.024 | -0.024 | 0.143 | 0.168 |
| | | | | | | | | | | | |
| $C_2H_2$•••ClF | 0.0238 | 0.0758 | 0.977 | -0.018 | 0.019 | 0.000 | 0.98 | -0.017 | -0.009 | 0.101 | 0.168 |
| $C_2H_2$•••ClCN | 0.0086 | 0.0332 | 0.577 | -0.005 | 0.007 | 0.002 | 0.72 | -0.005 | -0.003 | 0.042 | 0.128 |
| $C_2H_2$•••ClNC | 0.0138 | 0.0500 | 0.719 | -0.009 | 0.011 | 0.002 | 0.83 | -0.009 | -0.005 | 0.065 | 0.143 |
| $C_2H_2$•••ClCCH | 0.0076 | 0.0298 | 0.564 | -0.004 | 0.006 | 0.002 | 0.70 | -0.005 | -0.003 | 0.037 | 0.122 |
| $C_2H_2$•••ClOH | 0.0137 | 0.0502 | 0.868 | -0.009 | 0.011 | 0.002 | 0.83 | -0.009 | -0.005 | 0.064 | 0.140 |
| | | | | | | | | | | | |
| $C_2H_4$•••ClF | 0.0394 | 0.0917 | 1.628 | -0.032 | 0.027 | -0.004 | 1.16 | -0.035 | -0.013 | 0.139 | 0.248 |
| $C_2H_4$•••ClCN | 0.0092 | 0.0321 | 0.744 | -0.005 | 0.006 | 0.002 | 0.74 | -0.006 | -0.004 | 0.042 | 0.147 |
| $C_2H_4$•••ClNC | 0.0162 | 0.0516 | 0.962 | -0.010 | 0.012 | 0.001 | 0.88 | -0.012 | -0.006 | 0.069 | 0.171 |
| $C_2H_4$•••ClCCH | 0.0083 | 0.0309 | 0.612 | -0.004 | 0.006 | 0.002 | 0.70 | -0.005 | -0.003 | 0.039 | 0.131 |
| $C_2H_4$•••ClOH | 0.0175 | 0.0558 | 1.169 | -0.011 | 0.013 | 0.001 | 0.90 | -0.013 | -0.006 | 0.074 | 0.172 |
| | | | | | | | | | | | |
| $H_2$•••ClF | 0.0106 | 0.0429 | 0.240 | -0.008 | 0.009 | 0.002 | 0.82 | -0.008 | -0.006 | 0.057 | 0.137 |
| $H_2$•••ClCN | 0.0046 | 0.0197 | 0.153 | -0.002 | 0.004 | 0.001 | 0.66 | -0.003 | -0.003 | 0.026 | 0.127 |
| $H_2$•••ClNC | 0.0069 | 0.0289 | 0.182 | -0.004 | 0.006 | 0.002 | 0.74 | -0.005 | -0.004 | 0.038 | 0.132 |
| $H_2$•••ClCCH | 0.0042 | 0.0183 | 0.155 | -0.002 | 0.003 | 0.001 | 0.65 | -0.003 | -0.003 | 0.024 | 0.123 |
| $H_2$•••ClOH | 0.0067 | 0.0282 | 0.235 | -0.004 | 0.006 | 0.001 | 0.75 | -0.005 | -0.004 | 0.037 | 0.129 |

** $\rho$ is the electron density, $\nabla^2\rho$ is Laplacian of electron density, H is the total energy density which is the summation of density of potential energy 'V' and Lagrangian form of kinetic energy density 'G', $\lambda 1$, $\lambda 2$ and $\lambda 3$ are the curvature values, all at intermolecular BCP.*

Sosa and co-workers have proposed another characteristic of shared-shell interaction as the ratio $|\lambda_1|/\lambda_3$, which is greater than 1[19] (see Table VI. 4). Among the three eigen values of the Laplacian, $\lambda_1$, $\lambda_2$, and $\lambda_3$, the first two are in general negative and the third one positive as the electron density at BCP is maximum in the two directions orthogonal to the bond and it is a minimum along the bond path, leading to the (3,-1) bond critical points. Hence, when this ratio is more than one, the maximum (electron accumulation) is steeper than the minimum (electron depletion). In other words, this is the ratio of the perpendicular contraction to the parallel expansion along the bond path. They had considered only the hydrogen and halogen bonded complexes. We extend their approach for lithium-bonded complexes and also for the 'covalent' D-H/D-Cl and 'ionic' D-Li bonds in our work, see Figure VI. 7. The results presented in Figure VI. 7, in comparison with those from Figure VI. 4 and Figure VI. 5, suggest that the $|\lambda_1|/\lambda_3$ ratio for closed-shell interaction is less than 0.25. All intra-molecular bonds in Li-D and the intermolecular bonds in DLi•••A considered in our work have $|\lambda_1|/\lambda_3$ less than 0.25. For lithium bond, these ratios are almost constant for case I and overall variation is very small (0.161-0.192). On the other hand, this ratio for hydrogen bonds goes up to 0.42 for BrH•••$NH_3$. Based on these results, we propose the following. The $|\lambda_1|/\lambda_3$ ratio is less than 0.25 for closed-shell interaction and greater than 1 for shared-shell interaction. The values in between 0.25-1.00 represent an intermediated region.

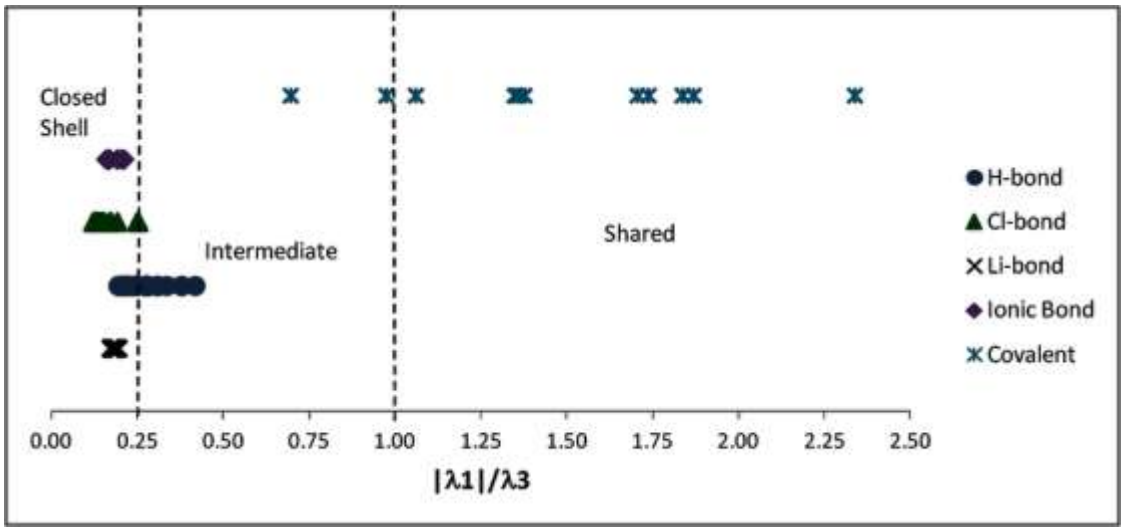


*Figure VI. 7. Plot of |λ1|/λ3 for various bonds having interactions classified as closed-shell, shared-shell and intermediate.*

Based on all the topological parameters derived from the Laplacian of electron density at BCP, sign of $\nabla^2\rho$, the ratio |V|/G, sign of H and $|\lambda_1|/\lambda_3$ ratio, it is clear that the 'ionic bond' in Li-D and the lithium bond in DLi•••A are both clearly closed-shell interactions. Hydrogen bond and chlorine bond on the other hand can be in the intermediate region where some extent of covalency can play a role. A natural bond orbital analysis can give the extent of covalency in all these interactions and that will be discussed later.

### VI.3.4.4. Mutual Penetration

Mutual penetration was considered as the necessary and sufficient condition for hydrogen bond by Koch and Popelier[18]. It is the summation of the difference between the non-bonded radii and bonded radii of both acceptor A and the bonded atom X. Non-bonded radii is the distance from nucleus to the point where the electron density value is 0.001 a.u. in monomer but the distance should be measured in the direction of approach of the bonded partner [18]. For hydrogen/chlorine bonded complexes, the binding energy is strongly correlated to the mutual penetration. In lithium bonded complexes, there are two regions: penetration linearly depends on binding energy and penetration remains constant as binding energy increases (Figure VI. 8). Generally for strongly bound complexes ( >63 kJ/mole) penetration remain constant e.g. for complexes $H_2O/NH_3$•••Li-D while in weakly bound complexes (<42 kJ/mole) it is linearly dependent (e.g. for complexes $CH_3/C_2H_4/H_2$•••Li-D, correlation coefficient is 0.96). For case II lithium bonded complexes, the bonded radii of both acceptor and Li-atom remain constant and penetration is therefore constant (Table VI. 5). Not surprisingly, the bonded radii of Li in the strongly bound complexes were very close to the ionic radii of $Li^+$, 0.73 Å. In the weaker complexes, such as $H_2$•••LiOH, the bonded radii of Li is 0.88 Å. As noted earlier, Li is equidistant between D and A in these strongly bound complexes. What is perhaps surprising is that LiD could form complexes with weak acceptors and these are not purely 'electrostatic'. For case 1 complexes, when the donor is kept fixed, the radii of both acceptor and lithium varied and showed linear relationship with a correlation coefficient 0.96 for all complexes (Table VI. 6).

*Table VI. 5. Mutual penetration between bonded atoms of complexes.*

| Complexes | $r_A^0$ | $r_A$ | Del $r_A$ | $r_X^0$ | $r_X$ | Del $r_X$ | Del $r_A$ + Del $r_X$ |
|---|---|---|---|---|---|---|---|
| **Hydrogen Bond** | | | | | | | |
| $CH_3$•••HBr | 1.98 | 1.26 | 0.72 | 1.27 | 0.74 | 0.53 | 1.25 |
| $CH_3$•••HCl | 1.98 | 1.34 | 0.64 | 1.22 | 0.78 | 0.44 | 1.08 |
| $CH_3$•••HF | 1.98 | 1.38 | 0.61 | 1.11 | 0.74 | 0.37 | 0.98 |
| $CH_3$•••HNC | 1.98 | 1.43 | 0.55 | 1.13 | 0.8 | 0.33 | 0.89 |
| $CH_3$•••HCN | 1.98 | 1.53 | 0.46 | 1.21 | 0.92 | 0.3 | 0.75 |
| $CH_3$•••HOH | 1.98 | 1.48 | 0.5 | 1.17 | 0.86 | 0.32 | 0.82 |
| $CH_3$•••HCCH | 1.98 | 1.53 | 0.46 | 1.25 | 0.94 | 0.32 | 0.77 |
| | | | | | | | |
| $H_2O$•••HBr | 1.88 | 1.2 | 0.68 | 1.27 | 0.63 | 0.64 | 1.32 |
| $H_2O$•••HCl | 1.88 | 1.2 | 0.68 | 1.22 | 0.62 | 0.61 | 1.29 |
| $H_2O$•••HF | 1.88 | 1.16 | 0.72 | 1.11 | 0.53 | 0.58 | 1.3 |
| $H_2O$•••HNC | 1.88 | 1.2 | 0.68 | 1.13 | 0.59 | 0.54 | 1.22 |
| $H_2O$•••HCN | 1.88 | 1.28 | 0.6 | 1.21 | 0.74 | 0.47 | 1.07 |
| $H_2O$•••HOH | 1.88 | 1.26 | 0.62 | 1.17 | 0.67 | 0.5 | 1.13 |
| $H_2O$•••HCCH | 1.88 | 1.33 | 0.55 | 1.25 | 0.8 | 0.45 | 1 |
| | | | | | | | |
| $NH_3$•••HBr | 2 | 1.14 | 0.86 | 1.27 | 0.52 | 0.75 | 1.61 |
| $NH_3$•••HCl | 2 | 1.18 | 0.82 | 1.22 | 0.54 | 0.68 | 1.5 |
| $NH_3$•••HF | 2 | 1.17 | 0.83 | 1.11 | 0.5 | 0.61 | 1.44 |
| $NH_3$•••HNC | 2 | 1.23 | 0.77 | 1.13 | 0.57 | 0.57 | 1.34 |
| $NH_3$•••HCN | 2 | 1.36 | 0.64 | 1.21 | 0.73 | 0.49 | 1.12 |
| $NH_3$•••HOH | 2 | 1.3 | 0.7 | 1.17 | 0.65 | 0.52 | 1.23 |
| $NH_3$•••HCCH | 2 | 1.41 | 0.59 | 1.25 | 0.78 | 0.47 | 1.07 |
| | | | | | | | |
| $C_2H_4$•••HBr | 2.14 | 1.41 | 0.74 | 1.27 | 0.82 | 0.45 | 1.18 |
| $C_2H_4$•••HCl | 2.14 | 1.43 | 0.71 | 1.22 | 0.8 | 0.42 | 1.13 |
| $C_2H_4$•••HF | 2.14 | 1.39 | 0.76 | 1.11 | 0.71 | 0.4 | 1.16 |
| $C_2H_4$•••HNC | 2.14 | 1.46 | 0.69 | 1.13 | 0.81 | 0.32 | 1.01 |
| $C_2H_4$•••HCN | 2.14 | 1.56 | 0.58 | 1.21 | 0.92 | 0.29 | 0.87 |
| $C_2H_4$•••HOH | 2.14 | 1.5 | 0.64 | 1.17 | 0.84 | 0.34 | 0.98 |
| $C_2H_4$•••HCCH | 2.14 | 1.58 | 0.56 | 1.25 | 0.95 | 0.3 | 0.86 |
| **Lithium Bond** | | | | | | | |
| $CH_3$•••LiCN | 1.98 | 1.5 | 0.48 | 1 | 0.86 | 0.14 | 0.63 |
| $CH_3$•••LiNC | 1.98 | 1.49 | 0.49 | 1 | 0.86 | 0.14 | 0.63 |
| $CH_3$•••LiBr | 1.98 | 1.48 | 0.51 | 0.98 | 0.85 | 0.14 | 0.65 |
| $CH_3$•••LiCl | 1.98 | 1.51 | 0.48 | 0.99 | 0.85 | 0.14 | 0.62 |
| $CH_3$•••LiCCH | 1.98 | 1.51 | 0.47 | 1 | 0.87 | 0.13 | 0.61 |
| $CH_3$•••LiH | 1.98 | 1.52 | 0.47 | 0.98 | 0.87 | 0.12 | 0.58 |

| | | | | | | | |
|---|---|---|---|---|---|---|---|
| $CH_3$•••LiF | 1.98 | 1.5 | 0.48 | 1.01 | 0.87 | 0.14 | 0.62 |
| $CH_3$•••LiOH | 1.98 | 1.53 | 0.45 | 1.01 | 0.88 | 0.12 | 0.58 |
| | | | | | | | |
| $H_2O$•••LiCN | 1.88 | 1.17 | 0.71 | 1 | 0.72 | 0.28 | 0.98 |
| $H_2O$•••LiNC | 1.88 | 1.17 | 0.71 | 1 | 0.72 | 0.28 | 0.99 |
| $H_2O$•••LiBr | 1.88 | 1.17 | 0.71 | 0.98 | 0.72 | 0.27 | 0.98 |
| $H_2O$•••LiCl | 1.88 | 1.17 | 0.71 | 0.99 | 0.72 | 0.27 | 0.98 |
| $H_2O$•••LiCCH | 1.88 | 1.18 | 0.7 | 1 | 0.73 | 0.28 | 0.98 |
| $H_2O$•••LiH | 1.88 | 1.18 | 0.7 | 0.98 | 0.73 | 0.26 | 0.96 |
| $H_2O$•••LiF | 1.88 | 1.18 | 0.7 | 1.01 | 0.73 | 0.28 | 0.98 |
| $H_2O$•••LiOH | 1.88 | 1.19 | 0.69 | 1.01 | 0.73 | 0.27 | 0.96 |
| | | | | | | | |
| $NH_3$•••LiCN | 2 | 1.28 | 0.72 | 1 | 0.74 | 0.26 | 0.98 |
| $NH_3$•••LiNC | 2 | 1.28 | 0.72 | 1 | 0.74 | 0.26 | 0.98 |
| $NH_3$•••LiBr | 2 | 1.27 | 0.73 | 0.98 | 0.73 | 0.25 | 0.98 |
| $NH_3$•••LiCl | 2 | 1.28 | 0.72 | 0.99 | 0.74 | 0.25 | 0.97 |
| $NH_3$•••LiCCH | 2 | 1.29 | 0.71 | 1 | 0.74 | 0.26 | 0.97 |
| $NH_3$•••LiH | 2 | 1.28 | 0.72 | 0.98 | 0.74 | 0.24 | 0.96 |
| $NH_3$•••LiF | 2 | 1.29 | 0.71 | 1.01 | 0.75 | 0.26 | 0.98 |
| $NH_3$•••LiOH | 2 | 1.3 | 0.7 | 1.01 | 0.75 | 0.25 | 0.95 |
| | | | | | | | |
| $H_2$•••LiCN | 1.56 | 1.18 | 0.38 | 1 | 0.87 | 0.13 | 0.51 |
| $H_2$•••LiNC | 1.56 | 1.17 | 0.39 | 1 | 0.86 | 0.14 | 0.53 |
| $H_2$•••LiBr | 1.56 | 1.14 | 0.42 | 0.98 | 0.85 | 0.14 | 0.56 |
| $H_2$•••LiCl | 1.56 | 1.17 | 0.4 | 0.99 | 0.86 | 0.13 | 0.53 |
| $H_2$•••LiCCH | 1.56 | 1.19 | 0.38 | 1 | 0.87 | 0.13 | 0.51 |
| $H_2$•••LiH | 1.56 | 1.19 | 0.37 | 0.98 | 0.87 | 0.11 | 0.48 |
| $H_2$•••LiF | 1.56 | 1.17 | 0.39 | 1.01 | 0.87 | 0.14 | 0.52 |
| $H_2$•••LiOH | 1.56 | 1.19 | 0.37 | 1.01 | 0.88 | 0.12 | 0.49 |
| | | | | | | | |
| $C_2H_4$•••LiCN | 2.14 | 1.49 | 0.65 | 1 | 0.83 | 0.17 | 0.82 |
| $C_2H_4$•••LiNC | 2.14 | 1.49 | 0.66 | 1 | 0.83 | 0.17 | 0.83 |
| $C_2H_4$•••LiBr | 2.14 | 1.46 | 0.68 | 0.98 | 0.82 | 0.16 | 0.84 |
| $C_2H_4$•••LiCl | 2.14 | 1.48 | 0.66 | 0.99 | 0.83 | 0.16 | 0.82 |
| $C_2H_4$•••LiCCH | 2.14 | 1.5 | 0.65 | 1 | 0.84 | 0.16 | 0.81 |
| $C_2H_4$•••LiH | 2.14 | 1.51 | 0.63 | 0.98 | 0.84 | 0.14 | 0.78 |
| $C_2H_4$•••LiF | 2.14 | 1.5 | 0.65 | 1.01 | 0.85 | 0.16 | 0.81 |
| $C_2H_4$•••LiOH | 2.14 | 1.51 | 0.63 | 1.01 | 0.85 | 0.15 | 0.78 |
| **Chlorine Bond** | | | | | | | |
| $CH_3$•••ClF | 1.98 | 1.28 | 0.7 | 1.79 | 1.33 | 0.46 | 1.16 |
| $CH_3$•••ClCN | 1.98 | 1.62 | 0.36 | 1.87 | 1.61 | 0.25 | 0.61 |
| $CH_3$•••ClNC | 1.98 | 1.46 | 0.53 | 1.82 | 1.48 | 0.34 | 0.87 |
| $CH_3$•••ClCCH | 1.98 | 1.64 | 0.34 | 1.88 | 1.66 | 0.22 | 0.56 |

| | | | | | | | |
|---|---|---|---|---|---|---|---|
| $CH_3$•••ClOH | 1.98 | 1.49 | 0.5 | 1.85 | 1.49 | 0.36 | 0.86 |
| | | | | | | | |
| $NH_3$•••ClF | 2 | 1.12 | 0.88 | 1.79 | 1.09 | 0.7 | 1.58 |
| $NH_3$•••ClCN | 2 | 1.47 | 0.53 | 1.87 | 1.46 | 0.41 | 0.94 |
| $NH_3$•••ClNC | 2 | 1.34 | 0.66 | 1.82 | 1.27 | 0.54 | 1.21 |
| $NH_3$•••ClCCH | 2 | 1.52 | 0.48 | 1.88 | 1.51 | 0.36 | 0.84 |
| $NH_3$•••ClOH | 2 | 1.31 | 0.69 | 1.85 | 1.29 | 0.56 | 1.25 |
| | | | | | | | |
| $C_2H_2$•••ClF | 2.04 | 1.36 | 0.68 | 1.79 | 1.34 | 0.45 | 1.13 |
| $C_2H_2$•••ClCN | 2.04 | 1.62 | 0.42 | 1.87 | 1.59 | 0.28 | 0.7 |
| $C_2H_2$•••ClNC | 2.04 | 1.5 | 0.54 | 1.82 | 1.46 | 0.35 | 0.89 |
| $C_2H_2$•••ClCCH | 2.04 | 1.65 | 0.39 | 1.88 | 1.62 | 0.26 | 0.65 |
| $C_2H_2$•••ClOH | 2.04 | 1.49 | 0.54 | 1.85 | 1.47 | 0.38 | 0.93 |
| | | | | | | | |
| $C_2H_4$•••ClF | 2.14 | 1.21 | 0.93 | 1.79 | 1.25 | 0.54 | 1.47 |
| $C_2H_4$•••ClCN | 2.14 | 1.61 | 0.53 | 1.87 | 1.58 | 0.29 | 0.82 |
| $C_2H_4$•••ClNC | 2.14 | 1.46 | 0.68 | 1.82 | 1.44 | 0.37 | 1.05 |
| $C_2H_4$•••ClCCH | 2.14 | 1.66 | 0.49 | 1.88 | 1.59 | 0.29 | 0.78 |
| $C_2H_4$•••ClOH | 2.14 | 1.43 | 0.71 | 1.85 | 1.43 | 0.42 | 1.13 |
| | | | | | | | |
| $H_2$•••ClF | 1.57 | 1.18 | 0.39 | 1.79 | 1.48 | 0.31 | 0.7 |
| $H_2$•••ClCN | 1.57 | 1.38 | 0.19 | 1.87 | 1.7 | 0.16 | 0.35 |
| $H_2$•••ClNC | 1.57 | 1.28 | 0.28 | 1.82 | 1.59 | 0.22 | 0.51 |
| $H_2$•••ClCCH | 1.57 | 1.39 | 0.18 | 1.88 | 1.73 | 0.15 | 0.33 |
| $H_2$•••ClOH | 1.57 | 1.28 | 0.28 | 1.85 | 1.6 | 0.25 | 0.53 |

*Radii of bonded ($r_A$ and $r_X$), non-bonded ($r_A^0$ and $r_X^0$) atoms, differences between them (Del $r_A$ , Del $r_X$) and summation of both differences i.e. mutual penetration (Del $r_A$ + Del $r_X$).*

For the chlorine bonded complexes, both case 1 and 2, there is a strong correlation between the overall penetration and binding energy. For hydrogen bonded complexes, there is a general correlation between penetration and binding energy. However, the correlation is better for case 1 than case 2 (Table VI. 6). However, it is clear that the hydrogen and halogen bonds behave differently compared to the lithium bonds. Interestingly, the difference could well be due to the fact that the donors (DH/DCl) are 'covalently bonded' in the former case and 'ionic' in the later case (DLi). This in turn influences the nature of the DX•••A bond.

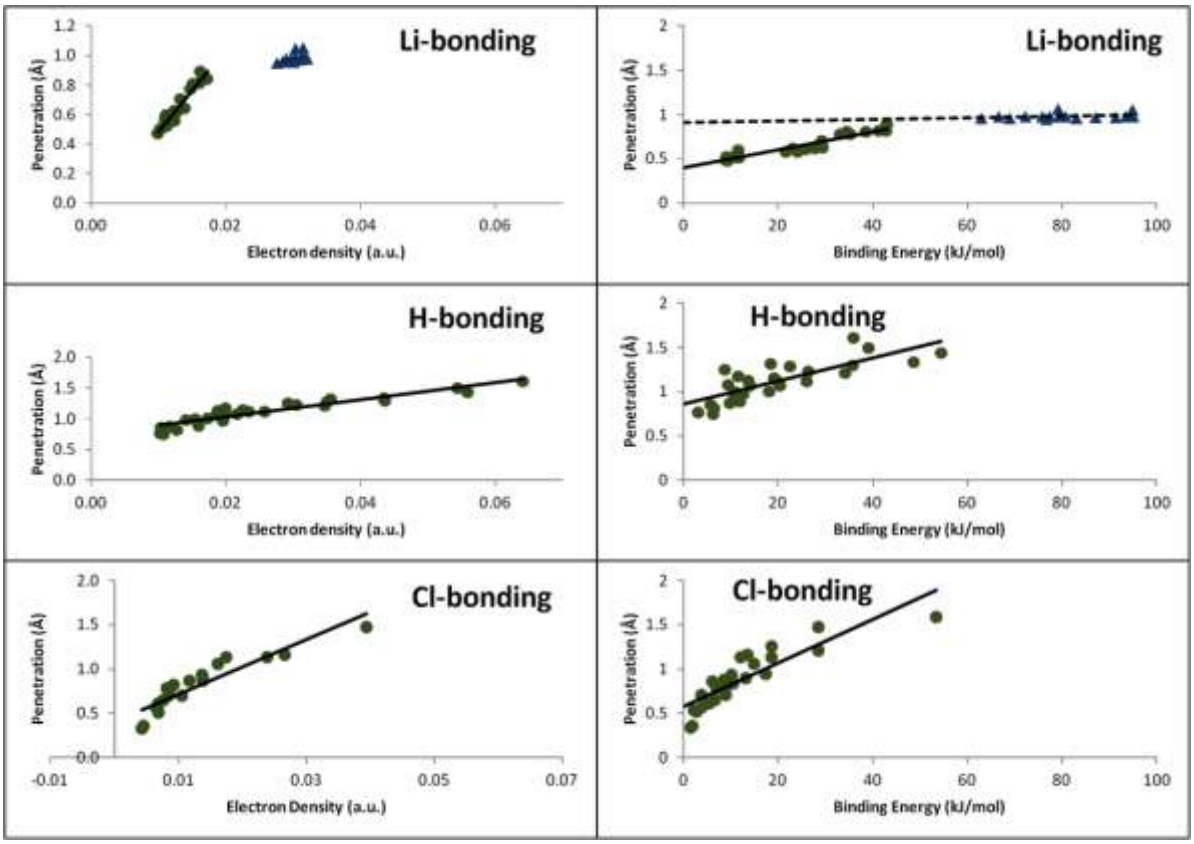


*Figure VI. 8. Correlation plots for penetration with electron density and binding energy.*

*Table VI. 6. Correlation coefficient (C.C.) for the correlation between mutual penetration and binding energy.*

| Complex | Li-Bonding | H-Bonding | Cl-bonding |
|---|---|---|---|
| Overall | CC=0.96# | CC=0.80 | CC=0.87 |
| | MP=0.001*BE+0.4 | MP=0.01*BE+0.7 | MP=0.02*BE+0.6 |
| | CC | CC | CC |
| | (CASE-I) Same Donor (X-D) , Different acceptor | | |
| A•••X-F | 0.96 | 0.96 | 0.90 |
| A•••X-Cl | 0.95 | 0.97 | xxx |
| A•••X-Br | 0.96 | 0.96 | xxx |
| A•••X-CN | 0.96 | 0.98 | 0.94 |
| A•••X-NC | 0.96 | 0.99 | 0.92 |
| A•••X-CCH | 0.96 | 0.77 | 0.95 |
| A•••X-OH | 0.96 | 0.97 | 0.95 |
| A•••X-H | 0.96 | xxx | xxx |
| | (CASE-II) Same acceptor (X) , Different Donor | | |
| $CH_3$ •••X-D | 0.79 | 0.48 | 0.95 |
| $NH_3$•••-X-D | 0.72 | 0.68 | 0.91 |
| $H_2O$•••X-D | 0.74 | 0.59 | Xxx |
| $C_2H_4$•••X-D | 0.83 | 0.64 | 0.95 |
| $C_2H_2$•••X-D | xxx | 0.55 | 0.93 |
| $H_2$•••X-D | 0.66 | xxx | 0.95 |

*#There are two type of correlation for Li-bonding. For Li-bonding in figure 7 (main text), Lower part shows linear dependence and upper part plateau. The correlation coefficient of the lower part is presented.*

Since binding energy correlates well with electron density and also with mutual penetration, it is logical to think about the correlation between electron density and penetration (Figure VI. 8). Surprisingly, this is the best correlation we observed among the binding energy vs electron density, binding energy vs penetration and electron density vs penetration (Table VI. 7). To the best of knowledge, electron density vs penetration correlation has not been analyzed before. This correlation assumes significance, given the fact that van der Waals radii are still used as the 'non-bonded radii' in analyzing crystal structures to make conclusion about penetration. For example, it was concluded that C-H•••O contacts are 'hydrogen bonds' and C-H•••π contacts are 'van der Waals interaction' using this arbitrary non-bonded radius to measure penetration.[63] However, both these interactions satisfied the other criteria of Koch and Popelier for 'hydrogen bonding'. The correlation between electron density and binding energy is useful for analyzing crystal structure and also intramolecular hydrogen bonds as there are no direct methods available for measuring the binding energy in these cases. In closing, we point out that the exclusion of $C_2H_2$•••H-D and $NH_3$•••Cl-D from H-bond and Cl-bond respectively, improves the correlation coefficient (Table VI. 7 and Figure VI. 8).

*Table VI. 7. Correlation coefficient for the correlation between electron density ( in a.u.) and mutual penetration (in Å).*

| Complex | Li-Bond | H-Bond | Cl-bond |
|---|---|---|---|
| Overall | CC=0.97# | CC=0.94$ | CC=0.92 |
| | MP=55.6*ρ-0.1 | MP=13.9*ρ+0.7 | MP=30.9*ρ+0.4 |
| | CC# | CC | CC** |
| (CASE-I) | Same Donor (X-D) , Different acceptor | | |
| A•••X-F | 0.94 | 0.96 | 0.99 |
| A•••X-Cl | 0.94 | 0.98 | xxx |
| A•••X-Br | 0.93 | 0.98 | xxx |
| A•••X-CN | 0.94 | 0.97 | 0.99 |
| A•••X-NC | 0.94 | 0.86 | 1.00 |
| A•••X-CCH | 0.94 | 0.96 | 0.99 |
| A•••X-OH | 0.94 | 0.85 | 0.99 |
| A•••X-H | 0.94 | xxx | xxx |
| (CASE-II) | Same acceptor (X) , Different Donor | | |
| $CH_3$ •••X-D | 0.96 | 0.99 | 0.96 |
| $NH_3$•••-X-D | 0.81 | 0.99 | 0.95 |
| $H_2O$•••X-D | 0.73 | 0.94 | xxx |
| $C_2H_4$•••X-D | 0.93 | 0.96 | 0.97 |
| $C_2H_2$•••X-D | xxx | 0.95 | 0.98 |
| $H_2$•••X-D | 0.97 | xxx | 0.98 |

*$ Without the values of $C_2H_2$•••H-D complexes. ** Without the values of $NH_3$•••Cl-D complexes for case 1 only. # Figure 7 of main text for Li-bonding, lower part depends linearly and upper part plateau. The correlation coefficient and equation are presented only for the lower part.*

### VI.3.4.5. Net Charge on Bonded Atoms

Net charge on atom is defined as the difference between nuclear charge and average number of electronic charge N(A) on the atom A. Koch and Popelier had observed that there is a loss of the charge on the hydrogen atom on hydrogen bond formation. The same is observed for Li atom in the lithium bonded complexes. However, for chlorine atom, there is gain of charge on chlorine bond formation and it has been noted in earlier work as well.[19] We note that in all complexes and monomers (Li-D), Li atom has charge close to +1 (Table VI. 8). In this criterion, H and Li behave similarly but Cl is different.

### VI.3.4.6. Energy of the Bonded Atoms

Generally H-atom is destabilized on hydrogen bond formation. However, both Li and Cl atoms get stabilized on X bond formation (Table VI. 8).

*Table VI. 8. Change in net charge of X-atom and change in net energy of X-atom on complex formation.*

| Complexes | N(X) in Complexes | N(X) in monomer | ΔN(X) | K(X) in Complex | K(X) in monomers | ΔK(X) |
|---|---|---|---|---|---|---|
| | | | **Lithium Bonding** | | | |
| $CH_3$---LiCN | 0.9099 | 0.9406 | -0.0306 | -7.3581 | -7.3549 | -0.0032 |
| $CH_3$---LiNC | 0.919 | 0.9408 | -0.0218 | -7.3536 | -7.3343 | -0.0193 |
| $CH_3$---LiBr | 0.903 | 0.9301 | -0.0271 | -7.3467 | -7.3336 | -0.0131 |
| $CH_3$---LiCl | 0.9151 | 0.934 | -0.0189 | -7.3513 | -7.3339 | -0.0174 |
| $CH_3$---LiCCH | 0.9081 | 0.9333 | -0.0252 | -7.3678 | -7.3639 | -0.0039 |
| $CH_3$---LiH | 0.8934 | 0.9122 | -0.0188 | -7.38 | -7.3628 | -0.0173 |
| $CH_3$---LiF | 0.9129 | 0.9437 | -0.0308 | -7.3629 | -7.3432 | -0.0197 |
| $CH_3$---LiOH | 0.9043 | 0.9319 | -0.0276 | -7.3633 | -7.3547 | -0.0086 |
| | | | | | | |
| $H_2O$---LiCN | 0.9155 | 0.9406 | -0.025 | -7.3685 | -7.3549 | -0.0136 |
| $H_2O$---LiNC | 0.9206 | 0.9408 | -0.0202 | -7.3647 | -7.3343 | -0.0304 |
| $H_2O$---LiBr | 0.907 | 0.9301 | -0.0231 | -7.3551 | -7.3336 | -0.0215 |
| $H_2O$---LiCl | 0.9105 | 0.934 | -0.0235 | -7.3565 | -7.3339 | -0.0226 |
| $H_2O$---LiCCH | 0.9096 | 0.9333 | -0.0236 | -7.3779 | -7.3639 | -0.014 |
| $H_2O$---LiH | 0.8955 | 0.9122 | -0.0167 | -7.3858 | -7.3628 | -0.023 |
| $H_2O$---LiF | 0.9149 | 0.9437 | -0.0287 | -7.3736 | -7.3432 | -0.0304 |
| $H_2O$---LiOH | 0.908 | 0.9319 | -0.0239 | -7.3734 | -7.3547 | -0.0187 |
| | | | | | | |
| $NH_3$---LiCN | 0.9071 | 0.9406 | -0.0334 | -7.3784 | -7.3549 | -0.0236 |
| $NH_3$---LiNC | 0.913 | 0.9408 | -0.0278 | -7.3741 | -7.3343 | -0.0398 |
| $NH_3$---LiBr | 0.8994 | 0.9301 | -0.0307 | -7.3624 | -7.3336 | -0.0288 |
| $NH_3$---LiCl | 0.9028 | 0.934 | -0.0312 | -7.3664 | -7.3339 | -0.0325 |
| $NH_3$---LiCCH | 0.9027 | 0.9333 | -0.0305 | -7.3859 | -7.3639 | -0.022 |
| $NH_3$---LiH | 0.8869 | 0.9122 | -0.0253 | -7.3942 | -7.3628 | -0.0314 |
| $NH_3$---LiF | 0.9068 | 0.9437 | -0.0369 | -7.3831 | -7.3432 | -0.0399 |

| | | | | | | |
|---|---|---|---|---|---|---|
| $NH_3$---LiOH | 0.9008 | 0.9319 | -0.0311 | -7.383 | -7.3547 | -0.0283 |
| | | | | | | |
| $H_2$----LiCN | 0.924 | 0.9406 | -0.0166 | -7.3496 | -7.3549 | 0.0052 |
| $H_2$----LiNC | 0.9284 | 0.9408 | -0.0124 | -7.3455 | -7.3343 | -0.0112 |
| $H_2$----LiBr | 0.9115 | 0.9301 | -0.0186 | -7.3384 | -7.3336 | -0.0048 |
| $H_2$----LiCl | 0.9161 | 0.934 | -0.0179 | -7.3382 | -7.3339 | -0.0043 |
| $H_2$----LiCCH | 0.9168 | 0.9333 | -0.0164 | -7.3609 | -7.3639 | 0.003 |
| $H_2$----LiH | 0.9021 | 0.9122 | -0.0101 | -7.3819 | -7.3628 | -0.0191 |
| $H_2$----LiF | 0.921 | 0.9437 | -0.0227 | -7.3552 | -7.3432 | -0.012 |
| $H_2$----LiOH | 0.9114 | 0.9319 | -0.0205 | -7.3578 | -7.3547 | -0.0031 |
| | | | | | | |
| $C_2H_4$---LiCN | 0.9099 | 0.9406 | -0.0306 | -7.3641 | -7.3549 | -0.0092 |
| $C_2H_4$---LiNC | 0.9145 | 0.9408 | -0.0263 | -7.3605 | -7.3343 | -0.0262 |
| $C_2H_4$---LiBr | 0.8987 | 0.9301 | -0.0314 | -7.3539 | -7.3336 | -0.0203 |
| $C_2H_4$---LiCl | 0.903 | 0.934 | -0.031 | -7.3542 | -7.3339 | -0.0204 |
| $C_2H_4$---LiCCH | 0.9041 | 0.9333 | -0.0292 | -7.3733 | -7.3639 | -0.0094 |
| $C_2H_4$---LiH | 0.8913 | 0.9122 | -0.0209 | -7.3814 | -7.3628 | -0.0186 |
| $C_2H_4$---LiF | 0.9089 | 0.9437 | -0.0348 | -7.3698 | -7.3432 | -0.0266 |
| $C_2H_4$---LiOH | 0.9006 | 0.9319 | -0.0314 | -7.3697 | -7.3547 | -0.0149 |
| **Hydrogen Bonding** | | | | | | |
| $CH_3$---HBr | 0.1461 | 0.0711 | 0.0749 | -0.5234 | -0.5439 | 0.0204 |
| $CH_3$---HCl | 0.3125 | 0.2961 | 0.0164 | -0.4692 | -0.4827 | 0.0135 |
| $CH_3$---HF | 0.7393 | 0.7539 | -0.0146 | -0.2535 | -0.2533 | -0.0002 |
| $CH_3$---HNC | 0.5662 | 0.5668 | -0.0006 | -0.3579 | -0.3651 | 0.0071 |
| $CH_3$---HCN | 0.2333 | 0.2378 | -0.0045 | -0.5183 | -0.5048 | -0.0135 |
| $CH_3$---HOH | 0.6064 | 0.6331 | -0.0267 | -0.3446 | -0.3286 | -0.016 |
| $CH_3$---HCCH | 0.1834 | 0.1712 | 0.0123 | -0.5428 | -0.5485 | 0.0057 |
| | | | | | | |
| $H_2O$---HBr | 0.2217 | 0.0711 | 0.1506 | -0.4981 | -0.5439 | 0.0457 |
| $H_2O$---HCl | 0.386 | 0.2961 | 0.0898 | -0.4413 | -0.4827 | 0.0413 |
| $H_2O$---HF | 0.7729 | 0.7539 | 0.019 | -0.2364 | -0.2533 | 0.0169 |
| $H_2O$---HNC | 0.6201 | 0.5668 | 0.0533 | -0.3327 | -0.3651 | 0.0324 |
| $H_2O$---HCN | 0.2859 | 0.2378 | 0.0481 | -0.4994 | -0.5048 | 0.0054 |
| $H_2O$---HOH | 0.6466 | 0.6331 | 0.0135 | -0.3262 | -0.3286 | 0.0024 |
| $H_2O$---HCCH | 0.2284 | 0.1712 | 0.0572 | -0.5272 | -0.5485 | 0.0213 |
| | | | | | | |
| $NH_3$---HBr | 0.3128 | 0.0711 | 0.2416 | -0.4459 | -0.5439 | 0.098 |
| $NH_3$---HCl | 0.423 | 0.2961 | 0.1269 | -0.4122 | -0.4827 | 0.0705 |
| $NH_3$---HF | 0.7586 | 0.7539 | 0.0047 | -0.2382 | -0.2533 | 0.0151 |
| $NH_3$---HNC | 0.6197 | 0.5668 | 0.0529 | -0.3239 | -0.3651 | 0.0412 |
| $NH_3$---HCN | 0.3036 | 0.2378 | 0.0658 | -0.4851 | -0.5048 | 0.0197 |
| $NH_3$---HOH | 0.6479 | 0.6331 | 0.0148 | -0.3189 | -0.3286 | 0.0098 |
| $NH_3$---HCCH | 0.2457 | 0.1712 | 0.0745 | -0.5149 | -0.5485 | 0.0336 |
| | | | | | | |
| $C_2H_4$---HBr | 0.1505 | 0.0711 | 0.0794 | -0.5239 | -0.5439 | 0.02 |
| $C_2H_4$---HCl | 0.325 | 0.2961 | 0.0289 | -0.4641 | -0.4827 | 0.0185 |
| $C_2H_4$---HF | 0.7436 | 0.7539 | -0.0103 | -0.2493 | -0.2533 | 0.004 |
| $C_2H_4$---HNC | 0.575 | 0.5668 | 0.0082 | -0.3514 | -0.3651 | 0.0136 |
| $C_2H_4$---HCN | 0.2439 | 0.2378 | 0.0061 | -0.5132 | -0.5048 | -0.0084 |
| $C_2H_4$---HOH | 0.6141 | 0.6331 | -0.019 | -0.3397 | -0.3286 | -0.0111 |

| | | | | | | |
|---|---|---|---|---|---|---|
| $C_2H_4$---HCCH | 0.1928 | 0.1712 | 0.0216 | -0.5384 | -0.5485 | 0.0101 |
| $C_2H_2$--HBr | 0.1458 | 0.0711 | 0.0747 | -0.5273 | -0.5439 | 0.0166 |
| $C_2H_2$--HCl | 0.3257 | 0.2961 | 0.0295 | -0.4656 | -0.4827 | 0.0171 |
| $C_2H_2$--HF | 0.7485 | 0.7539 | -0.0054 | -0.2482 | -0.2533 | 0.0052 |
| $C_2H_2$--HNC | 0.5784 | 0.5668 | 0.0117 | -0.3515 | -0.3651 | 0.0136 |
| $C_2H_2$--HCN | 0.2443 | 0.2378 | 0.0065 | -0.5139 | -0.5048 | -0.0091 |
| $C_2H_2$--HOH | 0.6168 | 0.6331 | -0.0163 | -0.3399 | -0.3286 | -0.0113 |
| $C_2H_2$--HCCH | 0.1932 | 0.1712 | 0.022 | -0.539 | -0.5485 | 0.0095 |
| **Chlorine Bonding** | | | | | | |
| $CH_3$--ClF | 0.3824 | 0.528 | -0.145 | -459.566 | -459.277 | -0.289 |
| $CH_3$--ClCN | 0.0271 | 0.012 | 0.015 | -459.763 | -459.623 | -0.14 |
| $CH_3$--ClNC | 0.3251 | 0.345 | -0.02 | -459.653 | -459.414 | -0.239 |
| $CH_3$--ClCCH | -0.0569 | -0.057 | 0 | -459.867 | -459.598 | -0.268 |
| $CH_3$--ClOH | 0.2456 | 0.22 | 0.026 | -459.469 | -459.394 | -0.074 |
| $NH_3$--ClF | 0.3145 | 0.528 | -0.213 | -459.599 | -459.277 | -0.323 |
| $NH_3$--ClCN | 0.0389 | 0.012 | 0.027 | -459.859 | -459.623 | -0.236 |
| $NH_3$--ClNC | 0.4415 | 0.345 | 0.096 | -459.473 | -459.414 | -0.059 |
| $NH_3$--ClCCH | -0.0305 | -0.057 | 0.026 | -459.865 | -459.598 | -0.267 |
| $NH_3$--ClOH | 0.2088 | 0.22 | -0.011 | -459.69 | -459.394 | -0.296 |
| $C_2H_2$--ClF | 0.3775 | 0.528 | -0.15 | -459.59 | -459.277 | -0.313 |
| $C_2H_2$--ClCN | 0.0171 | 0.012 | 0.005 | -459.872 | -459.623 | -0.249 |
| $C_2H_2$--ClNC | 0.3338 | 0.345 | -0.011 | -459.661 | -459.414 | -0.247 |
| $C_2H_2$--ClCCH | -0.0514 | -0.057 | 0.005 | -459.877 | -459.598 | -0.279 |
| $C_2H_2$--ClOH | 0.2057 | 0.22 | -0.014 | -459.703 | -459.394 | -0.308 |
| $C_2H_4$--ClF | 0.3195 | 0.528 | -0.208 | -459.612 | -459.277 | -0.335 |
| $C_2H_4$--ClCN | 0.0155 | 0.012 | 0.003 | -459.871 | -459.623 | -0.248 |
| $C_2H_4$--ClNC | 0.3249 | 0.345 | -0.02 | -459.662 | -459.414 | -0.248 |
| $C_2H_4$--ClCCH | -0.0597 | -0.057 | -0.003 | -459.763 | -459.598 | -0.165 |
| $C_2H_4$--ClOH | 0.197 | 0.22 | -0.023 | -459.703 | -459.394 | -0.309 |
| $H_2$--ClF | 0.4204 | 0.528 | -0.107 | -459.545 | -459.277 | -0.268 |
| $H_2$--ClCN | 0.0145 | 0.012 | 0.002 | -459.845 | -459.623 | -0.222 |
| $H_2$--ClNC | 0.3447 | 0.345 | 0 | -459.63 | -459.414 | -0.216 |
| $H_2$--ClCCH | -0.0549 | -0.057 | 0.002 | -459.847 | -459.598 | -0.248 |
| $H_2$--ClOH | 0.2161 | 0.22 | -0.004 | -459.67 | -459.394 | -0.275 |

*Atomic properties: N(X) is the average number of electronic charge on atom X and K(X) is the energy of atom X. 'diff.' is difference between complex to the monomer for the mentioned properties.*

### VI.3.4.7. Dipolar Polarization

According to this criterion, there is a loss in dipole moment of the H atom involved in hydrogen bonding. This has been observed for most of the H- and Cl-bonded complexes in this investigation. However, for most of the Li-bonded complexes, there is gain in the dipole

moment of Li-atom on complex (Table VI. 9). However, it is worth noting that the exceptions have values which are very close to zero.

### VI.3.4.8. Volume of the Bonded Atom

The last criterion is the change in atomic volume after complex formation. For C-H•••O, hydrogen bonds Koch and Popelier noted a decrease in atomic volume of H. It is observed in all hydrogen and chlorine bonded complexes in this work. However, for Li-bond, there is an increase in volume on complex formation (Table VI. 9).

Overall, it is clear that, the eight criteria found by Koch and Popelier for C-H•••O hydrogen bonds cannot be simply extended to other intermolecular bonding. Hydrogen and chlorine bonds behave more similarly and lithium bonds are different. The old periodic tables having hydrogen on top of both the alkali and halogen groups are indeed sensible.

*Table VI. 9. Change in dipole moment and change in volume of X-atom on complex formation.*

| Complexes | \| Mu(X) \| of complex | \| Mu(X) \| of monomer | ΔMu(X) | Vol (X) of complex | Vol (X) of monomer | diff.Vol( X) |
|---|---|---|---|---|---|---|
| **Lithium Bonding** | | | | | | |
| $CH_3$---LiCN | 0.0104 | 0.0024 | 0.0079 | 31.0 | 26.6 | 4.4 |
| $CH_3$---LiNC | 0.0177 | 0.0056 | 0.0121 | 30.0 | 26.7 | 3.3 |
| $CH_3$---LiBr | 0.0074 | 0.0033 | 0.0041 | 33.1 | 28.0 | 5.2 |
| $CH_3$---LiCl | 0.0107 | 0.0006 | 0.0101 | 30.6 | 27.4 | 3.2 |
| $CH_3$--- LiCCH | 0.0120 | 0.0003 | 0.0117 | 31.8 | 26.9 | 4.8 |
| $CH_3$---LiH | 0.0025 | 0.0008 | 0.0018 | 36.0 | 30.4 | 5.6 |
| $CH_3$---LiF | 0.0295 | 0.0182 | 0.0114 | 30.2 | 25.4 | 4.8 |
| $CH_3$---LiOH | 0.0318 | 0.0218 | 0.0100 | 32.0 | 26.7 | 5.4 |
| $H_2O$---LiCN | 0.0009 | 0.0024 | -0.0015 | 28.5 | 26.6 | 1.8 |
| $H_2O$---LiNC | 0.0060 | 0.0056 | 0.0004 | 27.3 | 26.7 | 0.6 |
| $H_2O$---LiBr | 0.0052 | 0.0033 | 0.0019 | 29.8 | 28.0 | 1.8 |
| $H_2O$---LiCl | 0.0006 | 0.0006 | 0.0000 | 29.0 | 27.4 | 1.6 |
| $H_2O$--- LiCCH | 0.0007 | 0.0003 | 0.0003 | 29.0 | 26.9 | 2.1 |
| $H_2O$---LiH | 0.0093 | 0.0008 | 0.0086 | 32.5 | 30.4 | 2.1 |
| $H_2O$---LiF | 0.0173 | 0.0182 | -0.0009 | 27.4 | 25.4 | 2.0 |
| $H_2O$---LiOH | 0.0190 | 0.0218 | -0.0028 | 28.6 | 26.7 | 1.9 |
| $NH_3$---LiCN | 0.0033 | 0.0024 | 0.0008 | 29.5 | 26.6 | 2.9 |
| $NH_3$---LiNC | 0.0099 | 0.0056 | 0.0043 | 28.3 | 26.7 | 1.7 |
| $NH_3$---LiBr | 0.0014 | 0.0033 | -0.0019 | 30.7 | 28.0 | 2.8 |
| $NH_3$---LiCl | 0.0035 | 0.0006 | 0.0029 | 30.1 | 27.4 | 2.7 |
| $NH_3$--- LiCCH | 0.0044 | 0.0003 | 0.0041 | 30.0 | 26.9 | 3.1 |
| $NH_3$---LiH | 0.0048 | 0.0008 | 0.0040 | 33.4 | 30.4 | 3.0 |

| | | | | | | |
|---|---|---|---|---|---|---|
| $NH_3$---LiF | 0.0214 | 0.0182 | 0.0033 | 28.4 | 25.4 | 3.0 |
| $NH_3$---LiOH | 0.0228 | 0.0218 | 0.0010 | 29.6 | 26.7 | 3.0 |
| | | | | | | |
| $H_2$----LiCN | 0.0050 | 0.0024 | 0.0025 | 29.2 | 26.6 | 2.6 |
| $H_2$----LiNC | 0.0126 | 0.0056 | 0.0070 | 28.3 | 26.7 | 1.7 |
| $H_2$----LiBr | 0.0025 | 0.0033 | -0.0008 | 31.2 | 28.0 | 3.2 |
| $H_2$----LiCl | 0.0068 | 0.0006 | 0.0062 | 30.4 | 27.4 | 3.0 |
| $H_2$----LiCCH | 0.0071 | 0.0003 | 0.0067 | 29.9 | 26.9 | 2.9 |
| $H_2$----LiH | 0.0020 | 0.0008 | 0.0012 | 33.5 | 30.4 | 3.1 |
| $H_2$----LiF | 0.0248 | 0.0182 | 0.0067 | 28.5 | 25.4 | 3.1 |
| $H_2$----LiOH | 0.0275 | 0.0218 | 0.0057 | 30.3 | 26.7 | 3.6 |
| | | | | | | |
| $C_2H_4$---LiCN | 0.0095 | 0.0024 | 0.0071 | 30.6 | 26.6 | 4.0 |
| $C_2H_4$---LiNC | 0.0168 | 0.0056 | 0.0112 | 29.9 | 26.7 | 3.2 |
| $C_2H_4$---LiBr | 0.0059 | 0.0033 | 0.0026 | 31.6 | 28.0 | 3.6 |
| $C_2H_4$---LiCl | 0.0106 | 0.0006 | 0.0099 | 31.9 | 27.4 | 4.5 |
| $C_2H_4$--- LiCCH | 0.0110 | 0.0003 | 0.0106 | 30.9 | 26.9 | 4.0 |
| $C_2H_4$---LiH | 0.0001 | 0.0008 | -0.0006 | 35.4 | 30.4 | 5.0 |
| $C_2H_4$---LiF | 0.0282 | 0.0182 | 0.0101 | 30.2 | 25.4 | 4.8 |
| $C_2H_4$---LiOH | 0.0301 | 0.0218 | 0.0083 | 31.8 | 26.7 | 5.1 |
| **Hydrogen Bonding** | | | | | | |
| $CH_3$---HBr | 0.0631 | 0.0649 | -0.0018 | 36.5 | 47.0 | -10.5 |
| $CH_3$---HCl | 0.1203 | 0.1367 | -0.0164 | 30.4 | 36.0 | -5.6 |
| $CH_3$---HF | 0.1178 | 0.1176 | 0.0003 | 11.4 | 13.9 | -2.5 |
| $CH_3$---HNC | 0.1411 | 0.1443 | -0.0032 | 20.1 | 22.1 | -2.1 |
| $CH_3$---HCN | 0.1203 | 0.1204 | -0.0001 | 37.1 | 38.5 | -1.3 |
| $CH_3$---HOH | 0.1610 | 0.1550 | 0.0060 | 19.6 | 19.4 | 0.2 |
| $CH_3$--- HCCH | 0.1271 | 0.1336 | -0.0065 | 39.8 | 41.1 | -1.3 |
| | | | | | | |
| $H_2O$---HBr | 0.0332 | 0.0649 | -0.0318 | 31.6 | 47.0 | -15.4 |
| $H_2O$---HCl | 0.0836 | 0.1367 | -0.0531 | 23.7 | 36.0 | -12.3 |
| $H_2O$---HF | 0.0839 | 0.1176 | -0.0336 | 7.0 | 13.9 | -6.9 |
| $H_2O$---HNC | 0.1053 | 0.1443 | -0.0390 | 13.4 | 22.1 | -8.7 |
| $H_2O$---HCN | 0.0955 | 0.1204 | -0.0249 | 30.4 | 38.5 | -8.1 |
| $H_2O$---HOH | 0.1281 | 0.1550 | -0.0269 | 13.6 | 19.4 | -5.8 |
| $H_2O$--- HCCH | 0.1061 | 0.1336 | -0.0275 | 34.4 | 41.1 | -6.7 |
| | | | | | | |
| $NH_3$---HBr | 0.0262 | 0.0649 | -0.0387 | 25.1 | 47.0 | -21.9 |
| $NH_3$---HCl | 0.0732 | 0.1367 | -0.0635 | 20.5 | 36.0 | -15.5 |
| $NH_3$---HF | 0.0852 | 0.1176 | -0.0323 | 7.2 | 13.9 | -6.7 |
| $NH_3$---HNC | 0.1043 | 0.1443 | -0.0400 | 12.9 | 22.1 | -9.2 |
| $NH_3$---HCN | 0.1024 | 0.1204 | -0.0180 | 29.4 | 38.5 | -9.1 |
| $NH_3$---HOH | 0.1289 | 0.1550 | -0.0261 | 13.2 | 19.4 | -6.2 |
| $NH_3$--- HCCH | 0.1116 | 0.1336 | -0.0221 | 33.4 | 41.1 | -7.7 |
| | | | | | | |
| $C_2H_4$---HBr | 0.0630 | 0.0649 | -0.0019 | 37.5 | 47.0 | -9.5 |
| $C_2H_4$---HCl | 0.1172 | 0.1367 | -0.0195 | 29.4 | 36.0 | -6.6 |
| $C_2H_4$---HF | 0.1127 | 0.1176 | -0.0049 | 9.8 | 13.9 | -4.1 |

| | | | | | | |
|---|---|---|---|---|---|---|
| $C_2H_4$---HNC | 0.1365 | 0.1443 | -0.0078 | 18.2 | 22.1 | -3.9 |
| $C_2H_4$---HCN | 0.1172 | 0.1204 | -0.0032 | 36.0 | 38.5 | -2.5 |
| $C_2H_4$---HOH | 0.1557 | 0.1550 | 0.0006 | 17.6 | 19.4 | -1.8 |
| $C_2H_4$---HCCH | 0.1246 | 0.1336 | -0.0091 | 39.0 | 41.1 | -2.1 |
| $C_2H_2$--HBr | 0.0598 | 0.0649 | -0.0052 | 38.6 | 47.0 | -8.3 |
| $C_2H_2$--HCl | 0.1144 | 0.1367 | -0.0224 | 29.8 | 36.0 | -6.2 |
| $C_2H_2$--HF | 0.1094 | 0.1176 | -0.0081 | 9.7 | 13.9 | -4.2 |
| $C_2H_2$--HNC | 0.1328 | 0.1443 | -0.0115 | 17.9 | 22.1 | -4.2 |
| $C_2H_2$--HCN | 0.1141 | 0.1204 | -0.0063 | 35.5 | 38.5 | -3.0 |
| $C_2H_2$--HOH | 0.1514 | 0.1550 | -0.0036 | 17.3 | 19.4 | -2.1 |
| $C_2H_2$--HCCH | 0.1219 | 0.1336 | -0.0117 | 38.7 | 41.1 | -2.4 |
| **Chlorine Bonding** | | | | | | |
| $CH_3$--ClF | 0.823 | 0.971 | -0.149 | 195.2 | 199.1 | -3.9 |
| $CH_3$--ClCN | 0.170 | 0.151 | 0.019 | 202.5 | 204.2 | -1.7 |
| $CH_3$--ClNC | 0.640 | 0.665 | -0.025 | 196.5 | 199.7 | -3.2 |
| $CH_3$--ClCCH | 0.190 | 0.196 | -0.007 | 211.0 | 209.6 | 1.4 |
| $CH_3$--ClOH | 0.759 | 0.734 | 0.025 | 203.1 | 209.3 | -6.2 |
| $NH_3$--ClF | 0.556 | 0.971 | -0.415 | 190.8 | 199.1 | -8.3 |
| $NH_3$--ClCN | 0.103 | 0.151 | -0.049 | 201.5 | 204.2 | -2.7 |
| $NH_3$--ClNC | 0.695 | 0.665 | 0.030 | 187.2 | 199.7 | -0.1 |
| $NH_3$--ClCCH | 0.143 | 0.196 | -0.053 | 207.6 | 209.6 | -2.0 |
| $NH_3$--ClOH | 0.584 | 0.734 | -0.151 | 200.9 | 209.3 | -8.4 |
| $C_2H_2$--ClF | 0.750 | 0.971 | -0.221 | 194.4 | 199.1 | -4.7 |
| $C_2H_2$--ClCN | 0.137 | 0.151 | -0.015 | 202.9 | 204.2 | -1.3 |
| $C_2H_2$--ClNC | 0.622 | 0.665 | -0.044 | 194.8 | 199.7 | -4.9 |
| $C_2H_2$--ClCCH | 0.176 | 0.196 | -0.021 | 210.0 | 209.6 | 0.4 |
| $C_2H_2$--ClOH | 0.667 | 0.734 | -0.067 | 204.5 | 209.3 | -4.8 |
| $C_2H_4$--ClF | 0.698 | 0.971 | -0.274 | 188.7 | 199.1 | -0.1 |
| $C_2H_4$--ClCN | 0.143 | 0.151 | -0.008 | 202.8 | 204.2 | -1.4 |
| $C_2H_4$--ClNC | 0.621 | 0.665 | -0.045 | 193.7 | 199.7 | -6.0 |
| $C_2H_4$--ClCCH | 0.182 | 0.196 | -0.014 | 206.9 | 209.6 | -2.7 |
| $C_2H_4$--ClOH | 0.661 | 0.734 | -0.073 | 202.3 | 209.3 | -7.0 |
| $H_2$--ClF | 0.817 | 0.971 | -0.154 | 201.2 | 199.1 | 2.1 |
| $H_2$--ClCN | 0.143 | 0.151 | -0.008 | 205.1 | 204.2 | 0.9 |
| $H_2$--ClNC | 0.650 | 0.665 | -0.015 | 199.0 | 199.7 | -0.7 |
| $H_2$--ClCCH | 0.184 | 0.196 | -0.012 | 211.3 | 209.6 | 1.7 |
| $H_2$--ClOH | 0.702 | 0.734 | -0.032 | 209.2 | 209.3 | -0.1 |

*Mu is the dipole moment of atom X and Vol is the volume of atom X. 'diff.' is difference between complex to the monomer for the mentioned properties.*

## VI.3.5. NBO Analysis

Bond elongation and weakening of D-H bond on complexation are well known features of the hydrogen bond. This leads to the signature red-shift for a hydrogen bond, though we now know of blue-shifting hydrogen bonds as well.[16,23] Weakening and lengthening of the D-H bond is attributed to the new 'bond' formed by H with A. Just by comparing the O-H bond distance with the H•••O bond distance in O-H•••O hydrogen bonds, Pauling[7] had concluded that the O•••H hydrogen bond should have a covalency of 5-10 %. Though, this interpretation supported by the red-shift in D-H has been well documented and accepted, as mentioned in the introduction the term 'hydrogen bond' has been considered incorrect by some. Of course, chemical bonding has itself been a source of confusion for long.[64] What is surprising is that most of the discussions about the ambiguity of 'chemical bonding' completely ignore 'ionic bond'. In this work, comparing the complexes of the 'covalent' DH and DCl along with the 'ionic' DLi has given us an opportunity to look at the ionicity and covalency of not only the donor D-X bond but also the intermolecular X•••A bond. Could one expect that the covalent D-H and D-Cl will become weaker and the H•••A/Cl•••A bond will gain that much covalency? What about the ionic D-Li bond? It is only natural that the ionicity of D-Li bond is reduced and the Li•••A bond gains that much ionicity. Will it also gain covalency? The NBO analysis reveals the answers to all these questions.

Weinhold's Natural Bond Orbital[37] method allows one to calculate the covalency and ionicity of the bonds in addition to determining the commonly used second order perturbation energy due to the n-$\sigma^*$ overlap. The later is the cause for the weakening D-H bond and the associated red-shift. It is indeed this overlap that gives covalency to the H•••A bond and legitimized the 'hydrogen bond' nomenclature. In this work, we focus on calculating

covalency and ionicity of both D-X and X•••N bonds for $H_3N$•••XD (D = F/Cl/Br, X= H/Li) and $H_3N$•••ClF complexes. There were four resonance structures considered by the NBO programme for these complexes and their weights are presented in Table VI. 10 and Figure VI. 9. The total ionicity of X-D bond in complex is calculated by summing the ionicity of resonance structure 1 and 2 while total covalency is same as covalency of structure 2 since structure 1 is purely ionic. Structure 3 has the X•••N bond but no D-X bond, with the D acquiring one more lone pair. This structure is the most important in this work as this considers the X•••N bond. Structure 4 has a bond between D and N with the X acquiring the lone pair. Structure 4 contributes about 1.5-2.5 % for DH complexes but does not contribute for DLi complexes. Structure 1 does not contribute for D-H and D-Cl complexes. With these resonance structures, the ionicity and covalency of both the D-X and X•••N bonds were calculated. The results are shown in Table VI. 10.

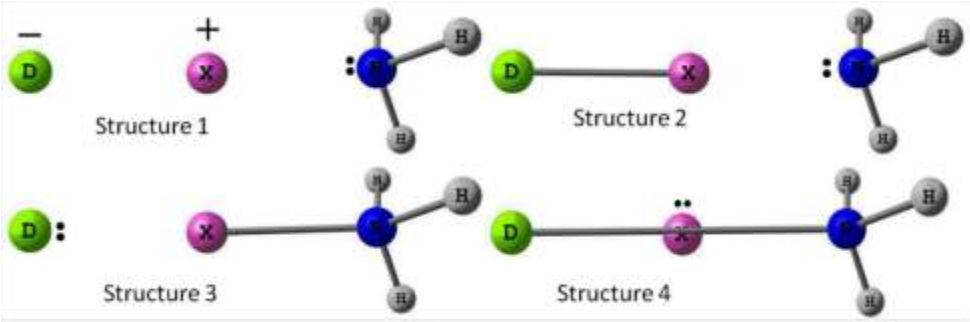


*Figure VI. 9. Various resonance structures of $H_3N$•••X-D complexes. A pair of dots represents a lone pair.*

*Table VI. 10. Percentage contributions of various resonance structures.*

| Complex | Weight (%) | | | | Complex (X•••A bond) Structure 3 | | Complex (D-X bond) Structure 1+ Structure 2 | | Monomer (D-X bond) | |
|---|---|---|---|---|---|---|---|---|---|---|
| D-X•••A | Structure 1 | Structure 2 | Structure 3 | Structure 4 | %Covalency | %Ionicity | %Covalency | %Ionicity | %Covalency | %Ionicity |
| F-H•••$NH_3$ | -- | 95.13 | 3.3 | 1.57 | 0.15 | 3.15 | 35.29 | 59.84 | 42.97 | 57.03 |
| Cl-H•••$NH_3$ | -- | 93.93 | 3.91 | 2.15 | 0.2 | 3.71 | 59.07 | 34.86 | 72.55 | 27.45 |
| Br-H•••$NH_3$ | -- | 92.53 | 4.89 | 2.57 | 0.31 | 4.59 | 62.65 | 29.89 | 79.78 | 20.22 |
| F-Li•••$NH_3$ | 96.64 | 1.44 | 1.91 | -- | 0.03 | 1.88 | 0.02 | 98.07 | 0 | 100 |
| Cl-Li•••$NH_3$ | 93.75 | 4.01 | 2.25 | -- | 0.05 | 2.19 | 0.19 | 97.56 | 0.09 | 99.91 |
| Br-Li•••$NH_3$ | 92.74 | 4.87 | 2.4 | -- | 0.06 | 4.56 | 0.3 | 97.3 | 0.16 | 99.84 |
| F-Cl•••$NH_3$ | -- | 68.92 | 29.3 | 1.78* | 6.82 | 25.4 | 36.31 | 33.25 | 62.22 | 37.78 |

*Percentage contributions of various resonance structures, (See Figure VI. 9), covalency and ionicity for A•••X bond, D-X bond in complex and D-X bond from NBO Calculations. * 1.78% is the collective weight of six resonance structures all of which involve N•••Cl bond formation at the expense of the three N-H bond in $NH_3$.*

The results given in Table VI. 10 reveal some obvious conclusions and some not so obvious. First, we mention the obvious one. The Li-D molecules are predominantly ionic, with the LiF being 100 % ionic and LiBr 99.84 % ionic. For the hydrogen halides, HF is more ionic (57.0) %) than HCl (27.5 %) and HBr (20.2 %), the rest being covalency. The ClF molecule is more covalent (62.2 %) than ionic. On complex formation, the DH molecules loose covalency. As a result, the D-H bond becomes more ionic and the H•••N bond is formed. The H•••N bond has significantly more ionic character but includes a small non-zero covalency. Interestingly, perhaps not surprisingly, the DLi molecules loose ionicity, making the D-Li bond little more covalent and also forming the Li•••N bond. The FCl•••$NH_3$ complex is different in that the Cl-F bond looses both covalency and ionicity on complex formation, resulting in a stronger Cl•••N bond. The X•••N bond in all these complexes are significantly ionic but all of them including Li•••N have a small non-zero covalency. Even with Li-F which is 100 % ionic according to this analysis, the lithium bond in FLi•••$NH_3$ has a small covalency! ! Moreover, the Li-F bond also gains marginal covalency on lithium bond formation From the data given in Table VI. 10, the hydrogen bond is about 5 % covalent, lithium bond is about 2 % covalent and the chlorine bond is about 21 % covalent. If one adds the covalency and ionicity in X•••N and D-X bonds, one can see that there is a conservation of bond order. For lithium bonds, structure 4 does not contribute and the sum of ionicity and

covalency in these two bonds add up to a 100 %. For hydrogen and chlorine bonds other resonance structures contribute about 1.5-2.5 %.

## VI.3.6. Electron Density at BCP: A Relook

Following the NBO analysis discussed above, it seemed obvious that the electron density at the BCP of D-X should decrease on complex formation and it might lead to the observed electron density at X•••A bond. It was decided to look at the correlation between the change in electron density at D-X BCP and X•••A BCP. To the best of our knowledge, and to our surprise, there appears to be no report of such an analysis. The correlation plots for hydrogen, chlorine and lithium bonds are shown in Figure VI. 10. The correlation coefficients are respectable at 0.84, 0.90 and 0.81, for H-, Cl- and Li-bonding, respectively.

The data given in Figure VI. 10 also shows that H- and Cl-bonding have some similarity and Li-bonding is different. The slopes for these correlation plots are close to one for hydrogen (0.9) and chlorine (1.1) bonding. This suggests that the weakening D-X bond is directly related to the formation of X•••A bond. The slope for Li-bonding is significantly larger at 4.7, though the electron density at Li•••A BCP as well as the difference in electron density at Li-D bond are both significantly smaller than those observed for H-/Cl-bonding cases. This in a way confirms the results from the NBO analysis, which suggests that the Li•••N bond has a small covalent character at the cost of loss of ionicity of Li-D bond. There are some H- and Cl-bonded complexes which have the electron density differences at D-X bond as negative. This implies that the electron density at the D-X BCP is actually increasing following the X•••N bond formation.

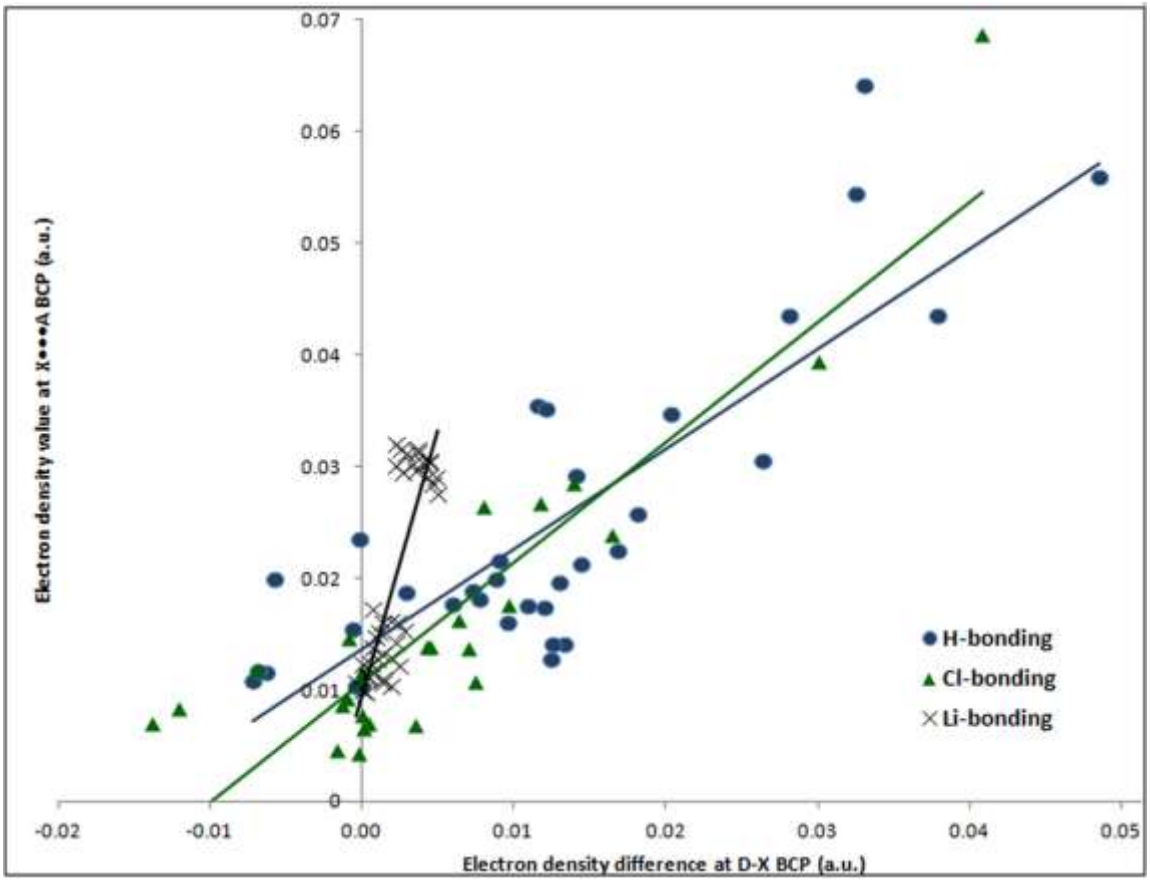


*Figure VI. 10. Correlation between difference in electron density at BCP of X-D with electron density at X•••A BCP.*

Clearly, one can expect a good correlation between the electron density difference at D-X with the binding energy and penetration and these plots are shown in Figure VI. 11. As noted earlier, for lithium bonded complexes, these plots also show a linear region for weakly bonded complexes (where $CH_3$, $C_2H_4$ and $H_2$ as acceptor) and a plateau for strongly bonded complexes ($H_2O$ and $NH_3$ as acceptor). Our analysis has focused on only the D-X and X•••A bonds and clearly both these bonds would be influenced by the other bonds in cases where both the donor and acceptor are polyatomic molecules. This is clearly shown in the case of A•••XCN (X = H/Cl) complexes, which show an increase in electron density at the X-C BCP following A•••X bond formation. A detailed analysis must include all the bonds in donors and acceptors. However, the overall correlation visible in Figure VI. 11 provides some justification for focusing on the X•••A and D-X bonds.

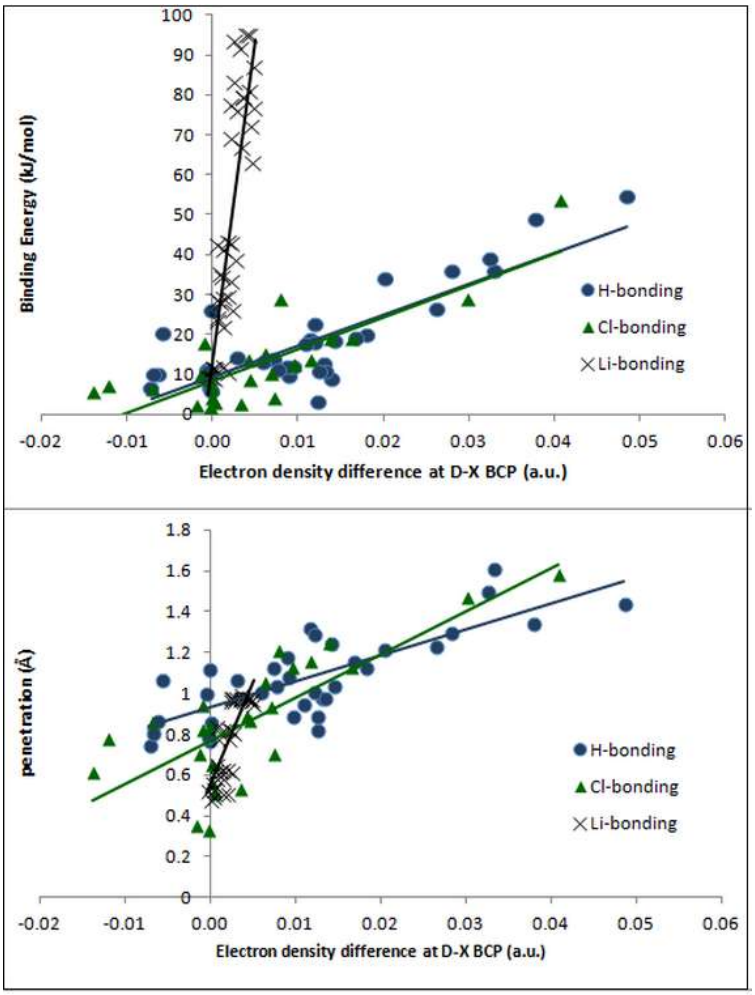


*Figure VI. 11.Correlation of differences in electron density of X-D on complex formation with binding energy (upper) and penetration (lower).*

It is worth reemphasizing that, irrespective of X from a D-X molecule involved in intermolecular bonding, the formation of X•••A bond leads to a conservation of bond order, if one takes care of both ionic and covalent character of both D-X and X•••A bonds. Clearly, the debate about whether all these intermolecular interactions should be called 'bonding' appears unnecessary. As mentioned earlier, much of the debate about the suitability of the term 'bond' ignores ionic bonding.

Before concluding, we must point out that conservation of bond order has been in the literature for long starting from the work of Pauling,[7] particularly with respect to the hydrogen bonding.[65] Coulson had used resonance structures, as in Table VI. 10, to point out the covalent contribution in hydrogen bonds.[66] Majerz and Olovsson have extended the bond order concept and have shown that the bond order for H is conserved along proton transfer

coordinate.[67] Mohri had discussed 'bond valences' in hydrogen bond with the assumption that the sum of bond valences for D-H and H•••A bonds is 1.[68] Golubev, Limbach and co-workers have used such valence bond order model to describe hydrogen bond coupling constants and chemical shifts observed in the NMR spectrum.[69] However, all these models have assumed that the D-H bond is 100 % covalent initially and on the D-H•••A bond formation, the D-H and H•••A bond orders are conserved to 1. In a way it is surprising, as rarely a chemical bond between two atoms in a molecule is 100 % covalent or 100 % ionic, as revealed by the data on monomers given in Table 3.

Pauling had estimated hydrogen bond to be about 5 % covalent just by comparing the H•••O bond length with the O-H bond length, assuming the later to be 100 % covalent, in an O-H•••O hydrogen bond.[7] However, our estimate of 5 % for covalency in hydrogen bond considers only the H•••A bond, suggesting that the rest of it is ionic. This was possible due to the extensive comparison of hydrogen and lithium bonding in this work. While the absolute estimates given for ionicity and covalency for D-X (in the monomer and complex) and X•••A bond could vary with the model and basis set, it is clear that assuming the D-X bond to be 100 % covalent is too simplistic. It is hoped that looking at the ionicity and covalency of D-X and X•••A bonds will bring chemistry back into the discussion on intermolecular interactions or should we say intermolecular bonding.

## VI.4. Conclusion

One hundred complexes formed between an acceptor A and donor DX, A•••X-D, have been theoretically investigated with X=H, Cl and Li at MP2(full)/aug-cc-pVTZ level. The unifying theme in all these one hundred complexes is that the angle D-X•••A is nearly linear for all X and A. If the X-bond acceptor has a well defined region of electron density such as one lone pair ($NH_3$), unpaired electron ($CH_3$), $\pi$ electrons ($C_2H_4$/$C_2H_2$), $\sigma$ electrons ($H_2$), the D-X approaches through this specific direction and it is enough to locate the other atoms in A. In all these specific cases, D-X approach A through the symmetry axis in A. If A has more than one region of electron density, as in $H_2O$ having two non degenerate lone pairs, the D-X•••O angle is linear, but that does not help in locating the $H_2O$ plane. For hydrogen/chlorine bonded complexes, the binding energy has a strong correlation with the charge on H/Cl in

DH/DCl, whereas for the lithium bonded complexes, there is a strong correlation with the dipole moment of DLi. In terms of the acceptors the binding energy increases as lone pairs > π-electron > unpaired electron > σ-electron. Lithium bonds are stronger than H-bond and Cl-bond.

We can summarize our results from the comprehensive AIM and NBO studies as follows.

1. There is a strong correlation between the electron density at the X•••A BCP and binding energy. The slopes of such correlation plots are similar for H-/Cl- bonding but distinctly different for Li- bonding. Extrapolation of these fitted lines leads towards ionic bond for Li-bonding and covalent bond for H-bonding and Cl-bonding. Moreover, there is a strong correlation between the electron density at X•••A BCP and mutual penetration. This could be very useful in determining the non bonded radii in crystal structures instead of using 'van der Waals' radii, which can lead to ambiguous conclusions.

2. Comparing the values of $\nabla^2\rho$, H, $|V|/G$ and $|\lambda_1|/\lambda_3$ ratio to differentiate closed-shell and shared-shell interactions leads us to suggest that $|\lambda_1|/\lambda_3 < 0.25$ be used as a limit for closed-shell interaction. For shared-shell interaction (i.e. a covalent bond), this ratio is 1.00 or more and the values between 0.25 – 1 could be considered as intermediate region.

3. Considering the ionicity and covalency of the D-X and X•••A bonds, it is clear that there is a conservation of bond order. When the ionicity and covalency are considered, it is also clear that the debate about whether 'hydrogen bond' is a misnomer is the result of a rather limited view of the term 'bond'.

4. Comparing the H-bond, with Li- and Cl-bonds have clearly shown that the difference in the nature of X•••A bonds for these three cases are significantly influenced by the nature of D-X bond. In any case, the X•••A bond has ionic (electrostatic) and covalent contributions for all X.

5. The conclusions reached here should be applicable for every atom in the periodic table, when it is involved in intermolecular bonding with another atom/bond centre.

## VI.5. Supporting Information

In this section, coordinates and normal mode vibrational frequencies with their intensity are presented for all one hundered complexes under investigation for hydrogen bonding, chlorine bonding and lithium bonding. The MP2(full)/aug-cc-PVTZ level of theory is used for the calculations.

## VI.6. References


1. G. Gilli and P. Gilli, *The Nature of the Hydrogen Bond: Outline of a Comprehensive Hydrogen Bond Theory*, Oxford University Press, Oxford, 2009.

2. S. J. Grabowski, *Hydrogen Bonding: New Insights (ed.)*, Dordrecht, The Neitherlands : Springer, 2006.

3. S. Scheiner, *Hydrogen Bonding: A theoretical perspective*, Oxford University Press, Oxford, 1997.

4. G. R. Desiraju and T. Steiner, *The weak hydrogen bond: In structural chemistry in biology.*, Oxford University Press, Oxford, 1999.

5. G. A. Jeffery and W. Saenger, *Hydrogen bonding in biological structure*, Springer Verlag, Berlin, 1991.

6. G. C. Pimentel and A. L. McClellan, *The Hydrogen Bond*, W. H. Freeman and Co., San Fransisco, 1960.

7. L. Pauling, *The Nature of the Chemical Bond and the Structure of Molecules and Crystals; An Introduction to Modern Structural Chemistry*, Cornell University Press, Ithaca, New York, 1960.

8. P. Hobza and K. Müller-Dethlefs, *Non-Covalent Interactions Theory and Experiment*, The Royal Society of Chemistry, Cambrdge, 2010.

9. Stone J. Anthony, *The Theory of Intermolecular Forces*, Clarendon Press, Oxford, 1996.

10. H. A. Benesi and J. H. Hildebrand, *J. Am. Chem. Soc.*, 1949, **71**, 2703.

11. R. S. Mulliken and W. B. Person, *Molecular complexes: A lecture and reprint volume*, Wiley Interscience, New York, 1969.

12. P. A. Kollman, J. F. Liebman, and L. C. Allen, *J. Am. Chem. Soc.*, 1970, **92**, 1142–1150.

13. A. Legon, *Angew. Chem. Int. Ed. Engl.*, 1999, **38**, 2686–2714.

14. “Odd Hassel - Facts”. Nobelprize.org. Nobel Media AB 2013. Web. 18 Jan 2014. <http://www.nobelprize.org/nobel_prizes/chemistry/laureates/1969/hassel-facts.html>, .

15. A. R. Voth, P. Khuu, K. Oishi, and P. S. Ho, *Nat. Chem.*, 2009, **1**, 74–9.

16. B. Raghavendra and E. Arunan, *J. Phys. Chem. A*, 2007, **111**, 9699–706.

17. R. F. W. Bader, *Atoms in Molecules: A Quantum Theory*, Oxford University Press, Oxford, 1990.

18. U. Koch and P. L. A. Popelier, *J. Phys. Chem.*, 1995, **99**, 9747–9754.

19. N. J. M. Amezaga, S. C. Pamies, M. Peruchena, N. M. Peruchena, and G. L. Sosa, *J. Phys. Chem. A*, 2010, **114**, 552–62.

20. X. Li, Y. Zeng, X. Zhang, S. Zheng, and L. Meng, *J. Mol. Model.*, 2011, **17**, 757–67.

21. A. J. Dingley and S. Grzesiek, *J. Am. Chem. Soc.*, 1998, **120**, 8293–8297.

22. E. D. Isaacs, A. Shukla, P. M. Platzman, D. R. Hamann, B. Barbiellini, and C. A. Tulk, *Phys. Rev. Lett.*, 1999, **82**, 600–603.

23. E. Arunan, G. R. Desiraju, R. a. Klein, J. Sadlej, S. Scheiner, I. Alkorta, D. C. Clary, R. H. Crabtree, J. J. Dannenberg, P. Hobza, H. G. Kjaergaard, A. C. Legon, B. Mennucci, and D. J. Nesbitt, *Pure Appl. Chem.*, 2011, **83**, 1619–1636.

24. S. J. Grabowski, *Chem. Rev.*, 2011, **111**, 2597–625.

25. L. Gross, F. Mohn, N. Moll, P. Liljeroth, and G. Meyer, *Science*, 2009, **325**, 1110–4.

26. M. L. Huggins, *J. Phys. Chem.*, 1936, **40**, 723–731.

27. J. N. Israelachvili, *Intermolecular and Surface Forces*, Academic Press, Third Edit., 2011.

28. P. L. A. Popelier, *Atoms in Molecules. An Introduction*, Pearson Education Ltd. Essex, England, 2000.

29. A. E. Reed, L. A. Curtiss, and F. Weinhold, *Chem. Rev.*, 1988, **88**, 899–926.

30. C. Møller and M. S. Plesset, *Phys. Rev.*, 1934, **46**, 618–622.

31. T. H. Dunning, *J. Chem. Phys.*, 1989, **90**, 1007–1023.

32. Frisch, M. J.; Trucks, G. W.; Schlegel, H. B.; Scuseria, G. E.; Robb, M. A.; Cheeseman, J. R.; Scalmani, G.; Barone, V.; Mennucci, B.; Petersson, G. A.; Nakatsuji, H.; Caricato, M.; Li, X.; Hratchian, H. P.; Izmaylov, A. F.; Bloino, J.; Zheng, G.; Sonnenberg, J. L.; Hada, M.; Ehara, M.; Toyota, K.; Fukuda, R.; Hasegawa, J.; Ishida, M.; Nakajima, T.; Honda, Y.; Kitao, O.; Nakai, H.; Vreven, T.; Montgomery Jr., J. A.; Peralta, J. E.; Ogliaro, F.; Bearpark, M.; Heyd, J. J.; Brothers, E.; Kudin, K. N.; Staroverov, V. N.; Kobayashi, R.; Normand, J.; Raghavachari, K.;

Rendell, A.; Burant, J. C.; Iyengar, S. S.; Tomasi, J.; Cossi, M.; Rega, N.; Millam, J. M.; Klene, M.; Knox, J. E.; Cross, J. B.; Bakken, V.; Adamo, C.; Jaramillo, J.; Gomperts, R.; Stratmann, R. E.; Yazyev, O.; Austin, A. J.; Cammi, R.; Pomelli, C.; Ochterski, J. W.; Martin, R. L.; Morokuma, K.; Zakrzewski, V. G.; Voth, G. A.; Salvador, P.; Dannenberg, J. J.; Dapprich, S.; Daniels, A. D.; Farkas, O.; Foresman, J. B.; Ortiz, J. V; Cioslowski, J.; Fox, D. J. Gaussian 09 Revision C.01..

33. S. F. Boys and F. Bernardi, *Mol. Phys.*, 1970, **19**, 553–566.

34. *AIMAll (Version 13.11.04), Todd A. Keith, TK Gristmill Software, Overl. Park KS, USA, 2013*.

35. B.-K. F and S. J, *AIM 2000 Version 2.0 Biegler-Konig, F.; Schonbohm J.; Univ. Appl. Sci. Bielefeld, Ger. 2002.*

36. E. D. Glendening and F. Weinhold, *J. Comput. Chem.*, 1998, **19**, 593–609.

37. E. D. Glendening, J. K. Badenhoop, A. E. Reed, J. E. Carpenter, J. A. Bohmann, C. M. Morales, C. R. Landis, and F. Weinhold, *NBO6.0*, 2006.

38. B. Raghavendra and E. Arunan, *Chem. Phys. Lett.*, 2008, **467**, 37–40.

39. S. R. Gadre and P. K. Bhadane, *J. Chem. Phys.*, 1997, **107**, 5625–26.

40. P. K. Mandal and E. Arunan, *J. Chem. Phys.*, 2001, **114**, 3880.

41. B. Lakshmi, A. G. Samuelson, K. V. J. Jose, S. R. Gadre, and E. Arunan, *New J. Chem.*, 2005, **29**, 371–377.

42. B. Raghavendra, P. K. Mandal, and E. Arunan, *Phys. Chem. Chem. Phys.*, 2006, **8**, 5276.

43. N. K. Karan and E. Arunan, *J. Mol. Struct.*, 2004, **688**, 203–205.

44. Y. Li, D. Wu, Z. Li, W. Chen, and C. Sun, *J. Chem. Phys.*, 2006, **125**, 084317–084324.

45. Z. Latajka and S. Scheiner, *J. Chem. Phys.*, 1984, **81**, 4014–4017.

46. G. V. Kulkarni and C. N. R. Rao, *J. Mol. Struct.*, 1983, **100**, 531–537.

47. M. M. Szczęśniak, H. Ratajczak, U. P. Agarwal, and C. N. R. Rao, *Chem. Phys. Lett.*, 1976, **44**, 465–467.

48. Q. Li, T. Hu, X. An, W. Li, J. Cheng, B. Gong, and J. Sun, *Chemphyschem*, 2009, **10**, 3310–5.

49. S. Salai Cheettu Ammal and P. Venuvanalingam, *J. Phys. Chem. A*, 2000, **104**, 10859–10867.

50. *CRC Handbook of chemistry and physics*, CRC press, Boca Raton London, 80th ed.

51. R. Parajuli and E. Arunan, *Chem. Phys. Lett.*, 2013, **568-569**, 63–69.

52. R.-Y. Li, Z.-R. Li, D. Wu, Y. Li, W. Chen, and C.-C. Sun, *J. Phys. Chem. A*, 2005, **109**, 2608–13.

53. P. Politzer, P. Lane, M. C. Concha, Y. Ma, and J. S. Murray, *J. Mol. Model.*, 2007, **13**, 305–11.

54. W. Wang, N. Wong, W. Zheng, and A. Tian, *J. Phys. Chem. A*, 2004, **108**, 1799–1805.

55. M. T. Carroll and R. F. W. Bader, *Mol. Phys.*, 1988, **65**, 695–722.

56. M. T. Carroll, C. Chang, and R. F. W. Bader, *Mol. Phys.*, 1988, **63**, 387–405.

57. D. Cremer and E. Kraka, *Angew. Chemie Int. Ed. English*, 1984, **23**, 627–628.

58. E. Espinosa, I. Alkorta, J. Elguero, and E. Molins, *J. Chem. Phys.*, 2002, **117**, 5529.

59. M. Jabłoński and M. Palusiak, *J. Phys. Chem. A*, 2010, **114**, 2240–4.

60. L. Bian, *J. Phys. Chem. A*, 2003, **107**, 11517–11524.

61. R. Parthasarathi, V. Subramanian, and N. Sathyamurthy, *J. Phys. Chem. A*, 2006, **110**, 3349–51.

62. R. F. W. Bader and H. Essen, *J. Chem. Phys.*, 1984, **80**, 1943–1960.

63. P. Munshi and T. N. Guru Row, *J. Phys. Chem. A*, 2005, **109**, 659–72.

64. E. Arunan, *Curr. Sci.*, 2011, **100**, 284–285.

65. L. Pauling, *J. Am. Chem. Soc.*, 1947, **69**, 542.

66. C. A. Coulson, *Res.*, 10AD, **1957**, 149–159.

67. I. Majerz and I. Olovsson, *Phys. Chem. Chem. Phys.*, 2010, **12**, 5462–5467.

68. F. Mohri, *J. mol. Struct.*, 2005, **756**, 25–33.

69. I. G. Shenderovich, P. M. Tolstoy, N. S. Golubev, S. N. Smirnov, G. S. Denisov, and H.-H. Limbach, *J. Am. Chem. Soc.*, 2003, **125**, 11710–20.

# *Supporting Information*

*Table VI. S. 1.Coordinates of the optimized geometry for all H-bonded complexes (35) under investigation at MP2(full)/aug-cc-PVTZ level of theory.*

| Atoms | X (Å) | Y (Å) | Z (Å) |
|---|---|---|---|
| $CH_3$•••HBr | | | |
| C | -1.9860 | 0.5816 | -2.5943 |
| H | -3.0377 | 0.5657 | -2.3783 |
| H | -1.4389 | -0.3418 | -2.6259 |
| H | -1.4506 | 1.5111 | -2.5447 |
| H | -2.2440 | 0.6682 | -4.5754 |
| Br | -2.4274 | 0.7297 | -5.9833 |
| $CH_3$•••HCl | | | |
| C | -1.9779 | 0.5783 | -2.5390 |
| H | -3.0321 | 0.5634 | -2.3367 |
| H | -1.4323 | -0.3451 | -2.5834 |
| H | -1.4447 | 1.5096 | -2.5099 |
| H | -2.2520 | 0.6707 | -4.6416 |
| Cl | -2.4172 | 0.7277 | -5.9137 |
| $CH_3$•••HF | | | |
| C | -1.9795 | 0.5790 | -2.5426 |
| H | -3.0344 | 0.5644 | -2.3432 |
| H | -1.4330 | -0.3447 | -2.5748 |
| H | -1.4459 | 1.5100 | -2.5071 |
| H | -2.2381 | 0.6614 | -4.6425 |
| F | -2.3507 | 0.6986 | -5.5629 |
| $CH_3$•••HNC | | | |
| C | -1.9575 | 0.5721 | -2.4347 |
| H | -3.0089 | 0.5558 | -2.2173 |
| H | -1.4124 | -0.3514 | -2.4899 |
| H | -1.4230 | 1.5028 | -2.4019 |
| H | -2.2737 | 0.6777 | -4.6400 |
| N | -2.4157 | 0.7254 | -5.6311 |
| C | -2.5820 | 0.7812 | -6.7907 |
| $NH_3$•••HOH | | | |
| N | -2.0934 | 0.6058 | -3.0416 |
| H | -2.9439 | 0.7627 | -2.5202 |
| H | -1.7233 | -0.2866 | -2.7467 |
| H | -1.4322 | 1.3116 | -2.7495 |
| H | -2.1403 | 0.7046 | -4.9864 |
| O | -2.0150 | 0.7766 | -5.9474 |
| H | -2.8895 | 0.6570 | -6.3196 |
| $NH_3$•••HCCH | | | |
| N | -1.9775 | 0.5799 | -2.7800 |
| H | -2.8410 | 0.5169 | -2.2596 |
| H | -1.4221 | -0.2252 | -2.5280 |
| H | -1.4871 | 1.3949 | -2.4399 |
| H | -2.3274 | 0.6959 | -4.9371 |
| C | -2.4972 | 0.7529 | -5.9850 |
| C | -2.6906 | 0.8177 | -7.1778 |
| H | -2.8600 | 0.8743 | -8.2222 |
| $C_2H_4$•••HBr | | | |
| H | -0.0026 | 0.0073 | 0.7165 |
| Br | -0.0155 | 0.0112 | -0.6951 |
| C | 0.6659 | -0.0002 | 2.9307 |
| C | -0.6657 | -0.0002 | 2.9314 |
| H | 1.2238 | 0.9225 | 2.9331 |
| H | 1.2239 | -0.9228 | 2.9284 |
| H | -1.2236 | 0.9225 | 2.9342 |
| H | -1.2236 | -0.9228 | 2.9295 |
| $C_2H_4$•••HCl | | | |
| C | 1.8203 | 0.6658 | 0.0000 |
| C | 1.8207 | -0.6657 | 0.0000 |

$CH_3$•••HCN

| | | | |
|---|---|---|---|
| C | -1.9402 | 0.5656 | -2.3296 |
| H | -2.9929 | 0.5454 | -2.1224 |
| H | -1.3914 | -0.3545 | -2.3908 |
| H | -1.4131 | 1.5005 | -2.3200 |
| H | -2.2908 | 0.6827 | -4.7461 |
| C | -2.4427 | 0.7347 | -5.7940 |
| N | -2.6090 | 0.7915 | -6.9420 |

$CH_3$•••HOH

| | | | |
|---|---|---|---|
| C | -1.9802 | 0.5972 | -2.5000 |
| H | -3.0457 | 0.6239 | -2.6251 |
| H | -1.4791 | -0.3461 | -2.3990 |
| H | -1.4387 | 1.5104 | -2.3452 |
| H | -1.9756 | 0.5963 | -4.8402 |
| O | -2.0672 | 0.5777 | -5.7971 |
| H | -1.1726 | 0.6916 | -6.1229 |

$CH_3$•••HCCH

| | | | |
|---|---|---|---|
| C | -1.9004 | 0.5521 | -2.1042 |
| H | -2.9550 | 0.5547 | -1.9082 |
| H | -1.3752 | -0.3788 | -2.1945 |
| H | -1.3570 | 1.4769 | -2.1205 |
| H | -2.2753 | 0.6776 | -4.5376 |
| C | -2.4357 | 0.7321 | -5.5806 |
| C | -2.6192 | 0.7943 | -6.7732 |
| H | -2.7800 | 0.8489 | -7.8187 |

$H_2O$•••HBr

| | | | |
|---|---|---|---|
| O | -1.2341 | 0.4427 | -3.7838 |
| H | -1.4146 | 1.2262 | -3.2585 |
| H | -1.5771 | -0.2887 | -3.2644 |
| H | -1.8553 | 0.5161 | -5.4969 |
| Br | -2.3438 | 0.5736 | -6.8288 |

$H_2O$•••HCl

| | | | |
|---|---|---|---|
| O | -1.3167 | 0.4964 | -3.9258 |
| H | -1.5821 | 1.2462 | -3.3878 |
| H | -1.6015 | -0.2766 | -3.4322 |
| H | -1.9016 | 0.5485 | -5.6432 |
| Cl | -2.3450 | 0.5853 | -6.8544 |
| H | 1.8210 | 1.2247 | 0.9222 |
| H | 1.8215 | 1.2248 | -0.9221 |
| H | 1.8218 | -1.2245 | 0.9222 |
| H | 1.8220 | -1.2246 | -0.9221 |
| Cl | -1.6897 | -0.0001 | 0.0000 |
| H | -0.4076 | 0.0002 | 0.0005 |

$C_2H_4$•••HF

| | | | |
|---|---|---|---|
| H | -0.0031 | 0.0064 | 0.7455 |
| F | -0.0127 | 0.0100 | -0.1850 |
| C | 0.6660 | 0.0002 | 2.8392 |
| C | -0.6665 | 0.0002 | 2.8398 |
| H | 1.2247 | 0.9223 | 2.8429 |
| H | 1.2247 | -0.9220 | 2.8409 |
| H | -1.2252 | 0.9223 | 2.8437 |
| H | -1.2252 | -0.9219 | 2.8417 |

$C_2H_4$•••HNC

| | | | |
|---|---|---|---|
| H | -0.0013 | 0.0063 | 0.6325 |
| N | -0.0126 | 0.0154 | -0.3720 |
| C | 0.6655 | 0.0000 | 2.8700 |
| C | -0.6660 | 0.0000 | 2.8701 |
| H | 1.2250 | 0.9221 | 2.8764 |
| H | 1.2245 | -0.9223 | 2.8736 |
| H | -1.2256 | 0.9221 | 2.8762 |
| H | -1.2251 | -0.9223 | 2.8734 |
| C | -0.0261 | 0.0163 | -1.5451 |

$C_2H_4$•••HCN

| | | | |
|---|---|---|---|
| H | -0.0019 | 0.0084 | 0.4953 |
| C | -0.0130 | 0.0150 | -0.5662 |
| C | 0.6648 | -0.0004 | 2.9556 |
| C | -0.6652 | -0.0004 | 2.9572 |
| H | 1.2245 | 0.9215 | 2.9613 |
| H | 1.2245 | -0.9223 | 2.9571 |
| H | -1.2249 | 0.9215 | 2.9639 |
| H | -1.2249 | -0.9222 | 2.9597 |
| N | -0.0255 | 0.0166 | -1.7289 |

$C_2H_4$•••HOH

| | | | |
|---|---|---|---|
| H | -0.0383 | -0.1578 | 0.4804 |
| O | -0.0708 | -0.4024 | -0.4495 |
| C | 0.6795 | -0.0138 | 2.7944 |

$H_2O$•••HF

| | | | |
|---|---|---|---|
| O | -1.3647 | 0.5055 | -4.1469 |
| H | -1.6344 | 1.2589 | -3.6163 |
| H | -1.6525 | -0.2661 | -3.6532 |
| H | -1.9385 | 0.5514 | -5.7400 |
| F | -2.2871 | 0.5768 | -6.6104 |

$H_2O$•••HNC

| | | | |
|---|---|---|---|
| O | -1.6928 | 0.5178 | -3.8793 |
| H | -1.2285 | 1.2407 | -3.4511 |
| H | -1.3509 | -0.2800 | -3.4693 |
| H | -2.0227 | 0.5626 | -5.6380 |
| N | -2.2206 | 0.5881 | -6.6300 |
| C | -2.4443 | 0.6172 | -7.7804 |

$H_2O$•••HCN

| | | | |
|---|---|---|---|
| O | -1.4829 | 0.4657 | -3.8215 |
| H | -1.3183 | 1.2105 | -3.2398 |
| H | -1.3640 | -0.3091 | -3.2685 |
| H | -1.9903 | 0.5448 | -5.7792 |
| C | -2.2565 | 0.5917 | -6.8074 |
| N | -2.5477 | 0.6429 | -7.9317 |

$H_2O$•••HOH

| | | | |
|---|---|---|---|
| O | -1.8802 | 0.5949 | -3.9118 |
| H | -1.2757 | 1.2692 | -3.5937 |
| H | -1.5371 | -0.2273 | -3.5545 |
| H | -1.9053 | 0.5510 | -5.8393 |
| O | -1.7915 | 0.5086 | -6.7969 |
| H | -2.6700 | 0.6501 | -7.1518 |

$H_2O$•••HCCH

| | | | |
|---|---|---|---|
| O | -1.5246 | 0.4678 | -3.9115 |
| H | -1.2665 | 1.1909 | -3.3370 |
| H | -1.4947 | -0.3100 | -3.3514 |
| H | -2.0460 | 0.5669 | -5.9792 |
| C | -2.3046 | 0.6161 | -7.0035 |
| C | -2.6002 | 0.6723 | -8.1747 |
| H | -2.8592 | 0.7215 | -9.2006 |

$NH_3$•••HBr

| | | | |
|---|---|---|---|
| N | -2.0155 | 0.5947 | -2.9961 |
| H | -2.8967 | 0.5661 | -2.5021 |
| C | -0.6483 | 0.0691 | 2.8184 |
| H | 1.2964 | 0.8688 | 2.8504 |
| H | 1.1792 | -0.9663 | 2.7206 |
| H | -1.1482 | 1.0214 | 2.8946 |
| H | -1.2649 | -0.8137 | 2.7649 |
| H | -0.0262 | 0.4322 | -0.9191 |

$C_2H_4$•••HCCH

| | | | |
|---|---|---|---|
| C | 2.0829 | -0.6025 | 0.0001 |
| C | 2.0756 | 0.6060 | 0.0001 |
| H | 2.0724 | 1.6638 | 0.0001 |
| H | 2.0931 | -1.6602 | 0.0001 |
| H | -0.4181 | -0.0087 | -0.0014 |
| C | -1.4751 | -0.0043 | -0.0006 |
| C | -2.6842 | 0.0008 | 0.0003 |
| H | -3.7430 | 0.0052 | 0.0011 |

$C_2H_2$•••HBr

| | | | |
|---|---|---|---|
| C | 2.6075 | -0.6031 | 0.0000 |
| C | 2.5991 | 0.6062 | 0.0000 |
| H | 2.5952 | 1.6641 | 0.0000 |
| H | 2.6187 | -1.6609 | 0.0000 |
| H | 0.3572 | -0.0070 | 0.0014 |
| Br | -1.0517 | -0.0004 | 0.0000 |

$C_2H_2$•••HCl

| | | | |
|---|---|---|---|
| C | 1.9440 | -0.6034 | 0.0000 |
| C | 1.9374 | 0.6060 | 0.0000 |
| H | 1.9351 | 1.6638 | 0.0000 |
| H | 1.9540 | -1.6613 | 0.0000 |
| H | -0.3010 | -0.0056 | 0.0012 |
| Cl | -1.5810 | -0.0007 | 0.0000 |

$C_2H_2$•••HF

| | | | |
|---|---|---|---|
| C | 1.2302 | -0.6028 | 0.0000 |
| C | 1.2211 | 0.6067 | 0.0000 |
| H | 1.2181 | 1.6649 | 0.0000 |
| H | 1.2446 | -1.6608 | 0.0000 |
| H | -0.8813 | -0.0080 | 0.0003 |
| F | -1.8099 | -0.0022 | 0.0000 |

$C_2H_2$•••HNC

| | | | |
|---|---|---|---|
| C | 1.8299 | -0.6020 | 0.0000 |

| | | | |
|---|---|---|---|
| H | -1.4926 | -0.2311 | -2.7393 |
| H | -1.5025 | 1.3991 | -2.6626 |
| H | -2.2498 | 0.6705 | -4.6379 |
| Br | -2.4572 | 0.7376 | -6.0909 |
| $NH_3$•••HCl | | | |
| N | -2.0097 | 0.5925 | -2.9558 |
| H | -2.8903 | 0.5641 | -2.4609 |
| H | -1.4874 | -0.2318 | -2.6931 |
| H | -1.4980 | 1.3961 | -2.6188 |
| H | -2.2487 | 0.6701 | -4.6578 |
| Cl | -2.4326 | 0.7302 | -5.9669 |
| $NH_3$•••HF | | | |
| N | -2.0228 | 0.5960 | -3.0316 |
| H | -2.9035 | 0.5689 | -2.5377 |
| H | -1.5016 | -0.2268 | -2.7638 |
| H | -1.5122 | 1.3994 | -2.6937 |
| H | -2.2491 | 0.6699 | -4.6907 |
| F | -2.3775 | 0.7138 | -5.6359 |
| $NH_3$•••HNC | | | |
| N | -2.0145 | 0.5943 | -2.9881 |
| H | -2.8842 | 0.5648 | -2.4737 |
| H | -1.4903 | -0.2298 | -2.7276 |
| H | -1.4972 | 1.3926 | -2.6463 |
| H | -2.2870 | 0.6831 | -4.7618 |
| N | -2.4432 | 0.7342 | -5.7780 |
| C | -2.6211 | 0.7925 | -6.9359 |
| $NH_3$•••HCN | | | |
| N | -1.9940 | 0.5870 | -2.8562 |
| H | -2.8617 | 0.5563 | -2.3390 |
| H | -1.4690 | -0.2354 | -2.5928 |
| H | -1.4779 | 1.3846 | -2.5116 |
| H | -2.3109 | 0.6913 | -4.9165 |
| C | -2.4737 | 0.7449 | -5.9736 |
| N | -2.6504 | 0.8031 | -7.1218 |
| C | 1.8187 | 0.6075 | 0.0000 |
| H | 1.8200 | 1.6659 | 0.0000 |
| H | 1.8518 | -1.6602 | 0.0000 |
| H | -0.3915 | -0.0128 | 0.0005 |
| N | -1.3950 | -0.0059 | 0.0002 |
| C | -2.5678 | 0.0026 | -0.0002 |
| $C_2H_2$•••HCN | | | |
| C | -2.0047 | -0.6021 | 0.0000 |
| C | -1.9954 | 0.6067 | 0.0000 |
| H | -1.9980 | 1.6648 | 0.0000 |
| H | -2.0246 | -1.6600 | 0.0000 |
| H | 0.4352 | -0.0136 | 0.0001 |
| C | 1.4961 | -0.0062 | 0.0000 |
| N | 2.6587 | 0.0026 | 0.0000 |
| $C_2H_2$•••HOH | | | |
| C | 1.3387 | 0.6046 | 0.0069 |
| C | 1.3391 | -0.6045 | 0.0068 |
| H | 1.3423 | -1.6621 | 0.0018 |
| H | 1.3412 | 1.6622 | 0.0027 |
| H | -0.9827 | -0.0003 | -0.0597 |
| O | -1.9431 | 0.0002 | -0.1049 |
| H | -2.2228 | -0.0020 | 0.8122 |
| $C_2H_2$•••HCCH | | | |
| C | 2.0829 | -0.6025 | 0.0001 |
| C | 2.0756 | 0.6060 | 0.0001 |
| H | 2.0724 | 1.6638 | 0.0001 |
| H | 2.0931 | -1.6602 | 0.0001 |
| H | -0.4181 | -0.0087 | -0.0014 |
| C | -1.4751 | -0.0043 | -0.0006 |
| C | -2.6842 | 0.0008 | 0.0003 |
| H | -3.7430 | 0.0052 | 0.0011 |

*Table VI. S. 2. Coordinates of the optimized geometry for all Cl-bonded complexes (25) under investigation at MP2(full)/aug-cc-PVTZ level of theory.*

| Atoms | X (Å) | Y (Å) | Z (Å) | Atoms | X (Å) | Y (Å) | Z (Å) |
|---|---|---|---|---|---|---|---|

$CH_3$•••ClF

| | | | |
|---|---|---|---|
| C | 2.3593 | 0.0002 | 0.0002 |
| H | 2.4418 | -0.7109 | -0.7997 |
| H | 2.4408 | 1.0486 | -0.2156 |
| H | 2.4408 | -0.3370 | 1.0161 |
| Cl | -0.2569 | -0.0003 | -0.0003 |
| F | -1.9014 | 0.0003 | 0.0003 |

$CH_3$•••ClCN

| | | | |
|---|---|---|---|
| C | -0.0521 | -0.0054 | 3.0848 |
| H | 0.4839 | 0.9227 | 3.1249 |
| H | -1.1245 | -0.0050 | 3.1023 |
| H | 0.4831 | -0.9342 | 3.1191 |
| Cl | -0.0129 | 0.0036 | -0.1534 |
| C | 0.0048 | 0.0078 | -1.7797 |
| N | 0.0176 | 0.0106 | -2.9495 |

$CH_3$•••ClNC

| | | | |
|---|---|---|---|
| C | 0.1501 | 0.2646 | 0.1056 |
| H | 0.0016 | 0.0025 | 1.1354 |
| H | 1.0684 | 0.0026 | -0.3836 |
| H | -0.5463 | 0.9182 | -0.3833 |
| Cl | -1.2177 | -2.1467 | -0.8557 |
| N | -1.9760 | -3.4841 | -1.3892 |
| C | -2.5259 | -4.4549 | -1.7773 |

$CH_3$•••ClCCH

| | | | |
|---|---|---|---|
| Cl | 0.2553 | -0.1792 | 0.1016 |
| C | -3.0339 | 0.0985 | 0.0655 |
| H | -2.9525 | 1.0152 | -0.4848 |
| H | -3.1352 | -0.8327 | -0.4563 |
| H | -3.0445 | 0.1162 | 1.1376 |
| C | 1.8832 | -0.3187 | 0.1215 |
| C | 3.0882 | -0.4219 | 0.1361 |
| H | 4.1383 | -0.5119 | 0.1489 |

$CH_3$•••ClOH

| | | | |
|---|---|---|---|
| C | 2.7026 | 0.3931 | -0.5854 |
| H | 3.5918 | 0.2861 | -1.1754 |
| H | 2.2577 | 1.3606 | -0.4586 |
| H | 2.3115 | -0.4497 | -0.0499 |
| Cl | 0.8228 | -0.1945 | -2.8118 |
| O | -0.3222 | -0.5335 | -4.0164 |

$C_2H_2$•••ClCCH

| | | | |
|---|---|---|---|
| C | -2.9532 | -0.5907 | -0.0022 |
| C | -2.8940 | 0.6167 | -0.0022 |
| H | -2.8449 | 1.6725 | -0.0018 |
| H | -3.0069 | -1.6462 | -0.0026 |
| C | 1.9732 | -0.0019 | -0.0006 |
| Cl | 0.3389 | -0.0125 | 0.0038 |
| C | 3.1829 | 0.0049 | -0.0039 |
| H | 4.2370 | 0.0117 | -0.0070 |

$C_2H_2$•••ClOH

| | | | |
|---|---|---|---|
| C | -2.3126 | -0.6047 | 0.0101 |
| C | -2.3123 | 0.6050 | 0.0101 |
| H | -2.3163 | 1.6621 | 0.0079 |
| H | -2.3171 | -1.6618 | 0.0081 |
| O | 2.3465 | 0.0003 | -0.0909 |
| Cl | 0.6477 | -0.0003 | -0.0147 |
| H | 2.5994 | 0.0006 | 0.8408 |

$C_2H_4$•••ClF

| | | | |
|---|---|---|---|
| C | -1.8815 | 0.6706 | 0.0001 |
| C | -1.8809 | -0.6705 | 0.0001 |
| H | -1.8942 | 1.2275 | 0.9224 |
| H | -1.8947 | 1.2274 | -0.9224 |
| H | -1.8934 | -1.2273 | 0.9224 |
| H | -1.8940 | -1.2272 | -0.9224 |
| Cl | 0.5749 | -0.0003 | -0.0001 |
| F | 2.2641 | 0.0005 | 0.0001 |

$C_2H_4$•••ClCN

| | | | |
|---|---|---|---|
| C | -2.7219 | 0.6654 | 0.0006 |
| C | -2.7203 | -0.6647 | 0.0006 |
| H | -2.7232 | 1.2247 | 0.9222 |
| H | -2.7290 | 1.2247 | -0.9209 |
| H | -2.7203 | -1.2241 | 0.9222 |
| H | -2.7261 | -1.2241 | -0.9209 |
| Cl | 0.4733 | -0.0010 | -0.0010 |
| C | 2.1010 | 0.0003 | 0.0001 |
| N | 3.2714 | 0.0013 | 0.0009 |

$C_2H_4$•••ClNC

| | | | |
|---|---|---|---|
| C | -2.5075 | -0.6657 | 0.0002 |
| C | -2.5063 | 0.6664 | 0.0002 |

| | | | |
|---|---|---|---|
| H | 0.2105 | -0.5382 | -4.8215 |

$NH_3$•••ClF

| | | | |
|---|---|---|---|
| N | 0.0000 | 0.0001 | -2.1208 |
| H | 0.4744 | 0.8218 | -2.4663 |
| H | -0.9489 | 0.0000 | -2.4663 |
| H | 0.4745 | -0.8218 | -2.4661 |
| Cl | 0.0000 | -0.0001 | 0.0865 |
| F | 0.0000 | 0.0000 | 1.7996 |

$NH_3$•••ClCN

| | | | |
|---|---|---|---|
| N | -0.0005 | 0.0002 | 2.7440 |
| H | 0.4680 | -0.8103 | 3.1241 |
| H | -0.9363 | 0.0003 | 3.1250 |
| H | 0.4678 | 0.8112 | 3.1233 |
| Cl | -0.0003 | -0.0002 | -0.1865 |
| C | 0.0005 | -0.0005 | -1.8157 |
| N | 0.0008 | -0.0008 | -2.9862 |

$NH_3$•••ClNC

| | | | |
|---|---|---|---|
| N | 0.0034 | 0.0000 | -2.4050 |
| H | 0.4733 | -0.8126 | -2.7788 |
| H | 0.4733 | 0.8126 | -2.7788 |
| H | -0.9342 | 0.0000 | -2.7814 |
| Cl | -0.0015 | 0.0000 | 0.2037 |
| N | -0.0057 | 0.0000 | 1.8461 |
| C | -0.0085 | 0.0000 | 3.0266 |

$NH_3$•••ClCCH

| | | | |
|---|---|---|---|
| N | -0.0005 | 0.0017 | -2.8316 |
| H | 0.9357 | 0.0079 | -3.2106 |
| H | -0.4756 | 0.8086 | -3.2101 |
| H | -0.4634 | -0.8139 | -3.2067 |
| Cl | 0.0008 | 0.0010 | 0.2059 |
| C | 0.0009 | -0.0006 | 1.8415 |
| C | 0.0009 | -0.0018 | 3.0520 |
| H | 0.0012 | -0.0030 | 4.1060 |

$NH_3$•••ClOH

| | | | |
|---|---|---|---|
| N | -0.0093 | -0.0464 | 1.9810 |
| H | 0.4666 | -0.8688 | 2.3227 |
| H | -0.9510 | -0.0658 | 2.3448 |
| H | 0.4530 | 0.7588 | 2.3780 |
| H | -2.5137 | -1.2246 | -0.9217 |
| H | -2.5101 | -1.2249 | 0.9218 |
| H | -2.5113 | 1.2253 | -0.9216 |
| H | -2.5077 | 1.2251 | 0.9221 |
| Cl | 0.3944 | -0.0003 | -0.0003 |
| N | 2.0255 | -0.0006 | 0.0001 |
| C | 3.2070 | 0.0006 | 0.0001 |

$C_2H_4$•••ClCCH

| | | | |
|---|---|---|---|
| C | -2.7486 | 0.6649 | 0.0006 |
| C | -2.7482 | -0.6648 | 0.0006 |
| H | -2.7469 | 1.2242 | 0.9221 |
| H | -2.7512 | 1.2242 | -0.9209 |
| H | -2.7462 | -1.2241 | 0.9221 |
| H | -2.7505 | -1.2241 | -0.9209 |
| Cl | 0.4924 | -0.0001 | -0.0002 |
| C | 2.1272 | 0.0009 | 0.0003 |
| C | 3.3371 | 0.0016 | 0.0007 |
| H | 4.3911 | 0.0022 | 0.0010 |

$C_2H_4$•••ClOH

| | | | |
|---|---|---|---|
| C | 2.1410 | -0.6660 | 0.0042 |
| C | 2.1407 | 0.6662 | 0.0043 |
| H | 2.1721 | -1.2248 | 0.9254 |
| H | 2.1112 | -1.2245 | -0.9170 |
| H | 2.1714 | 1.2250 | 0.9255 |
| H | 2.1104 | 1.2248 | -0.9169 |
| Cl | -0.7177 | -0.0001 | -0.0072 |
| O | -2.4216 | 0.0002 | -0.0974 |
| H | -2.6818 | -0.0005 | 0.8324 |

$H_2$•••ClF

| | | | |
|---|---|---|---|
| H | -2.9950 | 0.3727 | 0.0015 |
| H | -3.0007 | -0.3673 | 0.0016 |
| Cl | -0.3359 | -0.0008 | -0.0005 |
| F | 1.3006 | 0.0008 | 0.0006 |

$H_2$•••ClCN

| | | | |
|---|---|---|---|
| H | 0.1226 | 0.3749 | -3.5860 |
| H | -0.0028 | -0.3526 | -3.5681 |
| Cl | 0.0365 | 0.0513 | -0.4962 |
| C | 0.0258 | 0.0601 | 1.1292 |
| N | 0.0179 | 0.0663 | 2.2994 |

| | | | |
|---|---|---|---|
| Cl | 0.0336 | 0.2041 | -0.6120 |
| O | 0.0765 | 0.4533 | -2.3090 |
| H | -0.0694 | -0.4352 | -2.6551 |

$C_2H_2$•••ClF

| | | | |
|---|---|---|---|
| C | -2.1219 | -0.6053 | -0.0006 |
| C | -2.1206 | 0.6059 | -0.0006 |
| H | -2.1364 | 1.6637 | -0.0007 |
| H | -2.1398 | -1.6630 | -0.0008 |
| F | 2.2267 | 0.0001 | -0.0016 |
| Cl | 0.5700 | -0.0003 | 0.0013 |

$C_2H_2$•••ClCN

| | | | |
|---|---|---|---|
| C | -2.8552 | -0.5981 | -0.0018 |
| C | -2.8452 | 0.6109 | -0.0018 |
| H | -2.8461 | 1.6682 | -0.0015 |
| H | -2.8742 | -1.6551 | -0.0021 |
| C | 1.9796 | 0.0014 | -0.0009 |
| Cl | 0.3527 | -0.0098 | 0.0033 |
| N | 3.1499 | 0.0098 | -0.0037 |

$C_2H_2$•••ClNC

| | | | |
|---|---|---|---|
| C | -2.6585 | -0.6040 | -0.0011 |
| C | -2.6593 | 0.6056 | -0.0013 |
| H | -2.6730 | 1.6631 | -0.0011 |
| H | -2.6709 | -1.6616 | -0.0016 |
| N | 1.9274 | 0.0004 | -0.0009 |
| Cl | 0.3004 | -0.0016 | 0.0022 |
| C | 3.1086 | 0.0021 | -0.0024 |

$H_2$•••ClNC

| | | | |
|---|---|---|---|
| H | -0.3698 | 0.0740 | 3.4048 |
| H | 0.3679 | 0.0323 | 3.4057 |
| Cl | 0.0226 | 0.0607 | 0.5317 |
| N | 0.0351 | 0.0649 | -1.0883 |
| C | 0.0442 | 0.0680 | -2.2695 |

$H_2$•••ClCCH

| | | | |
|---|---|---|---|
| H | 0.3690 | 0.0983 | 3.6664 |
| H | -0.3642 | 0.0168 | 3.6891 |
| Cl | 0.0088 | 0.0486 | 0.5578 |
| C | 0.0401 | 0.0469 | -1.0749 |
| C | 0.0632 | 0.0452 | -2.2840 |
| H | 0.0831 | 0.0442 | -3.3378 |

$H_2$•••ClOH

| | | | |
|---|---|---|---|
| H | -1.0885 | 0.2692 | 4.0125 |
| H | -0.3669 | 0.1112 | 4.0068 |
| Cl | -0.8520 | -0.1369 | 1.1443 |
| O | -0.9410 | -0.4055 | -0.5244 |
| H | -0.7275 | 0.4620 | -0.8910 |

*Table VI. S. 3. Coordinates of the optimized geometry for all Li-bonded complexes (40) under investigation at MP2(full)/aug-cc-PVTZ level of theory.*

| Atoms | X (Å) | Y (Å) | Z (Å) |
|---|---|---|---|

$CH_3$•••LiCN

| | | | |
|---|---|---|---|
| C | -0.0483 | -0.0045 | 2.7636 |
| H | 0.4863 | 0.9227 | 2.8718 |
| H | -1.1211 | -0.0044 | 2.8426 |
| H | 0.4855 | -0.9331 | 2.8633 |
| Li | -0.0144 | 0.0038 | 0.4055 |
| C | 0.0008 | 0.0064 | -1.5112 |
| N | 0.0112 | 0.0090 | -2.6871 |

| Atoms | X (Å) | Y (Å) | Z (Å) |
|---|---|---|---|

$NH_3$•••LiH

| | | | |
|---|---|---|---|
| Li | 0.0747 | 0.0017 | 0.6698 |
| N | -0.0209 | 0.0003 | 2.6931 |
| H | -0.4858 | -0.8210 | 3.0563 |
| H | -0.5250 | 0.7987 | 3.0572 |
| H | 0.8945 | 0.0219 | 3.1235 |
| H | 0.1530 | 0.0029 | -0.9448 |

$NH_3$•••LiF

$CH_3$•••LiNC

| | | | |
|---|---|---|---|
| C | -0.0253 | 0.0045 | -2.3205 |
| H | 0.5108 | -0.9226 | -2.4207 |
| H | -1.0972 | 0.0044 | -2.4092 |
| H | 0.5095 | 0.9334 | -2.4099 |
| Li | -0.0116 | -0.0041 | 0.0281 |
| C | 0.0119 | -0.0088 | 2.9840 |
| N | 0.0020 | -0.0068 | 1.8035 |

$CH_3$•••LiBr

| | | | |
|---|---|---|---|
| C | -3.4924 | 0.0003 | -0.0001 |
| H | -3.5749 | 1.0426 | -0.2530 |
| H | -3.5958 | -0.7393 | -0.7740 |
| H | -3.5847 | -0.2997 | 1.0288 |
| Li | -1.1695 | -0.0009 | 0.0002 |
| Br | 1.0062 | -0.0001 | 0.0000 |

$CH_3$•••LiCl

| | | | |
|---|---|---|---|
| C | -0.2136 | -0.0087 | -0.5193 |
| H | -1.2625 | -0.0257 | -0.2822 |
| H | 0.3350 | -0.9333 | -0.5446 |
| H | 0.3244 | 0.9207 | -0.4584 |
| Li | -0.5432 | 0.1350 | -2.8498 |
| Cl | -0.8342 | 0.2941 | -4.8594 |

$CH_3$•••LiCCH

| | | | |
|---|---|---|---|
| C | -0.0436 | 0.0004 | 2.9944 |
| H | -1.1159 | -0.0293 | 3.0696 |
| H | 0.5168 | -0.9126 | 3.0883 |
| H | 0.4656 | 0.9428 | 3.0893 |
| Li | -0.0232 | 0.0002 | 0.6172 |
| C | -0.0086 | -0.0001 | -1.2805 |
| C | 0.0008 | -0.0003 | -2.5143 |
| H | 0.0090 | -0.0004 | -3.5744 |

$CH_3$•••LiH

| | | | |
|---|---|---|---|
| C | -0.2385 | 0.0066 | -0.6813 |
| H | -1.2872 | -0.0115 | -0.4452 |
| H | 0.3088 | -0.9180 | -0.7231 |
| H | 0.3012 | 0.9343 | -0.6161 |
| Li | -0.5678 | 0.1394 | -3.0411 |
| H | -0.7332 | 0.2056 | -4.6247 |
| Li | 0.0727 | 0.0000 | 0.6680 |
| N | -0.0216 | -0.0003 | 2.6998 |
| H | -0.4866 | -0.8196 | 3.0676 |
| H | -0.5249 | 0.7977 | 3.0646 |
| H | 0.8938 | 0.0220 | 3.1298 |
| F | 0.1513 | 0.0046 | -0.9351 |

$NH_3$•••LiOH

| | | | |
|---|---|---|---|
| Li | -0.0002 | 0.0005 | 0.2629 |
| N | 0.0000 | 0.0005 | -1.7886 |
| H | 0.4770 | -0.8038 | -2.1742 |
| H | 0.4575 | 0.8150 | -2.1763 |
| H | -0.9345 | -0.0112 | -2.1754 |
| H | 0.0001 | -0.0007 | 2.8224 |
| O | 0.0000 | -0.0003 | 1.8718 |

$H_2$•••LiCN

| | | | |
|---|---|---|---|
| H | -0.0191 | -0.4244 | 3.6190 |
| H | 0.0736 | 0.3094 | 3.6778 |
| Li | 0.0454 | 0.0806 | 1.5951 |
| C | 0.0411 | -0.0146 | -0.3145 |
| N | 0.0417 | -0.0753 | -1.4889 |

$H_2$•••LiNC

| | | | |
|---|---|---|---|
| H | -0.3829 | 0.1054 | 3.6102 |
| H | 0.3485 | -0.0001 | 3.6773 |
| Li | 0.1499 | 0.0098 | 1.6075 |
| N | 0.0697 | 0.0334 | -0.1590 |
| C | 0.0147 | 0.0515 | -1.3385 |

$H_2$•••LiBr

| | | | |
|---|---|---|---|
| H | 0.4154 | 0.0040 | 3.6810 |
| H | -0.3208 | 0.0941 | 3.6877 |
| Li | 0.0177 | 0.0161 | 1.6879 |
| Br | -0.0123 | -0.0141 | -0.4807 |

$H_2$•••LiCl

| | | | |
|---|---|---|---|
| H | 0.1027 | -0.3687 | -1.9771 |
| H | 0.2017 | 0.3663 | -1.9680 |
| Li | 0.0051 | 0.0009 | 0.0559 |
| Cl | -0.0300 | 0.0110 | 2.0870 |

$H_2$•••LiCCH

$CH_3$•••LiF

| | | | |
|---|---|---|---|
| C | -0.2404 | 0.0071 | -0.6797 |
| H | -1.2864 | -0.0114 | -0.4325 |
| H | 0.3062 | -0.9175 | -0.7291 |
| H | 0.2989 | 0.9352 | -0.6187 |
| Li | -0.5611 | 0.1348 | -3.0278 |
| F | -0.7296 | 0.2064 | -4.6039 |

$CH_3$•••LiOH

| | | | |
|---|---|---|---|
| C | -0.0004 | -0.0004 | 2.1867 |
| H | -1.0720 | -0.0003 | 2.2691 |
| H | 0.5353 | -0.9285 | 2.2693 |
| H | 0.5355 | 0.9276 | 2.2702 |
| Li | 0.0005 | 0.0010 | -0.2268 |
| O | 0.0005 | 0.0008 | -1.8181 |
| H | 0.0004 | 0.0007 | -2.7682 |

$H_2O$•••LiCN

| | | | |
|---|---|---|---|
| Li | 0.0000 | 0.0000 | -0.5609 |
| O | 0.0000 | 0.0000 | -2.4547 |
| H | 0.7653 | 0.0000 | -3.0341 |
| H | -0.7653 | 0.0000 | -3.0341 |
| C | 0.0000 | 0.0000 | 1.3717 |
| N | 0.0000 | 0.0000 | 2.5481 |

$H_2O$•••LiNC

| | | | |
|---|---|---|---|
| Li | 0.0000 | 0.0000 | -0.3927 |
| O | 0.0000 | 0.0000 | -2.2847 |
| H | -0.7653 | 0.0000 | -2.8637 |
| H | 0.7653 | 0.0000 | -2.8637 |
| N | 0.0000 | 0.0000 | 1.3987 |
| C | 0.0000 | 0.0000 | 2.5791 |

$H_2O$•••LiBr

| | | | |
|---|---|---|---|
| Li | 0.0000 | -0.0011 | -1.1834 |
| Br | 0.0000 | -0.0012 | 1.0093 |
| O | 0.0000 | 0.0001 | -3.0655 |
| H | -0.7649 | 0.0001 | -3.6450 |
| H | 0.7649 | 0.0001 | -3.6450 |

$H_2O$•••LiCl

| | | | |
|---|---|---|---|
| Li | -1.1817 | 0.3737 | 0.8496 |
| O | -0.1597 | 0.0289 | 2.4046 |
| H | -0.3032 | 0.0070 | 3.8247 |
| H | 0.4328 | 0.0068 | 3.7352 |
| H | 0.1008 | 0.0476 | -2.4536 |
| C | 0.0428 | 0.0436 | -1.3951 |
| C | -0.0250 | 0.0436 | -0.1634 |
| Li | -0.1482 | 0.0515 | 1.7263 |

$H_2$•••LiH

| | | | |
|---|---|---|---|
| H | 0.0000 | -0.3701 | -1.8510 |
| H | 0.0000 | 0.3709 | -1.8498 |
| Li | 0.0000 | -0.0021 | 0.2249 |
| H | 0.0000 | 0.0013 | 1.8126 |

$H_2$•••LiF

| | | | |
|---|---|---|---|
| H | 0.0000 | -0.3723 | 2.8694 |
| H | 0.0000 | 0.3690 | 2.8737 |
| Li | 0.0000 | 0.0083 | 0.8152 |
| F | 0.0000 | -0.0049 | -0.7666 |

$H_2$•••LiOH

| | | | |
|---|---|---|---|
| H | 0.0000 | 0.3705 | 3.0458 |
| H | 0.0000 | -0.3705 | 3.0458 |
| Li | 0.0000 | 0.0000 | 0.9623 |
| O | 0.0000 | 0.0000 | -0.6239 |
| H | 0.0000 | 0.0000 | -1.5738 |

$C_2H_4$•••LiCN

| | | | |
|---|---|---|---|
| Li | 0.0131 | -0.1713 | -0.0543 |
| C | -0.0003 | -0.6692 | 2.3140 |
| C | -0.0006 | 0.6596 | 2.1958 |
| H | -0.9231 | -1.2263 | 2.3729 |
| H | 0.9225 | -1.2248 | 2.3852 |
| H | -0.9231 | 1.2182 | 2.1498 |
| H | 0.9215 | 1.2198 | 2.1623 |
| C | 0.0115 | 0.0858 | -1.9574 |
| N | 0.0111 | 0.2625 | -3.1202 |

$C_2H_4$•••LiNC

| | | | |
|---|---|---|---|
| Li | 0.0276 | 0.0559 | -0.1372 |
| C | -0.0021 | 0.8546 | 2.1242 |
| C | -0.0036 | -0.4763 | 2.2195 |
| H | 0.9208 | 1.4142 | 2.1072 |
| H | -0.9241 | 1.4145 | 2.0829 |

| | | | |
|---|---|---|---|
| H | -0.4367 | 0.2405 | 3.2987 |
| H | 0.7073 | -0.3730 | 2.4882 |
| Cl | -2.4777 | 0.8520 | -0.6710 |

$H_2O$•••LiCCH

| | | | |
|---|---|---|---|
| Li | 0.0000 | 0.0000 | 0.5842 |
| C | 0.0000 | 0.0000 | -1.3322 |
| C | 0.0000 | 0.0000 | -2.5665 |
| H | 0.0000 | 0.0000 | -3.6266 |
| O | 0.0000 | 0.0000 | 2.4856 |
| H | -0.7652 | 0.0000 | 3.0645 |
| H | 0.7652 | 0.0000 | 3.0645 |

$H_2O$•••LiH

| | | | |
|---|---|---|---|
| Li | 0.0000 | 0.0000 | -1.3043 |
| O | 0.0000 | 0.0000 | 0.5985 |
| H | 0.0000 | -0.7651 | 1.1765 |
| H | 0.0000 | 0.7651 | 1.1765 |
| H | 0.0000 | 0.0000 | -2.9154 |

$H_2O$•••LiF

| | | | |
|---|---|---|---|
| Li | 0.0000 | 0.0000 | 0.2659 |
| O | 0.0000 | 0.0000 | -1.6444 |
| H | 0.0000 | 0.7647 | -2.2231 |
| H | 0.0000 | -0.7647 | -2.2231 |
| F | 0.0000 | 0.0000 | 1.8670 |

$H_2O$•••LiOH

| | | | |
|---|---|---|---|
| Li | 0.0000 | 0.0000 | 0.2679 |
| O | 0.0000 | 0.0000 | -1.6552 |
| H | 0.7649 | 0.0000 | -2.2335 |
| H | -0.7649 | 0.0000 | -2.2335 |
| O | 0.0000 | 0.0000 | 1.8754 |
| H | 0.0000 | 0.0000 | 2.8259 |

$NH_3$•••LiCN

| | | | |
|---|---|---|---|
| Li | 0.0000 | 0.0000 | -0.0036 |
| N | 0.0000 | 0.0000 | -2.0227 |
| H | -0.9337 | 0.0000 | -2.4132 |
| H | 0.4668 | -0.8086 | -2.4132 |
| H | 0.4668 | 0.8086 | -2.4132 |
| C | 0.0000 | 0.0000 | 1.9325 |
| N | 0.0000 | 0.0000 | 3.1089 |
| H | 0.9182 | -1.0339 | 2.2876 |
| H | -0.9271 | -1.0336 | 2.2633 |
| N | 0.0512 | 0.2140 | -1.9097 |
| C | 0.0655 | 0.3289 | -3.0847 |

$C_2H_4$•••LiBr

| | | | |
|---|---|---|---|
| Li | -0.2230 | -0.1007 | 1.1571 |
| C | 0.6464 | 0.0743 | 3.3393 |
| C | -0.6770 | 0.0224 | 3.5018 |
| H | 1.2460 | -0.8230 | 3.3331 |
| H | 1.1602 | 1.0157 | 3.2197 |
| H | -1.1871 | -0.9186 | 3.6415 |
| H | -1.2732 | 0.9218 | 3.5279 |
| Br | 0.1874 | -0.2106 | -0.9762 |

$C_2H_4$•••LiCl

| | | | |
|---|---|---|---|
| Li | 0.0363 | 0.0003 | 0.2827 |
| C | 0.8461 | -0.0030 | 2.5361 |
| C | -0.4840 | -0.0035 | 2.6385 |
| H | 1.4058 | -0.9251 | 2.5008 |
| H | 1.4052 | 0.9197 | 2.5034 |
| H | -1.0410 | -0.9265 | 2.6926 |
| H | -1.0416 | 0.9189 | 2.6952 |
| Cl | 0.1217 | 0.0043 | -1.7555 |

$C_2H_4$•••LiCCH

| | | | |
|---|---|---|---|
| Li | 0.2405 | 0.0651 | -0.0778 |
| C | -0.6600 | -0.0062 | 2.1533 |
| C | 0.6631 | -0.0141 | 2.3216 |
| H | -1.2156 | 0.9184 | 2.1184 |
| H | -1.2189 | -0.9246 | 2.0589 |
| H | 1.2186 | 0.9042 | 2.4362 |
| H | 1.2149 | -0.9401 | 2.3765 |
| C | -0.0344 | 0.1295 | -1.9572 |
| C | -0.2220 | 0.1703 | -3.1764 |
| H | -0.3827 | 0.2056 | -4.2239 |

$C_2H_4$•••LiH

| | | | |
|---|---|---|---|
| Li | 0.0000 | 0.0000 | -2.0677 |
| H | 0.0000 | 0.0000 | -3.6655 |
| C | -0.6667 | 0.0000 | 0.2785 |
| C | 0.6667 | 0.0000 | 0.2785 |
| H | -1.2270 | 0.9222 | 0.2886 |

| | | | |
|---|---|---|---|
| $NH_3$•••LiNC | | | |
| Li | -0.0015 | -0.0029 | 0.3544 |
| N | 0.0004 | 0.0003 | 2.3735 |
| H | 0.4680 | 0.8098 | 2.7613 |
| H | 0.4680 | -0.8072 | 2.7656 |
| H | -0.9324 | 0.0013 | 2.7662 |
| N | -0.0013 | -0.0012 | -1.4428 |
| C | -0.0012 | -0.0001 | -2.6234 |
| $NH_3$•••LiBr | | | |
| Li | 0.0099 | -0.0033 | -0.8175 |
| Br | -0.0002 | 0.0025 | 1.3787 |
| N | 0.0420 | -0.0005 | -2.8176 |
| H | 0.5414 | 0.7947 | -3.1942 |
| H | -0.8844 | 0.0293 | -3.2235 |
| H | 0.4914 | -0.8226 | -3.1991 |
| $NH_3$•••LiCl | | | |
| Li | -0.0022 | -0.0034 | -0.8076 |
| N | 0.0463 | 0.0000 | -2.8251 |
| H | 0.5407 | 0.7948 | -3.2090 |
| H | -0.8852 | 0.0289 | -3.2196 |
| H | 0.4910 | -0.8229 | -3.2110 |
| Cl | -0.1769 | -0.0109 | 1.2431 |
| $NH_3$•••LiCCH | | | |
| Li | 0.0000 | 0.0000 | 0.7001 |
| N | 0.0000 | 0.0000 | 2.7353 |
| H | -0.4672 | -0.8092 | 3.1229 |
| H | -0.4672 | 0.8092 | 3.1229 |
| H | 0.9344 | 0.0000 | 3.1229 |
| C | 0.0000 | 0.0000 | -1.2198 |
| C | 0.0000 | 0.0000 | -2.4544 |
| H | 0.0000 | 0.0000 | -3.5146 |
| H | -1.2270 | -0.9222 | 0.2886 |
| H | 1.2270 | 0.9222 | 0.2886 |
| H | 1.2270 | -0.9222 | 0.2886 |
| $C_2H_4$•••LiF | | | |
| Li | 0.0000 | 0.0000 | -2.0574 |
| C | -0.6669 | 0.0000 | 0.2797 |
| C | 0.6669 | 0.0000 | 0.2797 |
| H | -1.2268 | 0.9223 | 0.2906 |
| H | -1.2268 | -0.9223 | 0.2906 |
| H | 1.2268 | 0.9223 | 0.2906 |
| H | 1.2268 | -0.9223 | 0.2906 |
| F | -0.0390 | -0.0145 | -3.6459 |
| $C_2H_4$•••LiOH | | | |
| Li | 0.0000 | 0.0000 | 0.7022 |
| C | 0.0000 | 0.6667 | -1.6561 |
| C | 0.0000 | -0.6667 | -1.6561 |
| H | -0.9222 | 1.2268 | -1.6658 |
| H | 0.9222 | 1.2268 | -1.6658 |
| H | -0.9222 | -1.2268 | -1.6658 |
| H | 0.9222 | -1.2268 | -1.6658 |
| O | 0.0000 | 0.0000 | 2.2972 |
| H | 0.0000 | 0.0000 | 3.2478 |

*Table VI. S. 4. Normal modes vibrational frequencies and their intensities for all H-bonded complexes (35) under investigation at MP2(full)/aug-cc-PVTZ level of theory.*

| Frequency | Intensity | Frequency | Intensity | Frequency | Intensity |
|---|---|---|---|---|---|
| $CH_3$•••HBr | | $NH_3$•••HBr | | $C_2H_4$•••HCN | |
| 97.4898 | 5.6 | 173.3011 | 61.6 | 59.8641 | 3.9 |
| 214.1629 | 0.2 | 278.0534 | 17.0 | 77.3274 | 15.7 |

| | |
|---|---|
| 214.6903 | 0.2 |
| 459.505 | 5.3 |
| 459.5767 | 5.3 |
| 653.1767 | 104.0 |
| 1444 | 2.8 |
| 1444.145 | 2.8 |
| 2475.722 | 483.0 |
| 3178.462 | 1.0 |
| 3345.76 | 0.0 |
| 3345.863 | 0.0 |

$CH_3$•••HCl

| | |
|---|---|
| 115.3689 | 2.6 |
| 149.3663 | 0.9 |
| 150.55 | 0.9 |
| 370.5246 | 14.5 |
| 370.7982 | 14.5 |
| 610.0175 | 100.9 |
| 1445.221 | 2.7 |
| 1445.322 | 2.7 |
| 2851.56 | 457.6 |
| 3181.394 | 0.2 |
| 3348.038 | 0.0 |
| 3348.323 | 0.0 |

$CH_3$•••HF

| | |
|---|---|
| 140.8402 | 4.3 |
| 141.2743 | 4.3 |
| 143.5537 | 0.9 |
| 445.0153 | 96.2 |
| 445.0507 | 96.2 |
| 646.0955 | 85.7 |
| 1447.879 | 3.1 |
| 1447.9 | 3.1 |
| 3180.17 | 0.7 |
| 3346.896 | 0.0 |
| 3347.077 | 0.0 |
| 3930.968 | 526.9 |

$CH_3$•••HNC

| | |
|---|---|
| 132.5899 | 0.9 |
| 135.3727 | 8.0 |
| 135.3927 | 8.0 |
| 278.1317 | 17.0 |
| 924.127 | 12.5 |
| 924.1364 | 12.5 |
| 1123.764 | 99.8 |
| 1664.935 | 22.9 |
| 1665.008 | 22.9 |
| 1917.56 | 2677.0 |
| 3522.416 | 1.0 |
| 3653.733 | 28.0 |
| 3653.89 | 28.0 |

$NH_3$•••HCl

| | |
|---|---|
| 204.9563 | 33.9 |
| 257.8984 | 16.7 |
| 258.0933 | 16.7 |
| 874.7404 | 26.5 |
| 874.7427 | 26.5 |
| 1120.845 | 129.7 |
| 1665.301 | 21.1 |
| 1665.317 | 21.1 |
| 2318.694 | 2138.0 |
| 3524.802 | 0.2 |
| 3654.384 | 25.4 |
| 3654.439 | 25.4 |

$NH_3$•••HF

| | |
|---|---|
| 267.1708 | 9.5 |
| 267.5673 | 9.5 |
| 275.8024 | 8.7 |
| 998.5609 | 106.7 |
| 998.5982 | 106.8 |
| 1138.579 | 154.2 |
| 1668.321 | 17.7 |
| 1668.35 | 17.7 |
| 3345.278 | 1608.0 |
| 3532.152 | 5.7 |
| 3657.467 | 25.9 |
| 3657.612 | 25.9 |

$NH_3$•••HNC

| | |
|---|---|
| 145.1278 | 0.2 |
| 145.1447 | 0.2 |
| 226.3769 | 12.6 |
| 91.391 | 4.9 |
| 111.2407 | 0.4 |
| 158.541 | 14.7 |
| 773.6513 | 17.7 |
| 811.6667 | 0.5 |
| 835.0807 | 26.1 |
| 957.6517 | 0.6 |
| 999.6349 | 105.2 |
| 1069.992 | 0.0 |
| 1244.487 | 0.0 |
| 1383.847 | 0.3 |
| 1486.766 | 10.5 |
| 1686.968 | 0.4 |
| 2046.557 | 3.8 |
| 3173.483 | 4.4 |
| 3199.064 | 0.2 |
| 3254.662 | 0.0 |
| 3282.427 | 5.8 |
| 3471.715 | 308.5 |

$C_2H_4$•••HOH

| | |
|---|---|
| 68.8131 | 8.9 |
| 121.0651 | 6.8 |
| 127.7998 | 6.2 |
| 132.0242 | 1.0 |
| 183.6046 | 4.2 |
| 662.6866 | 57.5 |
| 808.5047 | 13.6 |
| 833.9347 | 73.6 |
| 965.342 | 1.5 |
| 1005.3 | 110.0 |
| 1075.885 | 0.0 |
| 1244.928 | 0.0 |
| 1382.838 | 0.6 |
| 1485.796 | 11.4 |
| 1682.263 | 1.0 |
| 2035.787 | 9.1 |
| 3174.703 | 2.7 |
| 3199.497 | 0.0 |
| 3256.357 | 0.0 |
| 3284.597 | 3.5 |
| 3647.786 | 1018.0 |

| | |
|---|---|
| 187.1863 | 3.1 |
| 187.2694 | 3.0 |
| 627.8227 | 93.9 |
| 789.2936 | 99.4 |
| 789.3266 | 99.4 |
| 1446.731 | 2.9 |
| 1446.776 | 2.9 |
| 2039.318 | 15.7 |
| 3178.996 | 1.7 |
| 3347.266 | 0.0 |
| 3347.435 | 0.0 |
| 3691.036 | 784.1 |

$CH_3$•••HCN

| | |
|---|---|
| 107.1112 | 6.5 |
| 108.6821 | 7.1 |
| 111.5159 | 0.3 |
| 158.1428 | 14.5 |
| 159.1892 | 14.0 |
| 571.6332 | 91.4 |
| 817.3104 | 29.0 |
| 817.5512 | 29.0 |
| 1445.952 | 2.6 |
| 1446.101 | 2.6 |
| 2200.406 | 10.8 |
| 3183.555 | 1.1 |
| 3348.937 | 0.3 |
| 3349.345 | 0.3 |
| 3493.931 | 224.6 |

$CH_3$•••HOH

| | |
|---|---|
| 18.482 | 93.1 |
| 108.3048 | 3.4 |
| 109.43 | 3.9 |
| 113.7264 | 7.7 |
| 240.9927 | 67.4 |
| 365.3432 | 72.3 |
| 558.3073 | 86.4 |
| 1445.557 | 2.8 |
| 1446.372 | 2.5 |
| 1629.003 | 49.1 |
| 3186.369 | 0.4 |
| 3350.629 | 0.2 |
| 328.3837 | 22.6 |
| 328.4388 | 22.6 |
| 1015.575 | 112.5 |
| 1015.597 | 112.5 |
| 1140.083 | 158.0 |
| 1668.433 | 17.5 |
| 1668.439 | 17.5 |
| 2016.257 | 15.2 |
| 3187.495 | 2032.0 |
| 3524.061 | 0.6 |
| 3648.766 | 23.9 |
| 3648.804 | 23.9 |

$NH_3$•••HCN

| | |
|---|---|
| 151.5436 | 0.2 |
| 151.583 | 0.2 |
| 171.8796 | 3.5 |
| 283.7645 | 53.1 |
| 283.9348 | 53.1 |
| 944.4849 | 38.2 |
| 944.4975 | 38.2 |
| 1102.604 | 154.2 |
| 1671.242 | 17.2 |
| 1671.269 | 17.2 |
| 2037.429 | 26.3 |
| 3312.853 | 595.4 |
| 3524.724 | 0.7 |
| 3650.779 | 16.7 |
| 3650.828 | 16.7 |

$NH_3$•••HOH

| | |
|---|---|
| 18.8665 | 69.4 |
| 175.9316 | 22.6 |
| 189.5797 | 39.6 |
| 209.8449 | 29.1 |
| 472.3078 | 83.0 |
| 743.9453 | 88.0 |
| 1091.016 | 152.6 |
| 1659.247 | 52.5 |
| 1668.561 | 18.8 |
| 1677.177 | 3.8 |
| 3528.865 | 3.2 |
| 3609.302 | 587.6 |

$C_2H_4$•••HCCH

| | |
|---|---|
| 51.8121 | 0.0 |
| 97.9731 | 1.0 |
| 106.651 | 0.2 |
| 135.4331 | 1.0 |
| 622.3516 | 0.0 |
| 640.4163 | 0.0 |
| 655.2721 | 9.0 |
| 670.529 | 15.8 |
| 752.3062 | 71.4 |
| 763.3253 | 102.5 |
| 805.436 | 58.6 |
| 849.7071 | 70.9 |
| 1976.232 | 4.0 |
| 1981.127 | 0.0 |
| 3405.986 | 178.6 |
| 3406.045 | 115.2 |
| 3538.785 | 1.1 |
| 3559.152 | 41.3 |

$C_2H_2$•••HBr

| | |
|---|---|
| 76.0569 | 0.8 |
| 100.8861 | 1.8 |
| 359.9031 | 2.4 |
| 379.8879 | 4.3 |
| 624.532 | 0.0 |
| 642.8642 | 0.0 |
| 756.8993 | 82.7 |
| 768.9998 | 110.3 |
| 1977.114 | 1.8 |
| 2672.716 | 398.4 |
| 3402.563 | 112.1 |
| 3543.92 | 0.4 |

$C_2H_2$•••HCl

| | |
|---|---|
| 83.2509 | 1.2 |
| 116.1754 | 1.6 |
| 331.1464 | 12.3 |
| 400.8808 | 7.6 |
| 635.4468 | 0.3 |
| 641.2103 | 0.0 |
| 755.5932 | 85.5 |

| | |
|---|---|
| 3353.827 | 0.3 |
| 3801.45 | 91.2 |
| 3936.92 | 128.6 |

$CH_3$•••HCCH

| | |
|---|---|
| 108.8718 | 0.1 |
| 110.4822 | 0.2 |
| 111.8679 | 0.2 |
| 156.6924 | 0.7 |
| 157.5605 | 0.7 |
| 528.2665 | 95.6 |
| 690.1392 | 18.0 |
| 690.2063 | 18.1 |
| 869.4205 | 57.8 |
| 869.4926 | 57.7 |
| 1446.56 | 2.4 |
| 1446.619 | 2.4 |
| 2031.433 | 1.9 |
| 3187.928 | 0.9 |
| 3354.79 | 0.5 |
| 3355.031 | 0.5 |
| 3411.51 | 164.3 |
| 3561.483 | 32.3 |

$H_2O$•••HBr

| | |
|---|---|
| 140.5833 | 7.2 |
| 208.4636 | 216.1 |
| 219.7729 | 6.9 |
| 548.6358 | 23.8 |
| 630.0749 | 16.1 |
| 1623.779 | 67.2 |
| 2531.085 | 758.5 |
| 3827.018 | 23.1 |
| 3946.06 | 103.4 |

$H_2O$•••HCl

| | |
|---|---|
| 163.4989 | 17.4 |
| 213.0067 | 189.7 |
| 215.1628 | 12.6 |
| 558.3887 | 45.8 |
| 663.9059 | 30.9 |
| 1624.35 | 69.5 |
| 2788.455 | 832.5 |
| 3656.972 | 18.3 |
| 3659.209 | 17.1 |
| 3927.498 | 80.6 |

$NH_3$•••HCCH

| | |
|---|---|
| 146.8774 | 22.8 |
| 147.3851 | 22.4 |
| 157.9971 | 1.8 |
| 225.1855 | 18.5 |
| 226.1893 | 18.9 |
| 700.6961 | 33.9 |
| 700.7187 | 33.9 |
| 1002.577 | 46.5 |
| 1002.887 | 46.4 |
| 1061.355 | 162.4 |
| 1670.929 | 17.0 |
| 1671.109 | 17.0 |
| 1967.21 | 17.2 |
| 3366.409 | 361.4 |
| 3512.546 | 51.0 |
| 3527.737 | 4.9 |
| 3657.763 | 13.5 |
| 3658.096 | 13.5 |

$C_2H_4$•••HBr

| | |
|---|---|
| 88.9051 | 0.4 |
| 103.2104 | 2.1 |
| 105.3519 | 0.7 |
| 429.249 | 4.4 |
| 439.9239 | 1.4 |
| 809.5107 | 0.0 |
| 940.4549 | 0.0 |
| 991.8566 | 118.0 |
| 1063.778 | 0.0 |
| 1243.403 | 0.0 |
| 1382.178 | 0.8 |
| 1483.38 | 10.1 |
| 1681.108 | 2.1 |
| 2637.669 | 542.2 |
| 3176.023 | 3.2 |
| 3202.43 | 0.0 |
| 3257.373 | 0.0 |
| 3285.676 | 3.8 |
| 772.4091 | 106.0 |
| 1977.295 | 1.4 |
| 2931.211 | 482.6 |
| 3402.07 | 114.6 |
| 3543.96 | 0.2 |

$C_2H_2$•••HF

| | |
|---|---|
| 94.5896 | 5.5 |
| 150.588 | 0.9 |
| 479.028 | 75.1 |
| 491.0554 | 50.7 |
| 640.7285 | 0.0 |
| 656.2307 | 8.1 |
| 757.2733 | 101.1 |
| 780.3306 | 97.8 |
| 1977.75 | 0.7 |
| 3399.143 | 124.2 |
| 3541.521 | 0.3 |
| 3923.57 | 645.8 |

$C_2H_2$•••HNC

| | |
|---|---|
| 51.3111 | 12.0 |
| 135.9237 | 1.1 |
| 152.6856 | 10.1 |
| 156.1055 | 3.4 |
| 615.744 | 16.3 |
| 640.3284 | 0.0 |
| 666.5087 | 50.8 |
| 751.211 | 31.2 |
| 778.5346 | 104.6 |
| 801.9012 | 146.4 |
| 1977.189 | 1.3 |
| 2038.148 | 10.1 |
| 3397.053 | 121.9 |
| 3536.354 | 2.2 |
| 3677.397 | 934.6 |

$C_2H_2$•••HCN

| | |
|---|---|
| 54.9674 | 10.7 |
| 115.0417 | 0.5 |
| 119.3402 | 8.9 |
| 144.0563 | 19.7 |
| 633.6751 | 0.0 |

| | |
|---|---|
| 3830.075 | 21.4 |
| 3948.123 | 106.0 |

$H_2O$•••HF

| | |
|---|---|
| 229.6191 | 43.2 |
| 241.0474 | 0.0 |
| 275.3735 | 151.9 |
| 727.8101 | 158.6 |
| 850.9137 | 119.5 |
| 1629.941 | 74.1 |
| 3718.94 | 975.8 |
| 3836.428 | 9.4 |
| 3949.209 | 118.1 |

$H_2O$•••HNC

| | |
|---|---|
| 134.1007 | 1.1 |
| 157.6704 | 22.6 |
| 197.1999 | 71.5 |
| 222.0251 | 148.7 |
| 311.8841 | 21.8 |
| 864.6601 | 118.5 |
| 896.2337 | 124.9 |
| 1632.821 | 68.8 |
| 2037.471 | 0.3 |
| 3513.703 | 1255.0 |
| 3835.433 | 18.4 |
| 3951.89 | 116.9 |

$H_2O$•••HCN

| | |
|---|---|
| 108.6103 | 1.9 |
| 110.0314 | 195.6 |
| 154.3844 | 2.6 |
| 166.5116 | 59.4 |
| 242.6192 | 76.7 |
| 860.2301 | 32.9 |
| 876.9635 | 40.8 |
| 1631.616 | 65.5 |
| 2049.678 | 11.1 |
| 3442.876 | 371.0 |
| 3843.823 | 15.4 |
| 3962.162 | 102.1 |

$H_2O$•••HOH

| | |
|---|---|
| 68.8131 | 8.9 |

$C_2H_4$•••HCl

| | |
|---|---|
| 85.8953 | 0.7 |
| 100.7063 | 1.4 |
| 117.1005 | 1.7 |
| 406.0216 | 11.7 |
| 424.7881 | 5.8 |
| 810.1207 | 0.0 |
| 952.6103 | 0.1 |
| 997.7781 | 112.3 |
| 1066.96 | 0.0 |
| 1243.808 | 0.0 |
| 1382.506 | 0.6 |
| 1484.402 | 10.3 |
| 1681.568 | 1.4 |
| 2897.154 | 596.5 |
| 3175.843 | 3.3 |
| 3202.654 | 0.0 |
| 3256.659 | 0.0 |
| 3284.946 | 4.0 |

$C_2H_4$•••HF

| | |
|---|---|
| 103.3125 | 3.0 |
| 127.0855 | 3.7 |
| 151.2792 | 0.9 |
| 510.7537 | 47.4 |
| 577.6034 | 78.3 |
| 808.8844 | 0.1 |
| 961.6811 | 1.6 |
| 1004.31 | 102.4 |
| 1070.844 | 0.0 |
| 1244.531 | 0.0 |
| 1383.038 | 0.3 |
| 1485.786 | 11.4 |
| 1680.258 | 0.6 |
| 3178.082 | 2.6 |
| 3204.504 | 0.0 |
| 3260.035 | 0.0 |
| 3289.408 | 3.2 |
| 3878.899 | 742.7 |

$C_2H_4$•••HNC

| | |
|---|---|
| 641.6253 | 0.0 |
| 753.9088 | 75.7 |
| 771.5444 | 101.1 |
| 790.599 | 20.5 |
| 826.6494 | 38.3 |
| 1979.581 | 0.8 |
| 2048.402 | 3.4 |
| 3401.62 | 112.0 |
| 3484.583 | 287.0 |
| 3536.467 | 0.2 |

$C_2H_2$•••HOH

| | |
|---|---|
| 51.4636 | 25.1 |
| 122.1007 | 0.1 |
| 123.4084 | 84.7 |
| 226.5249 | 75.7 |
| 386.2908 | 41.7 |
| 634.332 | 1.4 |
| 643.8759 | 0.2 |
| 756.3736 | 85.9 |
| 768.0823 | 97.7 |
| 1633.418 | 49.6 |
| 1978.947 | 0.4 |
| 3405.886 | 111.6 |
| 3547.807 | 0.2 |
| 3811.08 | 132.2 |
| 3938.391 | 150.9 |

$C_2H_2$•••HCCH

| | |
|---|---|
| 51.8121 | 0.0 |
| 97.9731 | 1.0 |
| 106.651 | 0.2 |
| 135.4331 | 1.0 |
| 622.3516 | 0.0 |
| 640.4163 | 0.0 |
| 655.2721 | 9.0 |
| 670.529 | 15.8 |
| 752.3062 | 71.4 |
| 763.3253 | 102.5 |
| 805.436 | 58.6 |
| 849.7071 | 70.9 |
| 1976.232 | 4.0 |
| 1981.127 | 0.0 |

| | | | | | |
|---|---|---|---|---|---|
| 129.7097 | 112.0 | 121.0651 | 6.8 | 3405.986 | 178.6 |
| 149.3167 | 60.9 | 127.7998 | 6.2 | 3406.045 | 115.2 |
| 152.0816 | 160.6 | 132.0242 | 1.0 | 3538.785 | 1.1 |
| 188.816 | 120.4 | 183.6046 | 4.2 | 3559.152 | 41.3 |
| 374.1169 | 50.2 | 662.6866 | 57.5 | | |
| 656.2128 | 91.1 | 808.5047 | 13.6 | | |
| 1625.997 | 87.6 | 833.9347 | 73.6 | | |
| 1650.474 | 38.0 | 965.342 | 1.5 | | |
| 3741.117 | 320.3 | 1005.3 | 110.0 | | |
| 3836.738 | 11.2 | 1075.885 | 0.0 | | |
| 3934.087 | 108.9 | 1244.928 | 0.0 | | |
| 3953.278 | 99.2 | 1382.838 | 0.6 | | |
| | | 1485.796 | 11.4 | | |
| $H_2O$•••HCCH | | 1682.263 | 1.0 | | |
| 48.543 | 232.1 | 2035.787 | 9.1 | | |
| 86.6364 | 43.2 | 3174.703 | 2.7 | | |
| 140.0204 | 1.5 | 3199.497 | 0.0 | | |
| 153.8923 | 0.0 | 3256.357 | 0.0 | | |
| 201.4615 | 19.9 | 3284.597 | 3.5 | | |
| 692.8666 | 24.7 | 3647.786 | 1018.0 | | |
| 695.9748 | 27.3 | | | | |
| 914.533 | 53.9 | | | | |
| 919.5771 | 61.7 | | | | |
| 1627.693 | 67.2 | | | | |
| 1975.854 | 8.5 | | | | |
| 3399.124 | 201.6 | | | | |
| 3561.936 | 72.9 | | | | |
| 3845.658 | 10.3 | | | | |
| 3966.423 | 90.6 | | | | |

*Table VI. S. 5. Normal modes vibrational frequencies and their intensities for all Cl-bonded complexes (25) under investigation at MP2(full)/aug-cc-PVTZ level of theory.*

| Frequency | Intensity | Frequency | Intensity | Frequency | Intensity |
|---|---|---|---|---|---|
| $CH_3$•••ClF | | $NH_3$•••ClOH | | $C_2H_4$•••ClNC | |
| 116.8 | 0.0 | 5.3 | 71.2 | 65.3 | 2.0 |
| 116.8 | 0.0 | 115.4 | 18.1 | 67.7 | 2.4 |
| 130.4 | 22.4 | 117.2 | 21.2 | 105.0 | 0.1 |
| 262.7 | 0.1 | 144.0 | 15.7 | 107.3 | 2.1 |
| 262.9 | 0.1 | 280.3 | 19.9 | 158.3 | 0.0 |
| 729.1 | 110.5 | 287.9 | 23.4 | 278.5 | 0.4 |
| 950.9 | 313.6 | 712.1 | 78.4 | 285.5 | 0.2 |
| 1447.8 | 3.0 | 1055.3 | 138.1 | 699.8 | 13.7 |
| 1447.8 | 3.0 | 1224.1 | 31.6 | 814.1 | 0.0 |

| | |
|---|---|
| 3182.8 | 1.3 |
| 3348.7 | 0.1 |
| 3348.7 | 0.1 |

$CH_3$•••ClCN

| | |
|---|---|
| 35.2 | 2.3 |
| 35.2 | 2.3 |
| 78.5 | 0.2 |
| 93.9 | 0.1 |
| 94.0 | 0.1 |
| 391.8 | 2.9 |
| 391.8 | 2.9 |
| 519.0 | 102.5 |
| 761.2 | 4.6 |
| 1444.6 | 2.3 |
| 1444.6 | 2.3 |
| 2200.1 | 21.5 |
| 3190.8 | 0.7 |
| 3352.7 | 0.4 |
| 3352.7 | 0.4 |

$CH_3$•••ClNC

| | |
|---|---|
| 58.8 | 1.8 |
| 58.8 | 1.8 |
| 102.3 | 2.7 |
| 160.5 | 0.2 |
| 160.5 | 0.2 |
| 271.5 | 0.1 |
| 271.5 | 0.1 |
| 586.8 | 116.4 |
| 712.9 | 2.0 |
| 1445.3 | 2.5 |
| 1445.4 | 2.5 |
| 2094.3 | 86.2 |
| 3187.2 | 1.3 |
| 3350.9 | 0.1 |
| 3350.9 | 0.1 |

$CH_3$•••ClCCH

| | |
|---|---|
| 30.9 | 0.1 |
| 31.5 | 0.1 |
| 59.6 | 0.2 |
| 60.8 | 0.2 |
| 1665.2 | 20.2 |
| 1666.2 | 19.2 |
| 3529.8 | 0.1 |
| 3663.0 | 17.7 |
| 3663.6 | 17.3 |
| 3808.6 | 74.6 |

$C_2H_2$•••ClF

| | |
|---|---|
| 121.1 | 0.3 |
| 126.0 | 9.3 |
| 144.4 | 0.0 |
| 172.8 | 0.1 |
| 633.6 | 0.0 |
| 642.7 | 0.0 |
| 737.1 | 194.3 |
| 754.5 | 81.4 |
| 769.7 | 42.6 |
| 1967.6 | 4.1 |
| 3403.2 | 119.7 |
| 3542.9 | 0.4 |

$C_2H_2$•••ClCN

| | |
|---|---|
| 39.2 | 2.6 |
| 44.8 | 2.7 |
| 79.5 | 0.0 |
| 82.4 | 0.3 |
| 391.7 | 3.2 |
| 393.1 | 3.1 |
| 626.0 | 0.0 |
| 645.5 | 0.0 |
| 756.0 | 4.9 |
| 756.3 | 83.0 |
| 762.8 | 107.0 |
| 1978.4 | 0.8 |
| 2156.7 | 15.9 |
| 3404.7 | 104.6 |
| 3551.6 | 0.7 |

$C_2H_2$•••ClNC

| | |
|---|---|
| 59.2 | 2.3 |
| 68.7 | 2.3 |
| 105.7 | 1.5 |
| 109.0 | 0.0 |
| 944.8 | 0.0 |
| 990.7 | 120.2 |
| 1060.4 | 0.0 |
| 1243.9 | 0.0 |
| 1380.6 | 1.1 |
| 1482.3 | 10.0 |
| 1678.9 | 2.8 |
| 2089.0 | 98.8 |
| 3175.9 | 3.3 |
| 3205.1 | 0.0 |
| 3255.6 | 0.0 |
| 3285.1 | 4.2 |

$C_2H_4$•••ClCCH

| | |
|---|---|
| 36.9 | 0.1 |
| 38.8 | 0.1 |
| 59.8 | 0.3 |
| 75.7 | 0.1 |
| 83.9 | 0.3 |
| 362.7 | 3.4 |
| 365.4 | 3.9 |
| 620.1 | 41.4 |
| 622.9 | 41.5 |
| 764.5 | 4.4 |
| 815.2 | 0.0 |
| 943.7 | 0.0 |
| 983.4 | 114.3 |
| 1061.9 | 0.0 |
| 1245.7 | 0.0 |
| 1383.1 | 0.2 |
| 1483.9 | 9.2 |
| 1686.0 | 0.3 |
| 2121.9 | 39.7 |
| 3174.8 | 6.2 |
| 3205.9 | 0.0 |
| 3251.6 | 0.0 |
| 3282.3 | 8.0 |
| 3526.8 | 96.0 |

$C_2H_4$•••ClOH

| | |
|---|---|
| 48.2 | 99.5 |
| 90.4 | 1.2 |

| | |
|---|---|
| 70.8 | 0.1 |
| 361.1 | 4.3 |
| 361.1 | 4.3 |
| 489.6 | 105.6 |
| 623.5 | 41.6 |
| 623.5 | 41.6 |
| 768.6 | 6.3 |
| 1444.2 | 2.2 |
| 1444.3 | 2.1 |
| 2132.9 | 39.9 |
| 3193.4 | 0.5 |
| 3355.2 | 0.7 |
| 3355.4 | 0.7 |
| 3527.2 | 95.7 |

$CH_3$•••ClOH

| | |
|---|---|
| 7.2 | 85.7 |
| 69.8 | 3.0 |
| 74.0 | 2.5 |
| 95.5 | 1.7 |
| 129.7 | 0.5 |
| 134.3 | 0.2 |
| 538.7 | 115.8 |
| 812.1 | 42.3 |
| 1252.8 | 39.2 |
| 1444.0 | 2.4 |
| 1444.6 | 2.2 |
| 3191.7 | 0.5 |
| 3354.9 | 0.3 |
| 3355.2 | 0.2 |
| 3799.5 | 88.0 |

$NH_3$•••ClF

| | |
|---|---|
| 212.8 | 4.7 |
| 212.8 | 4.7 |
| 250.8 | 109.0 |
| 525.8 | 16.6 |
| 525.9 | 16.7 |
| 627.2 | 240.4 |
| 1105.7 | 118.5 |
| 1657.5 | 26.4 |
| 1657.5 | 26.4 |
| 3525.2 | 15.3 |
| 276.1 | 0.2 |
| 277.8 | 0.2 |
| 627.4 | 0.0 |
| 646.3 | 0.0 |
| 714.9 | 7.7 |
| 757.2 | 82.2 |
| 765.9 | 109.8 |
| 1975.0 | 2.5 |
| 2093.3 | 79.0 |
| 3402.6 | 110.8 |
| 3546.0 | 0.9 |

$C_2H_2$•••ClCCH

| | |
|---|---|
| 33.2 | 0.1 |
| 43.4 | 0.2 |
| 65.3 | 0.4 |
| 75.7 | 0.1 |
| 362.1 | 3.7 |
| 363.1 | 4.0 |
| 620.3 | 6.2 |
| 623.2 | 35.2 |
| 624.4 | 41.4 |
| 644.1 | 0.0 |
| 754.9 | 82.7 |
| 756.5 | 108.8 |
| 766.7 | 5.5 |
| 1979.4 | 0.4 |
| 2122.8 | 41.0 |
| 3407.9 | 99.1 |
| 3526.2 | 95.5 |
| 3554.6 | 0.4 |

$C_2H_2$•••ClOH

| | |
|---|---|
| 69.4 | 41.4 |
| 82.2 | 59.0 |
| 93.7 | 3.0 |
| 98.6 | 1.7 |
| 119.7 | 0.2 |
| 622.1 | 0.0 |
| 644.5 | 0.0 |
| 746.7 | 94.9 |
| 754.9 | 79.7 |
| 758.3 | 55.2 |
| 96.6 | 3.9 |
| 104.7 | 1.4 |
| 134.0 | 0.6 |
| 176.5 | 1.2 |
| 728.6 | 70.1 |
| 813.0 | 0.0 |
| 938.8 | 0.0 |
| 984.1 | 111.6 |
| 1051.3 | 0.0 |
| 1239.3 | 36.6 |
| 1242.4 | 0.0 |
| 1379.8 | 0.6 |
| 1480.8 | 9.3 |
| 1677.8 | 2.1 |
| 3177.8 | 4.4 |
| 3206.9 | 0.1 |
| 3256.7 | 0.0 |
| 3286.4 | 5.3 |
| 3798.4 | 87.4 |

$H_2$•••ClF

| | |
|---|---|
| 109.1 | 0.0 |
| 118.9 | 0.0 |
| 193.9 | 3.0 |
| 348.9 | 1.2 |
| 800.4 | 39.3 |
| 4476.6 | 7.1 |

$H_2$•••ClCN

| | |
|---|---|
| 43.0 | 0.8 |
| 48.5 | 0.8 |
| 143.0 | 0.3 |
| 229.9 | 0.3 |
| 386.5 | 2.8 |
| 387.3 | 2.6 |
| 761.1 | 7.7 |
| 2158.9 | 16.3 |
| 4502.3 | 1.8 |

$H_2$•••ClNC

| | |
|---|---|
| 55.6 | 0.7 |
| 73.3 | 0.6 |
| 172.2 | 1.0 |

| | |
|---|---|
| 3663.7 | 39.8 |
| 3663.8 | 39.8 |

$NH_3$•••ClCN

| | |
|---|---|
| 58.6 | 0.2 |
| 58.7 | 0.2 |
| 118.8 | 2.0 |
| 198.5 | 45.5 |
| 198.6 | 45.5 |
| 406.1 | 1.2 |
| 406.1 | 1.2 |
| 748.7 | 1.6 |
| 1072.3 | 155.5 |
| 1668.7 | 17.3 |
| 1668.7 | 17.4 |
| 2154.1 | 15.7 |
| 3526.4 | 0.2 |
| 3653.2 | 13.8 |
| 3653.2 | 13.8 |

$NH_3$•••ClNC

| | |
|---|---|
| 90.4 | 0.5 |
| 90.4 | 0.5 |
| 159.5 | 15.3 |
| 250.7 | 21.7 |
| 250.7 | 21.7 |
| 341.3 | 14.8 |
| 341.3 | 14.8 |
| 672.7 | 25.2 |
| 1092.5 | 141.0 |
| 1668.1 | 19.7 |
| 1668.2 | 19.7 |
| 2088.4 | 100.8 |
| 3526.2 | 0.8 |
| 3655.1 | 19.4 |
| 3655.3 | 19.4 |

$NH_3$•••ClCCH

| | |
|---|---|
| 46.8 | 9.0 |
| 46.9 | 9.0 |
| 99.5 | 1.3 |
| 148.5 | 31.3 |
| 148.6 | 31.3 |
| 1247.7 | 39.0 |
| 1975.1 | 1.0 |
| 3408.0 | 104.3 |
| 3551.3 | 0.4 |
| 3798.6 | 86.1 |

$C_2H_4$•••ClF

| | |
|---|---|
| 132.9 | 37.6 |
| 165.2 | 0.0 |
| 181.0 | 0.1 |
| 237.9 | 0.4 |
| 359.3 | 0.1 |
| 646.4 | 284.8 |
| 814.7 | 0.1 |
| 947.9 | 0.1 |
| 1001.1 | 95.3 |
| 1039.0 | 0.0 |
| 1240.0 | 0.0 |
| 1370.7 | 2.3 |
| 1480.1 | 10.5 |
| 1655.0 | 8.2 |
| 3185.6 | 0.7 |
| 3210.0 | 0.9 |
| 3269.2 | 0.0 |
| 3297.1 | 0.5 |

$C_2H_4$•••ClCN

| | |
|---|---|
| 40.1 | 2.4 |
| 41.8 | 2.7 |
| 64.8 | 0.2 |
| 81.7 | 0.2 |
| 102.8 | 0.1 |
| 391.9 | 3.4 |
| 393.7 | 3.0 |
| 752.8 | 3.2 |
| 814.7 | 0.0 |
| 943.4 | 0.0 |
| 987.6 | 113.0 |
| 1062.5 | 0.0 |
| 1245.7 | 0.0 |
| 1382.9 | 0.4 |
| 1484.2 | 9.7 |
| 1684.9 | 0.6 |
| 256.2 | 0.0 |
| 261.7 | 0.1 |
| 281.0 | 0.7 |
| 736.5 | 0.0 |
| 2099.2 | 56.9 |
| 4495.5 | 4.2 |

$H_2$•••ClCCH

| | |
|---|---|
| 36.2 | 0.1 |
| 50.0 | 0.1 |
| 134.3 | 0.1 |
| 173.8 | 0.5 |
| 353.7 | 4.3 |
| 354.7 | 4.5 |
| 623.5 | 41.8 |
| 623.6 | 41.7 |
| 771.4 | 8.1 |
| 2126.5 | 37.8 |
| 3527.7 | 93.0 |
| 4507.4 | 0.7 |

$H_2$•••ClOH

| | |
|---|---|
| 55.6 | 0.7 |
| 73.3 | 0.6 |
| 172.2 | 1.0 |
| 256.2 | 0.0 |
| 261.7 | 0.1 |
| 281.0 | 0.7 |
| 736.5 | 0.0 |
| 2099.2 | 56.9 |
| 4495.5 | 4.2 |

| | | | |
|---|---|---|---|
| 372.8 | 5.9 | 2155.7 | 14.2 |
| 372.8 | 5.9 | 3174.3 | 5.1 |
| 611.9 | 43.4 | 3205.2 | 0.1 |
| 611.9 | 43.4 | 3251.0 | 0.0 |
| 761.9 | 3.3 | 3281.7 | 6.7 |
| 1051.5 | 164.4 | | |
| 1668.2 | 16.8 | | |
| 1668.2 | 16.8 | | |
| 2118.6 | 44.7 | | |
| 3526.5 | 83.7 | | |
| 3528.9 | 9.0 | | |
| 3657.9 | 11.8 | | |
| 3657.9 | 11.8 | | |

*Table VI. S. 6. Normal modes vibrational frequencies and their intensities for all Li-bonded complexes (40) under investigation at MP2(full)/aug-cc-PVTZ level of theory.*

| Frequency | Intensity | Frequency | Intensity | Frequency | Intensity |
|---|---|---|---|---|---|
| $CH_3$•••LiCN | | $H_2O$•••LiF | | $H_2$•••LiH | |
| 59.5 | 34.9 | 57.3 | 24.5 | 69.4 | 489.0 |
| 59.7 | 34.9 | 76.9 | 0.8 | 134.9 | 482.4 |
| 163.7 | 14.1 | 231.7 | 335.1 | 361.9 | 1.1 |
| 163.9 | 14.4 | 292.2 | 1.6 | 617.9 | 0.2 |
| 172.1 | 0.9 | 413.0 | 132.3 | 1428.1 | 290.5 |
| 222.1 | 25.2 | 910.7 | 183.8 | 4466.7 | 16.4 |
| 222.6 | 24.9 | 1650.0 | 97.3 | | |
| 655.6 | 144.0 | 3852.7 | 45.4 | $H_2$•••LiF | |
| 769.3 | 73.6 | 3959.7 | 153.9 | 29.9 | 60.0 |
| 1447.2 | 4.1 | | | 54.9 | 59.0 |
| 1447.3 | 4.1 | $H_2O$•••LiOH | | 347.4 | 0.1 |
| 2081.7 | 20.7 | 51.6 | 60.0 | 609.9 | 1.5 |
| 3161.4 | 3.2 | 67.8 | 4.2 | 901.6 | 171.5 |
| 3326.0 | 0.9 | 192.5 | 206.3 | 4461.2 | 12.1 |
| 3326.3 | 0.9 | 291.7 | 0.9 | | |
| | | 353.5 | 128.0 | $H_2$•••LiOH | |
| $CH_3$•••LiNC | | 355.7 | 59.0 | 52.5 | 21.4 |
| 40.0 | 40.5 | 405.3 | 150.9 | 117.1 | 24.1 |
| 40.6 | 40.4 | 939.8 | 222.7 | 328.7 | 0.0 |
| 147.7 | 9.4 | 1646.5 | 96.9 | 377.6 | 121.1 |
| 147.8 | 9.5 | 3851.9 | 44.5 | 381.8 | 119.6 |
| 177.0 | 0.7 | 3961.4 | 148.1 | 600.9 | 1.7 |
| 208.5 | 23.5 | 4010.6 | 28.1 | 949.8 | 199.9 |
| 209.0 | 23.5 | | | 4019.4 | 42.0 |

| | |
|---|---|
| 722.5 | 175.7 |
| 761.0 | 85.4 |
| 1447.0 | 4.1 |
| 1447.0 | 4.1 |
| 2082.0 | 98.7 |
| 3161.8 | 3.2 |
| 3326.2 | 0.9 |
| 3326.5 | 0.9 |

$CH_3$•••LiBr

| | |
|---|---|
| 45.6 | 28.0 |
| 49.9 | 28.8 |
| 156.0 | 1.3 |
| 195.2 | 15.4 |
| 199.2 | 14.6 |
| 604.5 | 124.7 |
| 754.9 | 82.4 |
| 1446.3 | 4.0 |
| 1447.3 | 4.0 |
| 3161.9 | 3.5 |
| 3325.1 | 1.1 |
| 3327.7 | 1.2 |

$CH_3$•••LiCl

| | |
|---|---|
| 58.6 | 41.6 |
| 61.0 | 41.4 |
| 164.5 | 0.8 |
| 205.3 | 13.9 |
| 206.8 | 14.1 |
| 663.0 | 147.9 |
| 752.3 | 78.1 |
| 1446.9 | 3.9 |
| 1447.1 | 4.0 |
| 3162.9 | 2.9 |
| 3327.0 | 0.9 |
| 3328.3 | 0.9 |

$CH_3$•••LiCCH

| | |
|---|---|
| 62.8 | 8.0 |
| 63.3 | 7.9 |
| 161.5 | 53.6 |
| 161.9 | 54.7 |
| 169.4 | 0.6 |

$NH_3$•••LiCN

| | |
|---|---|
| 78.6 | 9.9 |
| 78.6 | 9.9 |
| 183.5 | 16.2 |
| 183.5 | 16.2 |
| 263.1 | 9.3 |
| 479.6 | 95.3 |
| 479.6 | 95.3 |
| 710.7 | 133.2 |
| 1223.6 | 161.0 |
| 1672.7 | 19.7 |
| 1672.7 | 19.7 |
| 2078.6 | 16.3 |
| 3518.0 | 4.3 |
| 3628.6 | 35.5 |
| 3628.6 | 35.5 |

$NH_3$•••LiNC

| | |
|---|---|
| 48.4 | 19.3 |
| 48.7 | 19.3 |
| 148.0 | 7.8 |
| 148.1 | 7.8 |
| 271.9 | 8.0 |
| 474.6 | 94.8 |
| 474.8 | 94.8 |
| 749.9 | 174.3 |
| 1220.7 | 160.8 |
| 1672.1 | 19.7 |
| 1672.1 | 19.7 |
| 2078.8 | 85.5 |
| 3516.1 | 4.4 |
| 3626.6 | 35.5 |
| 3626.8 | 35.5 |

$NH_3$•••LiBr

| | |
|---|---|
| 68.5 | 11.0 |
| 69.8 | 11.2 |
| 223.1 | 9.1 |
| 460.9 | 73.9 |
| 461.9 | 73.7 |
| 674.1 | 117.3 |
| 1212.9 | 171.0 |
| 1672.7 | 20.5 |
| 4465.1 | 10.6 |

$C_2H_4$•••LiCN

| | |
|---|---|
| 40.3 | 27.7 |
| 69.6 | 29.5 |
| 137.3 | 0.8 |
| 164.9 | 5.3 |
| 165.4 | 8.3 |
| 203.6 | 28.0 |
| 223.6 | 28.5 |
| 661.5 | 142.4 |
| 817.9 | 0.1 |
| 991.7 | 4.0 |
| 1034.8 | 107.3 |
| 1093.4 | 0.0 |
| 1245.1 | 0.0 |
| 1383.8 | 1.0 |
| 1490.5 | 13.8 |
| 1678.4 | 0.9 |
| 2079.9 | 20.8 |
| 3167.8 | 0.0 |
| 3189.6 | 0.7 |
| 3250.5 | 0.0 |
| 3278.0 | 0.0 |

$C_2H_4$•••LiNC

| | |
|---|---|
| 11.6 | 37.4 |
| 51.4 | 38.5 |
| 116.1 | 0.5 |
| 148.9 | 7.2 |
| 157.2 | 7.6 |
| 187.5 | 13.5 |
| 216.0 | 22.4 |
| 725.0 | 183.2 |
| 816.9 | 0.1 |
| 985.8 | 4.2 |
| 1032.2 | 110.2 |
| 1090.3 | 0.0 |
| 1245.2 | 0.0 |
| 1383.2 | 1.0 |
| 1490.4 | 13.9 |
| 1677.3 | 0.9 |
| 2079.8 | 99.3 |

| | |
|---|---|
| 223.4 | 49.0 |
| 224.4 | 47.9 |
| 657.6 | 55.2 |
| 657.7 | 55.2 |
| 682.5 | 147.8 |
| 741.8 | 82.7 |
| 1448.0 | 3.8 |
| 1448.4 | 3.8 |
| 1931.2 | 8.1 |
| 3164.8 | 2.8 |
| 3330.5 | 0.7 |
| 3330.7 | 0.7 |
| 3448.1 | 11.9 |

$CH_3$•••LiH

| | |
|---|---|
| 107.9 | 375.5 |
| 110.0 | 366.8 |
| 206.0 | 183.8 |
| 206.3 | 180.2 |
| 231.4 | 0.5 |
| 724.6 | 72.3 |
| 1402.7 | 304.6 |
| 1446.2 | 3.7 |
| 1447.8 | 3.6 |
| 3165.5 | 1.9 |
| 3328.9 | 0.8 |
| 3330.2 | 0.7 |

$CH_3$•••LiF

| | |
|---|---|
| 77.3 | 61.4 |
| 81.8 | 63.8 |
| 174.0 | 0.2 |
| 187.6 | 29.6 |
| 192.2 | 26.9 |
| 722.2 | 66.4 |
| 891.1 | 185.2 |
| 1446.9 | 3.9 |
| 1447.2 | 3.9 |
| 3166.7 | 1.8 |
| 3329.0 | 0.5 |
| 3330.7 | 0.4 |

$CH_3$•••LiOH

| | |
|---|---|
| 1672.8 | 20.4 |
| 3518.7 | 4.7 |
| 3629.9 | 35.4 |
| 3631.1 | 35.4 |

$NH_3$•••LiCl

| | |
|---|---|
| 50.4 | 16.7 |
| 63.1 | 17.3 |
| 250.2 | 8.0 |
| 466.5 | 81.4 |
| 469.7 | 81.2 |
| 705.7 | 138.5 |
| 1212.2 | 165.0 |
| 1672.6 | 20.2 |
| 1673.4 | 19.9 |
| 3518.2 | 3.9 |
| 3629.3 | 34.7 |
| 3631.8 | 34.5 |

$NH_3$•••LiCCH

| | |
|---|---|
| 77.8 | 0.0 |
| 77.8 | 0.0 |
| 178.5 | 61.0 |
| 178.5 | 61.0 |
| 262.3 | 7.2 |
| 470.3 | 92.3 |
| 470.3 | 92.3 |
| 643.0 | 59.1 |
| 643.0 | 59.1 |
| 717.8 | 142.7 |
| 1210.0 | 166.7 |
| 1673.2 | 19.5 |
| 1673.2 | 19.5 |
| 1925.4 | 4.5 |
| 3446.9 | 10.5 |
| 3521.4 | 3.2 |
| 3635.0 | 32.9 |
| 3635.0 | 32.9 |

$NH_3$•••LiH

| | |
|---|---|
| 112.8 | 374.9 |
| 115.9 | 378.9 |
| 420.3 | 0.8 |
| 3167.6 | 0.0 |
| 3189.3 | 0.7 |
| 3250.3 | 0.0 |
| 3277.7 | 0.0 |

$C_2H_4$•••LiBr

| | |
|---|---|
| 54.1 | 21.5 |
| 77.3 | 27.9 |
| 137.8 | 1.8 |
| 198.3 | 11.7 |
| 202.5 | 10.2 |
| 625.7 | 123.8 |
| 819.1 | 0.1 |
| 986.4 | 3.2 |
| 1031.4 | 109.1 |
| 1087.6 | 0.0 |
| 1246.9 | 0.0 |
| 1383.0 | 0.8 |
| 1488.7 | 13.3 |
| 1676.8 | 0.8 |
| 3168.0 | 0.0 |
| 3192.0 | 0.9 |
| 3250.1 | 0.1 |
| 3278.3 | 0.0 |

$C_2H_4$•••LiCl

| | |
|---|---|
| 11.1 | 31.7 |
| 76.0 | 37.4 |
| 155.9 | 2.1 |
| 178.6 | 9.1 |
| 207.1 | 12.9 |
| 674.4 | 148.9 |
| 818.0 | 0.1 |
| 986.8 | 2.9 |
| 1031.2 | 107.8 |
| 1088.2 | 0.0 |
| 1246.5 | 0.0 |
| 1383.5 | 0.8 |
| 1489.7 | 13.4 |
| 1678.2 | 0.8 |
| 3168.9 | 0.0 |
| 3191.8 | 0.6 |
| 3251.2 | 0.0 |

| | |
|---|---|
| 86.8 | 25.7 |
| 86.8 | 25.7 |
| 168.3 | 0.1 |
| 199.5 | 12.3 |
| 199.5 | 12.3 |
| 375.1 | 117.4 |
| 375.1 | 117.5 |
| 709.6 | 73.7 |
| 937.5 | 218.5 |
| 1448.2 | 3.6 |
| 1448.2 | 3.6 |
| 3169.7 | 1.6 |
| 3334.2 | 0.4 |
| 3334.2 | 0.4 |
| 4015.1 | 37.3 |

$H_2O$•••LiCN

| | |
|---|---|
| 43.2 | 10.2 |
| 82.4 | 0.1 |
| 164.7 | 11.1 |
| 169.9 | 14.4 |
| 252.4 | 306.2 |
| 263.6 | 6.2 |
| 433.2 | 119.9 |
| 715.9 | 151.9 |
| 1655.6 | 100.9 |
| 2079.5 | 16.9 |
| 3841.7 | 58.5 |
| 3946.8 | 164.1 |

$H_2O$•••LiNC

| | |
|---|---|
| 32.1 | 16.9 |
| 59.5 | 0.1 |
| 130.7 | 3.6 |
| 135.4 | 10.1 |
| 230.2 | 311.1 |
| 274.1 | 4.9 |
| 427.1 | 120.5 |
| 771.7 | 194.3 |
| 1651.6 | 101.3 |
| 2080.0 | 87.3 |
| 3845.1 | 58.6 |
| 3949.7 | 164.6 |
| 464.1 | 185.3 |
| 467.8 | 181.3 |
| 1197.0 | 177.7 |
| 1351.3 | 347.7 |
| 1672.0 | 19.9 |
| 1673.0 | 19.9 |
| 3519.0 | 1.8 |
| 3630.2 | 32.8 |
| 3635.0 | 32.8 |

$NH_3$•••LiF

| | |
|---|---|
| 78.8 | 34.5 |
| 80.6 | 34.9 |
| 288.0 | 3.5 |
| 448.9 | 101.5 |
| 450.7 | 101.1 |
| 898.7 | 170.2 |
| 1197.8 | 156.3 |
| 1673.3 | 19.3 |
| 1673.5 | 19.3 |
| 3522.0 | 2.0 |
| 3633.3 | 31.4 |
| 3635.2 | 31.4 |

$NH_3$•••LiOH

| | |
|---|---|
| 100.0 | 7.9 |
| 100.5 | 8.0 |
| 286.7 | 2.4 |
| 357.4 | 85.6 |
| 357.4 | 85.9 |
| 450.5 | 100.7 |
| 451.2 | 100.4 |
| 931.9 | 212.3 |
| 1192.8 | 156.5 |
| 1674.3 | 19.4 |
| 1674.4 | 19.4 |
| 3522.2 | 1.8 |
| 3636.0 | 29.8 |
| 3636.6 | 29.8 |
| 4009.3 | 26.8 |

$H_2$•••LiCN

| | |
|---|---|
| 20.2 | 19.8 |
| 3278.8 | 0.0 |

$C_2H_4$•••LiCCH

| | |
|---|---|
| 55.8 | 8.1 |
| 67.7 | 6.8 |
| 134.8 | 20.2 |
| 153.2 | 41.1 |
| 155.6 | 20.5 |
| 205.4 | 43.8 |
| 224.1 | 53.0 |
| 649.9 | 55.3 |
| 651.0 | 55.1 |
| 686.8 | 149.3 |
| 818.7 | 0.1 |
| 987.8 | 3.9 |
| 1030.0 | 109.4 |
| 1091.0 | 0.0 |
| 1245.8 | 0.0 |
| 1383.7 | 0.8 |
| 1491.0 | 13.1 |
| 1679.1 | 0.7 |
| 1928.2 | 8.4 |
| 3168.9 | 0.1 |
| 3190.5 | 0.6 |
| 3251.6 | 0.1 |
| 3279.2 | 0.1 |
| 3445.0 | 11.3 |

$C_2H_4$•••LiH

| | |
|---|---|
| 84.2 | 376.9 |
| 114.7 | 226.5 |
| 171.8 | 140.1 |
| 236.0 | 308.2 |
| 260.1 | 0.0 |
| 817.7 | 0.1 |
| 984.8 | 2.9 |
| 1026.0 | 104.4 |
| 1086.0 | 0.0 |
| 1247.2 | 0.0 |
| 1383.9 | 5.8 |
| 1393.0 | 350.2 |
| 1490.6 | 12.7 |
| 1679.8 | 0.4 |

$H_2O$•••LiBr

| | |
|---|---|
| 25.1 | 6.8 |
| 100.3 | 0.3 |
| 221.7 | 6.2 |
| 258.9 | 284.0 |
| 423.3 | 98.3 |
| 682.2 | 140.3 |
| 1654.8 | 102.9 |
| 3846.1 | 60.9 |
| 3950.7 | 159.8 |

$H_2O$•••LiCl

| | |
|---|---|
| 28.8 | 13.2 |
| 89.0 | 0.4 |
| 240.0 | 296.1 |
| 254.8 | 5.0 |
| 426.8 | 105.9 |
| 719.3 | 158.7 |
| 1653.5 | 100.9 |
| 3847.9 | 56.4 |
| 3953.3 | 159.3 |

$H_2O$•••LiCCH

| | |
|---|---|
| 45.7 | 0.0 |
| 89.6 | 25.5 |
| 157.3 | 22.9 |
| 168.4 | 53.2 |
| 233.8 | 303.6 |
| 265.2 | 4.8 |
| 423.3 | 121.1 |
| 646.6 | 59.0 |
| 650.1 | 58.6 |
| 729.3 | 158.7 |
| 1653.9 | 101.6 |
| 1927.5 | 5.0 |
| 3449.2 | 10.7 |
| 3845.1 | 55.0 |
| 3953.0 | 155.9 |

$H_2O$•••LiH

| | |
|---|---|
| 52.5 | 344.9 |
| 77.8 | 27.9 |
| 106.3 | 11.8 |
| 166.9 | 31.9 |
| 172.6 | 36.9 |
| 352.3 | 2.6 |
| 632.6 | 5.8 |
| 663.3 | 138.7 |
| 2082.1 | 22.2 |
| 4453.2 | 19.5 |

$H_2$•••LiNC

| | |
|---|---|
| 25.7 | 24.8 |
| 104.8 | 13.1 |
| 139.1 | 20.0 |
| 153.3 | 27.5 |
| 359.3 | 1.8 |
| 619.9 | 2.6 |
| 737.5 | 181.9 |
| 2080.8 | 100.6 |
| 4451.9 | 19.2 |

$H_2$•••LiBr

| | |
|---|---|
| 37.2 | 22.2 |
| 122.7 | 22.3 |
| 350.9 | 7.4 |
| 623.9 | 121.8 |
| 645.1 | 3.8 |
| 4456.6 | 17.9 |

$H_2$•••LiCl

| | |
|---|---|
| 7.9 | 29.5 |
| 76.5 | 30.8 |
| 345.3 | 2.4 |
| 628.1 | 2.7 |
| 668.4 | 145.1 |
| 4456.6 | 16.9 |

$H_2$•••LiCCH

| | |
|---|---|
| 25.7 | 24.8 |
| 104.8 | 13.1 |
| 139.1 | 20.0 |
| 153.3 | 27.5 |
| 359.3 | 1.8 |
| 619.9 | 2.6 |
| 3169.9 | 0.1 |
| 3194.2 | 0.4 |
| 3251.7 | 0.0 |
| 3279.4 | 0.1 |

$C_2H_4$•••LiF

| | |
|---|---|
| 48.7 | 51.3 |
| 79.0 | 53.7 |
| 160.7 | 19.0 |
| 175.8 | 1.1 |
| 196.9 | 30.1 |
| 818.5 | 0.1 |
| 892.0 | 176.4 |
| 977.1 | 3.0 |
| 1023.5 | 105.6 |
| 1082.8 | 0.0 |
| 1246.3 | 0.0 |
| 1382.8 | 0.5 |
| 1489.0 | 13.4 |
| 1678.2 | 0.4 |
| 3170.0 | 0.2 |
| 3195.4 | 0.3 |
| 3251.5 | 0.0 |
| 3279.8 | 0.4 |

$C_2H_4$•••LiOH

| | |
|---|---|
| 33.0 | 19.4 |
| 82.2 | 23.8 |
| 157.9 | 5.5 |
| 172.9 | 0.4 |
| 201.3 | 9.9 |
| 371.1 | 111.7 |
| 372.7 | 113.6 |
| 817.6 | 0.1 |
| 931.6 | 206.6 |
| 980.6 | 2.2 |
| 1021.8 | 113.9 |
| 1082.8 | 0.0 |
| 1247.1 | 0.0 |
| 1382.9 | 0.4 |
| 1489.6 | 12.7 |
| 1679.1 | 0.4 |
| 3170.9 | 0.3 |

| | | | | | |
|---|---|---|---|---|---|
| 258.4 | 708.6 | 737.5 | 181.9 | 3194.6 | 0.3 |
| 424.9 | 237.5 | 2080.8 | 100.6 | 3252.6 | 0.0 |
| 428.9 | 0.0 | 4451.9 | 19.2 | 3280.7 | 0.5 |
| 1369.7 | 349.1 | | | 4008.0 | 36.3 |
| 1650.0 | 100.8 | | | | |
| 3854.6 | 46.6 | | | | |
| 3962.1 | 152.6 | | | | |

# Appendix A. Naming and Characterizing hydrogen bonding

## A. 1. Introduction

Intermolecular interactions are complex phenomena to understand. Hydrogen bonding was postulated in 1920[1] but even about after a century, new discovery[2] and visualization of hydrogen bond[3] is a active area of research. In last three years, two new intermolecular interactions have been described i.e. carbon bond[4] and pnicogen bond.[5–9] However, Matta et al.[10] introduced the term 'trihydrogen bonding'. However, their choice follow the naming of M-H•••H-X as 'dihydrogen bond'. It was soon realized that hydrogen bonding exactly the same as 'hydrogen bond' with the acceptor being a halide. Matta et al. named H-H•••$H^-$ as trihydrogen bond and claimed it to be a new be a new discovery. They seems unaware of previous work on H-H•••$X^-$ (X= F, Cl, Br). In the appendix, we compare H-H•••$F^-$ and H-H•••$H^-$ and show that they are very similar.

Recently, Arunan et al. have redefined the hydrogen bond through an IUPAC project.[11] In this work, hydrogen bond definition was revised considering results from many theoretical. The IUPAC definition points out that the linearity of D-H•••A is the most distinguishing future of the hydrogen bond. It also recognized that the ∠ D-H•••A could deviate from linearity. It has recommended a lower limit to this angle as 110°, though no reasons have been given for this.

The above mentioned two issues create confusion and one can ask simple question about them like why the so called new interaction named as 'trihydrogen bond' and why the hydrogen bond angle range vary between 110-180° range. Hereafter, same angle range will be denoted in its complementary form as 0-70°, instead of 110-180°. These both issues are discussed in the next sections.

## A. 2. Trihydrogen Bonding and its Naming

As rightly pointed out by the author that hydrogen bonding, dihydrogen bonding and trihydrogen bonding are primarily electrostatic in nature.[10] Contribution from the covalency are also significant and discussed in Chapter VI for hydrogen bond. The trihydrogen complex ($H_3^-$) have intermolecular interaction between $H_2$ with the $H^-$ (hydride) ion and denoted as H-H•••$H^-$ complex. The objective of this work is to compare this complex with H-H•••$F^-$

complex. The H-H•••$F^-$ complex has been investigated using spectroscopy and it is an intermediate in the reaction between $F^-$ and $H_2$.[12–15] Other halides H-H•••$X^-$ complexes (X= Cl, Br, I) are also study studied with great interest.[16,17] Neumark and co-workers have done a lot of investigations on such complexes.

Comparison of the above mentioned complexes has been done mainly using ab initio and AIM calculations. The optimized structures of both complexes are given in Figure A. 1 at MP2/6-311++G** level of theory. The distance between $F^-$ and $H_2$ is much shorter than the distance between $H^-$ and $H_2$. This difference in distances also appeared in their binding energies. For the H-H•••$F^-$ complex, the binding energy is 21.03 kJ/mol whereas for H-H•••$H^-$ complex binding energy is only 3.22 kJ/mol. At the same level of theory, H-H bond distance is 0.738 Å. Bond elongation is 0.036 Å for H-H•••$F^-$ complex whereas for H-H•••$H^-$ complex, bond elongation is 0.006 Å, much less in comparison to the former one. This effect was experimentally observed in form of red shift by 940 $cm^{-1}$ in H-H stretching frequency for H-H•••$F^-$.[13] At MP2/6-311++G** level of theory, the red shift is 667 and 116 $cm^{-1}$ for H-H•••$F^-$ and H-H•••$H^-$ complexes, respectively.

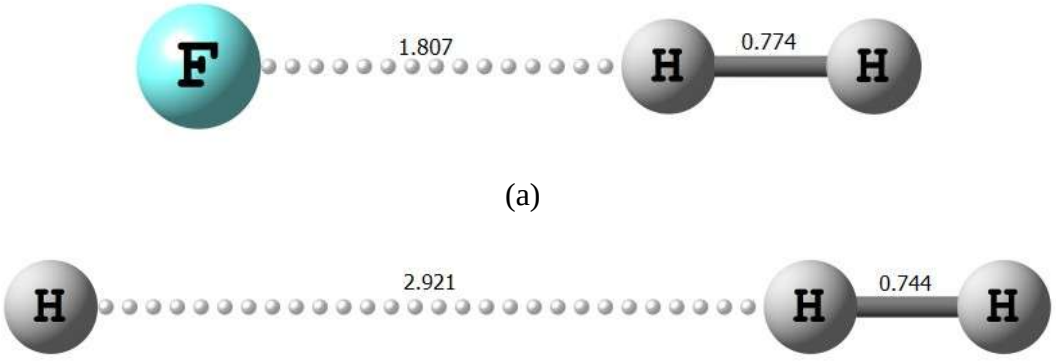


*Figure A. 1. Equilibrium structure of (a)H-H•••$F^-$ complex and (b) H-H•••$H^-$ at MP2/6-311++G**.Geometrical parameters are given in Å.*

AIM calculations have been performed for both complexes. In Figure A. 2, molecular graphs for these complexes are presented. The solid lines originating from the nuclear attractor (NA) are gradient of the electron density and they form atomic basin for a particular atom inside the molecule. In between two atoms, small green dots are the bond critical points (BCP),

which confirm that two atoms are bonded. The dividing surface of two atomic basins is called interatomic surface and in 2D plot it is shown by dashed black lines. The electron density is plotted in the form of a contour (red colour). Both figures look very similar and differences are noted only because of much stronger bonding in the first complex (a) than the second complex (b).

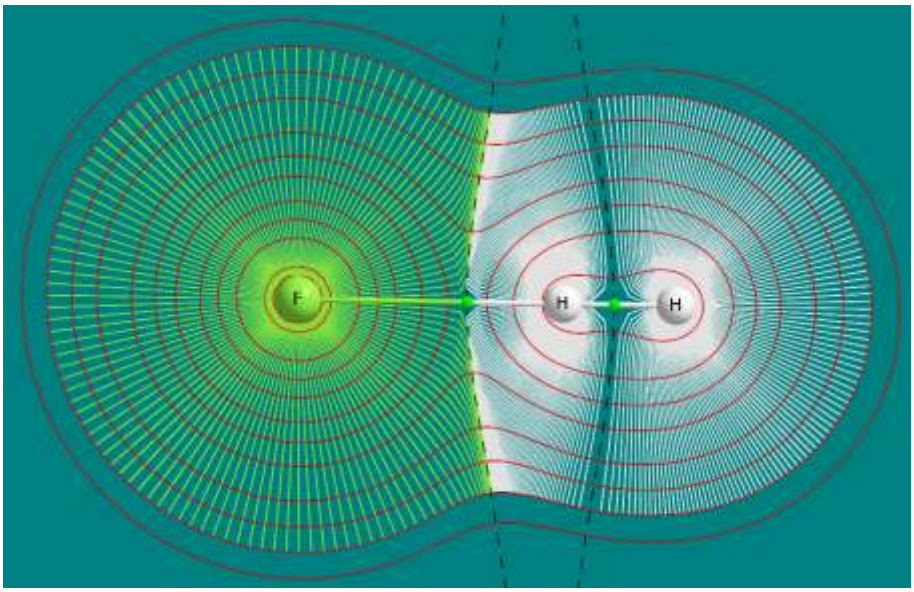


(a)

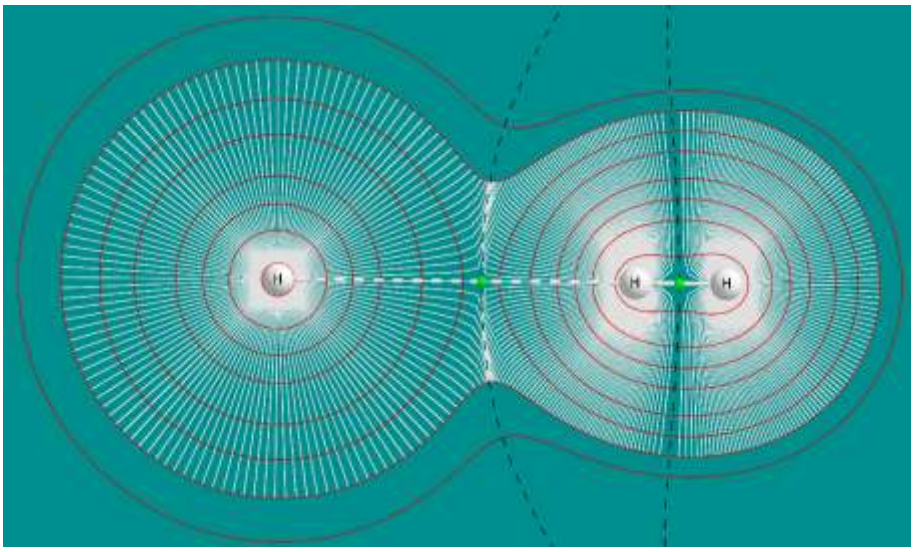


(b)

*Figure A. 2. Electron density contour, gradient of electron density, interatomic surface line are plotted for both complexes.*

Electron density at intermolecular BCP and at H-H bond are shown in Table A. 1. Intermolecular bond formed on the cost of monomer electron density. In table we can see that, $H_2$ molecule reduces its electron density on complex formation '$\Delta\rho$' by 0.0037 and 0.0246 a.u. for H-H•••$H^-$ and H-H•••$F^-$ complexes, respectively. Whereas at intermolecular BCP, electron density '$\rho$' values are 0.0036 and 0.0336 a.u. for H-H•••$H^-$ and H-H•••$F^-$ complexes, respectively. In Chapter VI, we have shown a linear correlation between $\Delta\rho$ and $\rho$ and the above mentioned values follow the same correlation. At intermolecular BCP, the value of Laplacian of electron density is positive for both complexes. Positive Laplacian is the signature of closed shell interaction. For covalent bond, its values are negative (Table A. 1).

There are many integrated atomic properties that can be monitored. All these properties exihib similar trend for both complexes. For example, trend of average charge on the atom is similar for both complexes. Bonded hydrogen atom (bonded with $H^-$ or $F^-$) should have partial positive charge. According to Koch and Popelier,[18] in the case of hydrogen bonding, bonded hydrogen atom should lose its charge on complex formation. Next property is the virial based total energy of an atom inside a molecule. According to the criterion, bonded hydrogen atom should destabilize on complex formation. In both the complexes, bonded hydrogen atoms are destabilized. In another criterion, there should be loss of dipole moment of the bonded hydrogen atom (H) on the complex formation. For strong H-H•••$F^-$ complex, there is significant loss in dipole moment but for the weak H-H•••$H^-$ complex, dipole moment is almost constant. The last criterion suggests that there should be decrement in the atomic volume. There is decrement in the volume of bonded hydrogen atom of H-H•••$F^-$ complex and almost constant for weak H-H•••$H^-$ complex.

In summary, H-H•••$H^-$ and H-H•••$F^-$ are both hydrogen bonded and a new name for the H-H•••$H^-$ seems unnecessary. The main difference between the two arises from the polarizability difference. The $F^-$ is strongly polarizing and $H^-$ is weak polarizing. The IUPAC recommendation mentioned that any hydrogen bond D-H•••A should have D more electronegative than H. In these examples, the polarizability of $X^-$ (X= F, Cl, Br) makes the $H_2$ molecule induces a dipole moment making the H interacts with $X^-$, more positive.

*Table A. 1. Electron density topological and integrated atomic properties from atoms in molecules calculations for the complex and monomer.*

| Properties | H-H•••$H^-$ | | H-H•••$F^-$ | | H-H |
|---|---|---|---|---|---|
| | Property at H•••$H^-$ BCP | Property at H-H BCP | Property at H•••$F^-$ BCP | Property at H-H BCP | Property at H-H BCP |
| Electron density | 0.0036 | 0.2599 | 0.0336 | 0.239 | 0.2636 |
| Laplacian | 0.0063 | -1.0548 | 0.1089 | -0.9322 | -1.0744 |
| | Property of $H^-$ | Property of H (cov. Bonded H) | Property of $F^-$ | Property of H (cov. Bonded H) | Property of bonded H |
| Avg. charge | -0.9693 | 0.0701 (-0.1008) | -0.9551 | 0.2201 (-0.2650) | 0 |
| Avg. Energy | -0.5238 | -0.5368 (-0.6073) | -99.7127 | -0.4837 (+0.6514) | -0.5802 |
| Dipolar polarization | 0.193 | 0.1171 (-0.1168) | 0.1121 | 0.0481 (-0.1253) | 0.1044 |
| Volumes at 0.001 a.u. | 272.0558 | 61.7961 (-67.8259) | 182.6825 | 38.538 (-83.3805) | 60.1341 |

*In small bracket, atomic property corresponds to other hydrogen of $H_2$ which is not participated in bonding directly.*

## A. 3. Suggested Angle Range for conventional Hydrogen Bonding

In Chapter V, for a particular hydrogen bond donor H-D, three different sets of hydrogen bond radii are suggested for three different strengths of the A•••H-D complexes i.e. strong, medium and weak. In the Figure A. 3, four different contours are plotted corresponding to 0.02, 0.005, 0.002, 0.001 a.u. electron density value for HF. Blue solid line denotes the interatomic surface in 2D contour plot. An interatomic surface or zero-flux surface separates an atom from rest of the molecule. It consists of a bunch of gradient path terminating at the bond critical point (BCP). As the name suggests, surface is a 3D property and in a 2D plane it appears as a line shown as solid blue line in Figure A. 3. This line intersects the 0.02, 0.005, 0.002, 0.001 a.u. contours at four different places denoted by four different dashed lines C1, C2, C3 and C4, respectively (Figure A. 3). For HF molecule, angles (θ) are 72, 66, 65 and 63° for C1, C2, C3 and C4 lines, respectively (Table A. 2). The values 0.02, 0.005, 0.002 a.u. correspond to strong, medium and weak bonds[19] (see Chapter V for details). Therefore, if the

A•••H-F complex is very strong, hydrogen bond angle range 0-72° can be considered as a conventional hydrogen bond. For medium and weak complexes, angle range 0-65° can be considered as a conventional hydrogen bond. This is more specific quantitative interpretation of the hydrogen bond angle range for HF molecule. It is little difficult to apply this method quickly as one should know the strength of the bond. In the next paragraph, easily applicable ranges are suggested for conventional hydrogen bond.

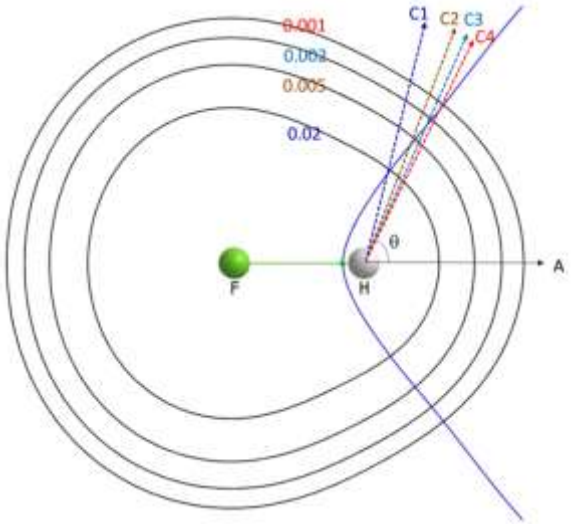


*Figure A. 3. Angle measurement for different contour plot for HF molecule.*

Because of the high electronegativity of F-atom, HF mostly forms either medium or strong type of complexes depending on the acceptor and there are no large differences between the angle ranges for them (72 and 66). For the HF molecule, 0-65° hydrogen bond angles can be considered as the conventional type of hydrogen bond, in general. The upper limit of the range (65) is the average of angles 66, 65 and 63, corresponding to 0.005, 0.002 and 0.001 contours, respectively. In the range 0-65°, strong bonds are underestimated by a small value. In such cases, one can see the Table A. 2, for more accurate value.

In similar way, angles are measured for the most popular hydrogen bond donors HD in the A•••H-D complexes where HD are HCl, HBr, $H_2O$, $H_2S$, HNC, $NH_3$, HCN, HCCH and $CH_4$ (Table A. 2). However, $NH_3$ and $CH_4$ rarely work as hydrogen bond donor and they are kept in the list for comparison. It is clear from the table that, change in hybridization of the D-atom (Nitrogen and Carbon) does not alter the angle range (unlike hydrogen bond radii, see Chapter V). However, moving downwards or leftwards to the periodic table, results in

increasing angle. Other HD molecules show their angle range higher than the IUPAC recommended angle range for conventional hydrogen bond (0-70°). For example, for H2S and HBr cases angle ranges are 0-94° and 0-89°, respectively.

*Table A. 2. Maximum hydrogen bond angle for the conventional type of hydrogen bonding.*

| | **0.02** | **0.005** | **0.002** | **0.001** | **Angle Range** |
|---|---|---|---|---|---|
| HF | 72 | 66 | 65 | 63 | 0-65 |
| HCl | 96 | 87 | 82 | 79 | 0-83 |
| HBr | 105 | 93 | 88 | 85 | 0-89 |
| $H_2O$ | 84 | 79 | 75 | 74 | 0-76 |
| $H_2S$ | 107 | 97 | 94 | 92 | 0-94 |
| HNC | 88 | 78 | 75 | 73 | 0-75 |
| $NH_3$ | 88 | 79 | 76 | 73 | 0-76 |
| HCN | 99 | 91 | 87 | 85 | 0-88 |
| HCCH | 99 | 91 | 88 | 84 | 0-88 |
| $CH_4$ | 100 | 90 | 86 | 84 | 0-87 |

So for, we have not included the effect of acceptor A on the hydrogen bond angle range in the A•••H-D complexes. We have selected two models, $NH_3$•••H-F and Ar•••H-F to calculate the hydrogen bond angle range. Bonding between A and H can be confirmed by observing a BCP between them. The BCP is bonded to the atoms through a bond path. Relaxed scan, an inbuilt method in G09 to get the potential surface along scanning coordinate, have been performed for the hydrogen bond angle at the step size of 3° from 0 to 70°. The AIM calculations have been performed for the structures at each steps of this relax scanning. Location of intermolecular BCP and the bond path are monitored for each structure. For $NH_3$•••H-F, when the angle changes from 63° to 67°, bond path changes its bonding from hydrogen to fluorine (see the change in bond path colour in Figure A. 4). Therefore, 63° is the upper limit of the hydrogen bond angle range for the conventional hydrogen bonding. This value is closed to the recommended hydrogen bond angle range (0-65°) for HF molecule. In another example, Ar•••H-F, bond path changes it bonding from hydrogen to

argon at the angle 54°. Clearly, the acceptor can alter the range of angles in which hydrogen bonding can occur.

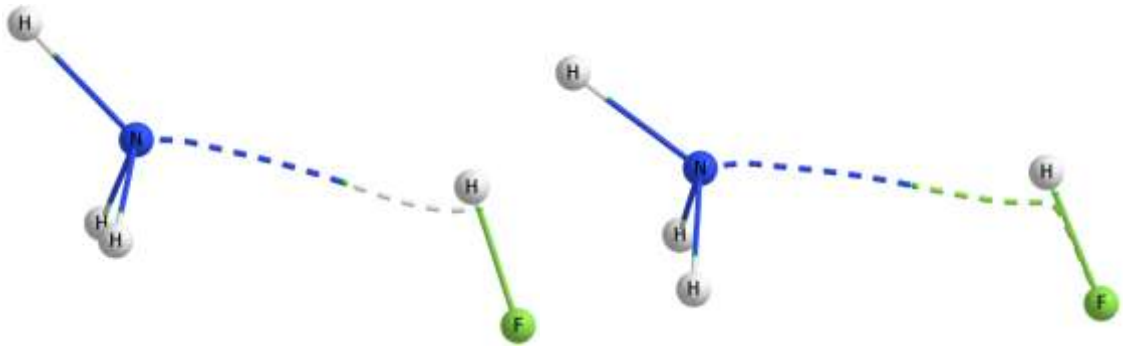


*Figure A. 4. Example of $NH_3$•••HF complex at two different angle.*
(117° (left side) and 114° (right side) or complimentary angle 63° or 67°)

## A. 4. Conclusion

In the first part, we have learned that all properties of H-H•••$H^-$ complex match with that of H-H•••$F^-$ complex. Author's claim about an unexpected molecular structure should be revised and giving a new name 'trihydrogen bond' is not needed because all atoms participate in the bonding are hydrogen.

In the second part, treating the complexes as a conventional hydrogen bond when the hydrogen bond angle is 0-70° (IUPAC recommended) may underestimate the $H_2S$, HBr, HCN bond donor. For these donors, the suggested range for hydrogen bond angle is 0-90°. Angle ranges largely depend on the donor part of the complex but not on the hybridization of D-atom of A•••H-D complex. The acceptor part can alter the angle bond range.

## A. 5. References

1. L. Pauling, *The Nature of the Chemical Bond and the Structure of Molecules and Crystals; An Introduction to Modern Structural Chemistry*, Cornell University Press, Ithaca, New York, 1960.

2. L. De Marco, M. Thämer, M. Reppert, and A. Tokmakoff, *J. Chem. Phys.*, 2014, **141**, 034502.

3. J. Zhang, P. Chen, B. Yuan, W. Ji, Z. Cheng, and X. Qiu, *Science*, 2013, **342**, 611–4.

4. D. Mani and E. Arunan, *Phys. Chem. Chem. Phys.*, 2013, **15**, 14377–83.

5. U. Adhikari and S. Scheiner, *Chem. Phys. Lett.*, 2011, **514**, 36–39.

6. S. Scheiner, 2011, **164313**, 1–9.

7. S. Scheiner, *Chem. Phys.*, 2011, **387**, 79–84.

8. M. Solimannejad, M. Gharabaghi, and S. Scheiner, 2011, **024312**, 1–6.

9. S. Scheiner, *J. Chem. Phys.*, 2011, **134**, 094315.

10. C. F. Matta, L. Huang, and L. Massa, *J. Phys. Chem. A*, 2011, **115**, 12451–8.

11. E. Arunan, G. R. Desiraju, R. a. Klein, J. Sadlej, S. Scheiner, I. Alkorta, D. C. Clary, R. H. Crabtree, J. J. Dannenberg, P. Hobza, H. G. Kjaergaard, A. C. Legon, B. Mennucci, and D. J. Nesbitt, *Pure Appl. Chem.*, 2011, **83**, 1619–1636.

12. B. Hartke and H. Werner, *Chem. Phys. Lett.*, 1997, **280**, 430–438.

13. D. A. Wild, R. L. Wilson, Z. M. Loh, and E. J. Bieske, *Chem. Phys. Lett.*, 2004, **393**, 517–520.

14. S. E. Bradforth, D. W. Arnold, D. M. Neumark, and D. E. Manolopoulos, *J. Chem. Phys.*, 1993, **99**, 6345.

15. A. Weaver, R. B. Metz, S. E. Bradforth, and D. M. Neumark, 1993, **5352**, 1989–1991.

16. T. a Grinev, A. A. Buchachenko, J. Kłos, and E. J. Bieske, *J. Chem. Phys.*, 2006, **125**, 114313.

17. E. Garand, J. Zhou, D. E. Manolopoulos, M. H. Alexander, and D. M. Neumark, *Science*, 2008, **319**, 72–5.

18. U. Koch and P. L. A. Popelier, *J. Phys. Chem. Chem.*, 1995, **99**, 9747–9754.

19. R. A. Klein, *Chem. Phys. Lett.*, 2006, **425**, 128–133.

# Appendix B. Preliminary studies on hexafluoroisopropanol dimer

## B. 1. Introduction

We have already discussed the microwave spectroscopic study of hexafluoroisopropanol and its complex with water in Chapter III and Chapter IV, respectively. From previous studies, we have learned many interesting property of the HFIP solvent and its aqueous solution. In addition to those properties, this molecule has strong self-aggregation power in condense phase. [1–10] HFIP is known for forming strong hydrogen bond as we have observed that HFIP forms a very strong hydrogen bond with water (Chapter IV). Suhm's group has done spectroscopic study of this molecule and showed the effect of fluorination on alcohols.[11]

## B. 2. Ab initio calculations

MP2 and LC-wPBE level of theory with 6-311++G** basis set produced a very close prediction for HFIP and HFIP•••water complex. These methods were used to predict the HFIP dimer properties as well. Binding energy, hydrogen bond length, rotational constants and dipole moment components are given in Table B. 1 at both level of theory. However, calculations at other level theories also have been performed and rotational constants are given in Table B. 2. The MP2/6-311++G** level of theory has been used for the prediction of the rotational transitions of HFIP-dimer. From Table B. 1, it is clear that the complex has non-zero *a*- and *c-dipole* moment component. The *b-dipole* moment component is zero for this complex, unlike HFIP and HFIP•••water where *b-type* transitions were the most intense signals.

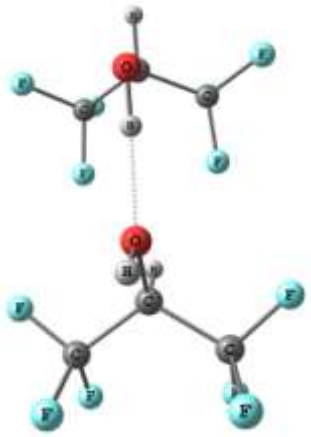

*Figure B. 1. Equilibrium structure of HFIP-dimer at MP2/6-311++G**.*

*Table B. 1. Important structural and spectroscopic properties of HFIP-dimer.*

| HFIP Dimer | mp2/6-311++g(d,p) | LC-wPBE/6-311++G** |
|---|---|---|
| Hydrogen Bond Length (Å) | 1.87 | 1.89 |
| Binding Energy (kcal/mol) | 4.99 | 4.39 |
| Dipole Moment (Debye) | | |
| $\mu_a$ | 0.07 | 0.34 |
| $\mu_b$ | 0 | 0 |
| $\mu_c$ | 0.85 | 0.76 |
| Rotational Constants | | |
| A /MHz | 483.72 | 486.57 |
| B /MHz | 212.68 | 199.60 |
| C /MHz | 174.82 | 165.48 |
| κ-parameter | -0.75 | -0.79 |

*Table B. 2. Calculated rotational constants of HFIP-dimer at different level of theory.*

| Level of theory | A /MHz | B /MHz | C /MHz | κ-parameter |
|---|---|---|---|---|
| MP2/6-311++G(d,p) | 483.72 | 212.68 | 174.82 | -0.75 |
| B3LYP/6-311++G** | 479.13 | 195.99 | 162.90 | -0.79 |
| LC-wPBE/6-311++G** | 486.57 | 199.60 | 165.48 | -0.79 |
| CAM-B3LYP/6-311++G** | 483.89 | 209.83 | 172.74 | -0.76 |
| wB97XD/6-311++G** | 481.86 | 208.95 | 171.82 | -0.76 |
| HF/6-311++G** | 492.36 | 194.80 | 162.11 | -0.80 |

## B. 3. Experiment and unassigned transitions

Rotational spectra have been predicted for HFIP-dimer on the basis of the calculated rotational constants. At MP2/6-311++G** level of theory, the predicted spectra are given in Table B.S 3 for *a*- and *c-type* transitions of R-branch. Ab initio calculations show that for HFIP-dimer, *b-dipole* moment is zero and therefore it should not show b-type transition. Certain patterns in the strong *c-type* transitions, which may help in assigning the transition, are presented in Table B. 3.

*Table B. 3. Predicted rotational transitions with certain pattern in between transitions and frequencies.*

| **J, $K_{-1}$, $K_{+1}$ <- J, $K_{-1}$, $K_{+1}$ (Transition)** | **Type** | **Frequency** | **Intensity** |
|---|---|---|---|
| 7, 0, 7 <- 6, 0, 6 | a-R | 2568.9542 | 6.9 |
| 7, 1, 7 <- 6, 1, 6 | a-R | 2543.8954 | 6.8 |
| 7, 1, 6 <- 6, 1, 5 | a-R | 2782.6945 | 6.8 |
| 7, 2, 6 <- 6, 2, 5 | a-R | 2684.3054 | 6.4 |
| 8, 0, 8 <- 7, 0, 7 | a-R | 2914.7785 | 7.8 |
| 8, 1, 8 <- 7, 1, 7 | a-R | 2898.1227 | 7.8 |
| 8, 1, 7 <- 7, 1, 6 | a-R | 3152.0209 | 7.7 |
| 8, 2, 7 <- 7, 2, 6 | a-R | 3056.2938 | 7.5 |
| 9, 0, 9 <- 8, 0, 8 | a-R | 3261.2385 | 8.8 |
| 9, 1, 9 <- 8, 1, 8 | a-R | 3250.7916 | 8.8 |
| 9, 1, 8 <- 8, 1, 7 | a-R | 3510.3327 | 8.7 |
| 9, 2, 8 <- 8, 2, 7 | a-R | 3424.3866 | 8.5 |
| 10, 0, 10 <- 9, 0, 9 | a-R | 3608.63 | 9.8 |

| | | | |
|---|---|---|---|
| 10, 1, 10 <- 9, 1, 9 | a-R | 3602.3438 | 9.8 |
| 10, 1, 9 <- 9, 1, 8 | a-R | 3859.5727 | 9.6 |
| 10, 2, 9 <- 9, 2, 8 | a-R | 3788.6706 | 9.5 |
| 11, 0, 11 <- 10, 0, 10 | a-R | 3956.8126 | 10.8 |
| 11, 1, 11 <- 10, 1, 10 | a-R | 3953.1429 | 10.8 |
| 11, 1, 10 <- 10, 1, 9 | a-R | 4203.3768 | 10.6 |
| 11, 2, 10 <- 10, 2, 9 | a-R | 4149.4457 | 10.5 |
| 12, 0, 12 <- 11, 0, 11 | a-R | 4305.5538 | 11.8 |
| 12, 1, 12 <- 11, 1, 11 | a-R | 4303.4601 | 11.8 |
| 12, 1, 11 <- 11, 1, 10 | a-R | 4545.4118 | 11.6 |
| 12, 2, 11 <- 11, 2, 10 | a-R | 4507.181 | 11.5 |
| 13, 0, 13 <- 12, 0, 12 | a-R | 4654.6557 | 12.8 |
| 13, 1, 13 <- 12, 1, 12 | a-R | 4653.4824 | 12.8 |
| 13, 1, 12 <- 12, 1, 11 | a-R | 4888.0494 | 12.6 |
| 13, 2, 12 <- 12, 2, 11 | a-R | 4862.4404 | 12.5 |
| 14, 0, 14 <- 13, 0, 13 | a-R | 5003.9792 | 13.8 |
| 14, 1, 14 <- 13, 1, 13 | a-R | 5003.331 | 13.8 |
| 14, 1, 13 <- 13, 1, 12 | a-R | 5232.2219 | 13.5 |
| 14, 2, 13 <- 13, 2, 12 | a-R | 5215.8007 | 13.5 |
| 15, 0, 15 <- 14, 0, 14 | a-R | 5353.4351 | 14.8 |
| 15, 1, 15 <- 14, 1, 14 | a-R | 5353.0812 | 14.8 |
| 15, 1, 14 <- 14, 1, 13 | a-R | 5577.9687 | 14.5 |
| 15, 2, 14 <- 14, 2, 13 | a-R | 5567.7853 | 14.5 |

## B. 3. 1. HFIP-Monomer Experiment

During the HFIP-monomer experiment, we observed some signals which are not in the list of fitted transitions for HFIP parent, C-13 (center) and C-13 (side) (Chapter III). Since HFIP molecule has strong tendency to self-aggregate, we suspect that some of these signals are from the HFIP-dimer. The overall molecular mass of the HFIP-dimer complex is large and therefore most of the predicted spectra are in the low frequency range. No attempts have yet been made to assign these transitions. These experimentally observed transitions are given in Table B. 4. Note that only helium gas was used during the experiments, which discarded the possibilities of complex formation between HFIP and helium, unlike when using argon as carrier gas.

*Table B. 4. Experimentally observed unassigned transitions during HFIP-monomer study.*

| | | | | | |
|---|---|---|---|---|---|
| 6705.9006 | 7941.9750 | 8471.1379 | 9747.8658 | 11633.5930 | 13031.3270 |
| 6705.9589 | 7958.5090 | 8478.1942 | 9846.3140 | 11643.5000 | 13107.6336 |
| 6706.2665 | 7958.6260 | 9089.1530 | 10103.4266 | 11789.2779 | 13107.8436 |
| 7026.8550 | 7958.6260 | 9110.8633 | 10203.7930 | 12001.2436 | 13481.0400 |
| 7042.7363 | 7968.3680 | 9137.0050 | 10215.2330 | 12015.0996 | 15129.3340 |
| 7246.5249 | 8059.2960 | 9595.7650 | 10232.6607 | 12015.0996 | 15129.6555 |
| 7833.6082 | 8073.1685 | 9597.2550 | 11099.3363 | 12692.5605 | 15129.8270 |
| 7862.1654 | 8139.8632 | 9597.4160 | 11174.3521 | 12696.4655 | 15131.9170 |
| | | | | | 15271.8980 |

## B. 3. 2. HFIP-Water experiment

We observed some transitions during the search for HFIP-water complex which are not in the final fitted transition list of HFIP-water complex (Chapter IV). There are many possibilities of the complex formation during HFIP-water experiment like HFIP-$(H_2O)_2$, HFIP-$(H_2O)_3$ etc. or some oligomer of water. Only helium gas was used throughout the experiments. Quantum calculations towards the prediction of rotational transitions have not yet been done.

*Table B. 5. Experimentally observed unassigned transitions during HFIP-Water complex experiment.*

| | | | |
|---|---|---|---|
| 8055.71700 | 8812.83650 | 10241.31200 | 10961.05150 |
| 8149.86600 | 8882.65900 | 10293.72700 | 11111.79450 |
| 8644.98050 | 8886.46100 | 10306.89050 | 11112.31750 |
| 8645.10750 | 8892.10000 | 10360.58050 | 11112.80200 |
| 8670.22400 | 8915.91500 | 10474.35600 | 11112.86450 |
| 8696.38500 | 8916.37800 | 10477.14900 | 11132.58550 |
| 8716.81500 | 8958.84350 | 10480.59100 | 11147.79250 |
| 8760.15250 | 8982.75660 | 10485.12950 | 11634.51000 |
| 8774.93100 | 8987.56300 | 10485.13900 | 12319.43900 |
| 8774.98900 | 9023.13900 | 10493.25300 | 12320.99500 |
| 8780.45330 | 9161.00600 | 10496.97550 | 12329.11900 |
| 8812.11900 | 9161.72800 | 10497.84350 | 12329.73600 |
| 8812.32400 | 9521.17350 | 10500.31900 | 12335.30750 |
| 8812.60200 | 10232.65550 | 10503.89050 | |

## B. 4. Conclusion

HFIP has self-aggregation property. Therefore, understanding the HFIP dimer and the type of interaction between two HFIP monomers is important to understand the phenomena of self-aggregation. Ab intito results showed that HFIP-dimer is strongly bound with strong hydrogen bonding interaction. Rotational constants are calculated at different level of theory and tentative predictions for the HFIP-dimer have been done. Unassigned transitions, observed during HFIP-monomer and HFIP-water dimer are tabulated.

## B. 5. Supporting Information

Coordinates of the HFIP-dimer complex at MP2/6-311++G** and LC-wPBE/6-311++G** level of theory have been given. Predicted rotational transitions for the HFIP-dimer are presented. This table includes the *a*- and *c*-type transition from the R-branch only. Note that the b-dipole moment is zero for this complex. The prediction has been done at MP2/6-311++G** level of theory.

## B. 6. References


1. J.-F. Berrien, M. Ourévitch, G. Morgant, N. E. Ghermani, B. Crousse, and D. Bonnet-Delpon, *J. Fluor. Chem.*, 2007, **128**, 839–843.

2. S. Takahashi, T. Katagiri, and K. Uneyama, *Chem. Commun. (Camb).*, 2005, 3658–60.

3. K. F. Purcell, J. A. Stikeleather, and S. D. Brunk, *J. Am. Chem. Soc.*, 1969, **91**, 4019–4027.

4. W. R. Moomaw, T. Liu, and J. E. Kenny, *J. Phys. Chem.*, 1995, **99**, 7320–7323.

5. N. C. Maiti, P. R. Carey, and V. E. Anderson, *J. Phys. Chem. A*, 2003, **107**, 9910–9917.

6. T. Katagiri, Y. Fujiwara, S. Takahashi, and K. Uneyama, *J. Fluor. Chem.*, 2005, **126**, 1134–1139.

7. M. Hyacinth, M. Chruszcz, K. S. Lee, M. Sabat, G. Gao, and L. Pu, *Angew. Chem. Int. Ed. Engl.*, 2006, **45**, 5358–60.

8. M. A. Muñoz, M. Galán, C. Carmona, and M. Balón, *Chem. Phys. Lett.*, 2005, **401**, 109–114.

9. J. Graton, M. Berthelot, F. Besseau, and C. Laurence, *J. Org. Chem.*, 2005, **70**, 7892–901.

10. A. Berkessel, J. A. Adrio, D. Hüttenhain, and J. M. Neudörfl, *J. Am. Chem. Soc.*, 2006, **128**, 8421–6.

11. H. Schaal, T. Häber, and M. a. Suhm, *J. Phys. Chem. A*, 2000, **104**, 265–274.

# *Supporting Information*

*Table B. S. 1. Coordinates (in Å) of HFIP-dimer at MP2/6-311++G** level.*

| | MP2/6-311++g(d,p) | | | LC-wPBE/6-311++G** | | |
|---|---|---|---|---|---|---|
| Atoms | X (Å) | Y (Å) | Z (Å) | X (Å) | Y (Å) | Z (Å) |
| F | 3.3171 | 1.3966 | 0.8836 | 3.3745 | 1.4073 | 0.9122 |
| C | 1.6199 | 0.0000 | 0.0025 | 1.7145 | 0.0000 | -0.0202 |
| C | 2.4373 | 1.2874 | -0.1281 | 2.5366 | 1.2870 | -0.1304 |
| C | 2.4375 | -1.2873 | -0.1286 | 2.5363 | -1.2871 | -0.1312 |
| O | 0.9279 | -0.0004 | 1.2266 | 0.9978 | -0.0002 | 1.1764 |
| H | 0.8741 | 0.0001 | -0.7928 | 0.9949 | 0.0004 | -0.8401 |
| H | 1.5695 | -0.0004 | 1.9488 | 1.6020 | -0.0006 | 1.9285 |
| F | 1.6180 | 2.3402 | -0.0692 | 1.7165 | 2.3385 | -0.1120 |
| F | 3.1083 | 1.3420 | -1.2802 | 3.2518 | 1.3359 | -1.2525 |
| F | 3.1085 | -1.3413 | -1.2808 | 3.2517 | -1.3354 | -1.2531 |
| F | 3.3172 | -1.3969 | 0.8831 | 3.3739 | -1.4085 | 0.9115 |
| F | 1.6183 | -2.3402 | -0.0704 | 1.7159 | -2.3384 | -0.1137 |
| F | -1.1846 | 1.3850 | -0.5687 | -1.3309 | 1.3951 | -0.6566 |
| C | -2.6593 | 0.0002 | 0.6803 | -2.6914 | 0.0003 | 0.7067 |
| C | -2.4578 | 1.2807 | -0.1356 | -2.5611 | 1.2811 | -0.1227 |
| C | -2.4578 | -1.2808 | -0.1350 | -2.5612 | -1.2810 | -0.1218 |
| O | -1.8455 | 0.0004 | 1.8102 | -1.7957 | 0.0006 | 1.7586 |
| H | -3.7002 | 0.0002 | 1.0149 | -3.7023 | 0.0005 | 1.1210 |
| H | -0.9149 | 0.0003 | 1.5297 | -0.8791 | 0.0004 | 1.4362 |
| F | -2.7099 | 2.3449 | 0.6308 | -2.7570 | 2.3424 | 0.6612 |
| F | -3.2606 | 1.3383 | -1.2035 | -3.4471 | 1.3365 | -1.1196 |
| F | -3.2608 | -1.3389 | -1.2028 | -3.4470 | -1.3369 | -1.1188 |
| F | -1.1847 | -1.3852 | -0.5682 | -1.3310 | -1.3956 | -0.6555 |
| F | -2.7098 | -2.3446 | 0.6320 | -2.7574 | -2.3417 | 0.6628 |

*Table B. S. 2. Normal mode vibrational frequencies ($cm^{-1}$) with their intensity for HFIP-dimer at LC-wPBE/6-311++G** level*

| Frequency | Intensity | Frequency | Intensity | Frequency | Intensity |
|---|---|---|---|---|---|
| 4.7 | 0.0 | 378.3 | 72.0 | 1160.5 | 159.5 |
| 18.4 | 0.1 | 465.4 | 7.0 | 1187.7 | 132.9 |
| 23.5 | 0.0 | 468.8 | 10.3 | 1208.7 | 27.4 |
| 27.8 | 0.2 | 520.7 | 7.9 | 1220.6 | 33.9 |
| 30.4 | 0.2 | 522.6 | 9.3 | 1233.9 | 473.8 |
| 34.5 | 0.1 | 536.3 | 5.8 | 1237.2 | 360.7 |
| 52.9 | 0.3 | 537.3 | 2.9 | 1270.5 | 276.0 |
| 58.7 | 0.5 | 551.2 | 6.9 | 1275.9 | 324.7 |
| 121.1 | 1.2 | 558.4 | 2.7 | 1282.9 | 155.8 |
| 129.3 | 4.5 | 589.5 | 100.3 | 1289.6 | 3.0 |
| 166.3 | 0.3 | 617.4 | 1.3 | 1291.2 | 304.7 |
| 169.0 | 0.4 | 619.6 | 1.6 | 1306.7 | 204.2 |
| 241.3 | 1.9 | 695.1 | 1.3 | 1340.5 | 147.0 |
| 247.5 | 2.7 | 698.0 | 119.6 | 1368.5 | 99.2 |
| 249.6 | 5.7 | 749.0 | 11.5 | 1426.7 | 280.0 |
| 252.9 | 1.8 | 752.4 | 19.5 | 1427.1 | 22.1 |
| 290.6 | 12.4 | 852.5 | 26.7 | 1444.1 | 3.8 |
| 295.3 | 2.1 | 858.0 | 63.6 | 1460.6 | 4.1 |
| 329.2 | 0.7 | 915.4 | 18.4 | 3155.0 | 4.9 |
| 330.1 | 0.4 | 923.7 | 69.4 | 3178.6 | 8.4 |
| 342.2 | 28.0 | 1133.8 | 220.4 | 3709.5 | 597.4 |
| 352.1 | 0.0 | 1138.0 | 75.8 | 3861.1 | 103.4 |

*Table B.S 3.Predicted rotational transitions (in MHz) for the HFIP-dimer at MP2/6-311++G** level.*

| J, K-1, K+1 <- J, K-1, K+1 | Type | Frequency | Intensity | J, K-1, K+1 <- J, K-1, K+1 | Type | Frequency | Intensity |
|---|---|---|---|---|---|---|---|
| 5, 1, 4 <- 4, 1, 3 | a-R | 2013.556 | 4.7 | 6 3 4 <- 5 2 4 | c-R | 3820.045 | 3.2 |
| 6, 1, 6 <- 5, 1, 5 | a-R | 2187.64 | 5.8 | 6 5 2 <- 5 4 2 | c-R | 4936.47 | 4.6 |
| 6, 0, 6 <- 5, 0, 5 | a-R | 2222.426 | 5.8 | 6 2 5 <- 5 1 5 | c-R | 3474.226 | 2.1 |
| 6, 2, 5 <- 5, 2, 4 | a-R | 2308.552 | 5.3 | 6 4 3 <- 5 3 3 | c-R | 4358.922 | 3.9 |
| 6, 5, 2 <- 5, 5, 1 | a-R | 2334.343 | 1.8 | 6 2 4 <- 5 1 4 | c-R | 3133.231 | 3.7 |
| 6, 5, 1 <- 5, 5, 0 | a-R | 2334.349 | 1.8 | 6 4 2 <- 5 3 2 | c-R | 4353.191 | 3.9 |
| 6, 4, 3 <- 5, 4, 2 | a-R | 2337.502 | 3.3 | | | | |
| 6, 4, 2 <- 5, 4, 1 | a-R | 2337.912 | 3.3 | 7 1 6 <- 6 0 6 | c-R | 3626.058 | 2.5 |
| 6, 3, 4 <- 5, 3, 3 | a-R | 2339.654 | 4.5 | 7 1 6 <- 6 2 4 | c-R | 2052.092 | 1.5 |
| 6, 3, 3 <- 5, 3, 2 | a-R | 2351.792 | 4.5 | 7 3 4 <- 6 2 4 | c-R | 4066.364 | 3.9 |
| | | | | 7 5 2 <- 6 4 2 | c-R | 5324.232 | 4.9 |
| 6, 1, 5 <- 5, 1, 4 | a-R | 2402.628 | 5.7 | 7 3 5 <- 6 2 5 | c-R | 4242.409 | 3.5 |
| 6, 2, 4 <- 5, 2, 3 | a-R | 2410.784 | 5.3 | 7 5 3 <- 6 4 3 | c-R | 5324.711 | 4.9 |
| 7, 1, 7 <- 6, 1, 6 | a-R | 2543.895 | 6.8 | 7 2 6 <- 6 1 6 | c-R | 3970.891 | 2.2 |
| 7, 0, 7 <- 6, 0, 6 | a-R | 2568.954 | 6.8 | 7 4 4 <- 6 3 4 | c-R | 4749.731 | 4.2 |
| 7, 2, 6 <- 6, 2, 5 | a-R | 2684.305 | 6.3 | 7 2 5 <- 6 1 5 | c-R | 3557.182 | 4.2 |
| 7, 5, 3 <- 6, 5, 2 | a-R | 2725.743 | 3.4 | 7 4 3 <- 6 3 3 | c-R | 4733.212 | 4.2 |
| 7, 5, 2 <- 6, 5, 1 | a-R | 2725.771 | 3.4 | | | | |
| 7, 4, 4 <- 6, 4, 3 | a-R | 2730.462 | 4.7 | 8 1 7 <- 7 0 7 | c-R | 4209.125 | 2.4 |
| 7, 3, 5 <- 6, 3, 4 | a-R | 2730.917 | 5.7 | 8 1 7 <- 7 2 5 | c-R | 2377.533 | 1.7 |
| 7, 4, 3 <- 6, 4, 2 | a-R | 2731.813 | 4.7 | 8 3 5 <- 7 2 5 | c-R | 4409.586 | 4.5 |
| | | | | 8 5 3 <- 7 4 3 | c-R | 5710.745 | 5.1 |
| 7, 3, 4 <- 6, 3, 3 | a-R | 2757.075 | 5.7 | 8 3 6 <- 7 2 6 | c-R | 4679.076 | 3.8 |
| 7, 1, 6 <- 6, 1, 5 | a-R | 2782.695 | 6.7 | 8 5 4 <- 7 4 4 | c-R | 5712.46 | 5.1 |
| 7, 2, 5 <- 6, 2, 4 | a-R | 2826.579 | 6.4 | 8 2 7 <- 7 1 7 | c-R | 4483.289 | 2.3 |
| 8, 1, 8 <- 7, 1, 7 | a-R | 2898.123 | 7.8 | 8 4 5 <- 7 3 5 | c-R | 5143.401 | 4.5 |
| 8, 0, 8 <- 7, 0, 7 | a-R | 2914.779 | 7.8 | 8 2 6 <- 7 1 6 | c-R | 4012.446 | 4.6 |
| 8, 2, 7 <- 7, 2, 6 | a-R | 3056.294 | 7.4 | 8 4 4 <- 7 3 4 | c-R | 5104.369 | 4.5 |
| 8, 5, 4 <- 7, 5, 3 | a-R | 3118.211 | 4.8 | | | | |
| 8, 5, 3 <- 7, 5, 2 | a-R | 3118.326 | 4.8 | 9 1 8 <- 8 0 8 | c-R | 4804.679 | 2.4 |
| 8, 3, 6 <- 7, 3, 5 | a-R | 3120.972 | 6.8 | 9 1 8 <- 8 2 6 | c-R | 2649.907 | 1.8 |
| 8, 4, 5 <- 7, 4, 4 | a-R | 3124.587 | 6 | 9 3 6 <- 8 2 6 | c-R | 4761.33 | 5.2 |
| | | | | 9 5 4 <- 8 4 4 | c-R | 6094.754 | 5.4 |
| 8, 4, 4 <- 7, 4, 3 | a-R | 3128.232 | 6 | 9 3 7 <- 8 2 7 | c-R | 5131.699 | 4 |
| 8, 1, 7 <- 7, 1, 6 | a-R | 3152.021 | 7.7 | 9 5 5 <- 8 4 5 | c-R | 6099.746 | 5.4 |
| 8, 3, 5 <- 7, 3, 4 | a-R | 3169.8 | 6.8 | 9 2 8 <- 8 1 8 | c-R | 5009.553 | 2.3 |
| 8, 2, 6 <- 7, 2, 5 | a-R | 3237.959 | 7.5 | 9 4 6 <- 8 3 6 | c-R | 5542.06 | 4.8 |
| 9, 1, 9 <- 8, 1, 8 | a-R | 3250.792 | 8.8 | 9 2 7 <- 8 1 7 | c-R | 4502.665 | 4.9 |
| 9, 0, 9 <- 8, 0, 8 | a-R | 3261.239 | 8.8 | 9 2 7 <- 8 3 5 | c-R | 2470.613 | 1.5 |
| 9, 2, 8 <- 8, 2, 7 | a-R | 3424.387 | 8.4 | 9 4 5 <- 8 3 5 | c-R | 5462.702 | 4.9 |
| 9, 3, 7 <- 8, 3, 6 | a-R | 3508.917 | 7.9 | | | | |
| 9, 1, 8 <- 8, 1, 7 | a-R | 3510.333 | 8.6 | 10 1 9 <- 9 0 9 | c-R | 5403.013 | 2.4 |
| 9, 5, 5 <- 8, 5, 4 | a-R | 3511.873 | 6.2 | 10 1 9 <- 9 2 7 | c-R | 2867.24 | 1.7 |
| | | | | 10 3 7 <- 9 2 7 | c-R | 5133.31 | 5.9 |
| 9, 5, 4 <- 8, 5, 3 | a-R | 3512.242 | 6.2 | 10 3 7 <- 9 4 5 | c-R | 2141.221 | 1 |
| 9, 4, 6 <- 8, 4, 5 | a-R | 3519.631 | 7.2 | 10 5 5 <- 9 4 5 | c-R | 6474.447 | 5.7 |
| 9, 4, 5 <- 8, 4, 4 | a-R | 3528.133 | 7.2 | 10 3 8 <- 9 2 8 | c-R | 5601.226 | 4.2 |
| 9, 3, 6 <- 8, 3, 5 | a-R | 3589.703 | 8 | 10 5 6 <- 9 4 6 | c-R | 6486.925 | 5.7 |
| 10, 1, 10 <- 9, 1, 9 | a-R | 3602.344 | 9.8 | 10 2 9 <- 9 1 9 | c-R | 5547.432 | 2.4 |
| 10, 0, 10 <- 9, 0, 9 | a-R | 3608.63 | 9.8 | 10 2 9 <- 9 3 7 | c-R | 2081.358 | 1 |
| 9, 2, 7 <- 8, 2, 6 | a-R | 3642.24 | 8.5 | 10 4 7 <- 9 3 7 | c-R | 5948.274 | 5.2 |
| 10, 2, 9 <- 9, 2, 8 | a-R | 3788.671 | 9.5 | 10 0 10 <- 9 1 8 | c-R | 2065.19 | 0.6 |
| 10, 1, 9 <- 9, 1, 8 | a-R | 3859.573 | 9.6 | 10 2 8 <- 9 1 8 | c-R | 5029.789 | 5 |
| 10, 3, 8 <- 9, 3, 7 | a-R | 3893.914 | 9 | 10 2 8 <- 9 3 6 | c-R | 2918.366 | 1.9 |
| | | | | 10 4 6 <- 9 3 6 | c-R | 5805.797 | 5.4 |
| 10, 5, 6 <- 9, 5, 5 | a-R | 3906.81 | 7.5 | | | | |
| 10, 5, 5 <- 9, 5, 4 | a-R | 3907.825 | 7.5 | 11 1 10 <- 10 0 10 | c-R | 5997.76 | 2.4 |
| 10, 4, 7 <- 9, 4, 6 | a-R | 3915.131 | 8.4 | 11 1 10 <- 10 2 8 | c-R | 3033.161 | 1.6 |
| 10, 4, 6 <- 9, 4, 5 | a-R | 3932.798 | 8.4 | 11 3 8 <- 10 2 8 | c-R | 5534.818 | 6.5 |
| 11, 1, 11 <- 10, 1, 10 | a-R | 3953.143 | 10.8 | 11 3 8 <- 10 4 6 | c-R | 2647.387 | 1.4 |
| 11, 0, 11 <- 10, 0, 10 | a-R | 3956.813 | 10.8 | 11 5 6 <- 10 4 6 | c-R | 6847.161 | 6.1 |
| 10, 3, 7 <- 9, 3, 6 | a-R | 4014.22 | 9.1 | 11 1 11 <- 10 2 9 | c-R | 2008.055 | 0.6 |
| 10, 2, 8 <- 9, 2, 7 | a-R | 4037.456 | 9.5 | 11 3 9 <- 10 2 9 | c-R | 6087.831 | 4.4 |
| 11, 2, 10 <- 10, 2, 9 | a-R | 4149.446 | 10.5 | 11 3 9 <- 10 4 7 | c-R | 2220.915 | 1.1 |
| 11, 1, 10 <- 10, 1, 9 | a-R | 4203.377 | 10.5 | 11 5 7 <- 10 4 7 | c-R | 6874.825 | 6.1 |
| | | | | 11 2 10 <- 10 1 10 | c-R | 6094.534 | 2.4 |
| 11, 3, 9 <- 10, 3, 8 | a-R | 4275.276 | 10.1 | 11 2 10 <- 10 3 8 | c-R | 2336.891 | 1.1 |
| 11, 5, 7 <- 10, 5, 6 | a-R | 4303.031 | 8.7 | 11 4 8 <- 10 3 8 | c-R | 6364.77 | 5.5 |
| 12, 1, 12 <- 11, 1, 11 | a-R | 4303.46 | 11.8 | 11 0 11 <- 10 1 9 | c-R | 2162.43 | 0.6 |
| 11, 5, 6 <- 10, 5, 5 | a-R | 4305.513 | 8.7 | 11 2 9 <- 10 1 9 | c-R | 5592.098 | 4.9 |
| 12, 0, 12 <- 11, 0, 11 | a-R | 4305.554 | 11.8 | 11 2 9 <- 10 3 7 | c-R | 3326.028 | 2.3 |
| 11, 4, 8 <- 10, 4, 7 | a-R | 4310.41 | 9.5 | 11 4 7 <- 10 3 7 | c-R | 6135.265 | 5.9 |
| 11, 4, 7 <- 10, 4, 6 | a-R | 4343.688 | 9.5 | | | | |

| | | | |
|---|---|---|---|
| 11, 2, 9 <- 10, 2, 8 | a-R | 4421.882 | 10.5 |
| 11, 3, 8 <- 10, 3, 7 | a-R | 4438.964 | 10.2 |
| 12, 2, 11 <- 11, 2, 10 | a-R | 4507.181 | 11.5 |
| 12, 1, 11 <- 11, 1, 10 | a-R | 4545.412 | 11.5 |
| 12, 3, 10 <- 11, 3, 9 | a-R | 4652.518 | 11.1 |
| 13, 1, 13 <- 12, 1, 12 | a-R | 4653.482 | 12.8 |
| 13, 0, 13 <- 12, 0, 12 | a-R | 4654.656 | 12.8 |
| 12, 5, 8 <- 11, 5, 7 | a-R | 4700.431 | 9.9 |
| 12, 4, 9 <- 11, 4, 8 | a-R | 4704.628 | 10.6 |
| 12, 5, 7 <- 11, 5, 6 | a-R | 4705.935 | 9.9 |
| 12, 4, 8 <- 11, 4, 7 | a-R | 4761.97 | 10.6 |
| 12, 2, 10 <- 11, 2, 9 | a-R | 4794.151 | 11.5 |
| 12, 3, 9 <- 11, 3, 8 | a-R | 4859.315 | 11.3 |
| 13, 2, 12 <- 12, 2, 11 | a-R | 4862.44 | 12.5 |
| 13, 1, 12 <- 12, 1, 11 | a-R | 4888.049 | 12.5 |
| 14, 1, 14 <- 13, 1, 13 | a-R | 5003.331 | 13.8 |
| 14, 0, 14 <- 13, 0, 13 | a-R | 5003.979 | 13.8 |
| 13, 3, 11 <- 12, 3, 10 | a-R | 5025.39 | 12.2 |
| 13, 4, 10 <- 12, 4, 9 | a-R | 5096.868 | 11.7 |
| 13, 5, 9 <- 12, 5, 8 | a-R | 5098.75 | 11 |
| 13, 5, 8 <- 12, 5, 7 | a-R | 5109.987 | 11 |
| 13, 2, 11 <- 12, 2, 10 | a-R | 5153.967 | 12.4 |
| 13, 4, 9 <- 12, 4, 8 | a-R | 5187.651 | 11.7 |
| 14, 2, 13 <- 13, 2, 12 | a-R | 5215.801 | 13.5 |
| 14, 1, 13 <- 13, 1, 12 | a-R | 5232.222 | 13.5 |
| 13, 3, 10 <- 12, 3, 9 | a-R | 5271.678 | 12.3 |
| 15, 1, 15 <- 14, 1, 14 | a-R | 5353.081 | 14.8 |
| 15, 0, 15 <- 14, 0, 14 | a-R | 5353.435 | 14.8 |
| 14, 3, 12 <- 13, 3, 11 | a-R | 5393.89 | 13.2 |
| 14, 4, 11 <- 13, 4, 10 | a-R | 5486.231 | 12.8 |
| 14, 5, 10 <- 13, 5, 9 | a-R | 5497.544 | 12.2 |
| 14, 2, 12 <- 13, 2, 11 | a-R | 5502.922 | 13.4 |
| 14, 5, 9 <- 13, 5, 8 | a-R | 5518.856 | 12.2 |
| 15, 2, 14 <- 14, 2, 13 | a-R | 5567.785 | 14.5 |
| 15, 1, 14 <- 14, 1, 13 | a-R | 5577.969 | 14.5 |
| 14, 4, 10 <- 13, 4, 9 | a-R | 5618.708 | 12.8 |
| 14, 3, 11 <- 13, 3, 10 | a-R | 5673.59 | 13.3 |
| 15, 3, 13 <- 14, 3, 12 | a-R | 5758.252 | 14.2 |
| 15, 2, 13 <- 14, 2, 12 | a-R | 5844.5 | 14.3 |
| 15, 4, 12 <- 14, 4, 11 | a-R | 5871.936 | 13.8 |
| 15, 5, 11 <- 14, 5, 10 | a-R | 5896.18 | 13.3 |
| 15, 5, 10 <- 14, 5, 9 | a-R | 5933.919 | 13.3 |
| 15, 4, 11 <- 14, 4, 10 | a-R | 6051.047 | 13.9 |
| 15, 3, 12 <- 14, 3, 11 | a-R | 6063.272 | 14.3 |
| 3 3 0 <- 2 2 0 | c-R | 2611.124 | 2.5 |
| 3 3 1 <- 2 2 1 | c-R | 2614.592 | 2.5 |
| 3 2 2 <- 2 1 2 | c-R | 2089.227 | 1.6 |
| <- | c-R | | |
| 4 1 3 <- 3 0 3 | c-R | 2036.995 | 2.2 |
| 4 3 1 <- 3 2 1 | c-R | 2992.193 | 2.7 |
| 4 3 2 <- 3 2 2 | c-R | 3008.86 | 2.7 |
| 4 2 3 <- 3 1 3 | c-R | 2532.847 | 1.8 |
| 4 4 1 <- 3 3 1 | c-R | 3580.511 | 3.5 |
| 4 2 2 <- 3 1 2 | c-R | 2359.182 | 2.4 |
| 4 4 0 <- 3 3 0 | c-R | 3580.296 | 3.5 |
| <- | c-R | | |
| 5 1 4 <- 4 0 4 | c-R | 2535.51 | 2.4 |
| 5 3 2 <- 4 2 2 | c-R | 3362.75 | 3 |
| 5 5 0 <- 4 4 0 | c-R | 4547.876 | 4.5 |
| 5 3 3 <- 4 2 3 | c-R | 3409.743 | 2.9 |
| 5 5 1 <- 4 4 1 | c-R | 4547.887 | 4.5 |
| 5 2 4 <- 4 1 4 | c-R | 2994.622 | 2 |
| 5 4 2 <- 4 3 2 | c-R | 3969.469 | 3.7 |
| 5 2 3 <- 4 1 3 | c-R | 2736.004 | 3.1 |
| 5 4 1 <- 4 3 1 | c-R | 3967.994 | 3.7 |
| <- | c-R | | |
| 6 1 5 <- 5 0 5 | c-R | 3065.79 | 2.5 |
| 6 3 3 <- 5 2 3 | c-R | 3720.073 | 3.4 |
| 6 5 1 <- 5 4 1 | c-R | 4936.372 | 4.6 |
| 12 1 11 <- 11 0 11 | c-R | 6586.359 | 2.4 |
| 12 1 11 <- 11 2 9 | c-R | 3156.69 | 1.5 |
| 12 3 9 <- 11 2 9 | c-R | 5972.251 | 7 |
| 12 3 9 <- 11 4 7 | c-R | 3163.014 | 1.7 |
| 12 5 7 <- 11 4 7 | c-R | 7209.408 | 6.5 |
| 12 1 12 <- 11 2 10 | c-R | 2162.069 | 0.6 |
| 12 3 10 <- 11 2 10 | c-R | 6590.903 | 4.5 |
| 12 3 10 <- 11 4 8 | c-R | 2563.023 | 1.3 |
| 12 5 8 <- 11 4 8 | c-R | 7264.846 | 6.4 |
| 12 2 11 <- 11 1 11 | c-R | 6648.572 | 2.4 |
| 12 2 11 <- 11 3 9 | c-R | 2568.796 | 1.2 |
| 12 4 9 <- 11 3 9 | c-R | 6794.123 | 5.8 |
| 12 4 9 <- 11 5 7 | c-R | 2140.213 | 1.1 |
| 12 0 12 <- 11 1 10 | c-R | 2264.607 | 0.6 |
| 12 2 10 <- 11 1 10 | c-R | 6182.873 | 4.9 |
| 12 2 10 <- 11 3 8 | c-R | 3681.216 | 2.6 |
| 12 4 8 <- 11 3 8 | c-R | 6458.271 | 6.6 |
| 12 4 8 <- 11 5 6 | c-R | 2258.497 | 1.1 |
| 13 1 12 <- 12 0 12 | c-R | 7168.855 | 2.4 |
| 13 1 12 <- 12 2 10 | c-R | 3250.589 | 1.4 |
| 13 3 10 <- 12 2 10 | c-R | 6449.777 | 7.4 |
| 13 3 10 <- 12 4 8 | c-R | 3672.722 | 2.2 |
| 13 5 8 <- 12 4 8 | c-R | 7557.426 | 6.9 |
| 13 1 13 <- 12 2 11 | c-R | 2308.371 | 0.6 |
| 13 3 11 <- 12 2 11 | c-R | 7109.112 | 4.6 |
| 13 3 11 <- 12 4 9 | c-R | 2883.785 | 1.5 |
| 13 5 9 <- 12 4 9 | c-R | 7658.967 | 6.8 |
| 13 2 12 <- 12 1 12 | c-R | 7207.552 | 2.4 |
| 13 2 12 <- 12 3 10 | c-R | 2778.719 | 1.2 |
| 13 4 10 <- 12 3 10 | c-R | 7238.473 | 6.1 |
| 13 4 10 <- 12 5 8 | c-R | 2536.65 | 1.3 |
| 13 0 13 <- 12 1 11 | c-R | 2373.851 | 0.6 |
| 13 2 11 <- 12 1 11 | c-R | 6791.427 | 4.8 |
| 13 2 11 <- 12 3 9 | c-R | 3975.867 | 2.7 |
| 13 4 9 <- 12 3 9 | c-R | 6786.606 | 7.3 |
| 13 4 9 <- 12 5 7 | c-R | 2740.212 | 1.4 |
| 14 1 13 <- 13 0 13 | c-R | 7746.421 | 2.5 |
| 14 1 13 <- 13 2 11 | c-R | 3328.844 | 1.3 |
| 14 3 11 <- 13 2 11 | c-R | 6969.4 | 7.5 |
| 14 3 11 <- 13 4 9 | c-R | 4158.661 | 2.7 |
| 14 5 9 <- 13 4 9 | c-R | 7888.63 | 7.4 |
| 14 1 14 <- 13 2 12 | c-R | 2449.261 | 0.6 |
| 14 3 12 <- 13 2 12 | c-R | 7640.562 | 4.7 |
| 14 3 12 <- 13 4 10 | c-R | 3180.808 | 1.6 |
| 14 5 10 <- 13 4 10 | c-R | 8059.644 | 7.2 |
| 14 2 13 <- 13 1 13 | c-R | 7769.871 | 2.4 |
| 14 2 13 <- 13 3 11 | c-R | 2969.129 | 1.2 |
| 14 4 11 <- 13 3 11 | c-R | 7699.313 | 6.4 |
| 14 4 11 <- 13 5 9 | c-R | 2924.132 | 1.5 |
| 14 0 14 <- 13 1 12 | c-R | 2489.78 | 0.6 |
| 14 2 12 <- 13 1 12 | c-R | 7406.3 | 4.8 |
| 14 2 12 <- 13 3 10 | c-R | 4207.111 | 2.7 |
| 14 4 10 <- 13 3 10 | c-R | 7133.637 | 8.1 |
| 14 4 10 <- 13 5 8 | c-R | 3248.933 | 1.6 |
| 15 1 14 <- 14 0 14 | c-R | 8320.41 | 2.5 |
| 15 1 14 <- 14 2 12 | c-R | 3403.891 | 1.3 |
| 15 3 12 <- 14 2 12 | c-R | 7529.75 | 7.5 |
| 15 3 12 <- 14 4 10 | c-R | 4603.225 | 3.1 |
| 15 5 10 <- 14 4 10 | c-R | 8203.841 | 7.9 |
| 15 1 15 <- 14 2 13 | c-R | 2586.542 | 0.6 |
| 15 3 13 <- 14 2 13 | c-R | 8183.013 | 4.8 |
| 15 3 13 <- 14 4 11 | c-R | 3452.829 | 1.7 |
| 15 5 11 <- 14 4 11 | c-R | 8469.592 | 7.5 |
| 15 2 14 <- 14 1 14 | c-R | 8334.325 | 2.5 |
| 15 2 14 <- 14 3 12 | c-R | 3143.024 | 1.2 |
| 15 4 12 <- 14 3 12 | c-R | 8177.359 | 6.6 |
| 15 4 12 <- 14 5 10 | c-R | 3298.524 | 1.7 |
| 15 0 15 <- 14 1 13 | c-R | 2610.994 | 0.6 |
| 15 2 13 <- 14 1 13 | c-R | 8018.578 | 4.8 |
| 15 2 13 <- 14 3 11 | c-R | 4378.022 | 2.5 |
| 15 4 11 <- 14 3 11 | c-R | 7511.094 | 8.8 |
| 15 4 11 <- 14 5 9 | c-R | 3781.125 | 2 |